Nonequilibrium critical phenomena : exact Langevin equations, erosion of tilted landscapes.

Charlie Duclut

UNIVERSITÉ PIERRE ET MARIE CURIE

ÉCOLE DOCTORALE
PHYSIQUE EN ÎLE-DE-FRANCE

T H È S E

pour obtenir le titre de

Docteur de l'Université Pierre et Marie Curie

Mention : PHYSIQUE THÉORIQUE

Présentée et soutenue par

Charlie DUCLUT

Nonequilibrium critical phenomena: exact Langevin equations, erosion of tilted landscapes.

Thèse dirigée par Bertrand DELAMOTTE

préparée au Laboratoire de Physique Théorique de la Matière Condensée

soutenue le 11 septembre 2017

devant le jury composé de :

M.	Andrea GAMBASSI	*Rapporteur*
M.	Michael SCHERER	*Rapporteur*
M.	Giulio BIROLI	*Examinateur*
Mme	Leticia CUGLIANDOLO	*Présidente du jury*
M.	Andrei FEDORENKO	*Examinateur*
M.	Bertrand DELAMOTTE	*Directeur de thèse*

Remerciements

First of all, I would like to thank the referees Andrea Gambassi and Michael Scherer for taking the time to carefully read the manuscript. I also thank the other jury members, Giulio Biroli, Leticia Cugliandolo, and Andrei Fedorenko, for accepting to get into my work and evaluate it.

Mes remerciements vont ensuite à Bertrand Delamotte, mon directeur de thèse, pour l'immense pédagogie dont il a su faire preuve pendant mes trois années de thèse. Je le remercie pour toutes les explications et les nombreux éclaircissements qu'il m'a donnés, pour le recul qu'il m'a permis de prendre sur mon travail. Sans lui, ce manuscrit n'aurait bien évidemment pas pu voir le jour.

Je remercie également chaleureusement Julien Vidal, parrain de thèse et d'escalade, pour ses nombreux conseils, son soutien, et les nombreuses escapades à Fontainebleau et en montagne, qui je l'espère continueront après mon départ du laboratoire. Je le remercie également, ainsi qu'Ivan Dornic, pour leur relecture de mon manuscrit.

Merci aussi à Hugues Chaté et Ivan, avec lesquels j'ai beaucoup apprécié collaborer, pour leurs conseils et recommandations pour ma recherche de postdoc.

Mon séjour de trois ans au LPTMC n'aurait pas été le même sans toutes les personnes qui le composent : en particulier, je remercie vivement Pascal Viot, son directeur, pour sa présence et sa disponibilité. Merci également aux secrétaires et comptables du laboratoire, Diane Domand, Sylvie Dalla Foglia et Liliane Cruzel pour leur gentillesse, leur patience et leur aide. Merci également à Michel Quaggetto pour les nombreux problèmes informatiques qu'il m'a aidé à résoudre.

Merci à Boris Mantisi et Annie Lemarchand pour leurs crumbles et autres gâteaux improvisés qui ont pu adoucir et réchauffer certaines après-midis d'hiver. Merci aux anciens thésards et postdocs qui m'ont précédé au laboratoire, Thibault Debelhoir, Frédéric Léonard, Simon Moulieras, Elena Tarquini, et Andréas Tresmontant pour toutes les pauses café et les soirées autour d'un verre. Merci en particulier à Fred et Thibault pour les discussions politiques, les ateliers pancartes et les discosoupes. Merci aussi à Fred de m'avoir initié à la gymnastique, et à Thibault pour toutes les discussions, pour sa gentillesse et son altruisme.

Un grand merci également aux doctorants de mon année avec lesquels j'ai beaucoup apprécié passer du temps dans et hors du labo : Chloé, Charlotte, Elsa, Félix, Nico et Stanley. En trois années ils sont devenus bien plus que des collègues et ils me manqueront beaucoup en Allemagne ! Merci en particulier à Chloé et Elsa pour avoir rendu bien plus faciles nos longues soirées de rédaction.

Merci à mes compagnons de grimpe, qui sans cesse me rappellent la valeur d'un *sandwiche* et d'un verre d'eau. Un immense merci à sketchy Tonio, le premier compagnon des sorties régulières à Bleau, à Alexis le téméraire, à Jean et à ses messages ambivalents voire ambidextres, et à John qui les déteste, à Édith le panda, à Quentin qui pourrait s'acheter un sac de sport, à Marion l'alpiniste qui revient de loin, et merci bien sûr à Léo, celui qui a choisi l'autre voie et qui m'a beaucoup fait douté. Merci aussi à Guillaume et Raphaël qui prennent la relève des grimpeurs parisiens ! Merci évidemment à l'AS de Jussieu (et ses nombreuses ramifications) et surtout à ses membres tous passionnés et passionnants : Adeline, Charlotte, Christophe, Constant, Flavien, Goki, Horace, Jeanne, Julia, Kévin, Lucie, Manu, Maria Belen, Marie, Maud,

Romain, Thomas, Thomas...

Merci également à mes colocataires pour les repas et tous les moments partagés, merci à Édouard – le seul vrai – pour les risottos, les mille-feuilles, et tous ses petits plats, et merci à ceux qui se sont succédés mais qui hantent encore les lieux : en particulier Baptiste, Marguerite, Joris, Arman et Thibaut. Un gigantesque merci à celles et ceux qui ne font pas (encore) d'escalade mais qui comptent beaucoup quand même : Delphine, Muriel, Marc l'insaisissable, Aïcha, Charlotte, Corentin, Erwan, Maxime mais également Lucie, Thibaut, Éléonore, David et bien d'autres.

Merci bien sûr aussi à Maya, à Paul et à Édouard, qui sont là depuis si longtemps, qui ont toujours cru en moi, ont toujours su me donner beaucoup de confiance et que je n'oublie pas une seconde.

Je remercie également mes parents, mon frère et ma sœur pour être simplement là, pour avoir su balayer mes hésitations lorsque j'en ai eues, pour m'avoir sans cesse soutenu dans mes choix et mes études.

To Bibu

Contents

Introduction

What are the challenges of modern physics? The description of matter and of its elementary components follows all the predictions of quantum mechanics and of the Standard Model, confirmed again in 2012 by the detection of the Higgs boson at the LHC. The detection of gravitational waves in 2015 by the LIGO detector supports the predictions of general relativity theory, which describes the physics at its largest scale. Despite their sweeping success since these theories were developed, major challenges still remain in the description of the fundamental laws: dark matter and dark energy are mainly phenomenological ingredients, necessary to explain the observed universe and yet not justified by any fundamental law. At the level of particles physics, the mass hierarchy problem is still unsolved, and a resolution of these paradoxical situations both in cosmology and high-energy physics probably requires a theory that would go beyond the Standard Model and the general relativity, which is probably the main challenge of the twenty-first century fundamental physics.

Does it mean that the comprehension of the world between these two extreme scales is now complete? Obviously not. Even if quantum mechanics explain with accuracy the microscopic interactions, many open problems still remain in condensed matter physics: what are the relevant mechanisms in high-temperature superconductivity? What is the nature of the glass transition that leads to the formation of amorphous solids? Fluid mechanics also has its share of problems and, for instance, turbulence that arises as solutions of the Navier–Stokes equation are still ill-understood. At the macroscopic level, physicists are now also puzzled by new situations stemming from biology, sociology, neurosciences: collective motion and behaviour of bacteria, animals or human beings, morphogenesis of living organisms, the understanding of gene expression or large networks of interacting neurons, are just examples of the wealth of open problems arising as physicists try to tackle more and more complex systems. In such systems, the larger entities formed by this collective behaviour display new and original features that were not present in the individual agents. This *emergence* phenomenon stirs more and more attention amongst scientists.

The main difficulty that comes up when studying these systems is that although the microscopic description of the interactions between each of the components may be well-established, the coupling of all these degrees of freedom rapidly makes an exact resolution intractable. Of course, recent progress in computational power has allowed for the simulations of systems described at their microscopic level (sometimes even by solving quantum mechanics equations) through molecular dynamics computation. However, if these new methods yield useful information about chemical reactions at the quantum level, proteins conformations, or solid properties, they usually deal at most with few thousands of particles, whereas macroscopic systems are composed of typically 10^{23} particles...

In the case of weakly-correlated systems, this large number of particles is yet not so demanding and statistical physics approaches have long proved their predictive power; classical equilibrium thermodynamics is an amazing example of the macroscopic description of systems composed of a very large number of particles. Complications, however, arise when the particles start to act in a collective fashion, such that they become strongly correlated, and the usual mean-field tools break down. This happens for example in the vicinity of second-order phase transitions where particles are correlated at larger and larger distances: at the critical point, par-

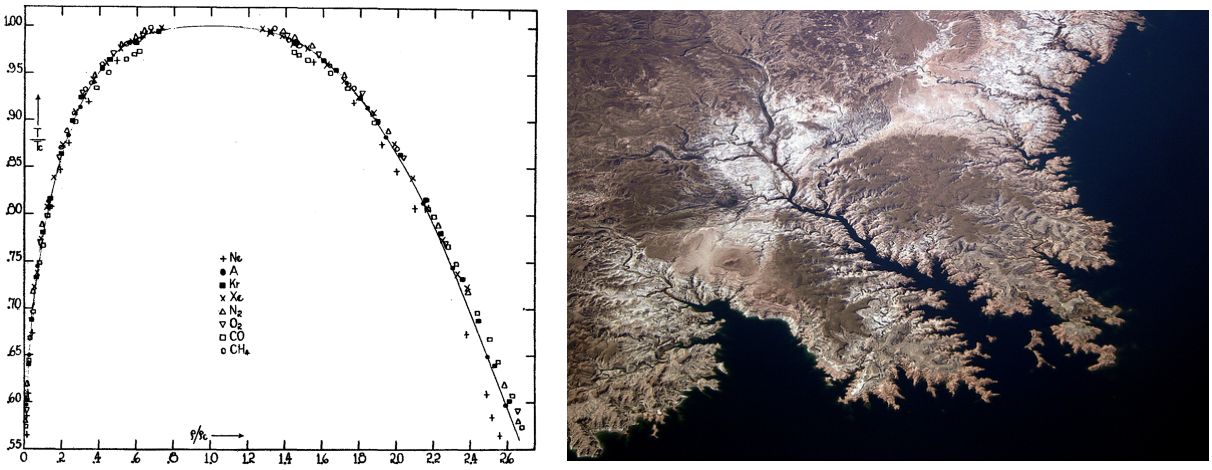

Figure 1 – ***(Left)*** *Reduced temperature T/T_c versus the reduced density ρ/ρ_c of coexisting liquid and gas phases for a number of simple molecular fluids. The experimental points support a data collapse to a universal curve (solid line). However, the curve does not have the behaviour predicted by the mean-field (van der Waals') theory and renormalization group techniques are needed to capture the correct physics. Picture from [2].* ***(Right)*** *Part of the coastline at Lake Mead, United States, displaying a fractal structure. Credits: Chris Moran, "Fractal Coast", 4 April 2010. Online Image. Flickr.*

ticles arbitrarily far apart will be correlated. In the 1940s, although the Onsager exact solution for the two-dimensional Ising model [1] showed that phase transitions can be understood via statistical physics tools, the overall situation of the critical phenomena remained puzzling: in 1945, Guggenheim showed that the mean-field approach failed to predict the scaling behaviour of various liquids near their critical temperature [2], suggesting that the strong correlations taking place in these systems were not taken into account properly by the mean-field theory (see Fig. 1).

The understanding of criticality on the theoretical point-of-view remained elusive for twenty more years. A major step was made in 1966 when Kadanoff developed the idea of coarse-graining variables to reduce the number of microscopic degrees of freedom while conserving the same macroscopic description [3]. Wilson then gave to these intuitions their full computational power by adapting the renormalization group techniques used in particles physics to the study of these strongly-correlated systems [4]. Kadanoff and Wilson approach relies in particular on the scale invariance of critical systems: at the critical point, the only relevant length scale, the correlation length, diverges, meaning that the critical system becomes scale free and looks self-similar at all scales. Using this simple idea, they constructed a theory that is able to explain the power-law behaviour observed near critical points, and also to give a justification to "universality" – the fact that different microscopic systems have the very same scaling properties near the critical point – observed in these phenomena.

Since this theoretical breakthrough, the renormalization group techniques have been applied with success to compute and understand the critical behaviour of various systems, even the more intricate such as topological phase transitions [5], or quantum phase transitions [6]. Open problems related to phase transitions of course still remain, in particular in systems that are not at the thermodynamics equilibrium, because of the variety of nonequilibrium phase transitions, and of the very peculiar features they may exhibit [7]. For instance, in the case of transitions to an absorbing state [8], one of the phases of the system is a state where there is no more fluctuation and from which the system cannot escape: this situation is of course very different from the phase transitions at equilibrium where fluctuations occur on both sides of the transition.

In addition, although at equilibrium the scaling behaviour requires the fine tuning of a pa-

rameter (for instance the temperature is fine-tuned to its critical value T_c) to be observed, some nonequilibrium systems display generic scaling, that is scaling without any fine tuning. This feature is obviously very interesting and may explain why fractal or scale-invariant phenomena are so common in nature: clouds, mountain ranges, coastlines have fractal shapes (see Fig. 1 for an illustration). When looking at the temporal correlations of many phenomena, a behaviour in $1/f^\alpha$ with f the frequency and $\alpha > 0$ is often observed. The preponderance of this "$1/f$ noise" in very diverse systems such as changes in yearly flood level of the river Nile, pitch fluctuations in music, etc. [9] have stirred a particular attention on this generic scaling feature, and many "self-organized criticality" (SOC) models appeared in the literature to explain these observations [10, 11]. Since then, it has become more and more obvious that many nonequilibrium systems (and not only the SOC models) such as the Navier-Stokes equation[1], or the Kardar-Parisi-Zhang (KPZ) equation describing roughening phenomena [13], display generic scaling.

These nonequilibrium systems have however often proved to be much more complicated to handle than their equilibrium counterparts: the KPZ equation, for instance, eludes most perturbative renormalization group approaches in $d > 1$, which urges toward the development of new tools for studying these phenomena. The nonperturbative[2] renormalization group (NPRG) figures amongst the candidates: relying on Wilson and Kadanoff's ideas as its perturbative counterpart, the nonperturbative renormalization group uses different (not dependent on a series expansion in a small parameter and hence nonperturbative) approximation schemes to describe phase transitions and critical phenomena [14]. In the context of nonequilibrium systems, it has proven very effective to tackle turbulence in Navier-Stokes equation for instance [15], or to describe the KPZ equation in $d = 2$ [16] (some theoretical difficulties still exist in dimensions $d > 2$).

Therefore, having in mind to keep on building a deeper understanding of critical phenomena in a nonequilibrium context, my Ph.D. work has been focused on applying nonperturbative techniques to nonequilibrium systems. The outline of this manuscript will be the following:

In the first chapter, a general description of critical phase transitions is given, as well as Wilson and Kadanoff's ideas that lead to the construction of the renormalization group. We show how the simple block-spin idea can be generalized and applied to critical systems. These simple yet general considerations already allow us to understand how universality arises in phase transitions. A presentation of the nonperturbative renormalization group in equilibrium is then given: we show how the NPRG takes care of the growing spatial fluctuations that arise near criticality through the use of a regulating function [14]. Some of its features are illustrated on the $O(N)$ model. Finally, comments about the approximation schemes performed within the NPRG formalism are made, and justifications are given to oppose the criticisms that are formulated against it. We show in particular how the regulator permits and validates the approximations that are performed within the NPRG context.

In the second chapter, the focus is shifted toward nonequilibrium systems, and in particular to the path-integral formulation of models describing out-of-equilibrium phenomena. These field theories are the starting point of the NPRG studies in the remaining chapters. Two different path-integral methods exist and stem from two different descriptions of the system: if a microscopic description at the particle level using a master equation is available – as it is the case for reaction-diffusion processes –, the Doi–Peliti method can be used to obtain an equivalent field-theoretical description [17]. On the other hand, if the description is made through a Langevin equation describing the coarse-grained dynamics of the system, the Martin–Siggia–Rose–de Dominicis–Janssen (MSRDJ) formalism provides the derivation of the field theory [18]. Furthermore, and this is the first main result of this manuscript [19], we connect the two previous approaches (Doi–Peliti and MSRDJ) to derive from the microscopic dynamics a Langevin

[1] Obviously the scaling in turbulence was known since the seminal work of Kolmogorov in 1941 [12], but its complete understanding from its mesoscopic Navier-Stokes description still remains an intricate problem.

[2] The terminology *functional* RG or *exact* RG can also be found in the literature.

equation that describes *exactly* (not in terms of a coarse-grained variable) the evolution of the system. Although this idea is not new, we show that the usual approach found in the literature is plagued with inconsistencies and generates Langevin equations with imaginary noises, which are difficult to manipulate and analyze [20]. By contrast, the approach we provide is consistent, well-justified and yields exact and *real* Langevin equations that give the correct description of the system at the microscopic level.

The third chapter has two purposes: on the one hand, starting from the field-theoretical description elaborated in the preceding chapter, we explain how the NPRG formalism can be extended from equilibrium to nonequilibrium systems [21]. On the other hand, and this is the second main result of this manuscript [22], we argue that nonequilibrium system requires, in addition to the usual space regulator which is the hallmark of the NPRG method, a time-regulator which ensures that the growing time fluctuations are taken care of in the same way as the spatial fluctuations are controlled. This issue, often overlooked in the literature, is in fact crucial for the sake of the approximations that are made in the NPRG context [23]. Furthermore, when engineering this frequency regulator, constraints such as causality and the symmetries of the model have to be taken into account. To benchmark this newly designed frequency regulator, we study it on simple relaxational models: the kinetic Ising model and the kinetic $O(N)$ model. We show that adding a frequency regulator yields better quantitative results for the computation of the dynamical exponent. Moreover, for these relaxational models, we show that designing a regulator that satisfies the fluctuation-dissipation theorem drastically simplifies the NPRG flow equations and is surely a desirable feature.

Finally, in the last chapter, light is shed on an anisotropic model describing the erosion of tilted landscapes. Understanding the erosion of landscapes, and how the fractal behaviour of natural landscapes arises has a long history [24]. Amongst the wealth of possible models for erosion, the Kardar–Parisi–Zhang (KPZ) is believed to provide a correct description of the observed phenomena and scaling behaviour of landscape erosion at large length scale [25]. However, at smaller length scale, the isotropic KPZ description breaks down and the existence of a preferred direction (that of the slope of the mountain) is believed to play a role. An alternative non-linear model including anisotropy was therefore proposed to describe the smaller length scale dynamics [26]. This model was the root of some misunderstandings concerning the relevance of the coupling constants, and was shown to possess infinitely many relevant coupling constants [27]. Its critical behaviour, instead of being determined by a discrete set of fixed points, was shown to possess a line of such fixed points, although their precise description – in particular their stability – was still eluding. The third and last main result of this manuscript [28] is to provide a comprehensive description of this model and its line of fixed points using the NPRG techniques developed in the preceding chapters. In particular, this whole line of fixed points is found to be attractive, indicating a non-universal behaviour of erosion at this scale, while preserving the scale-invariance feature that is indeed observed in real data.

Usual abbreviations

RG : renormalization group
NPRG : nonperturbative renormalization group
MSRDJ : Martin–Siggia–Rose–De Domicis–Janssen
KPZ : Kardar–Parisi–Zhang
PCPD : pair-contact process with diffusion
PCGV : parity conserving generalized voter

Usual notations

d : dimension of space
$\boldsymbol{x} \equiv (\vec{x}, t) \equiv (x, t)$: position and time
q, p : momenta
ω, ν : frequencies
a : microscopic scale (lattice spacing)
Λ : inverse lattice spacing ($\Lambda = 1/a$) or "ultraviolet" cut-off
k : RG momentum scale
$s \equiv \log(k/\Lambda)$: RG time (negative)
$\mathcal{Z}$: partition function
$\mathcal{S}$: microscopic action
Γ : Gibbs free energy or generating functional of the one-particle irreducible correlation functions.

All the hatted variables (for instance $\hat{\phi}$, $\hat{U}$, etc.) are dimensionless.

Short-hand notations

$$\int_{\boldsymbol{x}} \equiv \int_{x,t} \equiv \int \mathrm{d}^d x \, \mathrm{d}t$$

$$\int_{q,\omega} \equiv \left(\frac{1}{2\pi}\right)^{d+1} \int \mathrm{d}^d q \, \mathrm{d}\omega$$

$$\frac{\mathrm{d}f}{\mathrm{d}t} \equiv \partial_t f(t) \equiv \dot{f}(t)$$

Conventions

- We define the Fourier transform of a function f as (using abusively the same name for the function and its Fourier transform):

$$f(q, \omega) = \int_{x,t} f(x, t) \, \mathrm{e}^{-i(qx - \omega t)} \tag{1}$$

- All the Langevin equations are interpreted in the Itō (pre-point) sense.

Chapter I

Scale invariance, universality and renormalization group

Contents

When studying a physical system with many particles[1] far from a phase transition, one can often assume that the particles composing the system are weakly-correlated, and usual statistical physics tools allow us to compute the macroscopic laws of these systems: the law of perfect gases, the law of mass action are examples of this simple behaviour [29]. Adopting a slightly more probabilistic formulation, weakly-correlated particles can be seen as independent stochastic variables, and the fact that simple behaviours arise from very large system is a consequence of the central-limit theorem.

However, in the vicinity of a phase transition[2], the components of a statistical system start to behave in a collective fashion: correlations become non-negligible even at large scale, the

[1] Particles here should be understood as entities describing the system at its smallest scale, it can be individuals if one is interested in studying human or animal group phenomena, or atoms or molecules if one wishes to describe the phase transitions occurring in a liquid, or during a chemical reaction.

[2] In the case of second-order phase transition, that will be our focus in this whole manuscript.

central-limit theorem breaks down and the mean-field predictions become invalid. This theoretical difficulty is also accompanied by surprising facts: critical systems very different in their microscopic description behave similarly at the macroscopic scale. Such a feature – called universality – hints toward some kind of mechanism taking place at criticality that washes out the microscopic details. The second surprising fact is that at criticality, the fluctuations at all length scales of the system adds up in a coherent way, and no intrinsic length scale can be defined. This absence of intrinsic length scale also implies the self-similarity of the system at criticality.

These observations helped Wilson and Kadanoff to design the renormalization group, a theoretical tool that is unavoidable to study generic critical phenomena beyond their mean-field description (for an introduction to the renormalization group and its techniques see for instance [30, 31]). As we will see in this chapter, Wilson and Kadanoff use the scale invariance of the system to coarse-grain the microscopic details and obtain a simplified though correct large scale description of the system. In a sense, the renormalization group procedure generalizes the central-limit theorem for correlated variables [32], which is needed to give a correct description of these systems in the vicinity of a phase transition. In a first part of this chapter, we therefore describe the implementation of the renormalization group, and show how this formalism – although simple in the underlying ideas – explains qualitatively universality and the power-law behaviour that are the signature of second-order phase transitions.

After this rather general introduction, we introduce the nonperturbative renormalization group (NPRG) which is the tool we use throughout this manuscript (for a review, see [14], introductory courses can be found in [33, 34] and [35] is a very clear Ph.D. thesis in french on this matter). The NPRG, introduced by parallel works of Wetterich, Morris and Ellwanger [36–38], follows Wilson and Kadanoff's ideas of coarse-graining, but performs this task using a regulating function. This regulator has a major role in the NPRG context, and justifies the approximations that are made within this formalism. Notice that contrary to the usual perturbative renormalization group, the NPRG approximations do not rely on a series expansion with respect to a small parameter, and therefore depend crucially on this regulating term. We then briefly expose how the NPRG works on the example of the $O(N)$ model and present some usual methods to solve the nonlinear partial differential equations that one has to tackle when using the NPRG.

Finally, we try to review some of the criticisms that the NPRG has often been facing, and explain why many of them are unjustified; it will also be an opportunity to discuss the differences between the perturbative and the nonperturbative methods in order to understand why the usual perturbative approach sometimes breaks down and could be efficiently replaced by its nonperturbative counterpart.

I.1 Scale invariance and phase transitions

I.1.1 Phase transitions

I.1.1.a What is a phase transition?

A phase transition occurs when a small change of some external conditions (for instance the temperature, the pressure, an external magnetic field) induces a major change in some properties of the system. The simplest examples, usually known as phase changes, are familiar to anyone: it is for instance the freezing of water when placed below 0°C, or its vaporization when boiled above 100°C. These two examples are however called first-order phase transitions, while we will be interested in this manuscript only with second-order phase transitions.

The reason for this segregation is simple: in a first-order phase transition the two phases (for instance the boiling liquid water and its vapor) coexist at the transition point and the system is heterogeneous since all parts of the system do not undergo the transition at the same time (see Fig. I.1 for an illustration). In particular, the correlations between two particles of the

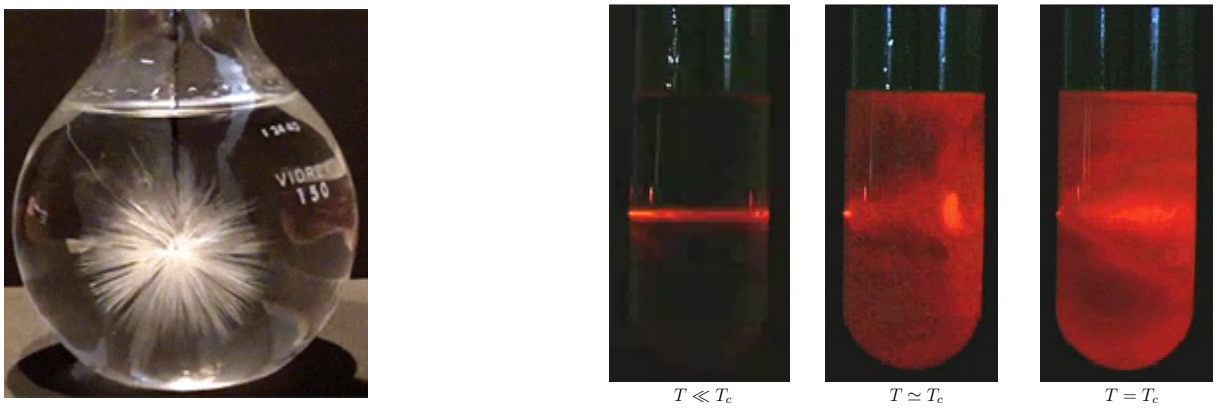

Figure I.1 – ***Left.*** *Ice formation from a seed in supercooled water. The transition is of first-order and one observes the coexistence of the two phases, ice and liquid water. Picture from [39].* ***Right.*** *Pictures of a laser beam shining through a test tube that contains a liquid near its critical temperature T_c. At $T = T_c$ the density fluctuations are very large in the system and cause a scattering of the light (critical opalescence). These large fluctuations are the signature of the second-order phase transition that occurs at $T = T_c$. From [40].*

system always remain finite. In the case of a second-order phase transition on the other hand, this correlation length diverges, meaning that all scales are contributing to the criticality and particles arbitrarily far apart are correlated. Paradoxically, we will see that this divergence of the correlation length allows for drastic simplifications when considering these systems since it reflects the fact that the microscopic details are washed out at criticality.

Examples of systems displaying a second-order phase transition are numerous: it is the case for instance of the liquid/gas phase transition at the critical point. In this example, the critical opalescence is the signature of fluctuations occurring at all scales and causing a scattering of light (see Fig. I.1 for an illustration). The ferromagnetic phase transition is also a classical example: below its critical temperature, the Curie point, a ferromagnetic material has a nonvanishing magnetization and acts as a magnet. When the temperature is raised above this critical value, the property of having a global ferromagnetic order is lost. The Ising model, which was first used to describe this transition, has become particularly famous in the physics of phase transitions, and will be used later on to introduce the renormalization group formalism.

As a teaser for the following of this manuscript, let us remark that out-of-equilibrium systems can also undergo phase transitions. Take the example of a toy-model for the spreading of epidemics: if the disease is very contagious, a large number of individuals in the population will soon be infected, the system is in an "active phase". On the other hand, if people recovers easily from the disease (or if the disease is not very contagious), the disease will soon be eradicated, the system is in the "absorbing phase". Notice that some out-of-equilibrium systems may become critical without fine-tuning of any parameter. In this case it would be abusive to refer to it as a phase transition (since the system does not slip from one phase to the other), but the same formalism can be used to understand these critical systems. It is the case of an erosion model presented in Chap. IV.

I.1.1.b The Ising model

In the following we focus on second-order phase transitions, and for concreteness we describe – at least in the beginning – this kind of transitions using the famous Ising model, which can be seen as a toy-model for the description of a magnetic material near the Curie point. To set the notations, we recall briefly the definition of the Ising model: at each point of a lattice in d dimensions is placed a spin S_i which can be either up or down ($S_i = 1$ or $S_i = 0$). Each spin

interacts with its nearest neighbours according to the Hamiltonian:

$$H[S_i, S_j] = -J \sum_{\langle i,j \rangle} S_i S_j \tag{I.1}$$

where $\langle i, j \rangle$ indicates that the sum is performed over the nearest neighbours and $J > 0$ is the strength of the interaction between two spins that energetically favours the spins pointing in the same direction.

At low temperatures, the system tries to minimize its energy, which means that neighbouring spins have a tendency to align with each other: there exists a global order and the system displays a nonvanishing magnetization. As the temperature increases, the spins are allowed to explore more states and they are less and less inclined to follow their neighbours. Above the critical temperature T_c, the global order is lost and the magnetization vanishes.

To describe accurately the phase transition that occurs at the Curie temperature T_c, we define the average magnetization per spin $M = L^{-d} \langle \sum_i S_i \rangle$, where L^d is the volume of the d-dimensional system, and M is called the order parameter of this system. An order parameter describes the state of the system: it vanishes in the disordered phase, and has a nonzero value in the ordered phase. Notice that here and in the following the average $\langle \cdot \rangle$ is an ensemble average made over realizations of the statistical system.

I.1.2 Universality in the second-order phase transitions

I.1.2.a Universality and critical exponents

The first important point to underline when studying continuous phase transitions is the emergence of universality. Intuitively, universality is the fact that near a phase transition, systems that may be *microscopically* very different act in a similar way because their collective behaviour at the critical point has washed out the microscopic details.

To be more specific in our description of universality, we need to be able to characterize the behaviour of a system near its critical point. As explained in the introduction, critical systems display a scaling behaviour, meaning that some of their properties display a power-law behaviour near the critical point, characterized by critical exponents. For instance, in the case of the Ising model, the magnetization has a power-law behaviour

$$M \underset{T \to T_c}{\sim} |T - T_c|^{\beta} \tag{I.2}$$

near the critical point and this defines a first critical exponent β[3] [29]. Other critical exponents that characterize the system near its critical point can be defined (see below).

A given set of critical exponents defines a universality class[4], which gathers all the systems that display the same critical behaviour. Quite naturally, because microscopic details play a limited role at the transition, most of fluids (independently of their composition) display the same set of exponents when they undergo a liquid/gas transition, and therefore belong to the same universality class. More surprisingly, the ferromagnetic transition at the Curie temperature also belong to this class, and the same holds true for the liquid/liquid demixion transition. In fact, the Ising model that we just presented, despite its simplicity, also belongs to the same universality class. Because it is minimalist and because it is the simplest model in this class, it is referred to as the Ising universality class.

[3] In this formula β denotes of course not the inverse temperature $1/k_B T$ but a critical exponent.

[4] This is not fully correct, in fact a universality class is defined by a set of critical exponents and scaling functions. For instance, in the Kardar-Parisi-Zhang model, one can identify two different universality classes (depending on the initial conditions) which differ by their scaling functions, although they have the same set of critical exponents [41].

I.1.2.b Order parameter and symmetries

In the example of the Ising model, we have seen that the phase transition is described by the order parameter, the magnetization M, which vanishes in the disordered (high-temperature) phase, and has a nontrivial value in the ordered (low-temperature) phase. The Ising model possesses a $\mathbb{Z}_2$ symmetry[5], that is, remains invariant if all the spins are flipped: $\{S_i\} \to \{-S_i\}$. The first point to notice is that the symmetry of the Ising model is *broken* in the ordered phase since the system acquires a nonvanishing magnetization. This *spontaneous symmetry breaking* that occurs at the critical point under the effect of a collective behaviour of the particles, has in fact far-reaching consequences: in high energy physics for instance, the Brout-Englert-Higgs mechanism [42, 43], that explains how particles acquire a mass, relies on a spontaneous symmetry breaking mechanism.

The symmetries of the order parameter (and of the Hamiltonian) therefore plays an important role for the critical properties of the system, and its belonging to a given universality class is mainly determined by symmetries, dimensionality and the range of the interactions between particles [29]. Landau's early description of phase transitions was therefore mainly based on symmetry considerations [44], and proved useful to give a description of the phenomenon at the mean-field level.

Beyond this mean-field description, symmetry considerations still are of paramount importance and constructing Hamiltonians that respect the symmetries of the system is capital. As an example, the "ϕ^4-model", involving a scalar order parameter ϕ and the following Hamiltonian:

$$H = \frac{1}{k_B T} \int \mathrm{d}^d x \left[\frac{1}{2} (\nabla \phi(x))^2 + \frac{r}{2} \phi^2 + \frac{g}{4!} \phi^4 \right] \tag{I.3}$$

also belongs to the Ising universality class and the Hamiltonian obeys a $\mathbb{Z}_2$ symmetry. Consequently, the study of phase transitions is often performed on a simplified model (the ϕ^4-model for instance is simpler to manipulate in the renormalization group context than the discrete Ising model) that respects the symmetries of the original model while neglecting microscopic features that are not relevant at the critical point for the universal quantities.

Symmetry considerations are usually the starting point for the construction of a model to describe a given physical system: once the order parameter is identified and the group $\mathcal{G}$ under which the system remains invariant has been established, one then builds a Hamiltonian that respects these symmetries and is invariant under the same group $\mathcal{G}$. The phase transition, which corresponds to a symmetry breaking, means that the order parameter in the ordered phase is invariant under the transformations of a subgroup of $\mathcal{G}$, even though the Hamiltonian itself remains invariant under the full group $\mathcal{G}$ [29].

Notice finally that the order parameter may not be a scalar but a vector: it is the case of the $O(N)$ model in which the field ϕ in the Hamiltonian (I.3) is replaced by a vector $\vec{\phi}$ with N components. Consequently, the Hamiltonian is invariant under the transformations of the orthogonal group $O(N)$ in N dimensions [31]. The $O(N)$ models have been extensively studied in the literature for they are relatively simple and have been the starting point of many renormalization group studies [30, 31], and also because they capture interesting physical models. For instance, the $O(2)$ [or $U(1)$] model is used to describe the breaking of the $U(1)$ symmetry in superfluid helium, and some phase transitions in liquid crystals are also captured by the $O(2)$ model [29].

I.1.2.c Correlation length

Another important notion when studying a continuous phase transition is the correlation length ξ, which we already alluded to, and which measures the typical length scale of correlations in the

[5] In addition to an invariance under time reversal, time translation, and spatial rotations and translations.

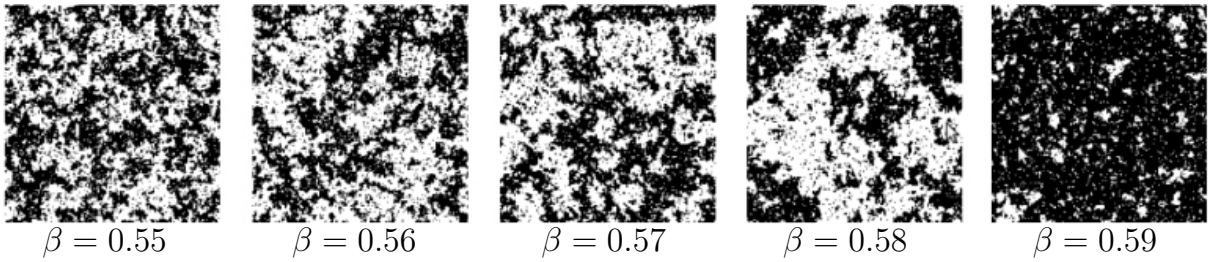

Figure I.2 – *Numerical simulation of the 2d Ising model from [45] for different inverse temperatures $\beta = 1/k_B T$. Up spins are in black and down spins in white. The critical (inverse) temperature is $\beta_c \simeq 0.586$. The correlation length ξ is the typical size of the Ising clusters (spins pointing in the same direction).*

system. For instance, in the case of the Ising model, the correlation length will be the typical size of a cluster of spins pointing in the same direction[6] (see Fig. I.2). Formally, the correlation length is defined via the spin-spin correlation function in the following way:

$$\langle S_i S_j \rangle \underset{r\to\infty}{\sim} \mathrm{e}^{-r_{ij}/\xi} \tag{I.4}$$

where r_{ij} is the distance between the spins i and j.

As the spin system gets closer to the critical point $T = T_c$, the size of the Ising clusters (clusters where all spins have the same orientation) grows more and more and the correlation length diverges as a power law:

$$\xi \sim |T - T_c|^{-\nu} \tag{I.5}$$

where ν is a second universal critical exponent. The fact that the correlation length diverges has far-reaching consequences. First, it means that the number of spins that have a collective behaviour is infinite. At $T = T_c$, there are thus percolating clusters of spins pointing in the same direction. Second, it means that besides the microscopic scale a (in the Ising case, the distance between two neighbouring spins on the lattice) which does not play a role anymore at criticality, the only other length scale is the correlation length ξ, which diverges. It means that there is no intrinsic length scale at criticality and the system becomes scale invariant, a characteristic feature that will be of paramount importance in the whole manuscript.

I.2 Renormalization group

Studying continuous phase transitions is a difficult task and requires new tools to tackle large number of correlated variables. This new tool is the renormalization group (RG), which relies on the scale invariance that arise at criticality, and that we will use throughout this manuscript to study critical phenomena.

I.2.1 Integrating the microscopic degrees of freedom step by step

I.2.1.a Kadanoff's block spin

In 1966, Kadanoff proposed to decrease in a systematic way the number of degrees of freedom of a critical system through the use of block-spin variables [3]. His idea is to describe the large-distance physics as aggregates of components at shorter distances. This simple yet powerful

[6] This picture, although true in $d = 2$, is not fully correct and requires some comments. In $d = 3$ for instance, the Ising clusters are percolating at a temperature $T_p < T_c$. One must in fact consider a subset of these Ising clusters, the Fortuin-Kasteleyn clusters, to have a percolation transition that coincides with the Ising phase transition at T_c [46].

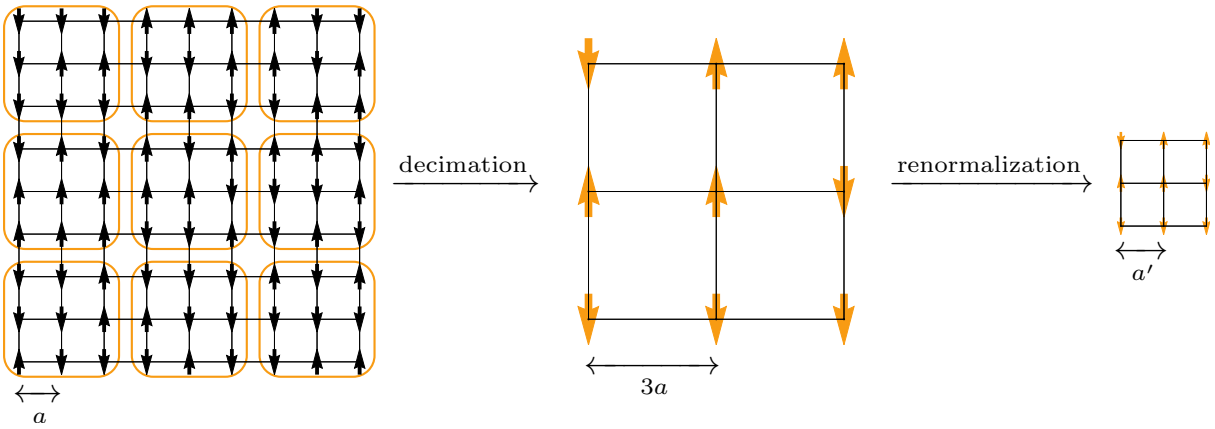

Figure I.3 – *Kadanoff's decimation and renormalization procedures on the two-dimensional Ising model. In a first step* ***(left)*** *the microscopic degrees of freedom (spins) are grouped in blocks (orange rounded squares). Each block-spin defines a new spin variable on a new lattice with four times less variables* ***(middle)****. This is the decimation. Notice that lattice spacing is twice as big as the original spacing a. The second step of the procedure, the renormalization, consists in rescaling all length with the new lattice spacing $a' = 3a$, such that the new lattice is identical to the original, except that the number of spins has been reduced by coarse-graining* ***(right)****.*

thought is the precursor of the renormalization group and is quite illuminating to understand the mechanism of second-order phase transitions. Let us describe this procedure in the case of the Ising model on a two-dimensional square lattice.

The partition function which describes the system is written as:

$$\mathcal{Z} = \sum_{\{S_i\}} \mathrm{e}^{-\beta H[S_i,S_j]} \tag{I.6}$$

where H is the Hamiltonian defined in Eq. (I.1), $\beta = 1/k_B T$ is the inverse temperature and the sum runs over all possible spin configurations. The difficulty of computing this partition function stems from the fact that the sum runs over infinitely many spins correlated to each other via a nearest neighbour interaction. Kadanoff's procedure consists in reducing the number of degrees of freedom by partitioning the lattice in blocks of 9 spins, and then assigning to each of these blocks a "block spin" variable S'_i (see Fig. I.3 for illustration). Each of these coarse-grained variables is of the same nature as the original microscopic spin, and its value is for example given by a majority rule from the values of the S_i. This step, called "decimation", reduces the number of microscopic degrees of freedom as desired.

However, the distance between each block after decimation is now twice the original lattice spacing $3a$, whereas it was a in the original microscopic configuration. Since the idea is to obtain a system which is a similar yet coarse-grained version of the previous one, we now redefine a new lattice spacing $a' = 3a$. This second step – a rescaling of the length scale – is called "renormalization". The combination of a decimation and a renormalization of the length scale is called a RG step.

One now computes the new Hamiltonian $H'[S'_i, S'_j]$ describing the interactions between block-spin variables[7]. Performing more and more of these decimation and renormalization steps, one obtains a family $\{H \to H' \to H'' \to \cdots\}$ of Hamiltonians which describe the system at a more and more coarse-grained level, although they all describe the same macroscopic thermodynamical system. This sequence of Hamiltonians is often referred to as a flow of Hamiltonians.

[7]Notice that $H'[S'_i, S'_j] \neq H[S_i, S_j]$ and is in fact much more complicated. Approximations will have to be made in order to use this procedure in a practical scheme.

Notice that we have achieved what we wanted: reducing step by step the microscopic degrees of freedom while keeping the same long-range description.

At criticality (and at a sufficiently coarse-grained scale), the scale invariance of the system implies that the flow of Hamiltonians converges to a fixed point H^* such that $(H^*)' = H^*$. It means that changing the scale of description of the system does not affect its behaviour any more, the system looks the same and the interactions between the new block-spin variables remain the same after the coarse-graining procedure.

I.2.1.b Decimation in continuous space

Before describing in more details the physical consequences of scale invariance and its implementation through the renormalization group, let us now describe RG transformations for more general systems. We adopt the language of field theory, and assume that our system is described by a partition function $\mathcal{Z}$:

$$\mathcal{Z} = \int \mathcal{D}\phi(x)\, \mathrm{e}^{-\mathcal{S}[\phi(x)]} \tag{I.7}$$

where $\mathcal{S} = \beta H[\phi(x)]$ is the action of the microscopic system and $\phi(x)$ is a scalar field describing the state of the system at position x. The sum over all possible spin configurations has been trade for a functional integral over all possible values of the field. Notice that, in the previous section, we could have chosen to compute the block-spin variables as an average over the previous ones rather than via a majority rule. Doing so, we would have lost the fact that our system remains an Ising spin system; on the other hand, after a few iterations the new "spins" variables would acquire a quasi-continuous range of value and a field description as Eq. (I.7) would have been justified. The formulation of the models in terms of a path integral will be the starting point of our RG studies in the following of the manuscript.

The idea of the renormalization group to study such a system near criticality is to perform the integration appearing in the previous definition only for the small (microscopic) length scale, such that we can rewrite the partition function as:

$$\mathcal{Z} = \int \mathcal{D}\phi(x > \ell a)\, \mathrm{e}^{-\mathcal{S}'[\phi(x>\ell a)]} \tag{I.8}$$

with

$$\mathrm{e}^{-\mathcal{S}'([\phi(x>\ell a)]} = \int \mathcal{D}\phi(x < \ell a)\, \mathrm{e}^{-\mathcal{S}[\phi(x)]}\,, \tag{I.9}$$

where ℓ is the rescaling factor and a is the smallest length scale of the system (the lattice spacing in the Ising model). Formally, one can thus write $\mathcal{R}(\mathcal{S}, \ell) = \mathcal{S}'$ with $\mathcal{R}(\cdot, \ell)$ an operator mapping the original action $\mathcal{S}$ to its coarse-grained version $\mathcal{S}'$. The mapping of $\mathcal{S}$ into $\mathcal{S}'$ is called a RG step, and the evolution $\mathcal{S} \to \mathcal{S}' \to \mathcal{S}'' \to \cdots$ is called a RG flow. Obviously, performing two successive coarse-graining of scale $\ell_1 a$ then $\ell_2 a$, or performing a single operation of scale $(\ell_1 \times \ell_2)a$ is equivalent, such that this procedure indeed has a semi-group structure:

$$\mathcal{R}\left(\mathcal{R}(\mathcal{S}, \ell_1), \ell_2\right) = \mathcal{R}(\mathcal{S}, \ell_1 \times \ell_2) \tag{I.10}$$

and this semi-group structure highlights the scale-invariant behaviour of the system. Indeed, right at the phase transition, the system is truly scale invariant since the only length scale – the correlation length ξ – diverges, which means that the system displays the same behaviour regardless the scale at which it is observed. It means that the critical action $\mathcal{S}^*$ must be a fixed point of the RG transformation:

$$\mathcal{R}(\mathcal{S}^*, \ell) = \mathcal{S}^*\,. \tag{I.11}$$

Notice at this point that if one were able to compute exactly $\mathcal{S}'$ from $\mathcal{S}$, then one could also compute exactly the partition function $\mathcal{Z}$, and the model would be integrable. Therefore, for the moment, the RG has not simplified the problem since one still has to perform the highly difficult functional integration Eq. (I.9). The power of the renormalization group will become clear when we will restrict the functional form of the successive actions: instead of considering a functional dynamical system, we will consider a function dynamical system, or even a dynamical system over a finite number of real variables. In the next section we will explain why the RG method already gives us highlights on which interactions can be neglected when studying a given phase transition, and how we can use this information to perform drastic approximations.

I.2.2 Universality seen by the renormalization group

I.2.2.a Renormalization group flow

As we have seen in previous parts, a RG transform modifies the length scale of the system $a \to \ell a \to \ell^2 a \to \cdots$, with $\ell > 1$ ($\ell = 3$ in the case of the block-spin example), as well as the action itself: $\mathcal{S} \to \mathcal{S}' \to \mathcal{S}'' \to \cdots$. We now write the successive actions in terms of an infinite number of couplings constants $\boldsymbol{K}$. For instance, in the case of the so-called "ϕ^4-model", the initial action reads

$$\mathcal{S} = \int \mathrm{d}^d x \left[\frac{1}{2}(\nabla\phi(x))^2 + \frac{r}{2}\phi^2 + \frac{g}{4!}\phi^4 \right] \tag{I.12}$$

where only two couplings r and g suffice to describe the model: $\mathcal{S}[\phi; K_1 = r, K_2 = g]$. For reasons that will become clearer in the following, the ϕ^4-model also belongs to the Ising universality class, and is therefore the field-theoretical counterpart of the discrete Ising model when one studies this universality class.

Although only two couplings r and g appear in the initial action, after a single RG step infinitely more coupling constants[8] will however be generated and one has $\mathcal{S}' \equiv \mathcal{S}'[\phi; K_1', K_2', K_3' \neq 0, \cdots]$. Therefore, instead of following the flow of actions, we now focus on the flow of the coupling constants $\boldsymbol{K} \to \boldsymbol{K}' \to \cdots$, and we write explicitly the dependence of the coupling constants in the RG dilatation factor: $\boldsymbol{K}_\ell$.

Let us now describe how the coupling constants evolve under an infinitesimal RG step, that is, compare the couplings $\boldsymbol{K}_\ell$ with the couplings $\boldsymbol{K}_{\ell(1+\varepsilon)}$ obtained after an infinitesimal RG transformation. This yields a differential equation that is the starting point of any RG procedure. By definition of the RG operator $\mathcal{R}(\cdot, \ell)$, the change in the coupling constants reads:

$$\boldsymbol{K}_{\ell(1+\varepsilon)} - \boldsymbol{K}_\ell = \mathcal{R}(\boldsymbol{K}_\ell, 1+\varepsilon) - \mathcal{R}(\boldsymbol{K}_\ell, 1) \tag{I.13}$$

where we have used the fact that $\mathcal{R}(\cdot, 1)$ is the identity. We therefore get:

$$\ell \frac{\mathrm{d}\boldsymbol{K}_\ell}{\mathrm{d}\ell} = \frac{\partial \mathcal{R}}{\partial \ell}|_{(\boldsymbol{K}_\ell, 1)} \tag{I.14}$$

and we define the $\boldsymbol{\beta}$ functions as:

$$\boldsymbol{\beta}(\boldsymbol{K}_\ell) = \frac{\partial \mathcal{R}}{\partial \ell}|_{(\boldsymbol{K}_\ell, 1)} \,. \tag{I.15}$$

We are now interested in studying the fixed point $\boldsymbol{K}^*$ and its vicinity. For this purpose we define the infinitesimal variation $\delta\boldsymbol{K} = \boldsymbol{K}_\ell - \boldsymbol{K}^*$. The linearization of the previous equation in the neighbourhood of $\boldsymbol{K}^*$ yields:

$$\ell \frac{\mathrm{d}\,\delta\boldsymbol{K}}{\mathrm{d}\ell} = M\,\delta\boldsymbol{K} \tag{I.16}$$

[8] Constrained however by the symmetries of the system one considers.

where the stability matrix M is defined as:

$$M_{i,j} = \frac{\partial \beta_i}{\partial K_{\ell,j}}|_{\boldsymbol{K}^*} \tag{I.17}$$

and we have used the fact that $\boldsymbol{\beta}(\boldsymbol{K}^*) = 0$ by definition, and $K_{\ell,j}$ is the j^{th} component of $\boldsymbol{K}_\ell$. Although M is in general not symmetric, we assume that it can be diagonalized:

$$M\boldsymbol{e}_i = \lambda_i \boldsymbol{e}_i \tag{I.18}$$

and that its (right) eigenvectors $\{\boldsymbol{e}_i\}$ form a complete basis, such that we can write

$$\delta \boldsymbol{K}_\ell = \sum_i v_i(\ell)\boldsymbol{e}_i \,. \tag{I.19}$$

Inserting the previous relation into the linearized flow near the fixed point, Eq. (I.16), we obtain:

$$\ell \frac{\mathrm{d}v_i(\ell)}{\mathrm{d}\ell} = \lambda_i v_i(\ell) \tag{I.20}$$

which can be integrated as:

$$v_i(\ell) = v_i(1)\ell^{\lambda_i} \,. \tag{I.21}$$

I.2.2.b Relevant and irrelevant coupling constants

From Eq. (I.21), we see that we can classify the eigenvalues λ_i into three categories, depending on their sign[9]:

- if $\lambda_i < 0$, then each RG iteration will make smaller the associated coupling v_i that will eventually go to zero and the coupling constant is thus called *irrelevant* under a RG transform.
- if $\lambda_i > 0$, then the associated coupling constant is called *relevant* under a RG transform. Notice that these relevant coupling constants correspond to unstable directions of the RG fixed point. If one wishes to reach the RG fixed point, all the relevant coupling constants have to be fine-tuned to 0. For instance, the reduced temperature $t = (T - T_c)/T_c$ or an external magnetic field are relevant coupling constants in the Ising model.
- if $\lambda_i = 0$, the associated coupling constant is called *marginal* and one must go to the next order to know its behaviour under a RG transform. Notice that the flow in this direction is slow since it is logarithmic instead of being a power law.

As we will see in the next paragraphs, these categories play an extremely important role in the RG formalism and in the insights we can obtain out of it. Very general considerations about the relevance of the coupling constants will yield universality, critical exponents and scaling behaviour.

I.2.2.c Critical exponents and scaling behaviour

Let us now show why these simple considerations can already explain the scaling behaviour we have described in the previous parts. We use again the example of the Ising model. In this case, there exist two relevant coupling constants: the external field h applied on the system,

[9] The eigenvalues could also be complex, in which case we are interested in the sign of their real part.

and the reduced temperature $t = (T - T_c)/T_c$; both of these parameters have to be fine-tuned to $t = h = 0$ in order to be at criticality.

Let us consider the effect of a RG transform on the correlation length ξ of the Ising model. This correlation length depends on all the coupling constants of the system, and after one RG iteration we get:

$$\xi(t', h', K_3', K_4', \dots) = \frac{1}{\ell}\xi(t, h, K_3, K_4, \dots) \tag{I.22}$$

where the $1/\ell$ in front of the right-hand side of the previous equation accounts for the rescaling (the renormalization) one has to perform during a RG step. In the neighbourhood of the critical point, that is near $t = h = 0$ we can use Eq. (I.21) and write[10]

$$\xi(t', h', K_3', K_4', \cdots) = \xi(t\ell^{\lambda_t}, h\ell^{\lambda_h}, K_3\ell^{-\lambda_3}, K_4\ell^{-\lambda_4}, \dots) = \frac{1}{\ell}\xi(t, h, K_3, K_4, \dots) \tag{I.23}$$

where all the λ_i have been defined to be positive (we recall that all the coupling constants but t and h are irrelevant). We now choose the renormalization parameter $\ell \gg 1$ such that the irrelevant coupling constants become negligible: $K_i\ell^{-\lambda_i} \ll 1$. Choosing furthermore ℓ in order to have $t\ell^{\lambda_t} = 1$ (which is consistent with the initial assumption of being near the critical point, since it means $t \ll 1$, i.e. in the critical regime for the temperature) yields:

$$\xi(t, h, K_3, K_4, \cdots) = t^{-1/\lambda_t}\xi(1, ht^{-\lambda_h/\lambda_t}, 0, 0, \cdots)\,. \tag{I.24}$$

Finally, setting the other relevant coupling to be zero: $h = 0$, we are left with the well-known power-law divergence of the correlation length at criticality, that is:

$$\xi(t, h, K_3, K_4, \cdots) \underset{t\to 0}{\sim} t^{-1/\lambda_t} \tag{I.25}$$

and the critical exponent ν defined above [Eq. (I.5)] is therefore found to be $\nu = 1/\lambda_t$. This corresponds to the leading behaviour of the correlation length as $t \to 0$. A similar proof yields $\beta = (d - \lambda_h)/\lambda_t$ [where the critical exponent β was defined in Eq. (I.2)], and all the critical exponents can in fact be expressed in terms of the two relevant eigenvalues λ_t and λ_h [31].

I.2.2.d Universality classes and critical surface

Let us now describe how universality and the universality classes we have described earlier arise naturally in the formalism of the renormalization group. Since a RG flow takes place in the space of the coupling constants, we define a point in the RG space as an (infinite) set of coupling constants $\boldsymbol{K}$.

Critical surface. Let us first introduce the notion of the critical surface. As stated earlier, a phase transition is characterized by the fact that its correlation length diverges: $\xi = \infty$. This means that if a point $\boldsymbol{K}$ in the RG space is critical (that is such that $\xi = \infty$), then after a RG transform, $\xi' = \xi/\ell = \infty$ and the system remains critical. We define the critical surface as the set of points $\boldsymbol{K}$ such that the correlation length diverges. Notice that in general, it is sufficient to fine-tune a few parameters (for instance the reduced temperature t and the external magnetic field h) to make the system critical. Therefore, in the space of the coupling constants, the critical surface has typically a low co-dimension (one or two). Notice also that if $\boldsymbol{K}$ belongs to the critical surface, then so does $\mathcal{R}(\boldsymbol{K})$: the critical surface is stable under RG transformations.

[10] Notice that in this formula we have assumed that t and h correspond to eigendirections of the RG flow. It is not necessarily the case, and the fact that they are both relevant parameters only means that they have a nonvanishing projection onto the relevant eigenvectors. We ignore this subtlety since it does not play a role for the following discussion.

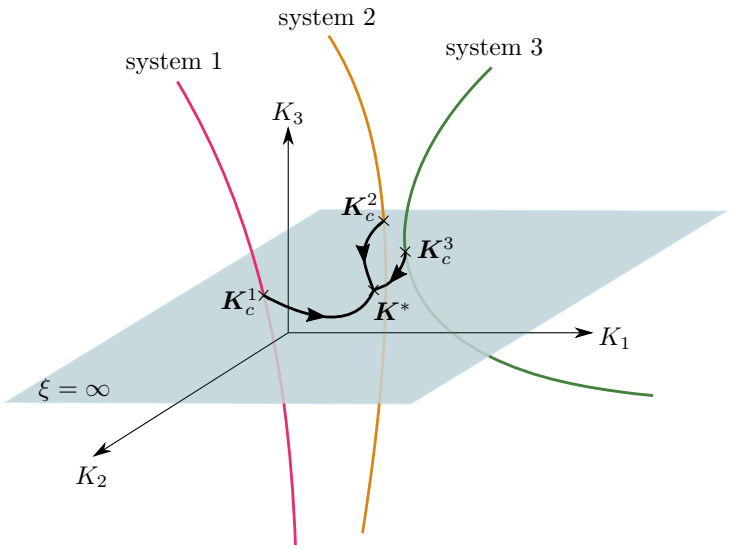

Figure I.4 – *Schematic representation of the coupling space; only three couplings K_1, K_2, K_3 are represented. The critical surface, defined as the hypersurface where the correlation length ξ diverges is represented by the blue plane. We pictured the "trajectory" of three physical systems: these trajectories are the evolution in the coupling space of these systems when a physical parameter (for instance the temperature) is varied. These systems are critical when their physical line crosses the critical surface (at the points $\boldsymbol{K}_c^1$, $\boldsymbol{K}_c^2$, $\boldsymbol{K}_c^3$). The black lines correspond to RG trajectories: under RG transformations, the three trajectories end up at the same fixed point $\boldsymbol{K}^*$. These three systems, although microscopically different (they have different critical temperature for instance), are all described by the same critical behaviour given by the fixed point and its vicinity: they all belong to the same universality class.*

Basin of attraction. We have seen that there exist fixed points of the RG transformations, that belong to the critical surface and that are such that $\boldsymbol{K}^* = \mathcal{R}(\boldsymbol{K}^*)$. If these fixed points are attractive, then all the points in the vicinity of $\boldsymbol{K}^*$ converge to it under RG transformations. The basin of attraction of a given fixed point $\boldsymbol{K}^*$ is then defined as the domain on the critical surface such that the flow of any point on this domain converges to $\boldsymbol{K}^*$.

Universality. Let us now consider a system, described by its *microscopic* coupling constants $\boldsymbol{K}^1$. If this system displays a (second-order) phase transition, it means that one can fine-tune the relevant coupling constants and obtain a set $\boldsymbol{K}_c^1$ of coupling constants which now belongs to the critical surface. Applying RG transformations on $\boldsymbol{K}_c^1$, we reach the fixed point $\boldsymbol{K}^*$, corresponding to the basin of attraction on which sits the physical critical system $\boldsymbol{K}_c^1$.

Let us now consider a second system $\boldsymbol{K}^2$, which differs at the microscopic level with the first one. We can also fine-tune it to its critical point $\boldsymbol{K}_c^2$. Now, although $\boldsymbol{K}_c^2 \neq \boldsymbol{K}_c^1$, if these two systems belong to the same basin of attraction, their respective RG flow converges toward the very same fixed point $\boldsymbol{K}^*$. Since the critical exponents and the critical behaviour in general is prescribed by the fixed point and its vicinity, the two *microscopically* different systems will have the same critical properties. The existence of these fixed points of the RG flow and their associated basin of attraction therefore gives an explanation for the appearance of universality classes to which very different models can belong (see Fig. I.4 for illustration).

The beauty of the RG now starts to become clear: without performing a single calculation, we have already explained (i) the existence of universality classes, regardless of the microscopic details of the system; (ii) the scaling behaviour of thermodynamical quantities in the vicinity of the critical point; (iii) the exact relations between critical exponents[11].

[11] We have not derived the scaling relations between the different critical exponents, but in Sec. I.2.2.c we have

I.2.3 An example: the central-limit theorem seen by the RG

As an illustration of the RG formalism and to explicit slightly the concepts seen above, we focus on the central-limit theorem which is probably the most famous example of universality. Indeed, the central-limit theorem states that the probability distribution of the mean value of n independent random variables with the same distribution $P(x)$ converges to a Gaussian distribution as $n \to \infty$, provided that P decays sufficiently rapidly at large x. Therefore, universality arises here in the sense that the initial distribution P of the "microscopic" variables is washed out and a universal Gaussian distribution arises at the "macroscopic" scale.

To prove this theorem, we follow [31] and use a RG approach, that is we use the decimation and renormalization procedure as explained earlier. For this purpose, we consider that there are initially $n = 2^m$ independent variables. We then proceed to the decimation of the variables by averaging recursively over pair of variables, and therefore decreasing the number of variables by a factor 2 at each iteration. To perform this decimation, we recall that the distribution of the sum of two independent random variables with the same distribution P is given by the transformation:

$$[\mathcal{R}P](x) = \int \mathrm{d}y\, P(y)P(x-y) \tag{I.26}$$

and we introduce a renormalization of this sum depending on the parameter λ such that

$$[\mathcal{R}_\lambda P](x) = \lambda \int \mathrm{d}y\, P(y)P(\lambda x - y)\,, \tag{I.27}$$

where $\lambda = 1$ corresponds to the sum, and $\lambda = 2$ to the mean of the initial variables. Using the Fourier transform defined in Eq. (1) and after a few calculations we get:

$$[\mathcal{R}_\lambda P](q) = P^2(q/\lambda)\,, \tag{I.28}$$

where we have kept the same name for $P(x)$ and its Fourier transform $P(q)$. In terms of the generating function of the cumulants, $w(q) = \log P(q)$, the last equality can be rewritten in a simpler, linear form:

$$[\mathcal{R}_\lambda w](q) = 2w(q/\lambda)\,. \tag{I.29}$$

Our goal is now to study the properties of the iterated transformation $\mathcal{R}_\lambda^m$ as $m \to \infty$. We assume that there exists a limiting distribution and therefore a fixed point of the transformation, that we write $w^*(q)$ and which verifies:

$$[\mathcal{R}_\lambda w^*](q) = w^*(q) = 2w^*(q/\lambda)\,. \tag{I.30}$$

Then we define the cumulants expansion of w^* as:

$$w^*(q) = -iw_1 q - \frac{1}{2}w_2 q^2 + \sum_{j=3} \frac{(-iq)^j}{j!} w_j \tag{I.31}$$

where the w_j are the cumulants ($w_1 = \langle x \rangle$ is the mean, $w_2 = \langle x^2 \rangle - \langle x \rangle^2$ is the variance, etc.), and $w_0 = 0$ by definition of w and by conservation of the probability ($P(q=0) = 1$). If we furthermore assume that the limiting distribution w^* is centred[12] (that is $w_1 = 0$), then identifying the q^2 term in Eq. (I.30) yields:

$$w_2 = \frac{2w_2}{\lambda^2} \tag{I.32}$$

seen that amongst the critical exponents, two only can be independent since there are only two relevant eigenvalues. It therefore exists scaling laws that link the critical exponents to each other [30, 33].

[12] The case of a non-centred distribution is also rather simple and is discussed in [31].

which means $\lambda = \sqrt{2}$ and this implies that all the other w_j must vanish. One can therefore perform an inverse Fourier transform to deduce the limiting probability distribution:

$$P^*(x) = \frac{1}{2\pi}\int \mathrm{d}q\, \mathrm{e}^{iqx - w_2 q^2/2} = \frac{1}{\sqrt{2\pi w_2}} \mathrm{e}^{-x^2/2w_2}\,, \tag{I.33}$$

which is indeed a Gaussian distribution, as expected from the central-limit theorem. We can also study the fixed-point stability by perturbing the fixed-point solution: $w(q) = w^*(q) + \delta w(q)$. It yields eigenvectors of the form $\delta w(q) = q^\alpha$ with eigenvalues $\sigma = 2^{1-\alpha/2}$, and therefore the following possibilities:

(i) $\alpha = 1 \Rightarrow \sigma = \sqrt{2} > 1$ which is an unstable direction since the corresponding eigenvector will diverge as $m \to \infty$. It is therefore a *relevant* perturbation in the RG language. Indeed, if $\alpha = 1$, the perturbation is linear in q which violates the centred condition $w_1 = 0$ that we assumed for the proof.

(ii) $\alpha = 2 \Rightarrow \sigma = 1$ is a marginal perturbation which only modifies the value of w_2.

(iii) $\alpha > 2 \Rightarrow \sigma < 1$ are irrelevant perturbations and their amplitudes go to 0 as $m \to \infty$.

I.3 The nonperturbative renormalization group

I.3.1 Exact renormalization group equation for the action

We describe in this section the ideas of the nonperturbative renormalization group (NPRG) and show how it can be used to study critical phenomena on a relatively simple example. As its denomination indicates, the NPRG follows very closely the RG ideas of Wilson and Kadanoff that we introduced in the previous section. However, and contrary to its perturbative counterpart, we will see that it calls upon approximations that are not Taylor expansions in terms of a small coupling constant, and is nonperturbative in this sense. However, the systems that we will be studying are far beyond the reach of exact methods, and the NPRG also resorts to approximation schemes. More details about the NPRG can also be found on the pedagogical reviews [33, 34], or on a more exhaustive one [14], or also on a thesis in french [35].

Before giving the modern implementation of the NPRG, which was formulated in parallel works of Wetterich, Morris and Ellwanger [36–38], we give a brief overview of its original formulations. These earlier formulations follow the ideas of the decimation in continuous space as described previously and translate it into a differential equation over the renormalization scale.

Because the equations we will derive in the following acquire a simpler form in Fourier space, we now switch to these variables, and define the Fourier transform of a function according to the convention Eq. (1). In particular, we now describe a RG transform in terms of the momentum scale $k = 1/(\ell a)$ and define the slow modes $\phi_< \equiv \phi(|q| < k)$ and the rapid modes $\phi_> \equiv \phi(|q| > k)$ accordingly. With this notation, we will now follow a flow of actions $\mathcal{S}_k$, evolving from the microscopic scale $k = \Lambda = 1/a$ down to the macroscopic scale $k = 0$.

In fact, this evolution between $k = \Lambda$ and $k = 0$ can be stated in terms of an *exact* differential equation over k by computing how the action $\mathcal{S}_k$ is modified by an infinitesimal change of the RG scale $\mathrm{d}k$. In its original version, this equation was derived by Wegner and Houghton [47] in the case where all the (slow) modes of scale $|q| < k$ were left untouched, whereas all the (rapid) modes with $|q| > k$ were integrated over; such a separation between the modes is called a "sharp cut-off", and we will see in the following that more sophisticated separation between the rapid and slow modes can be performed.

In fact, the problem of such a sharp cut-off is that it leaves no latitude for controlling the approximations that are made on the action $\mathcal{S}_k$ in order to find its fixed point; in addition, this kind of cut-off yields singularities in the flow of the actions $\mathcal{S}_k$, making it unusable in practice, but for the simplest approximation schemes. An alternative equation was then derived

by Polchinski [48] involving a smoother cut-off function. Instead of a sharp separation between slow and rapid modes, he introduced a cut-off function $K_k(q)$ separating smoothly the modes around scale k during the decimation procedure. An exact differential equation for the action $\mathcal{S}_k$, known as the Wilson-Polchinski equation was therefore derived, involving the cut-off function and its derivatives [48]. The Wilson-Polchinski flow equation is exact and contains all the physics of the model. However, written as such in terms of the action $\mathcal{S}_k$, this equation deals with very abstract objects, on which little physical insight can be expected in order to make sensible approximations. Indeed, the action $\mathcal{S}_k$ is a functional of the slow mode fields $\phi_<$, which are *not* the precursors of the order parameter (the magnetization), since there is still a path integral to perform. It is also a difficult task to extract the long-distance physics from the sequence of $\mathcal{S}_k$, which only describes the interactions between the slow modes, but in no case describes the thermodynamical properties of the system at scale k [33].

Since the physical thermodynamics properties of the system are rather encoded in the order parameter, and in the correlation functions (the moments of the probability distribution), it is much more convenient to work with the precursors of these objects, that is the precursor of the order parameter $\psi = \langle\phi\rangle$, and the precursor of the one-particle irreducible correlation functions, the Gibbs free energy Γ. This will be the task of the nonperturbative renormalization group (NPRG), which we introduce in the following section.

I.3.2 The effective average action method

Before introducing the NPRG formalism in details, let us summarize the ideas behind this formulation and which are refinements of the ideas already introduced in the previous approaches by Polchinski, Wegner and Houghton, Wilson and Kadanoff. (i) The integration over the fluctuations (over the microscopic degrees of freedom) appearing in the partition function will be performed step by step, or more precisely momentum shell by momentum shell, following the idea of the decimation of the degrees of freedom as proposed by Wilson and Kadanoff. (ii) This step-by-step integration allows for a reformulation of the complicated problem of computing path integrals with non-Gaussian weights for a (also complicated) problem of computing a functional partial differential equation, on which we will be able to perform controlled approximations in order to make the differential equation tractable. (iii) The separation between the rapid and slow modes will be performed in a subtle way by distorting the partition function and adding a regulator term to the action, as it is the case in the Wilson-Polchinski approach. As we will see in the following, this regulator plays a capital role in the justification of the approximations. (iv) Last but not least, the object of interest on which will be stated the exact renormalization flow equation is the effective average action Γ_k (a precursor of the Gibbs free energy Γ), a thermodynamical object on which one can have much more physical intuition than on the flow of actions in the case of the Wilson-Polchinski approach.

I.3.2.a The regulator

The whole idea of the RG is to integrate the fluctuations momentum scale by momentum scale. The NPRG keeps this idea and improves it by introducing a regulator term $\Delta\mathcal{S}_k$ in the partition function:

$$\mathcal{Z}_k[J] = \int \mathcal{D}\phi \, \mathrm{e}^{-\mathcal{S}[\phi]-\Delta\mathcal{S}_k[\phi]+\int_q J(q)\phi(-q)} \tag{I.34}$$

whose role is reminiscent of Wilson and Kadanoff's ideas to create a separation between the slow and rapid modes. Notice also that we add a source term $J(q)$ coupled linearly to the order parameter $\phi(-q)$ and that allows for the computation of the correlation functions.

In the NPRG context, the role of the regulator is to freeze the fluctuations at scale smaller than k. This is made possible by giving to $\Delta\mathcal{S}_k$ the shape of a "mass term", i.e. by writing it as:

$$\Delta\mathcal{S}_k[\phi] = \int_q \phi(q) R_k(q) \phi(-q)\,. \tag{I.35}$$

To understand why such a term can indeed play the role of a regulator and freeze the fluctuations at large length scale (i.e. at $|q| < k$), let us give an intuitive explanation. More explanations about the regulator will be given in a following section. Think of the Ginzburg-Landau approach to a phase transition [29]: in this case the description of the phase transition is done by assuming that the thermodynamic potential for the magnetization is given by:

$$\Gamma[\psi] = \int \mathrm{d}^d x \left[\frac{1}{2}(\nabla\psi)^2 + \frac{r}{2}\psi^2 + \frac{g}{4!}\psi^4\right] \tag{I.36}$$

where Γ is the Legendre transform of $\mathcal{W} = \log\mathcal{Z}$, defined as: $\Gamma[\psi] + \mathcal{W}[J] = \int_q J\psi$ (more details are given in the following). In this mean-field description, the temperature appears as $r \propto T - T_c^{\mathrm{MF}}$[13] in factor of the ψ^2 term, and therefore a vanishing factor in front of ψ^2 means that the system is critical (at the mean-field level). Adding a regulator term (I.35) also proportional to ψ^2 therefore modifies the temperature of the system and its distance to criticality. Within the RG formalism, the story is slightly different since the coupling r starts "running", that is, becomes dependent on the RG scale k: $r = r(k)$, but still characterizes the distance to criticality (at scale k). In particular, if $r(k = 0) = 0$, the non-regularized system is critical. Therefore, adding the regulator R_k and choosing it large for $|q| < k$ will in practice freeze the fluctuations of the modes with $|q| < k$, since the regulator places these fields with $|q| < k$ away from criticality, that is gives them a very large temperature such that they can be treated as non-fluctuating (or mean-field) fields.

In the language of quantum field theory, the term in factor of ψ^2 is the mass, and a massive particle interacts at a short range with other particles. The regulator can be seen in this case as an extra "mass term" which adds a large mass to the modes of the fields with $|q| < k$. The interaction of these particles with the others can thus be neglected: the fluctuations of these modes are frozen.

Now that we have some intuition about the regulator term $R_k(q)$, let us summarize the characteristics it must have. (i) The regulator must be large for $|q| < k$ in order to freeze the fluctuations at scale smaller than k. In particular, at $k = \Lambda$, *all* the fluctuations must be frozen, such that the model is described by its microscopic action. (ii) It should leave (almost) unaltered the fluctuations at scale $|q| > k$ since we want to compute these fluctuations. In particular, when $k = 0$, all fluctuations are integrated, which means $R_{k=0}(q) \equiv 0$. (iii) The regulator term $R_k(q)$ must have some regularity (at least be continuous), because we will see later that its derivatives play a role in the exact differential flow equation. From the points (i) and (ii) we deduce the following limits for the regulator:

$$\begin{cases} R_k(q) & \xrightarrow[k\to\Lambda]{} \infty \\ R_k(q) & \xrightarrow[k\to 0]{} 0\,. \end{cases} \tag{I.37}$$

Let us introduce two regulators that are commonly used in the NPRG context. The Θ-regulator [49]:

$$R_k^{\Theta}(q) = (k^2 - q^2)\Theta(k^2 - q^2)\,, \tag{I.38}$$

[13] Notice that the mean-field critical temperature T_c^{MF} is not equal to the actual critical temperature of the system, T_c. In practice, the fluctuations (that are neglected in the mean-field approximation) have a tendency to destabilize the system, such that the system remains in the ordered phase at a lower temperature than the one expected from the mean-field theory: $T_c < T_c^{\mathrm{MF}}$.

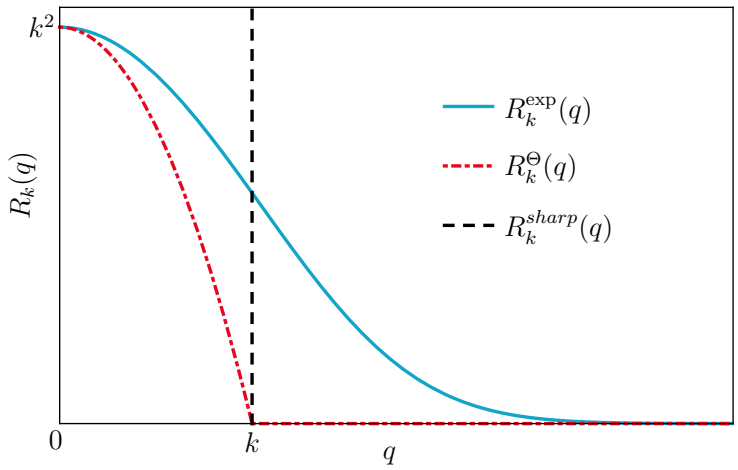

Figure I.5 – *Shape of the different regulator functions defined in Eqs.* (I.38) *and* (I.39)*. The sharp regulator* $R_k^{\text{sharp}}(q) = k^2(1/\Theta(q^2 - k^2) - 1)$ *can be seen as the old way to separate the slow and rapid modes as thought initially by Wilson.*

where $\Theta(q)$ is the Heavyside step-function ($\Theta(q < 0) = 0$ and $\Theta(q \geq 0) = 1$). This regulator is quite convenient (especially at the lowest order approximations) since it allows for analytical computations of the momentum integral in the RG flow Eq. (I.43). However, the presence of the step function yields singular contributions when higher-order approximation schemes are used [50]. The second commonly-used regulator is known as the "exponential" regulator:

$$R_k^{\exp}(q) = \frac{q^2}{\mathrm{e}^{q^2/k^2} - 1}\,, \tag{I.39}$$

which is more regular than the Θ-regulator, and therefore more versatile. However, it does not permit analytical computation of the momentum integral in the RG flow and they have to be computed numerically. The shape of these two regulators is displayed on Fig. I.5, and a comparison of these regulators is given in Sec. I.4.3.b.

Let us make several comments about the regulator term we have just introduced. Notice that adding the extra term $\Delta\mathcal{S}_k$ means that we have distorted the initial partition function $\mathcal{Z}$ into a one-parameter family of scale-dependent partition functions $\mathcal{Z}_k$. This family of partition functions interpolates smoothly between the mean-field scale $k = \Lambda$ where the physics is (usually) simple, and the macroscopic scale $k = 0$ where fluctuations play a major role and make the problem difficult to solve.

Although it might seem we are giving ourselves more objects to compute (all the k-family of partition functions), we will see that this formulation allows us to write down the evolution of the system when we add a little more fluctuations to it, i.e., when we go from the scale k to the scale $k - \mathrm{d}k$: we will be able to derive a differential equation over the scale k and that will be our task in the following. Even more crucially, we will see in the following that the regulator is the cornerstone of the NPRG formalism since it justifies the approximation schemes that are used. Indeed, because the NPRG does not rely on a series expansion with respect to a small parameter, the regulator ensures that the approximations made are controlled.

I.3.2.b The effective average action

As stated before, the partition functions $\mathcal{Z}_k$ are extremely abstract and complicated objects, since they involve a path integral and because the physics of the system cannot be simply extracted from them. We are therefore looking for a more practical object, which is given by the effective

average action Γ_k, defined as the (modified) Legendre transform of $\log Z_k$, that is:

$$\Gamma_k + \mathcal{W}_k = \int_q J(q)\psi_k(q) - \Delta\mathcal{S}_k[\psi_k] \tag{I.40}$$

where $\mathcal{W}_k[J] \equiv \log Z_k[J]$, and $\psi_k(x) = \frac{\delta \mathcal{W}_k}{\delta J(x)} = \langle \phi_k(x) \rangle$. Notice that in (I.40), there is an extra term $\Delta\mathcal{S}[\psi_k]$ in addition to the usual Legendre transform. This extra term enforces $\Gamma_{k=\Lambda} = \mathcal{S}$ (see for instance [33] for a proof).

The effective average action Γ_k has several advantages with regard to the partition function: (i) it is a functional of $\psi_k(x) = \frac{\delta \mathcal{W}_k}{\delta J(x)} = \langle \phi_k(x) \rangle$ which can be seen as the magnetization of a system of size $1/k^d$. The average effective action Γ_k can consequently be interpreted as the free energy of a smaller system of size $1/k^d$. (ii) It provides a smooth interpolation between the action $\Gamma_{k=\Lambda} = \mathcal{S}$ at the microscopic scale $k = \Lambda$, and the Gibbs free energy $\Gamma_{k=0} = \Gamma$ at the macroscopic scale $k = 0$. (iii) The Gibbs free energy Γ is the generating functional of the one-particle irreducible correlation functions. For example, the second derivative of Γ is the inverse of the propagator G and reads:

$$G^{-1}(x-y) \equiv \frac{\delta^2 \Gamma}{\delta\psi(x)\delta\psi(y)} = \langle \phi(x)\phi(y) \rangle_{\mathrm{c}}^{-1} \ . \tag{I.41}$$

and the effective average action Γ_k can therefore be seen as a (regularized) precursor of the generating functional of the one-particle irreducible correlation functions (see also next section).

Notice that the two-point correlation function $G(x-y)$ is a well-defined analytic function for $T \neq T_c$ but behaves as

$$G(x-y) \underset{|x-y|\to\infty}{\sim} \frac{1}{|x-y|^{d-2+\eta}} \tag{I.42}$$

at criticality ($T = T_c$), where this (nonanalytic) power-law behaviour is a signature of the scale invariance of the critical system. Notice that we have introduced the anomalous dimension $\eta > 0$ which can be understood as a shortening of the range of the correlations due to fluctuations. The important point is that the regulator term ensures that the effective average action Γ_k and its (functional) derivatives remain analytic for all $k \neq 0$ (it maintains the system out of criticality). In particular, R_k regularizes the nonanalytic behaviour of $G(x-y)$ for all $k \neq 0$, as we will see in the following. Ensuring that the derivatives of Γ_k are smooth functions of the momenta is the main role of the regulator, and it allows for performing approximations such as Taylor expansions in terms of the momentum, which is the essence of the approximation schemes that are used within the NPRG formalism and that we describe and justify in the following.

I.3.2.c Flow equation

Using the definitions of Γ_k and $\mathcal{Z}_k$, one can now compute the derivative of Γ_k with respect to k, that is, the "flow" of Γ_k when one goes from scale k to the scale $k - \mathrm{d}k$. Using the definition of Γ_k, Eq. (I.40), and performing a derivation with respect to the scale k, one finally obtains the Wetterich equation [36, 37]:

$$\partial_k \Gamma_k = \frac{1}{2} \int_q \partial_k R_k(q) \left[\Gamma_k^{(2)}(q) + R_k(q) \right]^{-1} \tag{I.43}$$

where we define the vertex functions:

$$\Gamma_k^{(n)}(\{x_i\}) = \frac{\delta^n \Gamma_k[\psi]}{\delta\psi(x_1)\cdots\delta\psi(x_n)} \tag{I.44}$$

and their Fourier transform are defined using the convention (1). Notice that in most cases the systems that we study have a translational invariance that is transmitted to the NPRG equations. This invariance imposes a vanishing sum of the momenta appearing in the Fourier transform of the integrands, and it is thus particularly convenient to use the short-hand notation for the two-points function: $\Gamma_k^{(2)}(q,-q) \equiv \Gamma_k^{(2)}(q)$. Notice that the flow equation is complemented by its boundary condition: when $k = \Lambda$, all the fluctuations are frozen by the regulator term and the system is described by its microscopic action: $\Gamma_{k=\Lambda} = \mathcal{S}$. When $k = 0$, all the fluctuations are taken into account and we have a description of the macroscopic system: $\Gamma_{k=0} = \Gamma$. We will neither derive the exact flow equation, nor prove that the initial condition $\Gamma_{k=\Lambda}$ is indeed equal to the microscopic action $\mathcal{S}$, but the interested reader can find these proofs in [14, 33] for instance.

Some comments about the Wetterich equation are needed:

- It is an *exact* equation, hence containing all the physics of the model, perturbative and nonperturbative, weak and strong couplings, topological excitations, etc.
- Although it is exact, its functional and nonlinear nature makes it non solvable without approximations, that we will present in the following. The nature of these approximations however will be nonperturbative in the sense that they do not rely on a Taylor expansion in a coupling constant. Notice however that if one performs *perturbative* approximations on the exact Wetterich equation, one retrieves the usual perturbative results, as expected.
- The regulator function $R_k(q)$ plays a major role in the flow equation. We will discuss its role in more details in the following, but notice already that it ensures that the propagator $[\Gamma_k^{(2)}(q)+R_k(q)]^{-1}$ does not become singular at criticality whenever $k \neq 0$. This is called an infrared (IR) regularization because its prevents the apparition of poles in the IR domain $q \to 0$. The ultraviolet (UV) regularization (when $q \to \Lambda$) is also tackled by the regulator, but this time by its derivative term $\partial_k R_k$, which decays sufficiently rapidly at large q to suppress the UV divergences.
- Finally, now that we have discussed three different versions (the Wegner-Houghton, the Wilson-Polchinski and the effective average action methods) of the exact flow equation, let us underline the differences between them. (i) The regulator function: the Wegner-Houghton approach differs from the two others by its regulator function. A very sharp cut-off function is used which discriminate between the slow modes and the rapid modes. In the modern implementation, it would mean that the regulator function $R_k(q)$ is a step function with $R_k(q) = 0$ if $q > k$, and $R_k(q) = \infty$ if $q < k$ (see Fig. I.5 for illustration). The Wilson-Polchinski approach, as the effective average method are thus more subtle with regard to the regularization, and use a smooth regulator function. (ii) The object of interest: in the Wegner-Houghton and in the Wilson-Polchinski approaches, the flow equation is written in term of an effective action $\mathcal{S}_k$. These actions are very abstract objects, since one still has to perform a path-integral in order to have access to the physical quantities. By contrast, although the Wetterich equation (I.43) is formally equivalent to the Wilson-Polchinski equation (see [37] for a proof), the former equation deals with the effective average action Γ_k, which bears more physical content. In particular, since the variable of the effective average action $\psi_k(x) = \frac{\delta \mathcal{W}_k}{\delta J(x)} = \langle \phi_k(x) \rangle$ can be seen as the magnetization of a system of size $1/k^d$, the average effective action Γ_k can consequently be interpreted as the free energy of a smaller system of size $1/k^d$.

I.3.2.d Approximation schemes

Although the Wetterich equation (I.43) governing the evolution of the effective average action Γ_k with the scale k is exact, its functional form makes it in practice unsolvable without resorting

to approximation schemes. Two main approximation schemes exist which are quite different in spirit and can be used to probe different properties of the critical systems. The most commonly used approximation within the NPRG context is called the derivative expansion (DE) and is quite natural since the idea is to restrict the functional form of Γ_k by imposing its shape via an ansatz [14, 37]. We will use it throughout the manuscript and will therefore describe it in details. The second approximation was introduced by Blaizot, Mendéz-Galain and Wschebor [51, 52] and does not rely on an ansatz for the action but is based on an approximation that allows one to obtain a closed set of flow equations on the correlation functions.

The derivative expansion (DE). The idea of this approximation [14, 37] is to transform the functional flow equation into a system of coupled partial differential equations describing the flow of "coupling" functions. For doing so, we therefore specify an ansatz for Γ_k that constrains its form. In other words, we perform a projection of Γ_k on a (much) simpler functional subspace. The ansatz we choose (i.e. the subspace) is an approximation of the exact functional and must therefore be chosen with great care. In particular, it must respect all the symmetries of the initial model, and one must be sure that the terms that have not been retained in the approximation are indeed negligible. A balance between the complexity of the ansatz (leading to more complicated analytical and numerical calculations) and the precision of the approximation will then have to be found.

When studying phase transitions, the physics of interest is that of large length scale, when all the microscopic degrees of freedom start to behave collectively and long-range order arises. It means that we are interested in the large-distance physics, or equivalently in the small-momentum physics $q \to 0$. For this reason, the spirit of the derivative expansion is to perform a Taylor expansion of the effective average action Γ_k near $q \to 0$, that is a Taylor expansion in power of the spatial derivatives. More details and justifications will be given in Sec. I.4.3.

For instance, in the context of the ϕ^4 model, this leads us to writing the effective average action as:

$$\Gamma_k[\psi] = \int \mathrm{d}^d x \left(U_k(\psi) + \frac{1}{2} Z_k(\psi) (\nabla\psi)^2 + O(\nabla^4) \right) \tag{I.45}$$

which is a derivative expansion at the second order in space derivative. Constraining the functional form of $\Gamma_k[\psi]$ means that Wetterich functional equation (I.43) translates into two coupled partial differential equations for the functions $U_k(\psi)$ and $Z_k(\psi)$. Evaluated in a uniform field configuration, $U_k(\psi)$ identifies to $\Gamma_k(\psi)$ up to a volume factor. Consequently, $U_{k=0}$ is proportional to the effective Γ[14], and we recall in App. A.1 that the thermodynamic potential $U = U_{k=0}$ is directly linked to the probability distribution of the magnetization (at least when the system is not critical). The function Z_k contains the physics of the configurations (slowly) variating in space. Notice that more drastic approximations can be made: setting $Z_k(\psi) = 1$ for instance is called the Local Potential Approximation (LPA) and usually yields already reasonably good quantitative results (except for the anomalous dimension η which is vanishing in this scheme). The LPA' is a slightly more refined approximations for which $Z_k(\psi) = Z_k$ is a mere number. This refinement allows us in particular to compute a nonvanishing η exponent. Finally, and we will discuss it a following section, a series expansions in ψ of the potential $U_k(\psi)$ may be performed (usually known as a field expansion), leading to further simplifications.

Let us already notice that the derivative expansion will allow us to calculate not only universal quantities, such as critical exponents (see for instance [53] for the computation of a nonequilibrium exponent in the kinetic Ising model after a critical quench, more examples are also given in the following), but also nonuniversal quantities defined at vanishing momenta,

[14] Since we have performed a derivative expansion, this is not the exact effective potential, but an approximation of it.

such as phase diagrams (see for example [54]). However, it does not give access to the full-momentum dependence of correlation functions, something desirable in many situations and that will be given by the BMW approximation (see for instance [55] for a detailed discussion about the differences between these two approximation schemes).

The Blaizot–Mendéz-Galain–Wschebor (BMW) approximation. The BMW scheme [51, 52] is very different in spirit to the derivative expansion: instead of restricting the form of Γ_k, this scheme limits the infinite number of coupled equations for the n-points functions $\Gamma_k^{(n)}$ into a closed system of equations. Indeed, because of the presence of $\Gamma_k^{(2)}$ in the right-hand side of the Wetterich equation (I.43), the flow of the $\Gamma_k^{(n)}$ contains all the vertex functions up to $\Gamma_k^{(n+2)}$.

For instance, let us derive the flow of the second derivative of the effective average action. We first define the Fourier transform of $\Gamma_k^{(2)}$ as:

$$\Gamma_k^{(2)}(p) \equiv \mathrm{FT}\left(\frac{\delta^2 \Gamma_k}{\delta\psi(x)\delta\psi(y)}\bigg|_{\psi=\psi^{\mathrm{unif}}} \right)(p,-p) \tag{I.46}$$

where $\mathrm{FT}(f)(p_1,p_2)$ is the Fourier transform of the function $f(x,y)$, using the convention (1). Notice that $\Gamma_k^{(2)}$ is evaluated at a uniform field configuration ψ^{unif}. We immediately drop the superscript for the uniform field ψ^{unif} to alleviate the notation and write $\psi = \psi^{\mathrm{unif}}$. To compute the flow of these quantities under a change of scale k we use the Wetterich equation (I.43). Writing the full propagator $G_k(q;\psi) \equiv [\Gamma_k^{(2)}(q) + R_k(q)]^{-1}$, the flow of $\Gamma_k^{(2)}$ reads:

$$\begin{aligned}\partial_k \Gamma_k^{(2)}(p) = \int_q \partial_k R_k(q) G_k(q;\psi) \Big[&\Gamma_k^{(3)}(q,-q-p,p) G_k(p+q;\psi) \Gamma_k^{(3)}(p+q,-q,-p) \\ &- \frac{1}{2}\,\Gamma_k^{(4)}(q,-q,p,-p) \Big] G_k(q;\psi)\,.\end{aligned} \tag{I.47}$$

We therefore see that the flow of the two-point function $\Gamma_k^{(2)}(p)$, given above, contains the vertices $\Gamma_k^{(3)}$ and $\Gamma_k^{(4)}$. The aim of the BMW scheme is to close this infinite hierarchy of equation[15] through an approximation, justified by the presence of the regulator function $R_k(q)$. Indeed, we recall that the regulator has two roles: (i) it ensures that the $\Gamma_k^{(n)}$ are smooth functions of the momenta (because the regulator places the system out of criticality where these functions are analytic) and (ii) it cuts off the momenta larger than $q \gtrsim k$ under the integral in the right-hand-side of the Wetterich equation (I.43) via the $\partial_k R_k$ term. This justifies to compute the vertices $\Gamma_k^{(n)}$ appearing under the integral at vanishing internal momentum q. For instance, in Eq. (I.47), one replaces:

$$\Gamma_k^{(3)}(q,-q-p,p) \to \Gamma_k^{(3)}(0,-p,p) \quad \text{and} \quad \Gamma_k^{(4)}(q,-q,p,-p) \to \Gamma_k^{(4)}(0,0,p,-p)\,. \tag{I.48}$$

This approximation then allows one to use the exact identity [51, 52]:

$$\Gamma_k^{(m+1)}(\{p_i\}, p_{m+1}=0) = \partial_\psi \Gamma_k^{(m)}(\{p_i\}) \tag{I.49}$$

which is the essential ingredient for closing the set of coupled equations. Using this formula, the flow of any vertex $\Gamma_k^{(n)}$ now contains vertices of order at most n. For instance, the flow of $\Gamma_k^{(2)}$ in Eq. (I.47) now reads:

$$\partial_k \Gamma_k^{(2)}(p) = \int_q \partial_k R_k(q) G_k(q) \left[\partial_\psi \Gamma_k^{(2)}(p) G_k(p+q) \partial_\psi \Gamma_k^{(2)}(p) - \frac{1}{2}\partial_\psi^2 \Gamma_k^{(2)}(p) \right] G_k(q)\,, \tag{I.50}$$

[15] The flow of $\Gamma_k^{(2)}$ depends on $\Gamma_k^{(3)}$ and $\Gamma_k^{(4)}$, whose flow depends on $\Gamma_k^{(5)}$, $\Gamma_k^{(6)}$, etc.

and it involves only $\Gamma_k^{(2)}(p)$.

The BMW scheme, because it keeps the full-momentum contribution of the vertices can be used to compute momentum-dependent quantities such as scaling functions (see for instance [56–58]), a task which is out-of-reach of the derivative expansion since this approximation is only valid at vanishing external momenta [55].

I.3.3 An example: the ϕ^4 theory

In this section, we give a pedagogical example of application of the NPRG on the archetypical ϕ^4 model. As stated in the previous section, the derivative expansion, at second order, reads:

$$\Gamma_k[\psi] = \int \mathrm{d}^d x \left(U_k(\psi) + \frac{1}{2} Z_k(\psi)(\nabla\psi)^2 + O(\nabla^4) \right) . \tag{I.51}$$

To solve this problem in this approximation scheme, we therefore have to find the flow of the functions $U_k(\psi)$ and $Z_k(\psi)$ that we define as:

$$U_k(\psi^{\mathrm{unif}}) = \frac{1}{\Omega}\Gamma_k(\psi^{\mathrm{unif}}) \tag{I.52}$$

$$Z_k(\psi^{\mathrm{unif}}) = \frac{1}{\Omega}\left[\partial_{p^2} \, \mathrm{FT}\left(\frac{\delta^2\Gamma_k}{\delta\psi(x)\delta\psi(y)}\bigg|_{\psi=\psi^{\mathrm{unif}}} \right)(p,-p) \right]\bigg|_{p=0} \tag{I.53}$$

where $\Omega \equiv \int \mathrm{d}^d x$ is the volume of the system, and $\mathrm{FT}(f)(p_1,p_2)$ is the Fourier transform of the function $f(x,y)$, using the convention (1). Notice that Γ_k and its derivatives are evaluated in a uniform field configuration ψ^{unif} (and again we immediately drop the superscript for the uniform field ψ^{unif} and write $\psi = \psi^{\mathrm{unif}}$). The flow of these quantities under a change of scale k is computed using the Wetterich equation (I.43), and we first have to write explicitly the full propagator $G_k(q;\psi) \equiv [\Gamma_k^{(2)}(q) + R_k(q)]^{-1}$ which is in this case rather simple:

$$G_k(q;\psi) = \frac{1}{R_k(q) + q^2 Z_k(\psi) + U_k''(\psi)} , \tag{I.54}$$

and we can now proceed to the computation of the flow of U_k.

I.3.3.a Calculation of the flow of U_k

The flow of U_k follows immediately from the Wetterich equation (I.43) and from the equation for the propagator (I.54). It reads:

$$\partial_k U_k(\psi) = \frac{1}{2}\int_q \frac{\partial_k R_k(q)}{R_k(q) + q^2 Z_k(\psi) + U_k''(\psi)} . \tag{I.55}$$

When describing the RG ideas in the block-spin example, we have seen that the rescaling (the renormalization) of the length after each decimation step was necessary in order to have a system that remains self-similar after each RG step. This rescaling means that we have to measure all the lengths in units of the running lattice spacing. In the NPRG formalism, the scale k is the analogue of the inverse running lattice spacing, and expressing the quantities appearing in the flow equations in the units of the running lattice is equivalent to writing the equations in a dimensionless form where the k-dependence is no longer explicit. To give a concrete example, if we compute directly Eq. (I.55) using the Θ-regulator (I.38) and setting $Z_k(\psi) = 1$, we obtain:

$$k\partial_k U_k(\psi) = \frac{4v_d}{d}\frac{k^{d+2}}{k^2 + U_k''(\psi)} . \tag{I.56}$$

Studying the large-distance physics $k \to 0$ in this form is obviously not convenient since the right-hand side of the equation seems to vanish in this limit. It is therefore important to follow the evolution of U_k and Z_k in the "co-moving" frame, that is, to zoom out as the scale k is modified. In practice, this is made possible by switching to dimensionless variables.

The starting point to switch to dimensionless variable is to notice that the effective average action Γ_k has the dimension of an action and is thus dimensionless: $[\Gamma_k] = [k^0]$. This allows us to deduce the dimension of the field and of the potential:

$$[\psi] = [k^{\frac{d-2}{2}}] \quad \text{and} \quad [U_k] = [k^d] \tag{I.57}$$

which we use to define the following dimensionless variables:

$$\hat{x} \equiv kx\,, \tag{I.58a}$$
$$y \equiv q^2/k^2\,, \tag{I.58b}$$
$$s \equiv \log(k/\Lambda)\,, \tag{I.58c}$$
$$\hat{\psi}(\hat{x}) \equiv k^{\frac{2-d}{2}} \bar{Z}_k^{1/2} \psi(x)\,, \tag{I.58d}$$
$$\hat{U}(\hat{\psi}) \equiv k^{-d} U_k(\psi)\,, \tag{I.58e}$$
$$\hat{Z}(\hat{\psi}) \equiv \bar{Z}_k^{-1} Z_k(\psi)\,, \tag{I.58f}$$
$$r(y) \equiv y^{-1} k^{-2} \bar{Z}_k^{-1} R_k(q)\,, \tag{I.58g}$$

where we have introduced the renormalization time s. Notice that the dimensionless variables are written with a hat [except for y, s and $r(y)$], and that their dependence in the renormalization time s is not explicit, for instance, $\hat{U}_s(\hat{\psi})$ is written $\hat{U}(\hat{\psi})$. Notice moreover that we have introduced the running coefficient $\bar{Z}_k$ to define the dimensionless function $\hat{Z}(\hat{\psi})$, and have modified the dimensionless field $\hat{\psi}$ and regulator $r(y)$ accordingly. This extra running coefficient is necessary to capture the anomalous dimension that appears at criticality [see Eq. (I.42)] and which can be seen as a shortening of the correlation length due to fluctuations. Indeed, according to Eq. (I.42), the fields are expected to have a scaling $\phi(q) \sim k^{(d-2+\eta/2)}$ as $k \to 0$, and the extra running coefficient $\bar{Z}_k$ scales as $\bar{Z}_k \sim k^{-\eta}$ when $k \to 0$ and captures this anomalous scaling.

In prevision to this power-law behaviour, we furthermore define a running anomalous dimension η_s as $\eta_s = -\partial_s \ln \bar{Z}_k$, matching the anomalous dimension η when $k \to 0$ (or equivalently when $s \to -\infty$): $\eta_{s=-\infty} = \eta$. Finally, $\bar{Z}_k$ is defined such that $\hat{Z}(\hat{\psi} = \hat{\psi}_0) = 1$, where $\hat{\psi}_0$ can be chosen arbitrarily but is in practice chosen as the (running) minimum of the potential $\hat{U}$.

We also define the $\mathbb{Z}_2$-invariant variable: $\hat{\rho} \equiv \hat{\psi}^2/2$. Using these dimensionless variables, we can now cast the flow equation (I.55) into a dimensionless form:

$$\partial_s \hat{U} = -d\hat{U} + (d - 2 + \eta_s)\hat{\rho}\hat{U}' + v_d \int_y y^{d/2} \frac{g(y)}{h(y, \hat{\rho})} \tag{I.59}$$

with $\hat{U} \equiv \hat{U}(\hat{\rho})$, $\hat{U}' \equiv \partial_{\hat{\rho}} \hat{U}$, where the integration factor $v_d^{-1} \equiv 2^{d+1}\pi^{d/2}\Gamma(d/2)$ comes from the spherical invariance of the integral over q, and we have defined $g(y) = -\eta_s r(y) - 2y r'(y)$ and $h(y, \hat{\rho}) = y(\hat{Z}(\hat{\rho}) + r(y)) + \hat{U}'(\hat{\rho}) + 2\hat{\rho}\hat{U}''(\hat{\rho})$.

I.3.3.b Calculation of the flow of Z_k

The flow of Z_k requires a little more work. First, we recall that the flow of the second derivative of the effective average action $\Gamma_k^{(2)}(p) \equiv \mathrm{FT}(\delta^2\Gamma_k/\delta\psi(x)\delta\psi(y)|_{\psi=\psi^{\mathrm{unif}}}$ reads:

$$\begin{aligned}\partial_k \Gamma_k^{(2)}(p) = \int_q \partial_k R_k(q) G_k(q;\psi) \Big[&\Gamma_k^{(3)}(q, -q-p, p) G_k(p+q;\psi) \Gamma_k^{(3)}(p+q, -q, -p) \\ &- \frac{1}{2}\, \Gamma_k^{(4)}(q, -q, p, -p) \Big] G_k(q;\psi)\,,\end{aligned} \tag{I.60}$$

where we have dropped the superscript for the uniform field ψ^{unif}. After some more computation and casting the equation into a dimensionless form using Eqs. (I.58), one obtains:

$$\partial_s \hat{Z} = \eta_s \hat{Z} + (d - 2 + \eta_s)\hat{\rho}\,\hat{Z}' + 2v_d \int_y y^{d/2} \frac{g}{h^2} \left[\frac{2\hat{\rho} f^2}{h^2} \left(\frac{4}{d} \frac{y h'^2}{h} - h' - \frac{2}{d} y h'' \right) + 4\hat{\rho}\hat{Z}' \frac{f}{h} \left(1 - \frac{2}{d} \frac{y h'}{h} \right) + \frac{2\hat{\rho}}{d} (\hat{Z}')^2 \frac{y}{h} - \frac{\hat{Z}'}{2} - \hat{\rho}\hat{Z}'' \right], \tag{I.61}$$

where $v_d^{-1} = 2^{d+1}\pi^{d/2}\Gamma(d/2)$, $\hat{\rho} = \hat{\psi}^2/2$, $h(y,\hat{\rho}) = y(\hat{Z}(\hat{\rho}) + r(y)) + \hat{U}'(\hat{\rho}) + 2\hat{\rho}\hat{U}''(\hat{\rho})$, $f(y,\hat{\rho}) = y\hat{Z}'(\hat{\rho}) + 3\hat{U}''(\hat{\rho}) + 2\hat{\rho}\hat{U}'''(\hat{\rho})$ and $g(y) = -\eta_s r(y) - 2y r'(y)$. We have omitted to write the dependence of the function on their variables, and have written $h' = \partial_y h$ to alleviate the notation.

I.3.3.c Finding the fixed-point solution

Our main interest when studying critical phenomena is usually the fixed-point solution of the flow equations, as stressed in the previous parts. Equations (I.59) and (I.61), together with the conditions $\hat{U}'(\hat{\kappa}) = 0$ (where $\hat{\kappa}$ is the running minimum of the potential, and therefore the precursor of the magnetization[16]) and $\hat{Z}(\hat{\kappa}) = 1$ (by definition) form a closed system of nonlinear partially differential equations. When searching for the fixed-point solution $\partial_s \hat{U} = 0$ and $\partial_s \hat{Z} = 0$ it becomes a system of nonlinear ordinary differential equations. This kind of system remains usually highly nontrivial to solve, and we therefore show in the following some usual techniques that can be tried on.

Numerical root finding. A first method consists in discretizing the fixed-point version of equations (I.59) and (I.61) over a grid $\hat{\rho} \in [0, \hat{\rho}_{\max}]$ and evaluating the derivatives using for example a "five-point stencil" method[17]. If the grid has N points, this yields a system of $2N$ coupled nonlinear algebraic equations. This system can then be solved using usual root-finding algorithms. Notice that one also has to perform a numerical integration of the integrals over the momenta. Using a Θ-regulator (I.38), which allows for an analytical computation of these integrals when $\hat{Z}$ is independent of $\hat{\rho}$, can therefore simplify the numerical task in this case. Notice moreover that these root-finding methods necessitate an initial condition for $\hat{U}$ and $\hat{Z}$, and they converges toward a solution only if the initial condition is realistic. To obtain such an initial condition, one can either start from a better known theory (for example, start at the upper critical dimension $d = 4$ in our case) and then approach the desired model (lower the dimension d). An alternative path can be to start with a simpler model (for instance set $Z_k = 1$), solve this model and then resume to the more complicated one. The two other methods we show in the following are therefore explained for the case $Z_k = 1$[18].

Shooting method. For this method, we assume that $Z_k = 1$. The idea of this technique is to solve directly the fixed-point version of equation (I.59) by numerical integration [60, 61]. A priori, this task is complicated since we only have one boundary condition, $\hat{U}'(\hat{\psi}_0) = 0$, whereas we have a second-order partial differential equation, and we therefore expect to have infinitely

[16] At vanishing external field, we have $\partial U/\partial\psi = J = 0$ and the magnetization therefore corresponds to the minimum of the potential.

[17] This method is simply a finite-difference approximation that uses the point and its four neighbours on the grid to compute the derivatives [59]. On the boundaries of the discretization box the computation of the derivatives is made using only the points inside the box.

[18] Setting $Z_k = 1$ means to neglect the field anomalous dimension, that is to set $\eta_s = 0$. This method is known in the NPRG context as the local potential approximation, since the renormalization of the space-dependent part of the effective average action is neglected.

many solutions, indexed by the value of $\hat{U}''(\hat{\psi}_0) \equiv b$[19]. In fact, the only physical solution b^* is the only solution of the previous equation that does not blow up at finite $\hat{\psi}$. The shooting method therefore consists in a dichotomy on b, trying to obtain the b for which the numerical solution exists for all values of $\hat{\psi}$. Notice that to perform this shooting, it has been proven more efficient to compute the asymptotic behaviour of $\hat{U}$ when $\hat{\psi} \to \infty$, and then to proceed to a shooting-to-origin rather than the more intuitive shooting from the origin method [61].

Conformal mapping. For the presentation of this method we also assume that $Z_k = 1$. As for the shooting method, the goal is to find the only value for which $\hat{U}$ has a physical solution. This time, all the potential solutions of Eq. (I.59) are indexed by $\hat{r} \equiv \hat{U}(0)$. The idea is the following [62]: a series expansion of $\hat{U}$ is performed:

$$\hat{U}(\hat{\rho}) = \sum_{n=0}^{M} \hat{u}_n \hat{\rho}^n \,, \tag{I.62}$$

and the coefficients $\hat{u}_n$ are determined by plugging this series expansion into the fixed-point version of Eq. (I.59) and solving it order by order. Doing so, the coefficients $\hat{u}_n$ are therefore function of the free parameter $\hat{r}$: $\hat{u}_n \equiv \hat{u}_n(\hat{r})$, and we want to find the value $\hat{r}^*$ corresponding to the non-blowing physical solution.

In fact, it can be proven that the series expansion (I.62) has a finite radius of convergence [63], and the idea is to perform a conformal mapping in order to obtain the large $\hat{\rho}$ behaviour of $\hat{U}$. Defining $\hat{w}$ the conformal variable, and $\hat{W} \equiv \hat{U}(\hat{w})$ the corresponding transformed potential, one can perform a series expansion of $\hat{W}$ as:

$$\hat{W}(\hat{w}) = \sum_{n=0}^{M} \hat{w}_n(\hat{r}) w^n \tag{I.63}$$

where the $\hat{w}_n(\hat{r})$ are functions of the $\hat{u}_n(\hat{r})$. This series expansion of the conformal potential in the conformal variable captures the large-field behaviour of the potential. The idea is then to compute $\hat{r}^*$ by assuming that if M is sufficiently large, the series expansion of W should converge and therefore the last term $\hat{w}_M$ can be neglected. Solving $\hat{w}_M(\hat{r}) = 0$ yields a polynomial on $\hat{r}$ and one of its roots is the value $\hat{r}^*$ we are seeking[20], and we can therefore compute (the series expansion of) $\hat{W}$ as a function of $\hat{r}^*$. An inverse conformal transformation finally yields a good approximation for $\hat{U}$.

I.3.3.d Solving the flow equations

Although the integration of the flow given by Eqs. (I.59) and (I.61) is a more complicated task than finding a fixed-point solution, it also yields more information. In particular, it provides us with flow in the vicinity of the fixed points, therefore allowing us to compute the critical exponents that characterize this approach[21], such as the exponent ν. Having access to the flow of the coupling constants can also yield information about non-universal quantities [64, 65] or information about crossover phenomena and finite-size scaling effects (see for instance [66]): if there exist other (unstable) fixed points, the flow may spend a long time in the vicinity of these fixed points before reaching the actual stable fixed point of the model. This effect has a concrete translation when one performs experiments or numerical simulations: the computed critical exponents can differ from the theoretical ones because of finite-size effects.

[19] The shooting method is in fact more effective on the function $\hat{U}'(\hat{\psi})$, which is reason why we define $\hat{U}''(\hat{\psi}_0) = b$ (rather than $\hat{U}(\hat{\psi}_0) = b$ for instance).

[20] The value $\hat{r}^*$ can be found amongst the other roots of the polynomial by checking the shape of the resulting $\hat{U}$, and its large-field behaviour for instance.

[21] The critical exponents can also be computed from the linear stability of the fixed point equations, as we will see in the following.

Field expansion. Solving numerically the two coupled nonlinear partial differential equations (I.59) and (I.61) can be a very tedious task, and one can therefore perform, on top of the derivative expansion, a series expansion of the functions $\hat{U}$ and $\hat{Z}$. For a generic function $\hat{F}_s(\hat{\rho}) \equiv \hat{F}(\hat{\rho})$, we define its Taylor expansion around its running minimum as:

$$\hat{F}(\hat{\rho}) = \sum_{n=0}^{M} \hat{f}_n (\hat{\rho} - \hat{\kappa})^n \tag{I.64}$$

where $\hat{\kappa}$ is the running (s-dependent) minimum of the potential, $\hat{U}'(\kappa) = 0$. Note that $\hat{F}$ and the $\hat{f}_n$ are functions of the renormalization time s as well. Performing this expansion, we transform the coupled partial differential equations (I.59) and (I.61) into a system of ordinary differential equations, which is easier to integrate numerically[22]. Notice that, contrary to the derivative expansion which is controlled because of the regulator R_k (this will be explained in Sec. I.4.3 in more details), the field expansion is a cruder approximation, and it must be checked carefully that the series expansion is indeed convergent by checking the convergence of the coupling constants/exponents as the order of the expansion M is increased. The convergence of this expansion for the $O(N)$ model has been well studied (see for instance [67, 68] and references therein). Although this convergence is very rapid for $3 \leq d \leq 4$, one has to include more and more terms as d is lowered to 2, and it is therefore preferable to work with the functions $\hat{F}$ rather than their series expansion as soon as $d < 3$ in these models.

Numerical integration. In the general case, the build-in numerical solvers are not able to deal with the flow equations, and a numerical code has to be written. A rather simple numerical scheme is usually sufficient: the field $\hat{\rho}$ is discretized over a finite grid $\hat{\rho} \in [0, \hat{\rho}_{\max}]$, the derivatives are computed using a finite-difference scheme (for instance a "five-point stencil" method [59]), and the renormalization flow is then integrated numerically starting from an initial condition at $k = \Lambda$ and using a Runge-Kutta algorithm [59]. Notice that the specification of the initial condition, for instance:

$$\hat{U}(\hat{\rho})|_{k=\Lambda} = \frac{1}{2}(\hat{\rho} - \hat{\kappa}_\Lambda)^2 \tag{I.65}$$

is equivalent to specifying the temperature of the system via $\hat{\kappa}_\Lambda$. Therefore, if $\hat{\kappa}_\Lambda > \hat{\kappa}_c$ (where $\hat{\kappa}_c$ is the critical value for $\hat{\kappa}_\Lambda$ which corresponds to $T = T_c$) then the system ends up in the ordered phase, while it ends up in the disordered phase if one started with a $\hat{\kappa}_\Lambda < \hat{\kappa}_c$. Finding the fixed-point solution therefore requires to start exactly at $\hat{\kappa}_\Lambda = \hat{\kappa}_c$. Numerically, we proceed by dichotomy to approach the critical value, and therefore approach the true fixed-point solution. We explain this in more details on a specific example in the following section.

I.3.4 Results

In this section we present the results of the numerical integration of the flow equations in the case of the XY model (or $O(2)$ model) in $d = 3$. For simplicity, we use a LPA' approximation, such that the ansatz for the effective average action reads:

$$\Gamma_k = \int \mathrm{d}x \left[\frac{1}{2}(\bar{Z}_k \nabla \vec{\psi})^2 + U_k(\rho) \right] \tag{I.66}$$

where $\rho = 1/2\, \vec{\psi}^2$ is the invariant of the $O(2)$ symmetry and $\bar{Z}_k$ is a mere number (not a function of ρ). With $\bar{Z}_k$ is associated a running anomalous dimension η_s such that $\eta_s = -\partial_s \log \bar{Z}_k$. We

[22] It can usually be performed using any numerical solver from Maple or Mathematica for instance.

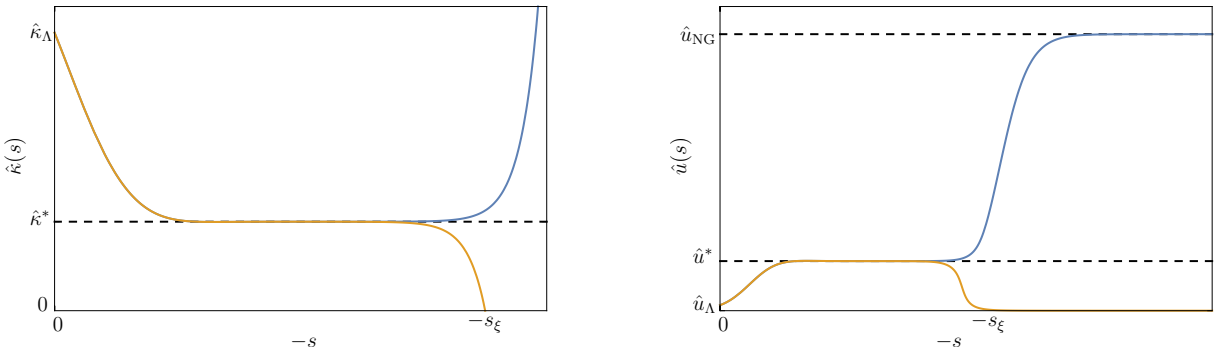

Figure I.6 – *Flows of the (dimensionless) minimum of the potential $\hat{\kappa}(s)$* ***(left)*** *and of the coupling constant $\hat{u}(s)$* ***(right)*** *as a function of the negative RG time $-s$. The blue curves correspond to an initial condition $\hat{\kappa}_\Lambda > \hat{\kappa}_c$, and as $s \to -\infty$, the system converges toward the low-temperature Nambu-Goldstone fixed point. The orange curves correspond to $\hat{\kappa}_\Lambda < \hat{\kappa}_c$ and ends up in the Gaussian fixed point. After a transient time, the flows reach a plateau corresponding to the vicinity of the Wilson-Fisher critical point. This plateau is left when $s \simeq s_\xi$, value at which the RG scale k is comparable to the inverse correlation length $1/\xi$ of the system.*

perform in addition a field expansion for the potential in its dimensionless form $\hat{U}$ at order 3 in $\hat{\rho}$ around its running minimum $\hat{\kappa}$, that is:

$$\hat{U}(\hat{\rho}) = \frac{\hat{u}}{2}(\hat{\rho} - \hat{\kappa})^2 + \frac{\hat{u}_3}{3!}(\hat{\rho} - \hat{\kappa})^3 \tag{I.67}$$

where $\hat{u}$, $\hat{u}_3$ and $\hat{\kappa}$ are the coupling constants and are renormalized along the flow. Even in this very crude approximation, the quantitative picture [compared to the flow we could obtain by integrating the flow of the functions $\hat{U}(\hat{\rho})$ and $\hat{Z}(\hat{\rho})$] is preserved and correct; it allows us to show a rather simple illustration of renormalization flows. The dimensionless flow equations may be found in App. A.2, and we just give in the main text the flow for $\hat{\kappa}$:

$$\partial_s \hat{\kappa} = (2 - d - \eta_s)\,\hat{\kappa} + \frac{8 v_d\,(2 + d - \eta_s)}{d(2+d)}\,\frac{2\hat{\kappa}^2\hat{u}^3 + 2\hat{\kappa}\hat{u}^2 + 2\hat{u} + \hat{\kappa}\hat{u}_3}{\hat{u}(2\hat{\kappa}\hat{u} + 1)^2}\,, \tag{I.68}$$

where d is the spatial dimension and $v_d^{-1} = 2^{d+1}\pi^{d/2}\Gamma(d/2)$ is the volume factor coming from the momentum integration. Notice that we have used a Θ-regulator [see Eq. (I.38)] to compute the momentum integrals. The initial condition for the numerical integration of the flow is given by:

$$\hat{U}(\hat{\rho})|_{k=\Lambda} = \frac{\hat{u}_\Lambda}{2}(\hat{\rho} - \hat{\kappa}_\Lambda)^2 + \frac{\hat{u}_{3,\Lambda}}{3!}(\hat{\rho} - \hat{\kappa}_\Lambda)^3 \tag{I.69}$$

with $\hat{u}_\Lambda = 10^{-2}$ and $\hat{u}_{3,\Lambda} = 10^{-5}$ and $\hat{\kappa}_\Lambda$ is tuned to be either in the low- or high-temperature phase. A fine-tuning of $\hat{\kappa}_\Lambda$ allows us to find the critical point $\hat{\kappa}_c$. Notice that to describe the flows we use the renormalization time $s \equiv \log(k/\Lambda)$, with $s = 0$ at the beginning of the flow (mean-field) and $s \to -\infty$ when all the fluctuations have been integrated over and the macroscopic state is reached.

I.3.4.a Flows of the dimensionless variables

We first focus on the flows of the dimensionless variables, which are simpler to study since they reach a (finite) fixed point when $\hat{\kappa}_\Lambda = \hat{\kappa}_c$. Depending on the initial value $\hat{\kappa}_\Lambda$, we expect the flow to end up either in the ordered, or disordered phase.

Flow near T_c. We choose a temperature T slightly smaller (resp. larger) than the critical temperature T_c, that is $\hat{\kappa}_\Lambda$ slightly larger (resp. smaller) than $\hat{\kappa}_c$. In both cases the flow of the coupling constants displays three regimes: (i) at the beginning of the renormalization procedure (at $s = 0$), the initial condition (I.69) describes the system at the mean-field level[23]. As soon as the renormalization procedure starts (s is lowered), that is as soon as fluctuations are taken into account, the coupling constants are renormalized and change rapidly, and, since the system is almost critical, they seem to converge toward their fixed-point value. (ii) Since $T \simeq T_c$, the flow is really slow near the critical point: a plateau in the flow can be observed, which is longer and longer as T is closer to T_c. In particular if $T = T_c$ the size of the plateau becomes infinite. (iii) For $T \neq T_c$, when the coarse-graining procedure has reached the correlation length of the system, that is when $k \simeq 1/\xi$ (we denote the RG time corresponding to this scale as s_ξ), the system realizes that it is not critical and the coupling constants start varying again. The plateau is left and the dimensionful[24] coupling constants converge now toward their true macroscopic value (see Fig. I.6 for an illustration).

Flow for $T > T_c$: the Gaussian fixed point. If $T > T_c$, the system ends up into the disordered phase as soon as the renormalization scale k is of order $1/\xi$, which corresponds to a RG time $s \simeq s_\xi$. In this phase the average magnetization vanishes, which means that the minimum $\hat{\kappa}$ vanishes at finite k. The flow below this scale (that is for $-\infty < s < s_\xi$) can be continued using a truncation of the form $\hat{U}(\hat{\rho}) = \hat{m}\hat{\rho} + \frac{1}{2}\hat{\lambda}\hat{\rho}^2$ [14].

Flow for $T < T_c$: the Nambu-Goldstone fixed point. If $T < T_c$, the system ends up in the ordered phase when $k \simeq 1/\xi$. The system shows a spontaneous magnetization $\psi_0 = \sqrt{2\rho_0}$ with ρ_0 the minimum of the potential. On Fig. I.6, one observes that the dimensionless minimum $\hat{\kappa}$ diverges as $s \to -\infty$ which seems to be in contradiction with having a finite spontaneous magnetization. In fact, the correct (physical) variable is the dimensionful minimum $\rho_0 = k^{d-2}\hat{\kappa}$: in $d = 3$, the scaling prefactor k^{d-2} goes to 0 when $k \to 0$, and the product $\rho_0 = k^{d-2}\hat{\kappa}$ has a finite, nonvanishing limit, as expected (see Fig. I.7). One also notices on Fig. I.6 that the potential is not quadratic since $\hat{u}$ reaches its Nambu-Goldstone fixed-point value $\hat{u}(s \to -\infty) = \hat{u}_{\rm NG}$.

Flow of the potential: approach to convexity. Observing the evolution of the dimensionful potential

$$U_k(\psi) = k^d \hat{U}(k^{-\frac{d-2}{2}}\psi) \tag{I.70}$$

is also illuminating. Indeed starting from the unphysical (because nonconvex) potential $U_{k=\Lambda}(\psi)$, one observes on Fig. I.8 that the potential $U_k(\psi)$ converges toward a convex potential, whose final shape depends on the final state of the system. If $T > T_c$, the potential evolves toward a parabola with a single minimum on $\psi = 0$ (we recall that we have to modify the ansatz to obtain this Gaussian fixed point). If $T < T_c$, the potential becomes completely flat between $-\psi_0$ and ψ_0, whereas if $T = T_c$, the system resembles the flat potential for $k \neq 0$, its flat part shrinks as $k \to 0$ such that there is finally a single minimum exactly at $k = 0$.

I.3.4.b The critical point

Although the flows of the coupling constants and of the potential are interesting and insightful, especially because they allow for a concrete picture of the often abstract RG flows, the true

[23] In particular, although $\hat{\kappa}_\Lambda \neq 0$ which means that the microscopic potential has a nontrivial minimum, the macroscopic system (i.e. when $k = 0$) is in the disordered phase $\hat{\kappa}_{k=0} = 0$ whenever $\hat{\kappa}_\Lambda < \hat{\kappa}_c$.

[24] To be more precise, the *dimensionful* quantities converge toward their macroscopic values. For instance, for $T < T_c$ the dimensionless minimum diverges as $k \to 0$ whereas its dimensionful counterpart will flow toward a finite value since the magnetization of the macroscopic system is finite.

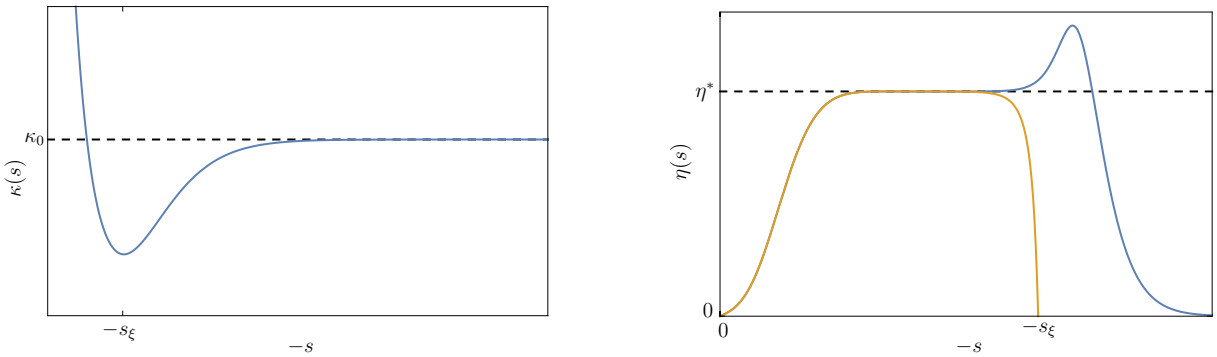

Figure I.7 – ***Left.*** *Flow of the* dimensionful *minimum of the potential $\kappa(s)$ for $T < T_c$ as a function of the negative RG time $-s$. After leaving the vicinity of the Wilson-Fisher fixed point at $s \simeq s_\xi$, the running minimum reaches its non-vanishing value κ_0, signaling that the system is indeed in the ordered phase.* ***Right.*** *Flow of the running anomalous dimension $\eta(s)$ for an initial condition $\hat{\kappa}_\Lambda > \hat{\kappa}_c$ (blue curve) and $\hat{\kappa}_\Lambda < \hat{\kappa}_c$ (orange curve) as a function of the negative RG time $-s$. After a transient time, the flows reach a plateau corresponding to the vicinity of the Wilson-Fisher critical point. This plateau is left when $s \simeq s_\xi$, value at which the RG scale k is comparable to the inverse correlation length $1/\xi$ of the system. The anomalous dimension η vanishes both in the Gaussian and in the Nambu-Goldstone fixed points.*

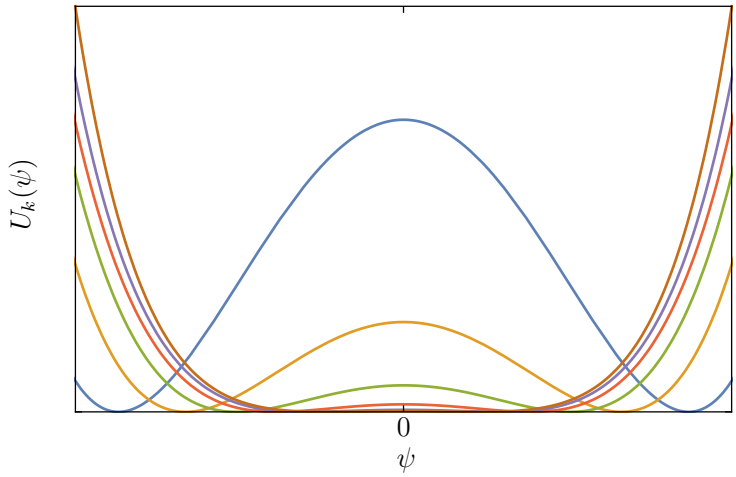

Figure I.8 – *Approach to convexity of the potential $U_k(\psi)$ in the ordered phase. Each curve corresponds to a different value of the RG scale k. At $k = \Lambda$ (blue curve), the initial condition is a nonconvex potential, but as k is lowered, the bump at $\psi = 0$ shrinks and the flow converges toward a convex potential with a completely flat region between $-\psi_0$ and ψ_0, the spontaneous magnetization.*

power of the RG blooms when studying a critical point and its vicinity. Indeed, the RG tools relies on the scale invariance of the system, which is truly effective when the system is critical. We therefore explain here how one can compute the critical exponents of a system using the NPRG formalism.

The anomalous dimension η. The anomalous dimension η is associated with the spatial fluctuations of the order parameter, and to an effective modification of the scaling behaviour of the correlations due to these fluctuations, as explained Sec. I.3.2.b. In the NPRG formalism, we have access to the running anomalous dimension, and the fixed point can be read directly on the flow if $T \simeq T_c$ (see Fig. I.7). Notice that to find the precise value of η^*, one therefore has to be as close to T_c as possible, which is usually done by dichotomy.

The approach to the fixed point and the exponent ν. The critical exponent ν is usually defined as the exponent characterizing the scaling behaviour of the correlation length ξ when one approaches the critical temperature, that is:

$$\xi \underset{T\to T_c}{\sim} |T - T_c|^{-\nu} \tag{I.71}$$

with $\nu > 0$ since the correlation length diverges when $T \to T_c$. As explained in Sec. I.2.2.a, this exponent can be directly computed from the first eigenvalue of the stability matrix computed at the nontrivial fixed point.

However, there exists an alternative path to compute the exponent ν, more suited to a dynamic integration of the flow equations: the exponent ν describes how the potential $\hat{U}$ (or any coupling constant) flows away from the fixed-point solution $\hat{U}^*$ when $T \simeq T_c$ but $T \neq T_c$. An expansion of the potential near its fixed-point value can therefore be written as:

$$\hat{U}(\hat{\rho}, s) \underset{T\sim T_c}{=} \hat{U}^*(\hat{\rho}) + \mathrm{e}^{-s/\nu} g_1(\hat{\rho}) + \mathrm{e}^{s\,\omega} g_2(\hat{\rho}) \tag{I.72}$$

where there is indeed a minus sign in the exponential defining ν since s is negative and ν describes how the potential escapes its unstable fixed point when the relevant coupling $(T - T_c)$ is not fine-tuned to 0. Notice that we also defined the exponent ω which describes the approach toward the fixed point, and is therefore related to the smallest positive eigenvalue of the stability matrix, associated to the "less irrelevant" coupling constant.

Notice that the other exponents (for instance β) can also be found using the RG flows but are not as simple to obtain as ν and η. Since there are only two independent critical exponents, all of them can be computed from ν and η using scaling relations [30, 33].

I.4 NPRG: some answers to its criticisms

Despite its successes in many domains – high-energy physics [69], frustrated magnets [70], quantum phase transitions [71], disordered systems [72] and out-of-equilibrium physics [21] – the NPRG methods are often undeservedly criticized for several reasons: (i) the NPRG is sometimes thought to be unable to retrieve the perturbative results, even at low order. (ii) The NPRG methods are (wrongly) accused to rely on unjustified approximations. (iii) The approximation schemes do not converge. (iv) The NPRG formalism is technically difficult and the underlying physics is therefore hidden by the technical details. In the following, we address these criticisms and try to justify why the NPRG is a useful tool, that should not be discarded blindly.

Obviously, the perturbative RG is also a very powerful tool and the Standard Model as well as the equilibrium statistical physics have thrived thanks to the tools of the perturbative RG. In many modern physics problems, the perturbative RG remains unavoidable and often allows for a very accurate resolution of some models, or it gives the first qualitative results to probe the underlying difficulties of more intricate problems. The NPRG does not claim to replace the perturbative RG: in some cases, it provides an alternative method for tackling a problem and therefore contest, refine or agree with the perturbative results. In some other cases, the intrinsic nonperturbative nature of the model makes it the only available option to address it. Finally, in some other context, the NPRG results are simply not (yet) available, or too difficult to implement, and the perturbative results may be the only ones available.

In the following, we give an answer to these criticisms by taking most of the time the example of the $O(N)$ model, for which many NPRG and perturbative RG results are available.

I.4.1 NPRG results

Before addressing the questions raised above, we present some of the NPRG results. Since the focus of this whole manuscript is on the nonequilibrium systems, this rapid review will

be focused on the nonequilibrium results obtained through the NPRG formalism, although this method has proven useful in various areas. Let us also remark that in this manuscript we are mainly interested in the computation of universal quantities (in particular critical exponents). However, to the contrary of the perturbative RG, the NPRG is also able to compute non-universal quantities such as critical temperatures (see for instance [64, 65]).

$O(N)$ model. The $O(N)$ model is probably the most studied model for phase transitions and is therefore a good benchmark for the NPRG. In Tables I.1 and I.2 we display the results for the critical exponents η and ν for different values of N in $d = 3$. We report the results obtained within the derivative expansion [73, 74] and the BMW [55] approximation schemes, together with results coming from the perturbative RG [75], Monte Carlo methods [76–80] and conformal bootstrap techniques [81] for comparison. One observes that the results of the NPRG are in reasonably good agreement with the Monte Carlo results, especially for the values of the ν (less than 1% error for its value in the case of the Ising model, $N = 1$). The results are comparable to those obtained with the perturbative RG, and differ from the expected numerical results by a few percents. For the $O(N)$ model, the conformal bootstrap methods are obviously the best suited.

Notice that similar results are available for the $d = 2$ case, in particular in $d = 2$ and $N = 2$ where the Berezinskii-Kosterlitz-Thouless phase transition is expected [82, 83]. We discuss this case in the following part. We finally report the results obtained in this manuscript for the kinetic $O(N)$ model in $d = 3$ in Table I.3. More details about these results are given in Chap. III.

Kardar–Parisi–Zhang equation. In one dimension, the Kardar–Parisi–Zhang (KPZ) equation [13] has been studied extensively and a mapping to the random matrix theory yields analytical and exact solutions in this case [41, 89]. In $d > 1$ however, the situation is more delicate and the perturbative approaches fail to capture the critical behaviour of this model, which is genuinely nonperturbative [90]. By contrast, the NPRG has proven quite effective in the study of the KPZ equation [16, 91]. The NPRG captures well the nonperturbative fixed point in $d = 2$ and is in good agreement with Monte Carlo results, see Table I.4. Nonetheless, the NPRG approach is still unable to capture the correct exponents for higher spatial dimensions [16]. To be slightly more precise, the NPRG results are expected to be correct yet less accurate up to dimension $d = 3.5$ but not reliable above dimension $d = 3.5$, where a more sophisticated approximation scheme is probably needed in order to yield consistent results (see [16] for more details about these issues).

Navier–Stokes equation. The NPRG has also been successful in the study of the Navier-Stokes equation in its turbulent regime, that is when an external stirring/energy injection is performed at the macroscopic scale to counterbalance the otherwise dissipative dynamics of the fluid dynamics equation [15, 92, 93]. Understanding the scaling behaviour of turbulence in the Navier–Stokes equation, and deriving Kolmogorov's scaling predictions from first principles still remains a challenge for the perturbative RG. The NPRG has therefore made a pioneering step in this direction by deriving, from the Navier-Stokes equation, predictions that go beyond the standard observations and Kolmogorov theory. For instance, a stretched exponential decay as $k^{-5/3}\exp(-\hat{\mu}(\lambda k)^{2/3})$ (with k the wave number, $\hat{\mu}$ a non-universal constant and λ the Taylor scale[25]) of the energy spectrum is predicted – and observed – in the dissipative (small-scale) range (see Fig. I.9).

[25]The Taylor scale is given by $\lambda \sim LR_\lambda^{-1/2}$ where L is the "integral" (large scale) length at which the energy is injected and R_λ is the Reynolds number.

N	DE	BMW	PFT	MC	CBS
0	0.039 [74]	0.034 [55]	0.0272(3) [75]	0.0303(3) [76]	
1	0.0443 [73]	0.039 [55]	0.0318(3) [75]	0.03627(10) [77]	0.036298(2) [81]
2	0.049 [74]	0.041 [55]	0.0334(2) [75]	0.0381(2) [78]	0.03852 [81]
3	0.049 [74]	0.040 [55]	0.0333(3) [75]	0.0375(5) [79]	0.03856 [81]

Table I.1 – *Values of the anomalous dimension η in $d = 3$ for the $O(N)$ model for different values of N and different methods. See [55] for the references of the different values. The NPRG results are reported for the derivative expansion (DE) and for the BMW approximation schemes. PFT stands for Perturbative Field Theory, MC for Monte Carlo studies, and CBS for Conformal Bootstrap methods.*

N	DE	BMW	PFT	MC	CBS
0	0.590 [74]	0.589 [55]	0.5886(3) [75]	0.5872(5) [80]	
1	0.6307 [73]	0.632 [55]	0.6306(5) [75]	0.63002(10) [77]	0.629971(4) [81]
2	0.666 [74]	0.674 [55]	0.6700(6) [75]	0.6717(1) [78]	0.6719 [81]
3	0.704 [74]	0.715 [55]	0.7060(7) [75]	0.7112(5) [79]	0.7121 [81]

Table I.2 – *Values of the critical exponent ν in $d = 3$ for the $O(N)$ model for different values of N and different methods. See [55] for the references of the different values. The NPRG results are reported for the derivative expansion (DE) and for the BMW approximation schemes. PFT stands for Perturbative Field Theory, MC for Monte Carlo studies, and CBS for Conformal Bootstrap methods.*

N	DE	PFT	MC
1	2.024 [22]	2.0237(55) [84]	2.032(4) [85]
2	2.025 [22]	2.026 [86]	
3	2.022 [22]	2.026 [86]	

Table I.3 – *Values of the dynamical exponent z in $d = 3$ for the kinetic $O(N)$ model (model A) for different values of N and different methods. The derivative expansion (DE) results are those of this manuscript and are derived in Chap. III, using a frequency regulator. For $N = 1$, the results are obtained at the second-order of the DE, whereas for $N = 2, 3$ they are obtained at the LPA'. PFT stands for Perturbative Field Theory and MC for Monte Carlo studies. The dynamic exponent z for $N = 2, 3$ is computed using the value of η from [87] and the relation $z = 2 + c\eta$ from [86], which is a relation obtained perturbatively at order ϵ^4, with $\epsilon = 4 - d$. Very few MC studies exist for the determination of z. More details on the determination of this exponent can be found in [88].*

d	1	2	3	4
α (LO)	1/2	0.330(8)	0.173(5)	0.075(4)
α (NLO)	1/2	0.373(1)	0.179(4)	
α (literature)	1/2	0.379(15)	0.300(12)	0.246(7)

Table I.4 – *Values of the roughness exponent α of the Kardar-Parisi-Zhang equation in various dimensions d. LO (Leading Order) and NLO (Next to the Leading Order) are from the NPRG approach in [16]. The references for the literature values can be found in [16]. In $d = 1$ the value of α is known exactly. In $d = 2$ the NPRG is able to reproduce the simulations results to the contrary of the perturbative RG. In $d > 2$ on the other hand the NPRG approach seems to break down as well.*

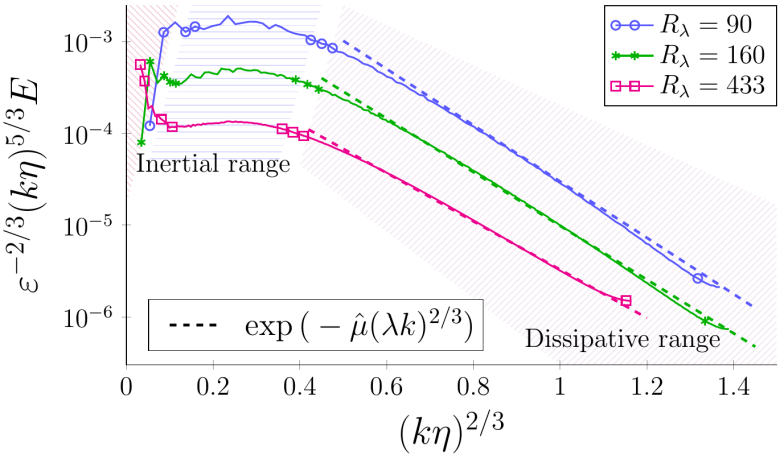

Figure I.9 – *Figure from [15]. Kinetic energy spectra in $d = 3$ obtained from direct numerical simulations at different Taylor-scale Reynolds numbers R_λ plotted in a rescaled dimensionless form against $(k\eta)^{2/3}$ where η is the Kolmogorov length scale at which the energy cascade is finally dissipated, and k is the wave-number. The NPRG predicts a crossover from the $k^{-5/3}$ power-law to a stretched exponential decay $\exp(-\hat{\mu}(\lambda k)^{2/3})$ in the dissipative range (dashed lines), which is observed in the numerical data (plain lines with symbols).*

Reaction-diffusion processes. The reaction-diffusion processes will be the focus of the Chap. II and we will give more details about these systems. But let us already mention that in the case of branching and annihilating random walks (BARW) with the reactions $A \xrightarrow{\sigma} 2A$, $2A \xrightarrow{\lambda} \emptyset$ for instance (see Fig. I.10), the perturbative RG approach is unable (at all orders) to find a phase transition to the absorbing state in dimension greater than two [94] because the phase transition is not perturbatively accessible [95, 96]. This fact is made easily understood when we have access to the phase diagram (see Fig. I.10), on which we see that for $d > 2$ the transition occurs at for a finite value of λ/D. This finite value cannot be reached from a perturbative expansion near $\lambda = 0$. The NPRG, on the other hand, successfully predicts a phase transition in all dimensions [95] (see Fig. I.10), a fact that is corroborated by Monte Carlo simulations, an exact result in the single-site approximation [97], and more recently, by a new perturbative RG approach done in the vicinity of the pure annihilation fixed point ($2A \to \emptyset$) and perturbative in σ [96]. NPRG methods have also provided satisfactory quantitative results for the computation of the critical exponents in these systems [98].

I.4.2 Retrieving the one-loop perturbative results

Let us now address the point (i) of the criticism expressed in the beginning of this section. We show that the NPRG allows us to retrieve the one-loop perturbative results in the general case, and we then give more details in the case of the $O(N)$ model.

I.4.2.a General case

The starting point of the proof is to rewrite the Wetterich equation (I.43) as:

$$\partial_k \Gamma_k = \frac{1}{2} \tilde{\partial}_k \int_q \log\left(\Gamma_k^{(2)} + R_k\right) , \tag{I.73}$$

where $\tilde{\partial}_k$ acts only on the k dependence of R_k, that is

$$\tilde{\partial}_k \equiv \frac{\partial R_k}{\partial k} \frac{\partial}{\partial R_k} . \tag{I.74}$$

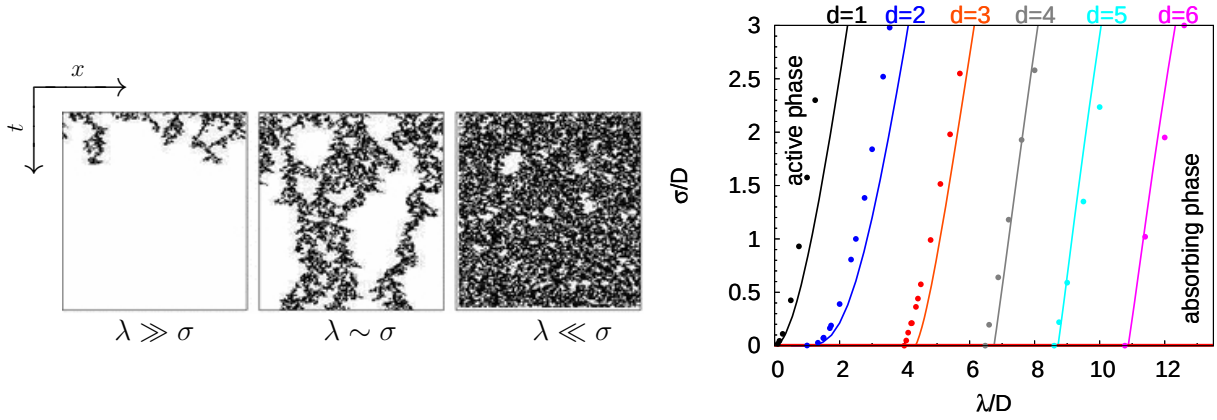

Figure I.10 – *Branching and Annihilating Random Walk with the reactions* $A \xrightarrow{\sigma} 2A$, $2A \xrightarrow{\lambda} \emptyset$ *and diffusion coefficient* D. ***Left:*** *Space-time diagrams of a one-dimensional BARW, from [8]. When* $\lambda \gg \sigma$, *the annihilation dominates and the system ends up in the absorbing state after a finite time, whereas when* $\lambda \ll \sigma$, *the system remains in the active phase. A phase transition occurs for* $\lambda \sim \sigma$. ***Right:*** *Phase diagrams for the same BARW in dimensions* $d = 1$ *to* $d = 6$, *from [54]. Lines present NPRG results, symbols follow from numerical simulations. Whereas the perturbative RG predicts the absence of a phase transition in dimension greater than two, the NPRG is able to capture the transition in all dimensions.*

Written in this form (I.73), the Wetterich equation closely resembles a one-loop equation. Indeed, if one replaces $\Gamma_k^{(2)}$ in the right-hand side by the (second derivative of the) classical action $S^{(2)}$, then the derivative $\tilde{\partial}_k$ can in fact be replaced by the usual derivative ∂_k, and the integration over k can be performed and yields:

$$\Gamma_k[\psi] = \mathcal{S}[\psi] + \frac{1}{2}\int_q \log\left(\mathcal{S}^{(2)}[\psi] + R_k\right) , \tag{I.75}$$

which is the usual one-loop result [14], and we give examples in the following.

I.4.2.b The example of the $O(N)$ model

We now provide slightly more details in the case of the $O(N)$ model, and show how the perturbative results for the critical exponents at the one-loop order can be retrieved from the NPRG flow equations. Even more interestingly, we will see that the NPRG results provide *at least* a clever interpolation between the one-loop perturbative results in $d = 2 + \varepsilon$ and $d = 4 - \varepsilon$.

Since we want to compare the NPRG results with those of the perturbative renormalization group, we consider a similar approximation scheme. We therefore proceed to a lowest-order field expansion of the potential:

$$\hat{U}(\hat{\rho}) = \frac{1}{2}\hat{\lambda}(\hat{\rho} - \hat{\kappa})^2 , \tag{I.76}$$

where the couplings $\hat{\lambda}$ and $\hat{\kappa}$ depend on the scale k, and $\hat{\lambda}$ is the usual ϕ^4 coupling whereas $2\hat{\lambda}\hat{\kappa}$ is the mass term. Within this approximation, the NPRG flow equations for any dimension d and any spin component N reads (details of the calculations can be found in [70]):

$$\partial_s \hat{\kappa} = -(d - 2 + \eta_s)\,\hat{\kappa} + 2v_d(N-1)\ell_1^d(0) + 6v_d\ell_1^d(2\hat{\lambda}\hat{\kappa}) , \tag{I.77a}$$

$$\partial_s \hat{\lambda} = (d - 4 + 2\eta_s)\,\hat{\lambda} + 2v_d(N-1)\hat{\lambda}^2\ell_2^d(0) + 18v_d\hat{\lambda}^2\ell_2^d(2\hat{\lambda}\hat{\kappa}) , \tag{I.77b}$$

$$\eta_s = \frac{16v_d}{d}\hat{\kappa}\hat{\lambda}^2 m_2^d(2\hat{\lambda}\hat{\kappa}) , \tag{I.77c}$$

where v_d is a volume factor, and the functions ℓ_i^j and m_i^j are called the threshold functions, they involve an integration over the momentum y and depend on the regulator $r(y)$ (and its derivatives). Their exact form is not interesting for us and can be found in [70]. Notice however that a signature of the nonperturbative approach is the fact that these threshold functions are non-polynomial. More importantly, notice that in the equations appear a term proportional to $N-1$, and a term in factor of $\ell_1^d(2\hat{\lambda}\hat{\kappa})$. The latter term corresponds to the longitudinal mode (parallel to ψ) which has a mass $2\hat{\lambda}\hat{\kappa}$. The former term correspond to the $N-1$ transverse (or Goldstone) modes, which are massless. In this form, the flow equations reflect explicitly the spontaneous symmetry breaking that occurs at low temperatures [70].

Study in $d = 4 - \varepsilon$. The upper critical dimension of the $O(N)$ model is $d = d_c = 4$, above which the ϕ^4 coupling becomes irrelevant and the long-distance physics is described by a vanishing ϕ^4 coupling: $\hat{\lambda} = 0$. The usual perturbative approach therefore studies the model in dimension $d = 4 - \varepsilon$ where the coupling $\hat{\lambda}$ at the fixed point is of order ε and one can thus performed a series expansion in $\hat{\lambda}$.

We therefore proceed to a series expansion at the lowest nontrivial order in $\hat{\lambda}$ of our Eq. (I.77), that is at second order. At this order, the equation for η_s is of order 3 in $\hat{\lambda}$ and therefore the anomalous dimension vanishes, $\eta_s = 0$. Using the properties of the threshold functions, one can rewrite Eq. (I.77) at lowest order in $\hat{\lambda}$. One obtains:

$$\partial_s \hat{\kappa} = -(2-\varepsilon)\,\hat{\kappa} + \frac{N+2}{16\pi^2}\ell_1^4(0) - \frac{3}{8\pi^2}\hat{\lambda}\hat{\kappa}\,, \tag{I.78a}$$

$$\partial_s \hat{\lambda} = -\varepsilon\hat{\lambda} + \frac{N+8}{16\pi^2}\hat{\lambda}^2\,, \tag{I.78b}$$

$$\eta_s = 0\,. \tag{I.78c}$$

These equations admit a trivial (Gaussian) fixed point $(\hat{\kappa}^* = (N+2)\ell_1^4(0)/(32\pi^2), \hat{\lambda}^* = 0)$ which is stable for $\varepsilon < 0$ (that is $d > 4$), and the nontrivial Wilson-Fisher fixed point [99]:

$$(\hat{\kappa}^*, \hat{\lambda}^*) = \left(\frac{(N+2)\ell_1^4(0)}{32\pi^2}, \frac{16\pi^2\varepsilon}{N+8}\right)\,, \tag{I.79}$$

which becomes stable as soon as $\varepsilon > 0$. We can now compute the expression of the critical exponent ν, which describes how the correlation length ξ diverges near the critical point. This is done by computing the eigenvalues of the stability matrix at the nontrivial fixed point, as explained in Sec. I.2.2.a. One gets:

$$\nu = \frac{1}{2} + \frac{\varepsilon}{4}\frac{N+2}{N+8}\,, \tag{I.80}$$

which does not depend on the regulator, and which indeed coincides with the one-loop perturbative result [31].

Study in $d = 2 + \varepsilon$. We now focus on the lower critical dimension $d = 2$ at which the critical temperature becomes zero for $N > 2$[26]. The usual perturbative approach consists in a low-temperature expansion of the nonlinear σ-model [31]. To compare the NPRG results with those of the usual perturbative approach, we therefore have to link the couplings $\hat{\kappa}$ and $\hat{\lambda}$ to the parameters of the nonlinear σ-model, whose partition function is given by:

$$\mathcal{Z} = \int \mathcal{D}\vec{\phi}\,\delta(\vec{\phi}^2 - 1)\mathrm{e}^{-\frac{1}{2T}\int \mathrm{d}^d x\,(\nabla\vec{\phi})^2}\,. \tag{I.81}$$

[26] For $N = 2$ the $O(2)$ model in $d = 2$ is known as the XY-model, and it undergoes a "topological" phase transition at $T_c \neq 0$, the Berezinskii–Kosterlitz–Thouless phase transition [82, 83].

Therefore, re-expressing the hard unity constraint as an exponential and after a change of variable $\vec{\phi} \to \sqrt{T}\vec{\phi}$, we get:

$$\mathcal{Z} = \int \mathcal{D}\vec{\phi}\, \mathrm{e}^{-\frac{1}{2}\int \mathrm{d}^d x \left[(\nabla\vec{\phi})^2 - g(\vec{\phi}^2 T - 1)^2\right]} \tag{I.82}$$

when $g \to \infty$. This implies that the minimum of the potential $\vec{\phi}^2 = 1/T$ diverges when $T \to 0$, and the low-temperature expansion in this model therefore corresponds to a large $\hat{\kappa}$ (which is the minimum of the potential) expansion in the NPRG approach. Therefore, setting this time $d = 2 + \varepsilon$ and performing a series expansion in $1/\hat{\kappa}$, Eq. (I.77) yields:

$$\partial_s \hat{\kappa} = -\varepsilon\hat{\kappa} + \frac{N-2}{4\pi} \tag{I.83a}$$

$$\partial_s \hat{\lambda} = -2\hat{\lambda} + \frac{N-1}{4\pi}\hat{\lambda}^2 \ell_2^2(0) \tag{I.83b}$$

$$\eta_s = \frac{1}{4\pi\hat{\kappa}} \tag{I.83c}$$

which reproduces the one-loop results of the nonlinear σ-model (after setting $T = 1/2\hat{\kappa}$) and leads to the critical exponents:

$$\nu = \frac{1}{\varepsilon} \quad \text{and} \quad \eta = \frac{\varepsilon}{N-2}\,, \tag{I.84}$$

in agreement with the perturbative expansion at one-loop of the nonlinear σ model [31].

Some remarks about the $O(N)$ model. In the case of the $O(N)$ model, the NPRG proves extremely powerful since the same (lowest-order) approximation (I.76) allows us to retrieve the one-loop perturbative results in $d = 4 - \varepsilon$ and $d = 2 + \varepsilon$. Notice that in the perturbative case, a different model is used for the different dimensions, whereas the NPRG uses the same model and therefore provides an interpolation between the one-loop results between $d = 2$ and $d = 4$.

Of course, between $d = 2$ and $d = 4$ one can compute using the NPRG, with accuracy and with a good quantitative agreement with the experimental/numerical results, the critical exponents of the $O(N)$ model for any value of N (see for instance Tables I.1 and I.2 for the values of the exponents η of ν computed via the NPRG and other methods in $d = 3$. Similar results are available in $d = 2$).

An even more striking result of the NPRG is its ability to capture the physics of the XY-model (or $O(2)$ model) in $d = 2$. Indeed, in $d = 2$, the XY model undergoes a topological phase transition at $T_c \neq 0$ known as the Berezinskii-Kostelitz-Thouless (BKT) phase transition [82, 83], which is usually solved using the Villain approach, which introduces *explicitly* the vortex configurations in the action. The power of the NPRG approach is that at the second-order of the derivative expansion, the qualitative and quantitative features of the BKT phase transition is obtained directly from the microscopic degrees of freedom, and without having to introduce *by hand* the vortex configurations [14, 70, 74].

Finally, the limit $N \to \infty$ is also particularly illuminating since the flow equation for the effective potential $\hat{U}$ can be computed analytically [14, 100, 101]. Indeed, in this limit the flow equation is drastically simplified[27] and for instance the exact values of the critical exponents in $d = 3$ can be computed:

$$\nu = 1 \qquad \beta = 0.5 \qquad \delta = 5 \qquad \gamma = 2 \qquad \eta = 0 \tag{I.85}$$

in agreement with the perturbative results [31].

[27] In the limit $N \to \infty$, the flow of $\hat{U}$ do not depend on $\hat{Z}(\hat{\rho})$, which can be set to one. Accordingly, the anomalous dimension η vanishes.

Two-loop result. Notice that the two-loop perturbative results can also be retrieved using a NPRG scheme (see for instance [23]). Indeed, one can recursively plug the one-loop result (I.75) into the right-hand side of the flow equation (I.73). Performing the k integration, one therefore gets a two-loop equation that allows for retrieving the perturbative results at this order of approximation.

We recall that the Wetterich equation (I.43) being exact, any perturbative approximation can be used on it and yields the corresponding perturbative results. It is however usually not the best way to proceed, and the two-loop results are already quite cumbersome to retrieve through the NPRG formulation.

I.4.3 Controlling the approximations

A common attack from the detractors of the NPRG is the lack of control on the approximations that are performed in the NPRG context, and the dependence on the regulator of the NPRG results. In this subsection, we explain why these claims are unsubstantiated. We focus on the case of the derivative expansion, although the justification for the BMW approximation stems from the same arguments.

I.4.3.a Theoretical justification

The principle of the derivative expansion that has been introduced previously, is that we are mostly interested in the long-distance physics, that is the small-momentum region $|q| \to 0$ of the model. Therefore, when designing an ansatz for the effective average action Γ_k, we perform a series expansion in $|q|$, that is in terms of the derivatives of the magnetization $\nabla\psi$, while keeping all the field dependence. Notice at this point that if we perform on top of the derivative expansion a field expansion, and retain only the lowest nontrivial order, we would get the following ansatz:

$$\Gamma_k[\psi] = \int_x \left[\frac{r_k}{2}\psi^2 + \frac{g_k}{4!}\psi^4 + \frac{1}{2}(\nabla\psi)^2 \right] \tag{I.86}$$

which looks very much like the usual Ginzburg-Landau-Wilson Hamiltonian from which one usually starts a perturbative approach in the coupling constant of the quartic term. The tremendous difference is that this ansatz is for the effective average action Γ_k and not the action $\mathcal{S}$. It will therefore *not* be the starting point of a perturbative expansion, but will be inserted into the *exact* flow equation (I.43).

Let us now give some reasons why the derivative expansion is expected to be a well-behaved approximation. Let us first give a justification based on physical arguments, that we will then refine. The RG scale k, together with the regulator $R_k(q)$ act as if one was considering a system of size k^{-1} instead of an infinite-size system[28]. Therefore, as long as $k > 0$, the system remains away from the phase transition (which occurs only at infinite system size). Thus, even though the free energy Γ is singular at $T = T_c$, this is not the case for the regulated effective average action Γ_k which remains a smooth function as long as $k > 0$. This justifies a series expansion in $\nabla\psi$.

To be more specific, we recall that the Wetterich equation (I.43) involves an integral over all the momenta $0 < |q| < \infty$. If one performs a series expansion of Γ_k at low momentum $|q| \to 0$, and thus of the term $\Gamma_k^{(2)}(q)$ in Eq. (I.43), the question of the validity of this expansion at large $|q|$ has to be asked. This seemingly uncomfortable situation is in fact tackled by the

[28] As we have seen in Sec. I.3.2.a, the role of the regulator is to freeze the fluctuations of the fields with $|q| < k$, which means that their fluctuations decouple from the rest of the system (for which the regulator is almost vanishing). Therefore, the regularized system is not exactly of size k^{-1}, but the modes of the field above this scale do not interact with the rest of the system and may therefore be overlooked.

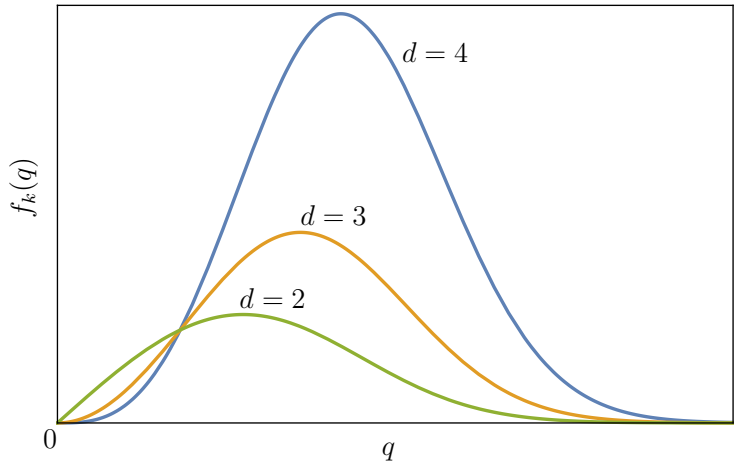

Figure I.11 – *Typical shape of the integrand appearing in the right-hand side of the flow equation (I.43), $f_k(q) = |q|^{d-1}\partial_k R_k(q) G_k(q)$, for various dimension. The factor $|q|^{d-1}$ in $f_k(q)$ comes from the rotational invariance of the integrand. The bumps of the curves are located near $q \simeq k$, which means the momenta which are integrated with a nonvanishing weight are obtained for $q \sim k$.*

regulator term $R_k(q)$ and its derivative $\partial_k R_k$ which ensure that the integrand is nonvanishing only for values of $|q| \lesssim k$, see Fig. I.11. Therefore, the regulator R_k validates a series expansion of Γ_k in power of $|q|/k$ inside the integral, and ensures that the terms with large $|q|$ (where the approximation is not valid) are effectively cut off. We will discuss this question in more details in the introduction of Chap. III.

This justification of the derivative expansion as a meaningful approximating scheme raises two questions (i) the role of the regulator and its influence on the (approximate) results and (ii) the convergence of the expansion as higher and higher terms in the series expansion in $|q|/k$ are added. We discuss these points in the following.

I.4.3.b Role of the regulator

If we were able to solve exactly the flow equation (I.43), the precise choice of the regulator would have no influence on the final result (provided that it vanishes when $k \to 0$ and diverges when $k \to \Lambda$). However, once approximations enter into the game, the specific choice of the regulator affects the quantitative results (see for instance [102]). The influence of the regulator has however to be negligible to validate the whole NPRG formalism.

Of course, the question of the influence of the regulator, and of the choice of an "optimal" regulator are quite difficult to answer since the regulators live in an infinite dimensional space, and the minimal properties that they have to comply with (fast decay when $|q| > k$ etc.) still leave us with infinitely many choices. Many attempts to find the optimal regulator have been carried out, in particular by Litim [49, 103] who argued that the Θ-regulator

$$R_k^{\Theta}(q) = a(k^2 - q^2)\Theta(k^2 - q^2) \tag{I.87}$$

with $a = 1$ is optimal (using a "gap criterion") in the case of the $O(N)$ model and at the lowest order of the derivative expansion (LPA). Moreover, this propagator has the advantage of allowing analytical computation of the momentum integrals [for instance in Eqs. (I.55) and (I.60)]. However, it is not clear whether this regulator is still optimal beyond the LPA [67], and because of the Θ step function, this propagator yields singular contributions to the flow equations when higher order approximations (such as the derivative expansion at the fourth order) are performed and can simply not be used any more [73].

Alternative approaches for finding an optimal regulator have therefore be experimented, for example by adding an extra free parameter a in the definition of the regulator (see for instance [67]). For the exponential regulator, it reads:

$$R_k^{\exp}(q) = \frac{a\, q^2}{\mathrm{e}^{q^2/k^2} - 1}\,. \tag{I.88}$$

This extra parameter a is used to find the "optimal" regulator according to Stevenson's principle of minimal sensitivity (PMS) [104] (see also App. C.2) for each regulator and each approximation scheme.

Fortunately, on the simple $O(N)$ model, the specific choice of the regulator is usually marginal – provided a PMS criterion is used – and the qualitative picture is not influenced by this choice. The quantitative results – especially the value of the critical exponents – are more sensitive to this choice, although the differences are usually small (up to 5%, depending on the critical exponent computed) [67].

This debate is far from being closed: while Litim gap criterion is not satisfactory beyond the LPA, the PMS criterion – although simple to set up for a given choice of regulator – does not allow for a comparison between regulators (Θ versus exponential regulator for instance). Alternative approaches for finding an optimal regulator within a given model and approximation scheme have therefore been proposed in [105] and more recently in [106].

I.4.3.c Approximations and scheme dependence

The question of the regulator, as emphasized throughout this chapter, is crucial, and the fact that the physical quantities eventually depend on it is of course problematic. Finding an optimal regulator also seems difficult and is probably model- and approximation scheme-dependent. However, it is important to recall that this problem is in fact not specific to the NPRG, but is rather inherent to the use of approximations.

In the perturbative RG context, if one were able to compute the perturbative series at all orders, the final result would not depend on the specific scheme used to perform the series expansion. However, since a truncation of this series is made, the arbitrary choices that are made influence crucially the physical quantities that are computed [104]. This is reflected at several levels:

- The choice of the perturbative scheme itself, that is, what is considered as a small parameter in the initial model, is crucial. For instance, we have seen previously that in the case of the directed percolation model, the perturbative RG near the usual, Gaussian fixed point yields wrong prediction, whereas a perturbative scheme near the pure annihilation fixed point is in agreement with NPRG and Monte Carlo results [96]. More generally, the "improved" or "optimized" perturbation theory is often based on perturbative schemes near a fixed point that is not the Gaussian one [104].

- The "scheme dependence": in addition to the crucial dependence on what is considered as a perturbation in the initial mode, the perturbative expansion is also dependent on the several arbitrary choices that are made during the renormalization procedure. For instance, the choice of the renormalization point or of the very definition of the coupling constants used to perform the expansion are arbitrary [107].

- The different resummation schemes that are used to obtain more precise results within a given order of approximation is also subject to many discussions. Indeed, within the RG formalism, the series expansion obtained in terms of the coupling constant is at best

asymptotic, and usually not convergent[29]. However, to extract as much information as possible from the computed terms, Borel resummation techniques can be used on the perturbative series. All the resummation techniques (involving Padé approximants, etc.) would be equivalent if infinitely many terms were available. Since it is not the case, the final result obtained using these different techniques are also dependent on the precise scheme that is used [107].

Of course, physical quantities must be independent of the particular scheme used to renormalize the theory, but this independence breaks down as soon as approximations are made, in the case of the NPRG as well as in the case of the perturbative RG. For the NPRG, the choice of the regulator bears almost entirely this difficulty, while in the perturbative RG the choice of the scheme (which specifies the coupling constant on which the perturbative series expansion is performed) is as crucial as in the nonperturbative case, although this arbitrariness is often overlooked.

I.4.3.d Convergence of the approximations

The last important issue to address concerns the convergence of the approximations: as the order of the series expansion in $|q|/k$ is increased, we expect to obtain results more and more accurate, and that the critical exponents converge toward their exact values. A systematic study of the convergence of the approximations has been carried out for the $O(N)$ model where the derivative expansion has been studied at the order 2, 4 [67, 68], and it is currently under investigation at order 6 [108]. At order 6, the derivative expansion finds critical exponents that are in even better agreement with the Monte Carlo and conformal bootstrap methods than the order 4 of this approximation. For instance, in $d = 3$ and for the Ising model ($N = 1$), one gets the following exponents [108]:

$$\eta = 0.0358 \quad \text{and} \quad \nu = 0.6301\,, \tag{I.89}$$

which can be compared with the results already displayed in Tables I.1 and I.2, and indeed seems to show the convergence of the derivative expansion in the case of the $O(N)$ model.

As a remark, notice that in order to observe the convergence of the derivative expansion, it is necessary to apply the PMS to select the best[30] value of the parameter a appearing in the regulator. This nontrivial convergence of the derivative expansion seems to emphasize the importance of having a criterion to select one particular regulator amongst the family of regulators indexed by the parameter a.

I.5 Conclusion

In this chapter we introduced the nonperturbative renormalization group (NPRG) which is the tool that will be used throughout this manuscript to tackle nonequilibrium critical systems. We have shown that the NPRG is based on Wilson and Kadanoff's idea to compute the fluctuations step by step and in a controlled way. To perform this task, the cornerstone of the NPRG approach is its regulator function $R_k(q)$ which freezes the fluctuations that take place at scales $|q| \lesssim k$. The regulator combines two roles: (i) by freezing the small momenta fluctuations it puts the system out of criticality as long as $k \neq 0$, and one therefore manipulates functions that are analytic. (ii) It ensures, during the integration of the fluctuations which is performed smoothly

[29] Notice that in quantum electrodynamics (QED), the coupling constant (the fine-structure constant) is indeed small and the first orders of the perturbative expansion usually yield good predictions. The situation is different in critical systems where the coupling constants are usually of order one.

[30] That is the value which renders stationary the dependence of the physical results on the regulator (see also App. C.2).

using a partial differential equation, that only the fluctuations that are well-described by the approximation schemes are computed, the non-controlled part being cut off by the regulator. Because of its key importance, Chap. III will be devoted to designing a proper regulator for out-of-equilibrium systems. Indeed, as we will see, in a nonequilibrium context, the temporal fluctuations have to be treated on the same footing as the spatial fluctuations.

We have also tried in this chapter to highlight some of the successes of the NPRG approach, focusing on the nonequilibrium systems that are our main interest here. However, this does not mean in any way that a perturbative RG method is always useless: the perturbative approach still remains a powerful theoretical tools that have cracked many problems out-of-equilibrium and it often offers a first theoretical description of the phenomena. However, when indications hint toward nonperturbative features (as it is the case in the KPZ equation for instance), or when the perturbative approach breaks down for unknown reasons (as it is the case for the pair-contact process with diffusion (PCPD), a reaction-diffusion process that we describe in the next chapter), alternative options such as nonperturbative methods should not be discarded.

To conclude, the NPRG formalism is not miraculous and relies on approximations as well as the perturbative RG. Higher-order approximation schemes such as the derivative expansion at fourth order are as computationally demanding as high-order loop expansion in a perturbative scheme. The regulator dependence in the NPRG context is also problematic, and so is the scheme dependence in the perturbative RG procedure. Finally, although we have shown some examples where the NPRG approach is promising (and we will see more of them in the following chapters), some physical systems are still beyond the reach of the NPRG: it is a tool amongst others, that should be used to validate and support other approaches, or replace them when they fail.

Chapter II

Out-of-equilibrium phase transitions

Contents

In the previous chapter we have given a description of the phase transitions occurring at equilibrium, and have underlined the scaling-behaviour they display at criticality. Surprisingly, systems which are sometimes very different at the microscopic level are found to display the same critical behaviour (that is, share the same set of critical exponents and scaling functions), hence forming a universality class. We have also introduced the renormalization group (RG) – and especially its nonperturbative version – which is able to explain qualitatively the existence of these universality classes by showing that the microscopic details are in fact washed out at criticality when the system acts as a whole. The RG techniques have also proven very powerful to compute, quantitatively, the value of the critical exponents of some universality classes at equilibrium.

In this chapter and in the following, we will be interested in phase transitions and critical phenomena that take place out of equilibrium. Out-of-equilibrium phenomena are of course much more numerous, rich and widespread than their equilibrium counterparts, but they are also more difficult to tackle on the theoretical point of view, since some basic tools of equilibrium statistical physics are not as efficient out of equilibrium. In this context, one can wonder how the global understanding we have of phase transitions translates to nonequilibrium systems:

are there universality classes? Is there an equivalent to the Ising model, that is a simple model that would allow us to fully understand critical properties? Can we apply the perturbative or nonperturbative RG techniques to compute the associated critical exponents?

The answer to these questions is not straightforward. As this chapter and the following ones will illustrate, there exist many "out-of-equilibrium" physics, and one of the difficulty that arises when leaving the equilibrium world is to deal with the plethora of systems that come up. Some systems for instance are said to be close to equilibrium – usually because some variant of a fluctuation-dissipation theorem holds –, and are relatively well-understood. For this reason, they are the starting point of a theoretical study in Chap. III.

On the other hand, many systems are said to be far from equilibrium and may display very exotic behaviours: this is the case of systems with an absorbing state on which we focus in this chapter. These systems have the peculiarity of possessing a state which, once reached by the system, cannot be left. This state is therefore called absorbing and is very different from what is known at equilibrium because the system stops fluctuating once it has reached it, and the dynamics is stopped. Other systems, and that will be the case of erosion models in Chap. IV, are also very peculiar because they display criticality without fine-tuning any parameter (usually the temperature). Scale-invariance (in landscapes for instance) will therefore appear naturally in these systems, and the RG will be the tool of choice to handle them.

Despite the large variety of nonequilibrium models and the nontrivial behaviour they display, many progresses in characterizing them have been achieved in the last decades. Through the systematic use of numerical simulations and RG techniques, several very broad universality classes have emerged, such as the Kardar-Parisi-Zhang (KPZ) universality class which gather models describing growth processes, front propagation and kinetic roughening phenomena (such as the front of a forest fire or coffee particles accumulating at the edge of a coffee drop), randomly stirred fluid (Burgers' equation), directed polymers in random media [109, 110], landscape erosion [25], random matrix theory [41], etc. Another vast universality class that we will encounter in this manuscript is the directed percolation (DP) universality class, which, initially stated for the description of a fluid flowing by gravity through a porous medium, has been found to describe epidemics processes – at least at the metaphorical level –, forest fire, diffusion in disordered media, catalytic chemical reactions, etc.

However, the picture is not as bright as one could imagine: in the case of the KPZ universality class for instance, RG techniques have long been doomed to failure in space dimension greater than one until recent advances made by the NPRG[1] [16]. As for the directed percolation class, the situation is also much more complicated and discussions about the very existence of the transition above two dimensions[2] was at stake until recently (more details will be given in the following). In addition, a process that looks much alike to directed percolation , the pair-contact process with diffusion for instance, is still elusive to a proper characterization and both numerical and theoretical studies are unable to prove whether it belongs to an already existing universality class or if it forms a different one [111].

These unanswered questions and theoretical difficulties therefore require proper tools to be addressed. In this chapter, we will therefore explain how nonequilibrium models can be described, either in a coarse-grained version using Langevin equations, or taking into account the microscopic details via a master equation approach. Our main goal will be to derive the field theory associated both to the Langevin and to the master equation formalism, which will be our starting point for translating the NPRG formalism to nonequilibrium systems in Chap. III and IV.

In this chapter we also provide a novel approach – and this is one of the main results of this manuscript [19] – to derive an *exact* (that is not stated in terms of a coarse-grained field)

[1] Notice that if the NPRG is able to give results in $d = 2$ for the KPZ equation, it still encounters difficulties in $d > 3$.

[2] For a particular reaction-diffusion process for which the one-particle decay is not considered in the microscopic description [35].

Langevin equation describing the dynamics of a microscopic system. Although similar methods have long existed in the literature to achieve such exact description, we will show that these approaches are either incorrect, or lead to ambiguous imaginary-noise Langevin equations that are unusable in practice for both numerical and theoretical treatment.

II.1 Summary of the different Langevin equations

At the end of this chapter (page 92) is displayed Table II.1 that summarizes the different approaches that will be discussed throughout this chapter and that lead to a Langevin equation for a reaction-diffusion process. The two first methods (Gillespie's and van Kampen's) are only approximate methods, and the Langevin equations obtained using them are therefore stated in terms of a coarse-grained variable. The approximate coarse-graining procedure makes these methods particularly efficient when applied to complicated systems possibly involving several species of particles. These methods however break down when the particle number is low, for instance near a transition to an absorbing state. These methods are explained and derived in Sec. II.4.1.

The three other methods (Poisson representation, *formal* field-theoretical method and duality formalism) are on the other hand supposed to describe the *exact* dynamics of the microscopic reaction-diffusion process, and are therefore not stated in terms of a coarse-grained variable, but on an auxiliary variable which does not have a direct physical meaning [and the table also provides the link between the moments of the reaction-diffusion (RD) process and those of the Langevin variable (LE)]. For this reason, they are believed to be an efficient tool for studying transitions to an absorbing state. The usual derivation of the Poisson representation and the formal field-theoretical method are given in Sec. II.4.2, where we will argue that they are incorrect and lead to inconsistencies. The corresponding Langevin equations in these two cases should therefore be treated with care, especially when they involve imaginary noise (more details will be given in the following).

Accordingly to the purpose of studying low-density states and having an exact description of the microscopic dynamics, the last method (the duality formalism) stands out of the crowd since it provides only *real* Langevin equations, to the contrary of the two others that can also produce complex Langevin equations. For reasons that we explain later on in this chapter, complex Langevin equations are usually not useful in practice, and their numerical integration is plagued with instabilities. The derivation of these dual Langevin equation is the first main result of this manuscript, and is given in Sec. II.5.

II.2 Mesoscopic description: the Langevin equation

Historically, the description of nonequilibrium phenomena has started with the study of the Brownian motion, first experimentally with the seminal work of Robert Brown in 1828 and its description of the erratic motion of a pollen particle in water[3] [113]. A more formal description then appeared in the works of Louis Bachelier [114] and Albert Einstein [115], and then Paul Langevin [116], who gave its name to the stochastic equations on which the focus is set in this section.

The description of the Brownian motion of a particle led to several mathematical difficulties: how to take into account the stochastic nature of the motion? How to write an equation of motion for a process that is continuous but nowhere differentiable? On this aspect, the works of several mathematicians such as Wiener, Kolmogorov, and Itō (amongst many) gave the proper

[3] In fact, Jan Ingen-Housz had already noticed in 1784 the erratic motion of ground charcoal in alcohol [112].

background for a well-defined description of the phenomenon and set the bases of the stochastic calculus, which is now widely used in the study of nonequilibrium phenomena.

In this section we will therefore briefly introduce the formalism and some of the difficulties than can be encountered. We also highlight some reasons that can explain why the Langevin formalism has become so popular to describe nonequilibrium phenomena. In essence, there are at least two main reasons that explain the enthusiasm for Langevin equations: (i) they provide a simple heuristic description at a mesoscopic scale, such that the perfect knowledge of the underlying microscopic dynamics is not necessary. (ii) They are the starting point for both numerical and theoretical treatments (in particular, we will show in a second part how a Langevin equation can be cast into a path-integral formulation).

II.2.1 A phenomenological approach

Langevin equations are ubiquitous in out-of-equilibrium statistical physics [117] because they offer a simple and intuitive way of describing nonequilibrium systems [118, 119]. Indeed, in addition to the classical, macroscopic description of a system by an equation of motion, one adds a noise term represents the effects of the microscopic degrees of freedom not taken into account in the macroscopic equation. The deterministic part of the Langevin equation therefore expresses the "mean-field" description of the model while the noise term appears as a correction to this mean-field terms coming from the microscopic fluctuations. The Langevin description is therefore made at a mesoscopic scale: the microscopic degrees of freedom are coarse-grained into a noise term, while the macroscopic forces are also acting on the dynamics. This mesoscopic, coarse-grained description is probably the key of the success of this description, because a precise knowledge of the microscopic details is not required to write down a sensible Langevin equation that yet captures the correct macroscopic picture. Despite the simplicity of this phenomenological approach, we will see with a few examples that designing the properties of the noise term is of crucial importance and therefore requires a particular care. Indeed, by contrast to the equilibrium case, in the nonequilibrium context there is no simple equivalent of the fluctuation-dissipation theorem to dictate the form of the noise correlations [7].

II.2.1.a Brownian motion

To illustrate the Langevin approach, let us start with the simple and historical description of the motion of a pollen particle of mass m in water, the Brownian motion. The Langevin equation of motion takes the following form:

$$m\partial_t v(x,t) = -\gamma v(x,t) + \zeta(x,t) \tag{II.1}$$

where $v(x,t)$ is the speed of the pollen particle, γ is the drag coefficient, and $\zeta(x,t)$ is a Gaussian white noise. The simplicity of the Langevin description in this simple case is striking: to the Newton's equation of motion which describes the macroscopic motion of the particle is added the noise term which takes into account the shocks of the water molecules with the Brownian pollen particle and accounts for its erratic motion. Of course, despite this simple form, the underlying mathematical and physical content is already rich and nontrivial.

II.2.1.b Law of mass action

To unveil more subtleties of the Langevin description, we focus on the description of a chemical reaction which provides us with an example of non-Gaussian noise term.

Describing a chemical reaction using a differential equation has a long history since it started in 1850 when Ludwig Wilhelmy used an (ordinary) differential equation to characterize the

evolution of the concentration in the conversion of sucrose into glucose [120]. For example, a reaction $A + B \xrightarrow{\mu} C$ is described at the mean-field level by the law of mass action, which reads:

$$\partial_t \rho_A(t) = -\mu \rho_A(t) \rho_B(t) \tag{II.2}$$

where $\rho_{A,B}(t)$ are respectively the density of particles A or B at time t, assuming that the system is perfectly stirred. A richer description is possible by allowing spatial heterogeneity in the system:

$$\partial_t \rho_A(x,t) = -\mu \rho_A(x,t) \rho_B(x,t) + D_A \nabla^2 \rho_A(x,t) + D_B \nabla^2 \rho_B(x,t) \tag{II.3}$$

where $D_{A,B}$ are the diffusion coefficients of the particles A and B. This description therefore allows for spatial fluctuations of the density and a very rich physics can already be described through this formalism: pattern formation (for example in morphogenesis [121]), oscillating reactions [122], genetics [123, 124], etc.

However, this description remains at a mean-field level and do not capture all the physics, especially when the density of particles becomes small. In fact, we know from quantum mechanics that a chemical reaction is also subject to an intrinsic randomness and the encounter of a particle A and a particle B does not surely imply a chemical reaction. Furthermore, as in the case of the Brownian motion, the motion of the particles is also erratic. We can therefore treat this randomness heuristically and introduce for this purpose a reaction rate (that is, a probability that the reaction occurs) and refine our description by including a noise $\xi(\rho_{A,B}; x, t)$ modelling the randomness of the microscopic details. This time, the noise itself should depend on the density of particles, and one expects in particular that when either $\rho_A = 0$ or $\rho_B = 0$, the noise term vanishes since no reaction can happen. This starts to highlight the difficulties that can be encountered when writing a noise term and the question of finding the precise form of the noise probability distribution will be the guiding thread of this chapter.

II.2.1.c Noise term

The previous example highlights one of the main difficulty when describing a system by a Langevin equation: its noise term. This noise term obviously accounts for a large part of the underlying physics, and different noise terms describe very different physical systems.

Additive noises. Even in the case of a noise term that does not depend on the density field ρ but only on time and/or space – an additive noise –, the behaviour of the system can change dramatically when the noise probability distribution is modified. The simpler Langevin systems usually involve a Gaussian white noise, as it is the case for the Brownian motion (II.1). This kind of noise is in fact quite ubiquitous in nature since it reflects the central-limit theorem, and the fact that if the underlying degrees of freedom represented by the noise term are not correlated, then the sum of their contributions has a Gaussian distribution. Therefore, even if the Gaussian white noise represents the simplest additive noise term, it already encompasses a wealth of phenomena. For instance, in Chap. III, we will see that the fluctuations of the dynamics of the Ising model are well taken into account by this simple noise.

The family of the additive noises is of course infinitely larger than the Gaussian noises, since they may display any probability distribution. A famous family amongst the non-Gaussian noises are the Lévy flights (or Lévy processes) for which the probability distribution does not have a fast decay as in the Gaussian case, but rather has an heavy-tailed probability distribution and a decay in power law. This kind of noises are used to describe for instance the foraging behaviour of animals or bacteria (see for instance [125]), but can also be used to describe epidemics propagation since they catch to some extend the basics of human mobility patterns (for instance [126]).

Multiplicative noises. In addition to the probability distribution of the noise, which itself plays a major role, the dependence of the noise in the density field makes the Langevin description even more richer, and complicated. A first classification of these noise terms depending on the fields can be done by expanding them in term of the density and writing:

$$\xi(\rho; x, t) = \rho^{\gamma}\zeta(x, t) \tag{II.4}$$

where $\zeta(x, t)$ is now a Gaussian noise (possibly not δ-correlated). Such a noise is called multiplicative, because a Gaussian noise is multiplied to the density field to a certain power γ. Depending on the exponent γ, very different behaviours are expected. For example,

- $\gamma = 0$ corresponds to an additive noise.
- $\gamma = 1/2$ appears when describing reaction-diffusion processes, that we will encounter and present in more details in the next section. This kind of noise is usually associated with systems displaying a phase transition between an active phase – in which the system has nontrivial activity and fluctuations – and an absorbing phase – where the system is trapped forever once it has reached it and where no fluctuation occurs. We will have a special interest in these phase transitions in the following.
- $\gamma = 1$ appears for instance in the famous Kardar-Parisi-Zhang equation[4] which was first derived in the context of the growth of an interface [13], but is also the main representative of a quite broad universality class. Moreover, we shall see in Chap. IV that the KPZ equation is also a sensible model for the erosion of landscape.

These few examples illustrate the crucial role of the noise term when describing a nonequilibrium process, since an unmotivated choice can easily lead to a completely different model and a different universality class. For this reason, models for which the noise term can be deduced from the microscopic dynamics play a special role and have been studied accordingly. A large part of this chapter is devoted to the derivation of noise terms, either in an approximate, or exact manner.

II.2.1.d Transition to an absorbing state

Amongst the Langevin equations with multiplicative noise, we are particularly interested in those describing a system with an absorbing state (see Fig. II.1 for an example of a reaction-diffusion system exhibiting a transition to an absorbing state). In general, such processes can be written as a Langevin equation with a square-root noise and take the form:

$$\partial_t\rho(x, t) = D\nabla^2\rho + A(\rho) + \sqrt{2B(\rho)}\,\zeta(x, t) \tag{II.5}$$

where $\rho(x, t)$ is for instance a density field, D is the diffusion constant and $\zeta(x, t)$ is a Gaussian noise. The function $A(\rho)$ is a drift term, and $B(\rho)$ is positive and vanishes for some values ρ_0. An absorbing phase is a special state of the system which once reached cannot be left: in the previous equation, it corresponds to ρ_0 with the extra condition $A(\rho_0) = 0$, and a system may have several absorbing states. Such transitions to an absorbing state are genuinely out-of-equilibrium because, by definition, there cannot be microscopic reversibility near such a state. The two phases, the absorbing phase from which the system cannot escape, and the active phase where the system evolves according to a given dynamics, are therefore very unlike. In particular, the absorbing state is not subject to fluctuations (the noise term $B(\rho_0)$ vanishes), which is very different from the equilibrium picture where fluctuations exist on the both sides of a phase transition.

[4] In its Cole-Hopf version involving a "density" field rather than the usual description in terms of the height of the interface.

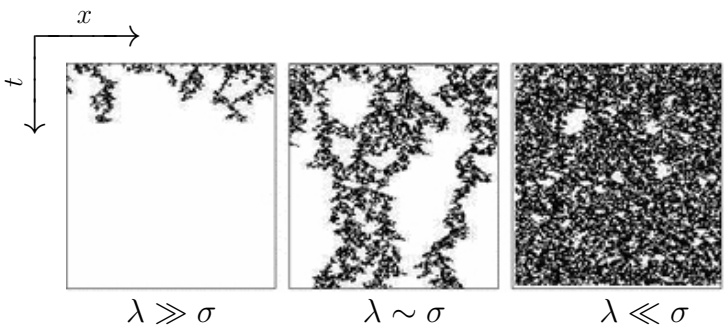

Figure II.1 – *Figure from [8]. Temporal evolution of a one-dimensional reaction-diffusion process with reactions* $A \xrightarrow{\sigma} 2A$ *and* $2A \xrightarrow{\lambda} \emptyset$*. Initially there is a particle on each site on the* x *axis. When the branching rate* σ *is large compared to the annihilation rate* λ*, the particles keep reacting and the system is in the active state, where nontrivial density fluctuations are observed* ***(right panel)****. To the contrary, if annihilation dominates, all particles annihilate exponentially fast and the system terminates in a nonfluctuating absorbing state from which it cannot escape* ***(left panel)****.*

This very special kind of transitions has therefore stirred a very enthusiastic research and some major steps have been achieved, for example the existence of a very wide universality class, called the directed percolation (DP) universality class (on which we give more details in the following), was unravelled. However, and in particular because of the numerical difficulties that such transitions imply, many shades of unknown still remain: some processes, very similar to those belonging to the directed percolation universality class still have an unclear status, and whether they belong to the directed percolation class or if they form a new universality class with different critical exponents is still an open question (see Sec. II.3.1.c). We shall come back on this matter later in this chapter when we discuss reaction-diffusion processes.

Finally, note that the systematic study of these processes using numerical simulations is a quite demanding task: as we will see in the next section, some tricks are necessary to solve them without violating the positivity condition on $B(\rho)$. The other difficulty that arises in the vicinity of these special states comes from the fact that the particle density is usually low, and approximate methods for deriving Langevin equations generally rely on a large density assumption (see Sec. II.4.1). These methods are usually unable (or even false) to describe properly the phase transition, especially near an extinction transition where the particle density ρ goes to zero. Our goal in the following will therefore be to derive an *exact* Langevin equation for this kind of systems, in order to have a precise description of the low density regions which play a crucial role near the phase transition.

II.2.2 Numerical resolution of a Langevin equation

The great versatility of the Langevin equations, and the fact that they are relatively simple to write imply that they often appear in the description of out-of-equilibrium systems. A numerical resolution of these equations is often a first step for studying them, or is used to compare the numerical results with the theoretical predictions. Also, because a Langevin equation is usually a coarse-grained approach of a complicated microscopic system, simulating a Langevin equation can be much easier than simulating (usually with Monte Carlo methods) the underlying microscopic process. Having a fast and reliable numerical scheme to solve these equations is therefore often a necessary condition for studying out-of-equilibrium processes.

However, some Langevin equations, in particular those involving square-root multiplicative noises such as Eq. (II.5), which correspond to systems with absorbing states, are especially difficult to solve numerically, and we explain rapidly what are the usual schemes that overcome these difficulties. This kind of Langevin equations raise numerical difficulties if not treated

properly: for instance, even a zero-dimensional version of the Eq. (II.5), studied using an explicit Euler scheme reads:

$$\rho(t+\Delta t) = \rho(t) + A(\rho(t))\Delta t + \sqrt{2B(\rho(t))\Delta t}\,\mathcal{N}(0,1) \tag{II.6}$$

where $\mathcal{N}(0,1)$ is a normal random variable. At each time step $\Delta t > 0$, there is a finite probability that $B(\rho)$ becomes negative, which is unphysical. These nonphysical values of ρ happen all the more often as one gets closer to the values where $B(\rho) \simeq 0$, which is also the absorbing state and thus the interesting point when studying transitions to an absorbing state. Another route, which would trade the square-root noise term for a less singular term using for example a Cole-Hopf transform (of the form $\rho = \mathrm{e}^{-\phi}$) is also a dead end since it generates pathological deterministic terms when the original variable ρ goes to 0 [127].

To tackle this numerical issue, several schemes have been proposed that guarantee the positivity of the Langevin variable at all time, and we now review them quickly.

Dickman's algorithm. Dickman for instance proposed to discretize the values that can be taken by the field ρ [128]. Quite ironically, this scheme breaks the continuous nature of the Langevin equation and retrieves the discrete nature that was the signature of the original microscopic system. This is in fact problematic since this algorithm is then plagued with the same long transients near the phase transitions as the microscopic models. Finally, as for the Euler approximation (II.6), Dickman's approach has a precision of order $\mathcal{O}(\sqrt{\Delta t})$ as $\Delta t \to 0$.

Balanced implicit methods. The balanced implicit methods (BIM) is an algorithm introduced by Schurz and co-workers [129, 130] which uses implicit Euler methods to impose the nonnegativity of the solution. It has the same order of convergence as the Euler algorithm, that is an error of order $\mathcal{O}(\sqrt{\Delta t})$ as $\Delta t \to 0$ for approximations of individual trajectories, but it guarantees that the term appearing under the square-root remains positive. However, as well as for the Euler approximation (II.6), Schurz's algorithm fails to reproduce the large density fluctuations at low density.

Splitting-operator scheme. The so-called "splitting-operator" scheme was first proposed by Pechenik and Levine [131] and then improved by Dornic, Chaté and Muñoz [127]. Let us describe this algorithm in zero-dimension for simplicity, although the main asset of this algorithm is that it can be used for spatially-extended systems as well. The idea is to split the Langevin equation (II.5) into two parts, (i) the deterministic part $A(\rho)$, and (ii) the stochastic term $\sqrt{2B(\rho)}\,\zeta$. In a first step, the noise term (ii) is sampled *exactly*, that is not by using a Gaussian random number (which would lead to negative ρ), but using directly the probability distribution computed from the Fokker-Planck equation associated with the noise term $\sqrt{2B(\rho)}\,\zeta$. In other words, a random number ρ^* is generated using the exact probability distribution $p(\rho,t)$, which is computed by solving the Fokker-Planck equation associated with $\partial_t \rho = \sqrt{2B(\rho)}\,\zeta$, that is $\partial_t p(\rho,t) = \partial_\rho^2[B(\rho)p(\rho,t)]$. We then use this number ρ^* to evolve the remaining part (the deterministic part) of the Langevin equation, that is $\rho(t+\Delta t) = \rho^* + A(\rho^*)$. Notice that although this algorithm is very powerful and enables to probe much larger simulation times than Dickman's algorithm for instance (see Fig. II.2), the implementation of this algorithm yet requires to know exactly the probability distribution corresponding to the Fokker-Planck equation $\partial_t p(\rho,t) = \partial_\rho^2[B(\rho)p(\rho,t)]$. If this is not the case, then one has to sample this distribution using a Monte-Carlo method and the algorithm looses its computational efficiency. For more details see [127, 132], and [133] for a comparison between Dickman, BIM and splitting-operator algorithms (and see also [134] for a proof of the equivalence between the different splitting-operator algorithms).

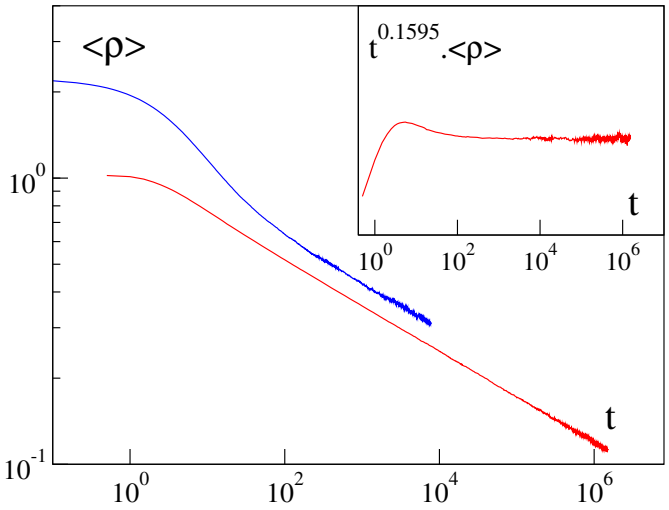

Figure II.2 – *Figure from [127]. Density decay* $\langle\rho\rangle \equiv \langle\rho(x,t)\rangle_x \sim t^{-\theta}$ *in a directed percolation process at criticality in dimension* $d = 1$*. The upper (blue) curve is obtained using Dickman's method with* $\Delta t = 10^{-3}$ *while the lower (red) curve is obtained using the Splitting-operator scheme, with* $\Delta t = 0.25$*. The inset shows the plateau of the decay exponent.*

II.2.3 Field theory for a Langevin equation

Now that we have shown how a nonequilibrium process can be stated in terms of a Langevin equation, we discuss how this equation can be cast into a field theory, in order to be able to apply standard and nonperturbative renormalization group techniques and thus study phase transitions occuring in this out-of-equilibrium context. The usual approach – derived by Martin, Siggia and Rose [135] – consists in employing an auxiliary field, called the response-field for reasons that will become clear in the following, to express the Langevin equation in a path-integral formalism. This auxiliary field is then used to build a response functional whose formulation originates from parallel works of Janssen [136] and De Dominicis [137]. For these reasons, the formalism is usually known in the literature as the MSRDJ or response-field formalism, and its derivation goes as follow: starting from a generic Langevin equation of the form

$$\partial_t \phi(x,t) = F(\phi) + K(\phi)\,\zeta(x,t) \tag{II.7}$$

where $\phi(x,t)$ is a coarse-grained field, F a macroscopic force acting on it (possibly involving diffusion), $\zeta(x,t)$ is a Gaussian white noise and K is the noise kernel, depending on the field ϕ and possibly adding space or time correlations to the white noise.

The starting point for the response-function formalism is to write down the expectation value [over the realizations of the noise $\zeta(x,t)$] of an observable $\mathcal{O}[\phi(x,t)]$:

$$\langle \mathcal{O}[\phi] \rangle_\zeta = \int \mathcal{D}\zeta\, P(\zeta) \mathcal{O}[\phi_\zeta] \tag{II.8}$$

where $\phi_\zeta \equiv \phi_\zeta(x,t)$ is the solution of the Langevin equation (II.7) for a given realization $\zeta(x,t)$ of the noise, and $P(\zeta)$ is the distribution of the noise. Since it is a Gaussian white noise, it reads:

$$P(\zeta) \propto \mathrm{e}^{-1/4 \int_{\boldsymbol{x}} \zeta(\boldsymbol{x})^2} \tag{II.9}$$

where we have defined $\boldsymbol{x} \equiv (x,t)$ and $\int_{\boldsymbol{x}} \equiv \int_{x,t}$. The above formula yields in particular the following correlations:

$$\left\langle \zeta(\boldsymbol{x})\zeta(\boldsymbol{x}') \right\rangle = 2\,\delta(t-t')\delta^d(x-x')\,. \tag{II.10}$$

The average value of the observable $\mathcal{O}$ can be rewritten as:

$$\langle \mathcal{O}[\phi] \rangle_\zeta = \int \mathcal{D}\zeta \, P(\zeta) \int \mathcal{D}\phi \, \delta \left[\phi(\boldsymbol{x}) - \phi_\zeta(\boldsymbol{x}) \right] \mathcal{O}[\phi] \, . \tag{II.11}$$

Using, by analogy, the usual property of the Dirac distribution $\delta(x - x_0) = |f'(x_0)| \, \delta(f(x))$, the previous formula now reads:

$$\langle \mathcal{O}[\phi] \rangle_\zeta = \int \mathcal{D}\zeta \, P(\zeta) \int \mathcal{D}\phi \, \delta(\mathcal{C}[\phi(x,t)]) \mathcal{J}[\phi] \mathcal{O}[\phi] \tag{II.12}$$

where $\mathcal{C}[\phi(\boldsymbol{x})] = \partial_t \phi(\boldsymbol{x}) - F(\phi) - K(\phi) \, \zeta(\boldsymbol{x})$ and $\mathcal{J}[\phi]$ is the Jacobian of the transformation, that is $\mathcal{J}[\phi] = |\det \left(\delta \mathcal{C}[\phi] / \delta \phi \right)|$. We prove in the following that choosing an Itō discretization in the initial Langevin equation is equivalent to setting this Jacobian to unity, and we therefore set $\mathcal{J}[\phi] = 1$ from now on.

Then, using the integral definition of the Dirac distribution $\delta(x) = \int_q \mathrm{e}^{-iqx}$, one gets:

$$\langle \mathcal{O}[\phi] \rangle_\zeta = \int \mathcal{D}\zeta \, P(\zeta) \int \mathcal{D}\phi \mathcal{D}\tilde{\phi} \, \mathrm{e}^{- \int_{\boldsymbol{x}} \tilde{\phi}(\boldsymbol{x}) [\partial_t \phi(\boldsymbol{x}) - F(\phi) - K(\phi) \, \zeta(\boldsymbol{x})]} \mathcal{O}[\phi] \tag{II.13}$$

where we have introduced the response-field $\tilde{\phi}(\boldsymbol{x})$, which is a purely imaginary field. At this point, one notices that the integration over the noise $\zeta(\boldsymbol{x})$ can be easily computed since it is a Gaussian integral. Integrating over the noise therefore finally yields the field-theoretical description of the Langevin equation (II.7):

$$\langle \mathcal{O}[\phi] \rangle_\zeta = \int \mathcal{D}\phi \mathcal{D}\tilde{\phi} \, \mathrm{e}^{-\mathcal{S}_{\mathrm{LE}}[\phi, \tilde{\phi}]} \mathcal{O}[\phi] \tag{II.14}$$

where $\mathcal{S}_{\mathrm{LE}}[\phi, \tilde{\phi}]$ is the Janssen-De Dominicis [136, 137] response functional, also called action by analogy with its equilibrium counterpart, and reads:

$$\mathcal{S}_{\mathrm{LE}}[\phi, \tilde{\phi}] = \int_{x,t} \tilde{\phi} \left(\partial_t \phi - F(\phi) - K(\phi)^2 \, \tilde{\phi} \right) , \tag{II.15}$$

and we have omitted the time and spatial dependence of the fields for simplicity. By analogy with equilibrium, one usually defines the "partition function" $\mathcal{Z}_{\mathrm{LE}}[J, \tilde{J}]$ which is in fact the generating functional of the correlation and response functions, and reads:

$$\mathcal{Z}_{\mathrm{LE}}[J, \tilde{J}] = \int \mathcal{D}\phi \mathcal{D}\tilde{\phi} \, \mathrm{e}^{-\mathcal{S}_{\mathrm{LE}}[\phi, \tilde{\phi}] + \int_{x,t} (J\phi + \tilde{J}\tilde{\phi})} \, . \tag{II.16}$$

Notice that within this formalism, the linear response function $\chi(\boldsymbol{x}, \boldsymbol{x}')$ is defined to be the variation of the mean value of the field ϕ at time t and position x caused by the variation of the external source J coupled to ϕ at time t' and position x'. Mathematically, it reads:

$$\chi(\boldsymbol{x}, \boldsymbol{x}') \equiv \left. \frac{\langle \delta \phi(\boldsymbol{x}) \rangle}{\delta J(\boldsymbol{x}')} \right|_{J \to 0} . \tag{II.17}$$

According to the generating function $\mathcal{Z}_{\mathrm{LE}}$ defined just above in Eq. (II.96), the response function reads:

$$\chi(\boldsymbol{x}, \boldsymbol{x}') = \left\langle \tilde{\phi}(\boldsymbol{x}') \phi(\boldsymbol{x}) \right\rangle , \tag{II.18}$$

and for this reason the auxiliary field $\tilde{\phi}$ is usually known as the response-field.

II.2.3.a Onsager-Machlup action

Notice that an alternative description of the same stochastic process can be obtained by integrating at an earlier stage over the noise, and therefore not introducing the response-field $\tilde{\phi}$. It yields a more complicated action, but depending only on a single field. We remind from the previous section that we had:

$$\langle \mathcal{O}[\phi] \rangle_\zeta = \int \mathcal{D}\zeta \, P(\zeta) \int \mathcal{D}\phi \, \delta(\mathcal{C}[\phi(\boldsymbol{x})]) \mathcal{J}[\phi] \mathcal{O}[\phi] \tag{II.19}$$

$$\propto \int \mathcal{D}\phi \mathcal{D}\zeta \, \mathcal{J}[\phi] \mathcal{O}[\phi] \mathrm{e}^{-\frac{1}{4}\int_{\boldsymbol{x}} \zeta(\boldsymbol{x})^2} \delta\left[\partial_t \phi(\boldsymbol{x}) - F(\phi) - K(\phi)\,\zeta(\boldsymbol{x})\right] \tag{II.20}$$

The integration over the noise is straightforward and yields the Onsager-Machulp functional:

$$\langle \mathcal{O}[\phi] \rangle_\zeta = \int \mathcal{D}\phi \, \mathcal{J}[\phi] \mathcal{O}[\phi] \, \exp\left(-\frac{1}{2} \int_{\boldsymbol{x}} \left[\partial_t \phi - F(\phi)\right]^2 K^{-1}(\phi) \right) . \tag{II.21}$$

This alternative formulation, which we will not use in the following, is more common in the context of the large-deviation theory for instance [138]. Notice moreover that under this form, the positivity of the generating functional (II.96) is made obvious because the path-integral is performed over real fields, whereas we had to deal with an imaginary response-field in the previous case. The positivity of $\mathcal{Z}$ is crucial in the following chapters since we will be taking its logarithm to define the effective average action Γ_k.

II.2.3.b Jacobian and Itō discretization

Let us now discuss in more details the computation of the Jacobian $\mathcal{J}[\phi] = |\det(\delta\mathcal{C}[\phi]/\delta\phi)|$. For this purpose we discretize time, and write $t_i = i\Delta t$. For the field and the noise we use the shorthand notations $\phi_i = \phi(x, t_i)$, $F_i = F(\phi_i)$, $K_i = K(\phi_i)$ and $\zeta_i = \zeta(x, t_i)$. The force $F(\phi)$ can then be evaluated at any point in the interval $[t_{i-1}, t_i]$. One can choose the point at which it is evaluated, such that the discretized version of the Langevin equation (II.7) now reads:

$$\mathcal{C}[\phi_i] = \frac{\phi_i - \phi_{i-1}}{\Delta t} - \tau F_i - (1-\tau) F_{i-1} - \tau K_i \zeta_i - (1-\tau) K_{i-1} \zeta_i \tag{II.22}$$

Notice that $\tau = 0$ corresponds to the Itō "pre-point" discretization, and $\tau = 1/2$ to the Stratonovich "mid-point" scheme. The matrix whose determinant yields the Jacobian is therefore simple since most of the terms are zero, except for those on the diagonal and lower diagonal. Thus, the determinant is the product of the diagonal terms and reads:

$$\mathcal{J} = \prod_i \left(\frac{1}{\Delta t} - \tau \frac{\delta F_i}{\delta \phi_i} - \tau \frac{\delta K_i}{\delta \phi_i} \zeta_i \right) \tag{II.23}$$

$$= \left(\frac{1}{\Delta t} \right)^n \prod_i \left(1 - \tau \Delta t \frac{\delta F_i}{\delta \phi_i} - \tau \Delta t \frac{\delta K_i}{\delta \phi_i} \zeta_i \right) \tag{II.24}$$

$$\underset{\Delta t \to 0}{\sim} \left(\frac{1}{\Delta t} \right)^n \exp\left[-\tau \sum_i \Delta t \left(\frac{\delta F_i}{\delta \phi_i} + \frac{\delta F_i}{\delta \phi_i} \zeta_i \right) \right] \tag{II.25}$$

We can then resume to a continuous description of the model: the term $(1/\Delta t)^n$ is absorbed in the integration measure $\mathcal{D}\phi$, the sum becomes an integral, and the argument of the exponential in Eq. (II.14) now reads:

$$-\int_{x,t} \left[\tilde{\phi} \left(\partial_t \phi - F(\phi) - K(\phi)\,\zeta \right) + \tau \frac{\delta F}{\delta \phi} + + \tau \frac{\delta K}{\delta \phi} \zeta \right] \tag{II.26}$$

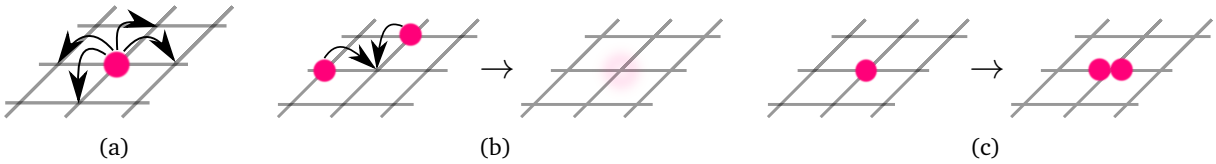

Figure II.3 – *Reaction-diffusion process: on a d-dimensional lattice, particles diffuse* ***(a)*** *and react, for instance annihilate* ***(b)*** *according to the reaction $2A \to \emptyset$, or generate offsprings* ***(c)*** *according to $A \to 2A$.*

which is consistent with the announced result, that $\mathcal{J}[\phi] = 1$, and is therefore coherent with Eq. (II.15), since the Itō representation means taking $\tau = 0$. Notice also that in the path-integral representation of an Itō process, one must take great care when performing a change of variables, and additional terms – corresponding to the additional terms in the Itō formula for Langevin equations (see App. B.1) – have to be added in the action. This issue has been made very clear recently in the following paper [139].

II.3 Microscopic description: the master equation

The other popular approach for describing a stochastic process – this time at the microscopic level – is the master equation [118, 119]. The master equation provides a description of a stochastic system stated as the time evolution of its microscopic probability distribution, and can be used whenever the states of the microscopic process at each time are countable. This is the case for instance of chemical reactions where one can label each molecule individually, or for an epidemics propagation where one is interested in following the fate of each individual. The master equation can also be cast into a field-theoretical form, as we show in the following, which is especially interesting if we have in mind to apply renormalization group techniques.

In the following, we focus only on a special kind of such processes called reaction-diffusion processes. These processes have a special status in the nonequilibrium phase transition world for several reasons: (i) as we will see in the following, they are formulated in a very simple way, and in this perspective they are often regarded as the equivalent of an Ising description of systems out of equilibrium. (ii) Similarly to the Ising model, some of these processes are believed to be the (simplest) representatives of universality classes. (iii) Although they are stated at the microscopic level, they can be cast into a field-theoretical form, which, in turn, can be identified with a Langevin equation. This third point will be our focus in the core of this chapter and will be discussed in details, in particular because it raised numerous paradoxical situations. (iv) Because these systems offer a master equation, a field-theoretical and a Langevin equation description, they provide very different techniques to be studied and understood, and have often been for these reasons the reference models for theorists.

II.3.1 Reaction-diffusion processes

II.3.1.a Definition

Reaction-diffusion processes are defined in the following way: on a lattice of dimension d, "particles"[5] are allowed to react and to diffuse (see Fig. II.3 for an illustration). These reactions and diffusion occur with some given probability or rate. To be more specific, a simple reaction-

[5]These particles can be actual particles as in chemical reaction, but they can as well be a model for infected/sound human beings in a disease-spreading model, trees in a forest fire model, genes in a population genetics model, etc.

diffusion process is given by the following reactions:

$$A + \emptyset \overset{D}{\leftrightarrow} \emptyset + A \tag{II.27a}$$

$$A \overset{\mu}{\rightarrow} \emptyset \tag{II.27b}$$

where particles diffuse (hop to a neighbouring site) at rate D, and may spontaneously decay at rate μ. More complicated processes involving different reactions and more particles can be added, such as coagulation $2A \to A$, annihilation $2A \to \emptyset$, creation of offsprings: $A \to 2A$, $2A \to 3A$ etc.

It is important to emphasize at this point that although we chose to describe the microscopic system using the language of chemical reactions, the variety of systems whose physics can be captured by this simple modelization is much broader. Indeed, as well as in equilibrium where the language of magnetization – the Ising model – is used to describe a whole universality class, out of equilibrium these reaction-diffusion systems are expected to represent universality classes, encompassing many different physical phenomena. We present in the following some of these universality classes.

II.3.1.b The directed percolation conjecture

Directed percolation (DP). Amongst the universality classes that can be represented by a reaction-diffusion scheme, the most famous and studied is probably the directed percolation (DP) universality class. This universality class, first studied in the context of percolation with a preferred direction (hence the name *directed* percolation), has been found to characterize also the critical behaviour of very various systems such as oil or gas in a porous rock, forest fires, diffusion in disordered media, some catalytic chemical reactions, the propagation of an infectious disease [8, 140], and more recently it has been shown to describe the turbulence in liquid crystals [141] or in a Couette flow [142].

Before introducing the directed percolation in the reaction-diffusion context, let us state it in its original setting [140]. Let be a lattice in d dimension where each bond between two neighbouring sites has a probability p to be open, and a probability $1 - p$ to be closed. This is the simple model of isotropic percolation. Directed percolation adds a preferred direction to the model by imposing a direction for choosing the links. It is therefore a basic model for studying the flow of a liquid (water, or oil...) into a porous medium, the preferred direction is that of gravity, and a bond being open means that the liquid can flow through it. Notice that when $p = 0$, all bonds are closed and the fluid does not flow at all. To the contrary, $p = 1$ means all bonds are open and the fluid go all the way to the bottom of the lattice. Now, starting from $p = 0$ and increasing this probability, the depth that a fluid reaches becomes larger and larger. For a critical value p_c, these paths stripe the whole lattice from top to bottom, forming a percolating path of open bonds. There exists therefore a phase transition at $p = p_c$ between the "dry" phase where the water never flow throughout the whole lattice, and the "wet" phase in which there are percolating paths.

In dimension $d = 1$, the percolation of a path necessitate all the bonds to be open, which means that the transition occurs only for $p_c = 1$. For an infinite dimension, that is for a Bethe lattice where all nodes are connected to the other nodes, as soon as $p > 0$, there is at least one open bond between two nodes and therefore always a path of infinite length. The dry phase is therefore reduced to $p = 0$ whereas the system is in the wet phase as soon as p is nonvanishing. For any other dimension $d > 1$ the system undergoes a second-order phase transition at $0 < p_c < 1$ [54].

The directed percolation model can be translated in the language of reaction-diffusion and

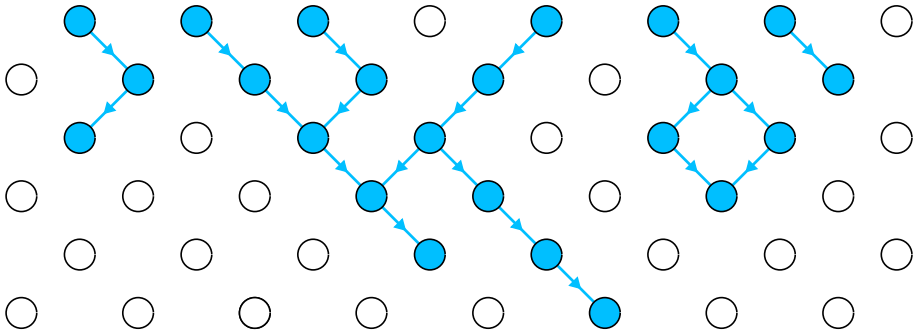

Figure II.4 – *Example of a two-dimensional directed percolation on a lattice. Water (in blue) flows in the preferred direction (bottom) whenever a link is open. Alternatively, the directed percolation process can be seen as a reaction-diffusion process with reactions (II.28) in one dimension, the vertical axis being the time.*

is given by a process obeying the following rules:

$$A + \emptyset \overset{D}{\longleftrightarrow} \emptyset + A \quad \text{diffusion} \tag{II.28a}$$

$$A \xrightarrow{\alpha_0} \emptyset \quad \text{spontaneous decay} \tag{II.28b}$$

$$A \xrightarrow{\alpha_2} 2A \quad \text{offspring creation} \tag{II.28c}$$

$$2A \xrightarrow{\beta_1} A \quad \text{coagulation} \tag{II.28d}$$

and the static directed percolation set-up in d dimensions can be translated to this reaction-diffusion scheme in $d-1$ dimensions where the time plays the role of the preferred direction (see Fig. II.4 for illustration). Notice that one can trade the coagulation reaction for an annihilation reaction $2A \to \emptyset$[6], and/or remove the spontaneous decay while remaining in the same universality class [8].

Mean-field study. Let us describe the directed percolation at the mean-field level to understand some characteristics of a transition to an absorbing state. We are interested in the average density of particles A that we denote $n(t)$, and we start by assuming that the system is well-stirred, such that we can neglect the spatial fluctuations (and the diffusion). The law of mass action for the reactions (II.28) reads:

$$\partial_t n(t) = (\alpha_2 - \alpha_0) n(t) - 2\beta_1 n(t)^2 \,, \tag{II.29}$$

where the coagulation occurs when two particles meet at the same site and is therefore proportional to $n(t)^2$. The assumption made when writing this equation is the absence of density fluctuations, such that the mean-field equation (II.29) is directly written in term of the average density $n(t)$. If $\Delta = (\alpha_2 - \alpha_0) < 0$, the density decreases until all particles have disappeared and the stationary state is $n_{\text{abs}} = 0$. If $\Delta = (\alpha_2 - \alpha_0) > 0$, a balance between creation and decay of particles is met and the density saturates at the stationary value:

$$n_{\text{act}} = \frac{\Delta}{2\beta_1} \,. \tag{II.30}$$

The full temporal solution of Eq. (II.29), for an initial density n_0, reads:

$$n(t) = \frac{n_0\, n_{\text{act}}}{n_0 + (n_{\text{act}} - n_0)\mathrm{e}^{-\Delta t}} \,, \tag{II.31}$$

[6] There is in fact an exact mapping between these two processes (see [143]).

which goes to the stationary solution $n_{\rm abs}$ or $n_{\rm act}$ depending on the sign of Δ. Notice that these two stationary states are reached exponentially fast. By contrast, if $\Delta = 0$, the density decreases algebraically to the absorbing state:

$$n(t) = \frac{n_0}{1 + 2\beta_1 n_0\, t}\,, \tag{II.32}$$

which is the signature of the phase transition between the absorbing state $n_{\rm abs} = 0$ and the active state $n_{\rm act} = \Delta/2\beta_1$. The fact that the dynamics switch from an exponential behaviour to an algebraic decay at the phase transition is typical in these phenomena and is known as the critical slowing down (see also Fig. II.1 for an illustration of the behaviour of the system in the different phases).

Mean-field exponents. At the mean-field level, we can compute the critical exponents describing the power-law behaviour of the system in the same manner as we did for equilibrium systems. Although at equilibrium two independent critical exponents are sufficient to characterize completely the critical scaling behaviour [30], one needs an additional exponent (the dynamical critical exponent) to describe nonequilibrium critical behaviour [7].

Similarly to the equilibrium case, we first define β, the exponent that characterizes how the order-parameter vanishes near its critical point:

$$n_{\rm act} \underset{\Delta\to 0}{\sim} |\Delta|^{\beta}\,, \tag{II.33}$$

and thus $\beta = 1$ in the mean-field approximation, according to Eq. (II.30). Furthermore, we define the dynamical critical exponent z which characterizes the divergence of the order-parameter dynamics upon approaching the transition as [7]:

$$t_{\rm relax} \underset{\Delta\to 0}{\sim} |\Delta|^{-\nu z}\,, \tag{II.34}$$

where $t_{\rm relax}$ is the relaxation time, and ν is the last critical exponent we need to compute and which characterizes the divergence of the correlation length ξ:

$$\xi \underset{\Delta\to 0}{\sim} |\Delta|^{-\nu}\,. \tag{II.35}$$

The relaxation time $t_{\rm relax}$ can be easily computed from the exponential decay of Eq. (II.31): $t_{\rm relax} = 1/\Delta$, and we immediately deduce $\nu z = 1$. Computing the correlation length necessitates to include spatial fluctuations in our simple model and write a "local" mean-field equation:

$$\partial_t n(t) = (\alpha_2 - \alpha_0 + D\nabla^2) n(t) - 2\beta_1 n(t)^2\,, \tag{II.36}$$

with D the diffusion coefficient. Since the diffusion up to a distance d takes a time of order $\sqrt{t}$, we deduce:

$$\xi \sim \sqrt{t_{\rm relax}} \underset{\Delta\to 0}{\sim} |\Delta|^{-1/2} \tag{II.37}$$

and we finally have the following mean-field exponents:

$$\beta = 1\,, \quad \nu = \frac{1}{2}\,, \quad z = 2\,. \tag{II.38}$$

These mean-field exponents are valid as long as the fluctuations remain negligible, which is the case when the spatial dimension is large. For directed percolation, the upper critical dimension above which the mean-field theory predicts the correct exponents is $d_c = 4$. Below this upper critical dimension, the exponents differ from their mean-field values and have been computed by the means of the NPRG in [54, 144], the perturbative RG [145], in experimental settings [141] and through Monte Carlo simulations [146] (see also [8] for a review).

The directed percolation conjecture. The prominence of the directed percolation universality class and its apparition in a large variety of settings led to the statement of a conjecture, the directed percolation conjecture, originally stated by Janssen [147] and Grassberger [148]. The directed percolation conjecture states that any process displaying a transition from an active to an absorbing state and satisfying the following conditions will fall under the directed percolation universality class:

(i) single absorbing state,
(ii) scalar order parameter,
(iii) spatially and temporally local microscopic dynamics,
(iv) absence of other symmetry,
(v) absence of quenched disorder.

However, although the directed percolation universality class seems quite common in natural settings, experiments that would unambiguously yield the directed percolation exponents have long remained elusive despite intensive experimental trials (see references in [141]). Until 2007 and a clear characterization of the directed percolation critical exponents (in two spatial dimensions) in an experiment involving turbulent liquid crystals [141], the directed percolation class and its conjecture were thus in a somewhat awkward situation of being virtually ubiquitous in the models involving a transition to an absorbing state both in theory and in numerical simulations, and yet nowhere to be found on the experimental side.

Notice also that the directed percolation is an example for which the perturbative RG breaks down qualitatively since it is unable to predict the correct phase diagram, while the NPRG performs very well. Indeed, taking $\alpha_0 = 0$, the perturbative RG claims that there is no phase transition for $d \geq 2$ [94, 149] and that the system remains in the active phase. On the other hand, the NPRG and Monte Carlo studies predict a phase transition between an absorbing and an active phase in all dimensions $d > 2$ [54, 144]. The explanation for this qualitative failure of the perturbative RG is subtle [35]: in $d < 2$, a phase transition occurs because particles encounter sufficiently often by diffusion so that they can effectively annihilate and reach the absorbing phase. On the other hand, in $d > 2$, diffusion is less effective and particles that are far apart may never meet each other. The only process that then may lead to an effective decay is the combination $A \to 2A$ followed by $2A \to \emptyset$. This is possible when the ratio β_0/D is large (that is large annihilation rate or sufficiently slow diffusion), and this somehow explains why the perturbative expansion fails: the usual perturbative approach is performed as an expansion at small reaction rates β_0/D and α_2/D, and therefore cannot probe the large β_0/D region where the transition indeed occurs. The NPRG, on the other hand, does not rely on such an expansion and do conclude in a phase transition in all dimensions. This conclusion and explanation was also highlighted by a more recent perturbative approach, this time done in the vicinity of the pure annihilation fixed point (that is, the perturbative expansion is done in terms of α_2/D, whereas β_0/D is arbitrarily large), which supports the NPRG predictions of a transition in all dimensions [96, 150]. See also Sec. (I.4.1) for some additional comments.

II.3.1.c Some other (presumed) universality classes

Pure annihilation (PA). This universality class is represented by the simple process where the only reaction is the pair annihilation:

$$A + \emptyset \overset{D}{\longleftrightarrow} \emptyset + A \tag{II.39a}$$

$$2A \xrightarrow{\beta_0} \emptyset \tag{II.39b}$$

This set of reactions without branching always reaches in the long-time limit the empty absorbing state. The response-functions are however nontrivial and the long-distance physics is governed by a non-Gaussian RG fixed point in $d < 2$. This simple class has been the subject

of intense discussions, in particular because its description in terms of a microscopic Langevin equation yields an imaginary noise term, whose physical interpretation is complicated. This point will be discussed thoroughly in the following.

Parity conserving generalized voter (PCGV). The parity conserving generalized voter universality class is the twin version of the directed percolation scheme in the case where the parity of the number of particles is locally preserved:

$$A + \emptyset \overset{D}{\longleftrightarrow} \emptyset + A \tag{II.40a}$$

$$A \xrightarrow{\alpha_2} 3A \tag{II.40b}$$

$$2A \xrightarrow{\beta_0} \emptyset \tag{II.40c}$$

hence the name. However, the parity conserving property has been shown not to be a relevant criterion for belonging to this universality class [151], but the more important characteristics is the existence of two symmetric absorbing states[7], a feature that is represented by the generalized voter universality class [151, 153]. Despite quite intensive numerical [151, 152] and theoretical works (perturbative RG [94, 149], NPRG [95] and perturbative RG near the pure annihilation (PA) fixed point [96, 150]), even a clear picture of the phase diagram is not yet known, and the precise value of the upper critical dimension d_c (which should lie between $d = 1$ and $d = 2$) remains elusive.

Pair-contact process with diffusion (PCPD). The pair-contact process with diffusion is different from the directed percolation and PCGV processes in that all reactions now require at least two particles to meet. A set of reactions for this process is the following:

$$A + \emptyset \overset{D}{\longleftrightarrow} \emptyset + A \tag{II.41a}$$

$$2A \xrightarrow{\beta_3} 3A \tag{II.41b}$$

$$2A \xrightarrow{\beta_0} \emptyset \tag{II.41c}$$

$$3A \xrightarrow{\gamma_0} \emptyset \tag{II.41d}$$

where the last reaction is a limiting reaction (otherwise the number of particles blows up in finite time in the active phase).

Although the microscopic requirement that all processes necessitate at least a pair of particles is not expected to be a relevant ingredient for defining a new universality class, the PCPD has largely resisted to analysis so far [111] in such a dramatic way that it is not even known whether the PCPD forms a new universality class or whether it belongs to the directed percolation class (see [154] and references therein). Even the status of its upper critical dimension is unclear. Usual numerical and theoretical methods (RG and NPRG) have proven so far ineffective to tackle this peculiar reaction-diffusion process.

More species. Obviously, even in the case of single species processes, it may exist other universality classes in addition to the few we just presented. The example of the PCPD for which the addition of a seemingly irrelevant reaction to the directed percolation class possibly change the universality class is quite worrying in this regard.

In the case of reactions involving more species of particles, the situation is therefore even more complex, and the theory beyond the mean-field level, still in its infancy. Even the simplest

[7] In $d = 1$, the particles of the PCGV in a space-time diagram can be seen as interfaces between "+" and "-" domains in a spin system (see for instance [152]), and the two absorbing states are the $\mathbb{Z}_2$-symmetric states of the spin system.

two-species reaction $A + B \to \emptyset$, first studied in [155, 156], and whose critical behaviour above its critical dimension $d_c = 2$ is quantitatively understood, still remains out-of-reach of RG procedure in $d \leq 2$[8] [157]. In more complicated cases such as $2A \to \emptyset$, $A + B \to \emptyset$ and $2B \to \emptyset$, results are sometimes available beyond the mean-field level, but they usually rely on assumptions (for instance for this model, the limit where the density of either A or B is much greater than that of the other) [158]. Amongst these obviously infinite possible reaction schemes, let us also mention the variants of the directed percolation class with several species: in some cases, for instance the case of particles A and B both subject to the directed percolation reactions with the additional coupling reactions $A \to 2B$ and $2A \to B$, the inclusion of these extra reactions happen not to change the critical properties since the corresponding couplings are in fact irrelevant in the RG sense [157]. In some other cases such as directed percolation coupled to a non-critical conserved density (DP-C), the model is renormalizable but yields a new critical point [159]. On the other hand, its related model where only the active individuals can diffuse, known as the conserved directed percolation (C-DP) model, is now known to belong to another different universality class known as the Manna class [160, 161].

II.3.1.d Numerical difficulties

To the contrary of the usual coarse-grained Langevin equations, the description of systems displaying a transition to an absorbing state using a microscopic description is exact. One could therefore hope that the theoretical difficulties coming from an approximate Langevin equation could be clarified when studying directly the exact microscopic process. However, other hurdles appear near these transitions: a field-theoretical computation in the case of the directed percolation [162], establishes the following scaling form at criticality of the particle number probability distribution: $P_n(t) \approx t^{-(\eta+2\delta)}\Phi(n/t^{\eta+\delta})$. This form shows that the distribution of the $P_n(t)$ has a fat tail. It is therefore not possible for instance to try to make the approximation $P_n(t) = 0$ for some $n > M$ in order to truncate the infinite hierarchy of equations set by the master equation (that we introduce in the following). It therefore appears that a numerical studies of these phenomena near criticality have to take care of large number of particles during long time, a task that can be computationally demanding. We therefore briefly review some methods that have been used to study the reaction-diffusion processes we have just discussed above (especially the controversial PCPD model):

- **Monte Carlo methods.** Near the phase transition to an absorbing state, bursts of activity separated by long quiescent periods are often observed, and Monte Carlo simulations have thus to be run for very long time near the critical point. For some particular processes such as the PCPD, an unusual absence of scaling of the probability distribution of the number of particles at the critical point with the size of the system L is observed [163], indicating that some improvements are still needed. Monte Carlo methods remain however very popular for studying reaction-diffusion processes in their non-critical regime. As an illustration of this rich literature we can cite Gillespie's method (see [164] and references therein) for studying chemical reactions involving several species of reactants, or Moro's hybrid algorithm [165] used to compute the front propagation in the stochastic Fisher-Kolmogorov-Petrovsky-Piscunov (sFKPP) equation [124, 166].

- **Density matrix renormalization group (DMRG) study.** This method yields a direct access to the critical exponents through the eigenvalues of the master equation operator $\mathcal{L}$[9] over a finite lattice of length L. However, only small values of L are accessible ($L \lesssim 60$)

[8] At least in the case of equal initial concentrations of A and B where the RG calculations involve a difficult nonperturbative sum over the initial "surface" term [157].

[9] The operator $\mathcal{L}$ describe the evolution of the probability distribution in a reaction-diffusion process. It will be defined in the following, Eq. (II.52).

and the finite-size scaling extrapolations are affected by some ill-understood correction terms [111].

Therefore, at the end of this section we see that for some (difficult) problems such as PCPD and systems involving several species of particles, we are confronted to the following situation when studying transition to an absorbing state: the exact microscopic description involves many degrees of freedom which all play a role near the transition and become very difficult to handle numerically. The microscopic approach fails to provide results that can be faithfully extrapolated to infinite-size system. On the other hand, the Langevin description, which could hopefully describe properly this systems even near the phase transition, breaks down in the low density limit since the usual derivation of a Langevin equation rely on a large density approximation. In Sec. II.4, we show how an *exact* Langevin description can be derived directly from the microscopic description, hence giving an answer to these difficulties. Before that we explain in the following how the microscopic description of a reaction-diffusion process can be cast into a field-theoretical formulation.

II.3.2 Master equation for reaction-diffusion processes

We now derive the master equation which describes the evolution of the probability distribution of the different configurations in a reaction-diffusion process. As we illustrate later on, this equation results simply in a book-keeping of the gains and losses of probability due to the microscopic reactions which occurs with given rates.

In more general context, that is for a generic Markov process (a memoryless process), the master equation is usually derived by considering the general Chapman-Kolmogorov equation [118, 119]. This general form is then adapted to the case of reaction-diffusion processes[10]. Since in this chapter we are only interested in reaction-diffusion processes, we derive the master equation directly for this kind of processes and our approach follow [164, 167] which have in mind the description of chemical reactions. After deriving the master equation for very general processes, we will furthermore simplify it and drastically restrict the reactions that we allow.

II.3.2.a General case

We consider a system of volume Ω containing N (chemical) species $\{S_1, \cdots, S_N\}$ that can react through M (chemical) reactions $\{R_1, \cdots, R_M\}$. In this section we consider that the system is well-mixed and that we can therefore neglect spatial inhomogeneities, which simplifies because the densities are then no longer space-dependent. The spatially-extended case including the diffusion of the different species can however be tackled, as explained for instance in [168].

The state of the system at time t is completely given by the vector $\boldsymbol{X}(t) \equiv (X_1(t), \cdots, X_N(t))$ where $X_i(t)$ is the number of particles of species S_i at time t. Our goal is to describe the evolution of the state vector $\boldsymbol{X}(t)$, given that the system was in state $\boldsymbol{X}(t_0) \equiv \boldsymbol{x}_0$ at the initial time t_0. Following [164, 167], we define for each reaction R_j:

(i) $a_j(\boldsymbol{x})\mathrm{d}t$ the probability, given $\boldsymbol{X}(t) = x$, that one R_j reaction will occur inside the system during the next time interval $[t, t + \mathrm{d}t[$,

(ii) $\boldsymbol{\nu}_j \equiv (\nu_{1,j}, \cdots, \nu_{N,j})$ the change in the $\{S_i\}$ particles population caused by one R_j reaction. Hence, if the system is in a state $\boldsymbol{x}$, it will jump at $t + \mathrm{d}t$ to the state $\boldsymbol{x} + \boldsymbol{\nu}_j$ if the reaction R_j occurs.

Finally, if we define the probability

$$P(\boldsymbol{x}, t|\boldsymbol{x}_0, t_0) = \mathrm{Prob}\left(\boldsymbol{X}(t) = \boldsymbol{x} \text{ given that } \boldsymbol{X}(t_0) = \boldsymbol{x}_0\right) \tag{II.42}$$

[10] Also known as birth and death processes in the zero-dimensional case.

then the (chemical) master equation that describes the evolution of probabilities is directly given by:

$$\partial_t P(\boldsymbol{x}, t|\boldsymbol{x}_0, t_0) = \sum_{j=1}^{M} \left[a_j(\boldsymbol{x} - \boldsymbol{\nu}_j) P(\boldsymbol{x} - \boldsymbol{\nu}_j, t|\boldsymbol{x}_0, t_0) - a_j(\boldsymbol{x}) P(\boldsymbol{x}, t|\boldsymbol{x}_0, t_0) \right] . \tag{II.43}$$

and is in fact simply a book-keeping equation that states the conservation of probabilities. We give a very simple illustration of the master equation in the following.

II.3.2.b Restriction of the reactions

In the following we will be interested in a drastically simplified setting, for some points of our formalism cannot (yet!) tackle more complicated schemes. In particular, we consider only one species of particles, A, and restrict the allowed reactions to the following ones:

$$A + \emptyset \overset{D}{\longleftrightarrow} \emptyset + A \tag{II.44a}$$

$$A \xrightarrow{\alpha_p} pA \tag{II.44b}$$

$$2A \xrightarrow{\beta_q} qA \tag{II.44c}$$

and any combination of them. Although these processes are less general than those involved in the general setting we presented above, notice that they already describe most chemical reactions (involving a single species) since reactions involving three reactants or more are really unlikely in nature.

The state of the system at a time t can therefore be specified by the (stochastic) number of particles $N(t)$. For the introduction of the formalism and to lighten the proofs, we keep considering the case of a single-site system, but the whole formalism can be translated to a d-dimensional system (and this is shown in Sec. II.3.3.d).

The reaction-diffusion process (II.44) can be described by a master equation which follows the time evolution of the probability $P_n(t) \equiv \mathrm{Prob}(N(t) = n)$ and reads

$$\partial_t P_n(t) = \sum_m L_{nm} P_m(t) \tag{II.45}$$

where the elements of the rate transition matrix L are

$$L_{nm} = \sum_p \alpha_p m(\delta_{n+1-p,m} - \delta_{m,n}) + \sum_q \beta_q m(m-1) \left(\delta_{n+2-q,m} - \delta_{m,n}\right) . \tag{II.46}$$

This matrix is simply determined by computing the "gains" and "losses" of probability coming from the microscopic reactions. For instance, consider the reaction $A \xrightarrow{\alpha_0} \emptyset$: let us assume that we want to compute the probability of having n particle at time $t+\mathrm{d}t$, $P_n(t+\mathrm{d}t)$. This probability is formally given by:

$$P_n(t + \mathrm{d}t) = P_n(t) + \text{"gains"} - \text{"losses"} \tag{II.47}$$

A particle disappears during a time interval $\mathrm{d}t$ with probability $\alpha_0 \mathrm{d}t$. The probability of having n particles at time $t + \mathrm{d}t$ is increased if there were $n+1$ particles at time t and one of them disappeared, which means that the gain term reads:

$$P_{n+1}(t) \times (n+1)\alpha_0 \, \mathrm{d}t \, , \tag{II.48}$$

whereas the probability of having n particles at time $t + \mathrm{d}t$ is decreased if there were n particles at time t but one of them disappeared. Therefore the loss term is:

$$P_n(t) \times n\alpha_0 \, \mathrm{d}t \, , \tag{II.49}$$

which finally yields – for the reaction $A \xrightarrow{\alpha_0} \emptyset$ – the simple master equation:

$$\partial_t P_n(t) = \alpha_0 \left[(n+1) P_{n+1}(t) - n P_n(t) \right] . \tag{II.50}$$

II.3.3 Field theory for reaction-diffusion processes: the Doi-Peliti formalism

II.3.3.a Creation and annihilation operators

We now introduce a field-theoretical description for reaction-diffusion processes. Since the state of the system is entirely determined by the number of particles at time t, it has become natural to introduce a "second-quantized" form of the master equation. This formalism was first introduced by Doi [169] and Peliti [170] and is therefore often referred to as the Doi-Peliti formalism. Following [17, 157, 171], we now introduce the procedure that allows us to write a path-integral version of the master equation (II.45). We define a Hilbert space spanned by the "occupation number" vectors $\{|n\rangle\}$ which are the eigenvectors with eigenvalues n of the "number" operator $\hat{N} = a^\dagger a$, with a and $a^\dagger$ the "annihilation" and "creation" operators satisfying the relations: $[a, a^\dagger] = 1$, $a|0\rangle = 0$, $a|n\rangle = n|n-1\rangle$, and $a^\dagger|n\rangle = |n+1\rangle$. We also introduce the scalar product[11]: $\langle m|n\rangle = n!\delta_{mn}$ and $a^\dagger$ is the Hermitian conjugate of a.

From these definitions, we introduce the state vector $|P(t)\rangle$ associated with the set of probabilities $\{P_n(t)\}$:

$$|P(t)\rangle = \sum_{n=0}^{\infty} P_n(t)|n\rangle \tag{II.51}$$

and such that the master equation can now be rewritten in terms of the creation and annihilation operators:

$$\partial_t|P(t)\rangle = \mathcal{L}(a^\dagger, a)|P(t)\rangle \tag{II.52}$$

where $\mathcal{L}$ reads:

$$\mathcal{L}(a^\dagger, a) = A(a^\dagger)\, a + B(a^\dagger)\, a^2\,. \tag{II.53}$$

Notice that, by its very construction, $\mathcal{L}$ is automatically normal-ordered, that is all the $a^\dagger$ are to the left and the a to the right. The functions A and B are determined by the reaction rates through:

$$A(a^\dagger) = \sum_p \alpha_p[(a^\dagger)^p - a^\dagger] \quad \text{and} \quad B(a^\dagger) = \sum_q \beta_q[(a^\dagger)^q - (a^\dagger)^2]\,. \tag{II.54}$$

Notice that we have derived the operator $\mathcal{L}$ in the case of the reactions (II.44), and we further assume that $q < 2$ for the reaction (II.44c). This in prevision of what we show in the following and which depends crucially on these assumptions, although the Doi-Peliti formalism that we are presenting here is more general and can be applied to a generic reaction-diffusion system. Therefore, for the reactions we deal with, the coefficient of the second derivative reduces to a second order polynomial in $a^\dagger$:

$$B(a^\dagger) = (\beta_0 + \beta_1)(a^\dagger - \ell)(1 - a^\dagger), \quad \ell \equiv -\beta_0/(\beta_0 + \beta_1). \tag{II.55}$$

The master equation in its new form (II.52) now looks like an imaginary-time Schrödinger equation and we use some standard quantum mechanics tools to derive a path-integral formulation of this equation. Notice however that there are several differences compared to the Schrödinger equation: (i) the operator $\mathcal{L}(a^\dagger, a)$ is not necessarily Hermitian, (ii) the states are linear functions of the probabilities, rather than linear functions of the probability amplitudes as it is the case in quantum mechanics.

[11] Notice that the occupation number vectors $|n\rangle$ are not normalized to one ($\langle n|n\rangle \neq 1$), to the contrary of what is customary in quantum mechanics.

II.3.3.b Computing observables

As in quantum mechanics, we would like to use the scalar product to compute average of observables $\mathcal{O}(N(t))$:

$$\langle \mathcal{O}(N(t)) \rangle = \sum_n P_n(t) \mathcal{O}(n) \,. \tag{II.56}$$

For this purpose, we introduce the "projection" state $\langle \cdot |$ defined as:

$$\langle \cdot | \equiv \langle 0 | \mathrm{e}^a \,, \tag{II.57}$$

and we also "quantify" the observable $\mathcal{O}$ and associate with it the operator $\tilde{\mathcal{O}}$ which is simply obtained by replacing n by $a^\dagger a$ in the Taylor series of $\mathcal{O}$: $\tilde{\mathcal{O}} \equiv \mathcal{O}(a^\dagger a)$ and such that $\mathcal{O}$ is also normal-ordered. These new definitions allow us to write the average value of an observable as:

$$\langle \mathcal{O}(N(t)) \rangle = \langle \cdot | \tilde{\mathcal{O}} | P_n(t) \rangle \,. \tag{II.58}$$

II.3.3.c Path integral representation

Let us now compute observables starting from a given initial condition. Since the "quantum mechanics" form (II.52) of the master equation is linear in time, we can write its formal solution as:

$$|P(t)\rangle = \mathrm{e}^{\mathcal{L}(a^\dagger, a) t} |P(0)\rangle \,, \tag{II.59}$$

which yields for the average value of an observable:

$$\langle \mathcal{O}(N(t)) \rangle = \langle \cdot | \tilde{\mathcal{O}} \mathrm{e}^{\mathcal{L}(a^\dagger, a) t} | P(0) \rangle \,. \tag{II.60}$$

We now split the time interval t into infinitesimally small increments $\delta t = t/M$, and we use the Trotter formula to write:

$$\langle \mathcal{O}(N(t)) \rangle = \lim_{M \to \infty} \langle \cdot | \tilde{\mathcal{O}} \prod_{i=0}^{M} \mathrm{e}^{\mathcal{L}(a^\dagger, a) \delta t} | P(0) \rangle \,. \tag{II.61}$$

We now introduce between each infinitesimal time step a complete set of coherent states $|\phi\rangle$, such that:

$$\mathbb{1} = \frac{i}{2\pi} \int \mathrm{d}\phi \mathrm{d}\phi^* \, \mathrm{e}^{-\phi\phi^*} |\phi\rangle\langle\phi^*| \tag{II.62}$$

where the coherent states $|\phi\rangle$ are *defined* as the eigenvectors of the annihilation operator a with eigenvalue ϕ and read:

$$|\phi\rangle \equiv \mathrm{e}^{\phi a^\dagger} |0\rangle \,. \tag{II.63}$$

Our average therefore reads:

$$\langle \mathcal{O}(N(t)) \rangle = \lim_{M \to \infty} \int \{\mathrm{d}\phi_i\} \underbrace{\prod_{i=1}^{M} \left[\mathrm{e}^{-\phi_i \phi_i^*} \langle \phi_i^* | \mathrm{e}^{\mathcal{L}(a^\dagger, a) \delta t} | \phi_{i-1} \rangle \right]}_{A} \underbrace{\langle \cdot | \tilde{\mathcal{O}} | \phi_M \rangle}_{B} \underbrace{\langle \phi_0^* | P(0) \rangle}_{C} \tag{II.64}$$

where we have defined $\{\mathrm{d}\phi_j\} \equiv \prod_{k=0}^{M} i \, \mathrm{d}\phi_k \mathrm{d}\phi_k^* / (2\pi)$; note that the factor $i/(2\pi)$ has been included in the integration measure for convenience. Let us compute the terms appearing in

this formula. We first focus on the term A, composed of $M-1$ terms, in which the scalar product reads:

$$\langle\phi_i^*|\mathrm{e}^{\mathcal{L}(a^\dagger,a)\delta t}|\phi_{i-1}\rangle \underset{\delta t\to 0}{=} \langle\phi_i^*|1+\delta t\mathcal{L}(a^\dagger,a)|\phi_{i-1}\rangle \tag{II.65}$$

$$\underset{\delta t\to 0}{=} \langle 0|\mathrm{e}^{\phi_i^* a}(1+\delta t\mathcal{L}(a^\dagger,a))\mathrm{e}^{\phi_{i-1}a^\dagger}|0\rangle \tag{II.66}$$

$$\underset{\delta t\to 0}{=} \mathrm{e}^{\phi_i^*\phi_{i-1}}\langle 0|\mathrm{e}^{\phi_{i-1}a^\dagger}(1+\delta t\mathcal{L}(a^\dagger+\phi_i^*,a+\phi_{i-1}))\mathrm{e}^{\phi_i^* a}|0\rangle \tag{II.67}$$

where we have used the formulas:

$$\mathrm{e}^{\lambda a}f(a^\dagger) = f(a^\dagger+\lambda)\mathrm{e}^{\lambda a} \tag{II.68}$$

$$\mathrm{e}^{\lambda a^\dagger}f(a) = f(a-\lambda)\mathrm{e}^{\lambda a^\dagger} \tag{II.69}$$

and since $\mathcal{L}$ is normal-ordered, the whole formula is normal-ordered and the operator a (resp. $a^\dagger$) yields a vanishing contribution when acting on the ground-state $|0\rangle$ (resp. $\langle 0|$). We therefore get, after a re-exponentiation of the δt-term:

$$\langle\phi_i^*|\mathrm{e}^{\mathcal{L}(a^\dagger,a)\delta t}|\phi_{i-1}\rangle \underset{\delta t\to 0}{=} \mathrm{e}^{\phi_i^*\phi_{i-1}}\mathrm{e}^{\delta t\mathcal{L}(\phi_i^*,\phi_{i-1})}\,. \tag{II.70}$$

We can now compute the whole integral involving the A term:

$$\int\{\mathrm{d}\phi_i\}A \underset{\delta t\to 0}{=} \int\{\mathrm{d}\phi_i\}\,\mathrm{e}^{-\phi_0\phi_0^*}\prod_{i=1}^{M}\mathrm{e}^{-\phi_i^*(\phi_i-\phi_{i-1})+\delta t\mathcal{L}(\phi_i^*,\phi_{i-1})}\,. \tag{II.71}$$

Notice that in the continuous-time limit $\delta t\to 0$, the term $(\phi_i-\phi_{i-1})$ can be interpreted as the time-derivative of $\phi(t)$. Using this fact and the Trotter formula in the other way, we get a path-integral formulation:

$$\int\{\mathrm{d}\phi_i\}A \underset{\delta t\to 0}{=} \int\mathcal{D}\phi(t)\mathcal{D}\phi^*(t)\,\mathrm{e}^{-\phi(0)\phi^*(0)}\mathrm{e}^{-\mathcal{S}_{\mathrm{RD}}[\phi,\phi^*]} \tag{II.72}$$

where we have introduced the Doi-Peliti action $\mathcal{S}_{\mathrm{RD}}$ for a reaction-diffusion process as:

$$\mathcal{S}_{\mathrm{RD}}[\phi,\phi^*] \equiv \int\mathrm{d}t\;\left[\phi^*\partial_t\phi+\mathcal{L}(\phi^*,\phi)\right]\,. \tag{II.73}$$

Notice that when going to continuous time, we have interpreted the term $\mathcal{L}(\phi_i^*,\phi_{i-1})\to\mathcal{L}(\phi(t)^*,\phi(t))$ where both fields are evaluated at equal time. This choice means that the whole path integral must be interpreted in the Itō sense.

It now remains to evaluate the terms B and C. We have:

$$B = \langle 0|\mathrm{e}^{a}\tilde{\mathcal{O}}(a^\dagger,a)\mathrm{e}^{\phi_M a^\dagger}|0\rangle \tag{II.74}$$

$$= \langle 0|\mathrm{e}^{\phi_M a^\dagger}\tilde{\mathcal{O}}(a^\dagger+1,a+\phi_M)\mathrm{e}^{a}|0\rangle \tag{II.75}$$

$$= \mathrm{e}^{\phi_M}\tilde{\mathcal{O}}(1,\phi_M) \tag{II.76}$$

where we have followed the same tricks as before for evaluating this scalar product. The last term C will in fact depend on the choice of the initial state $|P(0)\rangle$ and we will compute it afterwards.

Finally, putting all the terms together we are able to express the average of an observable in terms of a path-integral over coherent states:

$$\langle\mathcal{O}(N(t))\rangle = \int\mathcal{D}\phi\mathcal{D}\phi^*\,\tilde{\mathcal{O}}(1,\phi(t))\,\mathrm{e}^{-\mathcal{S}_{\mathrm{RD}}[\phi,\phi^*]+\phi(t)}\,\mathrm{e}^{-\phi^*(0)\phi(0)}\langle\phi^*(0)|P(0)\rangle \tag{II.77}$$

Notice that if the initial distribution of particles is a Poisson distribution with parameter ϕ_{init}, that is the probability of having n particles at $t = 0$ is: $P_n(0) = \mathrm{e}^{-\phi_{\text{init}}}\phi_{\text{init}}^n/n!$, then the initial state is almost a coherent state and reads: $|P(0)\rangle = \mathrm{e}^{-\phi_{\text{init}}}|\phi_{\text{init}}\rangle$. This allows for a simplification of the previous formula:

$$\int \mathrm{d}\phi^*(0)\,\mathrm{e}^{-\phi^*(0)\phi(0)}\langle\phi^*(0)|P(0)\rangle = \int \mathrm{d}\phi^*(0)\,\mathrm{e}^{-\phi^*(0)[\phi(0)-\phi_{\text{init}}]}\mathrm{e}^{-\phi_{\text{init}}} \tag{II.78}$$

and the integral over $\phi^*(0)$ yields a δ-distribution, which determines the lower bound of the path integral at $\phi(0) = \phi_{\text{init}}$. In the case of an initial Poisson distribution, we therefore have:

$$\langle\mathcal{O}(N(t))\rangle = \int_{\phi(0)=\phi_{\text{init}}} \mathcal{D}\phi\mathcal{D}\phi^*\,\hat{\mathcal{O}}(1,\phi(t))\,\mathrm{e}^{-\mathcal{S}_{\text{RD}}[\phi,\phi^*]-\mathcal{S}_{\text{BC}}} \tag{II.79}$$

where we have introduced the boundary term $\mathcal{S}_{\text{BC}} \equiv \phi(0) - \phi(t)$. Finally, a common transformation in the literature is to perform a "Doi shift", that consists in changing ϕ^* to $\phi^* + 1$ which has the advantage of cancelling the boundary term $\phi(0) - \phi(t)$. Indeed, after a Doi-shift, one has:

$$\langle\mathcal{O}(N(t))\rangle = \int_{\phi(0)=\phi_{\text{init}}} \mathcal{D}\phi\mathcal{D}\phi^*\,\tilde{\mathcal{O}}(1,\phi(t))\,\mathrm{e}^{-\mathcal{S}_{\text{shift}}[\phi,\phi^*]} \tag{II.80}$$

where $\mathcal{S}_{\text{shift}}[\phi,\phi^*] = \int \mathrm{d}t\ [\phi^*\partial_t\phi + \mathcal{L}(\phi^*+1,\phi)]$, and the boundary term was killed by the time-derivative contribution, which yields after the Doi-shift: $\int \mathrm{d}t\,(\phi^*+1)\partial_t\phi = \phi(t) - \phi(0) + \int \mathrm{d}t\,\phi^*\partial_t\phi$.

Notice also that in the following we are interested in the stationary limit and we therefore assume that the boundary contribution has been washed out. This assumption allows us to write down, as we did in the case of the Langevin equation, a generating functional $\mathcal{Z}_{\text{RD}}$ that reads:

$$\mathcal{Z}_{\text{RD}}[J,\tilde{J}] = \int \mathcal{D}\phi\mathcal{D}\phi^*\,\mathrm{e}^{-\mathcal{S}_{\text{RD}}[\phi,\phi^*]+\int \mathrm{d}t\,(J\phi+\tilde{J}\phi^*)}\,. \tag{II.81}$$

II.3.3.d Spatially-extended case

As claimed in the beginning of this section, the whole formalism can be adapted to a d-dimensional lattice instead of focusing on a single site. In this case, we also introduce the diffusion of the particles as the reaction:

$$A + \emptyset \overset{D}{\leftrightarrow} \emptyset + A \tag{II.82}$$

where D is the diffusion coefficient and the diffusion acts as an exchange of a particle at a given site and its neighbouring sites. The description of a d-dimensional system also require to introduce the probability distribution $P_{\boldsymbol{n}}(t)$ where $\boldsymbol{n} = (n_1,\ldots,n_N)$ is the number of particles at site $1,2,\ldots,N$, and the master equation (II.45) now contains a sum over all the sites:

$$\partial_t P_{\boldsymbol{n}}(t) = \sum_i \partial_t P_{n_i}(t)\,, \tag{II.83}$$

where each $\partial_t P_{n_i}(t)$ is simply obtained by replacing n by n_i in the zero-dimensional case, and adding an extra term coming from the diffusion reaction (II.82). This extra term reads:

$$D\sum_{\{v\}}\left[(n_v+1)P_{(\ldots,n_i-1,n_v+1,\ldots)}(t) - n_i P_{(\ldots,n_i,n_v,\ldots)}(t)\right]\,, \tag{II.84}$$

where $\{v\}$ indicates the sites neighbouring site i.

The Doi-Peliti formalism is then straightforwardly extended to the d-dimensional case. The state vector becomes $|\boldsymbol{n}\rangle = |n_1, \dots, n_N\rangle$ while we now associate one creation $a_i^\dagger$ and annihilation a_i for each site i, and modify the commutation relation accordingly: $[a_i, a_j^\dagger] = \delta_{ij}$. The modification of the master equation then translates to the operator $\mathcal{L}(a^\dagger, a)$ defined in Eq. (II.52) which now involves all the $\{a_i, a_i^\dagger\}$ and displays a sum over the sites i. Finally, diffusion (II.82) adds the following term to $\mathcal{L}$:

$$-D \sum_{\{v\}} a_i^\dagger (a_v - a_i)\,. \tag{II.85}$$

After introducing the complex-conjugated coherent states ϕ_i and ϕ_i^* for each site of the lattice, this adds a contribution

$$-D \sum_{\{v\}} \phi_i^* (\phi_v - \phi_i) \tag{II.86}$$

to the action.

Continuous space limit. Finally, the last step to obtain a usual continuous space description in terms of a continuous variable x and coherent sates $\phi(x,t)$, we have to make the assumption that the lattice spacing a is infinitely small, and define the new continuous variables: $\phi_i \to a^d \phi(x)$, $\phi_i^* \to \phi^*(x)$ and $\sum_i \to a^{-d} \int \mathrm{d}^d x$. Then, the difference between nearest neighbours appearing in Eq.(II.86) becomes a Laplacian term at the first order of the continuous limit: $\sum_{\{v\}} (\phi_v - \phi_i) \to a^2 \nabla^2 \phi(x)$. Finally, redefining the reaction rates as $\alpha_p \to \alpha_p$, $\beta_q \to a^{-2d} \beta_q$ and $D \to a^{-2} D$, we obtain the following Doi-Peliti action:

$$\mathcal{S}_{\mathrm{RD}}[\phi, \phi^*] = \int \mathrm{d}^d x \mathrm{d}t \, \left[\phi^* (\partial_t - D\nabla^2)\phi + \mathcal{L}(\phi^*, \phi)\right] \tag{II.87}$$

where we have omitted the (x,t) dependence of the fields for clarity.

II.4 Langevin equations for reaction-diffusion processes

In the previous sections we have introduced two methods for studying out-of-equilibrium systems: the Langevin approach provides a very powerful and versatile tool, since a precise description of the microscopic degrees of freedom of the model is not needed. This is especially efficient when the small-scale details are not completely known or difficult to modelize, as it is the case for the study of landscape erosion (see Chap. IV). The other approach stems from a microscopic description and therefore has the great advantage of giving an exact description of the phenomenon. When studying some critical phenomena such as the transitions to an absorbing state, an exact description of the phenomenon is however requested since at the transition between the active and the absorbing state, keeping track of very low number of particles is extremely important.

In the case of reaction-diffusion processes, one notices that the Doi-Peliti generating functional (II.81) and the one of the response-field formalism (II.96) look *superficially* identical, the major difference being that the former is written in terms of complex conjugated fields whereas the latter involves a real and an imaginary fields. We would now like to make the connection between the microscopic reaction-diffusion description and the Langevin description.

This connection is important for several reasons: (i) Langevin equations are mostly phenomenological. Having derived a Langevin equation from the microscopic dynamics would give us some insight on how to derive them generically, and this is especially important for the determination of the noise term. (ii) As explained previously, when studying processes that display a

transition to an absorbing state, the microscopic description may not be numerically tractable, and a Langevin description could be more efficient in this perspective.

In the first (i) case, a mesoscopic approach is requested, and therefore an approximate derivation from the microscopic master equation to a coarse-grained Langevin equation is admissible. We will rapidly explain how this kind of derivation can be performed. On the other hand, in the second (ii) case, we would in fact like a Langevin process that would *not* be a coarse-grained version of the master equation, but rather a dual, *equivalent* version of the master equation.

II.4.1 Approximate derivation of a Langevin equation

Before describing in details the derivation of *exact* Langevin equations that are needed for the study of transitions to an absorbing state, we first quickly review the different approximate methods that exist for deriving a coarse-grained Langevin equation from a master equation. In many cases, an approximate Langevin equation is sufficient for describing the system at the mesoscopic level, and the coarse-grained nature of the equation obtained by this approximate approach makes it simpler to study both numerically and theoretically than the usually very complicated microscopic process. This coarse-graining procedure however relies on a large density limit, and therefore breaks down in the vicinity of a phase transition to an absorbing state, when the particle density is too low for approximations to remain valid.

II.4.1.a Kramers-Moyal expansion of a master equation

Starting from the master equation (II.43), the Kramers-Moyal expansion is in fact already an approximation since it will assume that the particle numbers $\boldsymbol{X}(t)$ appearing in Eq. (II.43) are real-valued (rather than integer-valued). Although this approximation is probably legitimate at large number of particles, it is definitely more controversial as soon as this number of particle is 0 or 1, which is the case near a transition to an absorbing state. A second assumption is that the functions $f_j(\boldsymbol{x}) \equiv a_j(\boldsymbol{x})P(\boldsymbol{x},t|\boldsymbol{x}_0,t_0)$ must be analytic in $\boldsymbol{x}$, such that we can write their series expansion:

$$f_j(\boldsymbol{x}-\boldsymbol{\nu}_j) = f_j(\boldsymbol{x}) + \sum_{n=1}^{\infty} \sum_{m_1+\cdots+m_N=n} \frac{1}{m_1!\cdots m_N!}(-\nu_{j,1})^{m_1}\cdots(-\nu_{j,N})^{m_N}\frac{\partial^n f_j(\boldsymbol{x})}{\partial x_1^{m_1}\cdots\partial x_N^{m_N}}\,. \tag{II.88}$$

The Kramers-Moyal expansion is then simply obtained by substituing this expression into the master equation (II.43). It yields [167]:

$$\partial_t P(\boldsymbol{x},t|\boldsymbol{x}_0,t_0) = \sum_{n=1}^{\infty}(-1)^n \sum_{m_1+\cdots+m_N=n} \frac{1}{m_1!\cdots m_N!}\frac{\partial^n}{\partial x_1^{m_1}\cdots\partial x_N^{m_N}}\left[\left(\sum_{j=1}^{M}(\nu_{j,1}^{m_1}\cdots\nu_{j,N}^{m_N})a_j(\boldsymbol{x})\right)P(\boldsymbol{x},t|\boldsymbol{x}_0,t_0)\right], \tag{II.89}$$

which is the starting point of many approximating schemes. Indeed, if one truncates this expansion at the second order, the previous equation boils down to a Fokker-Planck equation. This truncation obviously necessitates further arguments to be justified. We quickly present them and the resulting Langevin equations in the following.

II.4.1.b Truncation at second-order: Gillespie's chemical Langevin equation

In the limit of a large number of reactant molecule populations, Gillespie argued that the truncation at the second-order of the Kramers-Moyal expansion (II.89) is justified and therefore yields

a Fokker-Planck equation which can be translated to a Langevin equation, usually called the chemical Langevin equation (CLE), that reads [167]

$$\partial_t X_i(t) = \sum_{j=1}^{M} \nu_{j,i} a_j(\boldsymbol{X}(t)) + \sum_{j=1}^{M} \nu_{j,i} \sqrt{a_j(\boldsymbol{X}(t))}\, \zeta_j(t) \quad \text{for } i = 1, \dots, N \tag{II.90}$$

where the ζ_j are independent Gaussian white noises. Notice that in the simpler case of the master equation (II.45) there is only a single species and $\boldsymbol{X}(t)$ reduces to a single-component vector $X_1(t) = x(t)$. Moreover, for the reactions (II.44) the reactions probability are $a_1(x) = \alpha_p x$ and $a_2(x) = \beta_q x(x-1)$. The previous equation therefore takes the form:

$$\partial_t x = \sum_p (p-1)\alpha_p x + \sum_q (q-2)\beta_q x(x-1) + \sqrt{\sum_p (p-1)^2 \alpha_p x + \sum_q (q-2)^2 \beta_q x(x-1)}\, \zeta(t) \tag{II.91}$$

and one may notice already that the limit of small number of particles $x < 1$ is problematic. For instance, taking all the $\alpha_p = 0$ (that is, no reaction with a single reactant) yields a negative argument in the square-root for $x < 1$. This was indeed to be expected from the very derivation of this equation.

II.4.1.c Van Kampen's system-size expansion

Before Gillespie, van Kampen proposed a justification for performing a simplification of the Kramers-Moyal expansion of the master equation which involves only derivatives up to the second-order [172]. The idea of his approximation is to perform a large-volume expansion near the mean-field solution of the Kramers-Moyal expansion (II.89). Thus, the starting point of this approximation is to write the stochastic variable $\boldsymbol{X}(t) = \Omega \boldsymbol{\phi}(t) + \Omega^{1/2} \boldsymbol{y}(t)$ where Ω is the size of the system, $\boldsymbol{\phi}$ is the deterministic solution of the mean-field equation, and $\boldsymbol{y}$ is a stochastic variable which can be seen as a small perturbation of the mean-field behaviour. In the case of the reactions (II.44), this approximation yields the following Langevin equation for the stochastic variable $y(t)$ [173]:

$$\partial_t y = \left(\sum_p (p-1)\alpha_p + \sum_q (q-2)\beta_q (2\phi - 1) \right) y + \sqrt{\sum_p (p-1)^2 \alpha_p \phi + \sum_q (q-2)^2 \beta_q \phi(\phi - 1)}\, \zeta(t) \tag{II.92}$$

where ϕ is the solution of the (deterministic) mean-field rate equation:

$$\partial_t \phi(t) = \sum_p (p-1)\alpha_p \phi(t) + \sum_q (q-2)\beta_q \phi(t)(\phi(t) - 1)\,. \tag{II.93}$$

This approximation is very crude since on top of the large system-size expansion, a "linear noise" approximation is performed and the noise term does not depend on the stochastic variable y.

We emphasize that both Langevin equations (II.90) and (II.92) are only approximate, coarse-grained descriptions of the master equation (II.43) and valid only in the limit of a large number of reacting particles. In the following we will on the other hand derive *exact*, that is *microscopic* Langevin equations which describe in an equivalent fashion the dynamics of the master equation.

II.4.2 Microscopic Langevin equation and imaginary noise

In this section and in the following we consider the class of single-species reaction-diffusion processes involving at most two particles and all possible reactions of the form:

$$A \xrightarrow{\alpha_p} pA \tag{II.94a}$$

$$2A \xrightarrow{\beta_q} qA \tag{II.94b}$$

with p arbitrary and $q = 0$ or 1. For this class of reaction-diffusion processes, there exists a *formal* connection between the master equation description and a Langevin equation. This connection is known for a long time, and is either derived using Gardiner's Poisson representation [118] or via a field-theory formalism [17, 18], and we present both derivations in the following.

II.4.2.a Field theory formalism

The usual method found in the literature to obtain a microscopic Langevin equation stems from a *formal* comparison between the Doi-Peliti approach and the MSRDJ formalism. As we will see, this method is not correct and its derivation suffers several inconsistencies. The aim of the next section, which is also the first result of this manuscript [19], is to solve these inconsistencies and obtain an *exact* Langevin equation describing the microscopic dynamics.

In Sec. II.3.3, we have seen that using the Doi-Peliti formalism, we can write a "partition function" – that is the generating functional of the correlation and response functions – for a reaction-diffusion process written in terms of the master equation (II.45):

$$\mathcal{Z}_{\mathrm{RD}}[J,\tilde{J}] = \int \mathcal{D}\phi\mathcal{D}\phi^* \, \mathrm{e}^{-\mathcal{S}_{\mathrm{RD}}[\phi,\phi^*]+\int \mathrm{d}t\,(J\phi+\tilde{J}\phi^*)} \tag{II.95}$$

with the action $\mathcal{S}_{\mathrm{RD}}[\phi,\phi^*] = \int \mathrm{d}t\,[\phi^*\partial_t\phi - \mathcal{L}(\phi,\phi^*)]$ and where ϕ and ϕ^* are complex-conjugated fields.

On the other hand, we have seen in Sec. II.2.3, that a Langevin equation can generically be cast into a field theory, and the MSRDJ formalism allows us to write similarly the generating functional for a Langevin process:

$$\mathcal{Z}_{\mathrm{LE}}[J,\tilde{J}] = \int \mathcal{D}\psi\mathcal{D}\tilde{\psi} \, \mathrm{e}^{-\mathcal{S}_{\mathrm{LE}}[\psi,\tilde{\psi}]+\int \mathrm{d}t\,(J\psi+\tilde{J}\tilde{\psi})} \tag{II.96}$$

where this time, ψ is a real field, and $\tilde{\psi}$ is purely imaginary.

Because of the obvious similarity between Eqs. (II.95) and (II.96), virtually every physicists have been tempted to replace formally the complex-conjugated fields ϕ and ϕ^* by a real field ψ and an imaginary field $\tilde{\psi}$, and therefore obtain a Langevin equation[12] that describes the microscopic reaction-diffusion process. Although we will see why this formal replacement is not valid in the following, let us however show that it can be justified at all orders of the perturbation theory.

Perturbative mapping between the Doi-Peliti and the MSRDJ formalism. We review the usual (zero-dimensional) perturbative argument showing that the functional integral written in terms of complex-conjugate (coherent states) fields ϕ and ϕ^* can be equivalently written in terms of a purely real field ψ and a purely imaginary field $\tilde{\psi}$. The idea is to show that for the Gaussian measure this formal replacement is exact, and since the perturbative approach is simply a series

[12] By using the MSRDJ formalism in the reverse order.

expansion near this Gaussian measure the result follows immediately. The starting point is the following relations:

$$n!\,\delta_{mn} = \int_{-\infty}^{+\infty} \mathrm{d}x\, x^n \left(-\frac{d}{dx}\right)^m \delta(x) \tag{II.97}$$

$$= \frac{1}{2\pi}\int_{-\infty}^{+\infty} \mathrm{d}x\,\mathrm{d}y\, x^n (iy)^m \mathrm{e}^{-ixy}. \tag{II.98}$$

Now, working with a complex number z we have:

$$n!\,\delta_{mn} = \frac{1}{\pi}\int \mathrm{d}z\,\mathrm{d}z^*\, z^n (z^*)^m \mathrm{e}^{-|z|^2} \tag{II.99}$$

which is easily proven by considering polar variables and where, by definition, $\mathrm{d}z\,\mathrm{d}z^* = \mathrm{d}(\mathrm{Re}z)\mathrm{d}(\mathrm{Im}z)$. Thus, up to a factor 2, we find that for this integral we obtain the same result if we consider as in Eq. (II.99) that z and z^* are complex conjugate variables or if we take as in Eq. (II.98) that z is real ($z \to x$) and z^* imaginary ($z \to iy$) and independent of z. It follows that for any Gaussian measure (denoted by an index 0), we have:

$$\langle z^n (z^*)^m \rangle_0 = \langle x^n (iy)^m \rangle_0 \,. \tag{II.100}$$

Within perturbation theory, this is sufficient to prove the same equality:

$$\langle z^n (z^*)^m \rangle = \langle x^n (iy)^m \rangle \,, \tag{II.101}$$

for any theory since the non-Gaussian part of the action, that is, the non-quadratic part of the exponential, is expanded around the Gaussian measure. Of course, the weak point of this derivation is the interchange between the series expansion and the integration.

Inconsistencies in the *formal* replacement. Let us now show why the formal replacement of the complex-conjugates fields by real and imaginary fields cannot yield exact results. We consider as an illustrative example the pure annihilation case in zero dimension:

$$2A \xrightarrow{\beta_0} \emptyset \tag{II.102}$$

then applying the Doi-Peliti formalism, ones gets the following generating functional:

$$\mathcal{Z}_{\mathrm{PA}} = \int \mathcal{D}\phi\mathcal{D}\phi^*\, \mathrm{e}^{-\int \mathrm{d}t\, \left[\phi^*\partial_t\phi - \beta_0\phi^2 + \beta_0(\phi^*)^2\phi^2\right]} \,. \tag{II.103}$$

At this point, ϕ and ϕ^* are complex conjugated fields, and the leading term in the exponential is therefore $-\beta_0(\phi^*)^2\phi^2 = -\beta_0|\phi|^4 < 0$ meaning that the integral is convergent and well-defined. However, if one performs the formal transformation and identify ϕ as a real field and $\phi^* = i\tilde{\psi}$ as an imaginary field, then the leading term becomes $-\beta_0(i\tilde{\psi})^2\phi^2 = +\beta_0\tilde{\psi}^2\phi^2 > 0$ and the integral is strongly diverging. The perturbative expansion, since it considers the leading term in the exponential as a perturbation, has of course lost this crucial information.

In fact, this is not the only problem that arises when performing such a formal replacement and to see these others issues, let us finish the formal derivation. Using the MSRDJ formalism in the reverse order, one obtains the following Langevin equation[13]:

$$\partial_t\phi(t) = -2\beta_0\phi^2 + i\sqrt{2\beta_0}\phi\,\zeta(t) \,, \tag{II.104}$$

[13]Notice that one first has to perform a "Doi shift" $\phi^* \to \phi^* + 1$ such that the action is proportional to ϕ^* and the MSRDJ can be applied.

with ζ a Gaussian white noise. We now have an imaginary noise term and therefore even starting from a real initial condition, the field ϕ itself becomes *complex*! This yields two more inconsistencies: (i) in the previous step, we assumed that ϕ was a real field, and we now discover that it is in fact complex. (ii) Starting from Eq. (II.104), one would be quite embarrassed to perform the MSRDJ formalism since this formalism requires a Gaussian integration over the noise term. If the noise is purely imaginary, this integral is no longer convergent and the whole formalism breaks down.

Difficulties of a complex Langevin equation. Let us now point out the last problem stemming from this formal derivation: the complex Langevin equation itself. As stated by Cardy in its lecture notes [17], a complex Langevin equation is not problematic with regard to the physical interpretation: in the case of pure annihilation, two different particles survive if they do not diffuse in the same area, meaning that particles must be anti-correlated in this process. This anti-correlation for the density can be obtained only if the noise term in the Langevin equation governing the dynamics of the density is purely imaginary. The pure annihilation case is also associated with the narrowing of the initial Poisson distribution of particles, narrowing which can be obtained only with an imaginary noise, since a real noise always leads to a broadening of the initial distribution (see for example [171]). The fact that ϕ is a complex variable is neither a problem since ϕ is an auxiliary variable that has no physical meaning: only its moments are linked to the moments of the particle number[14]. For instance one may even have $\langle \phi(t)^2 \rangle < 0$ while having a positive variance for $N(t)$ [174]. The fact that the moments of the actual physical process $N(t)$ are indeed real-valued was proven to be true at least in the case of the zero-dimensional annihilation reaction $2A \to \emptyset$ [20].

This was the brighter side of the problem. In fact complex Langevin equations have a much more controversial status for several reasons: even if the moments are real-valued, their very existence is still unclear because some trajectories of the Langevin equation blow up in a finite time and may therefore jeopardize the existence of well-defined moments [20]. On the theoretical side, these complex Langevin equations are still lacking some understanding [174] and it is not completely clear whether they can lead to tractable computations in general cases.

Moreover, even if these complex Langevin equations do have some sense[15], they are not *numerically* tractable. Even in the zero-dimensional cases, these Langevin equations start to diverge after finite time [20, 171, 175]. This last point is quite problematic since we were seeking for these Langevin equations in order to solve the problems of Monte Carlo and/or direct master equation simulations which often break down near phase transitions.

A solution to these difficulties. The situation we have depicted here therefore seems quite dramatic: the whole field-theoretical derivation seems to be only formal and leads to major inconsistencies that jeopardize its whole derivation, while the corresponding Langevin equation that is obtained is plagued with theoretical and numerical hurdles when the noise is imaginary.

In fact, we will see in Sec. II.5 that all these hurdles can be overcome: the replacement of the complex conjugated fields by a real and imaginary fields can indeed be performed, at the condition of making proper contour deformations. This is *not* a formal step and it must be conducted carefully, that is by making sure that the integral of the Doi-Peliti formalism [for instance in Eq. (II.103)] remains convergent at all time during the contour deformations. Doing these transformations, we will get an *exact* and *real* Langevin equation, therefore solving all the previous issues.

[14] We will see in the following that the moments of ϕ are equal to the factorial moments of N, see Eq. (II.122).

[15] We remind however that the derivation of these Langevin equations in the case of the field theory formalism is not correct.

II.4.2.b Poisson representation

Before showing in details how the difficulties encountered above can be solved using contours deformations, we discuss the Poisson representation, which is an alternative method for *formally* deriving Langevin equations that leads to the same equations as in the previous section and is thus plagued with the same problems.

The reasons why the following derivation is only *formal* is not as obvious as in the previous case, and is not the subject of this manuscript; we only hint to the weakest points of the proof. This elegant method was first introduced by Gardiner and Chaturvedi [176, 177] and does not rely on a field-theoretical formalism but uses rather the probability-generating function $G(z,t)$ which is a standard tool when studying reaction-diffusion processes; it is defined as:

$$G(z,t) \equiv \sum_{n=0}^{\infty} P_n(t) z^n \,. \tag{II.105}$$

Notice that the probability-generating function $G(z,t)$ is a well-defined analytic function for z in the complex unit disk: $|z| \leq 1$. The probability normalization is encoded through $G(z=1,t)=1$, and the derivatives of G with respect to z and evaluated in $z=1$ give access to the (factorial) moments of the number of particles:

$$\partial_z^{(k)} G(z,t)|_{z=1} = \langle N(t)(N(t)-1)\cdots(N(t)-k+1)\rangle \,. \tag{II.106}$$

Some works in the literature have also shown how one can extract some rare-events statistics in reaction-diffusion systems from the behavior of $G(z,t)$ near $z=0$ [178].

Using the probability-generating function (II.105), the master equation (II.45) can be subsumed as an evolution equation for $G(z,t)$:

$$\partial_t G(z,t) = \mathcal{L}_z G(z,t) \tag{II.107}$$

where $\mathcal{L} \equiv \mathcal{L}(z,\partial_z)$ is a second-order evolution operator:

$$\mathcal{L}(z,\partial_z)\cdot = A(z)\partial_z \cdot + B(z)\partial_z^2 \cdot \tag{II.108}$$

with A and B determined by the reaction rates through:

$$A(z) = \sum_p \alpha_p (z^p - z) \quad \text{and} \quad B(z) = \sum_q \beta_q (z^q - z^2) \,. \tag{II.109}$$

Note that for the reactions we deal with, the coefficient of the second derivative reduces to a second order polynomial in z:

$$B(z) = (\beta_0 + \beta_1)(z-\ell)(1-z), \;\; \ell \equiv -\beta_0/(\beta_0+\beta_1). \tag{II.110}$$

Notice already that the operator $\mathcal{L}$ appearing in Eq. (II.107) is the very same operator as the one appearing in the master equation in its "quantum" form, Eq. (II.52). The second-order operator $\mathcal{L}$ is *not* a Fokker-Planck operator that could be associated with the number of particles $N(t)$. The goal of the Poisson representation is therefore to find an alternative Fokker-Planck equation for an auxiliary variable, which is then linked to the initial particle number.

Let us assume that we can expand $P_n(t)$ as a superposition of uncorrelated Poisson distributions:

$$P_n(t) = \int \mathrm{d}y \, \frac{\mathrm{e}^{-y} y^n}{n!} f(y,t) \tag{II.111}$$

which means that the probability-generating function G can be rewritten as:

$$G(z,t) = \int \mathrm{d}y \, \mathrm{e}^{(z-1)y} f(y,t) \tag{II.112}$$

and its substitution into Eq. (II.107) yields (see App. B.2):

$$\partial_t G = \int \mathrm{d}y\, \mathrm{e}^{(z-1)y} \partial_t f(y,t) = \int \mathrm{d}y\, \tilde{\mathcal{L}}(1+\partial_y, y) \mathrm{e}^{(z-1)y} f(y,t) \tag{II.113}$$

$$= \int \mathrm{d}y\, \mathrm{e}^{(z-1)y} \mathcal{L}(1-\partial_y, y) f(y,t) \tag{II.114}$$

where $\tilde{\mathcal{L}}(1+\partial_y, y)\cdot = yA(1+\partial_y)\cdot + y^2 B(1+\partial_y)\cdot$ and the last equality comes from an integration by parts and after dropping the surface terms. Assuming vanishing boundary terms is probably the weak point of this derivation and it implicitly assumes some convergence properties for the function $f(y,t)$. Drummond [179] already pointed out this weakness and suggested an alternative "gauge" Poisson representation to cope with this problem, and it seems that his method yields more behaved Langevin equations, yet still complex-valued.

This remark being made, the previous equality allows us to write a partial differential equation for f:

$$\partial_t f(y,t) = \mathcal{L}(1-\partial_y, y) f(y,t)\,. \tag{II.115}$$

This partial differential equation can be interpreted as a Fokker-Planck equation if it is at most of second-order, which is the case if we also impose $p \leq 2$. In this case, we can explicitly write the Fokker-Planck equation:

$$\partial_t f(y,t) = -\partial_y \left[\mu(y) f(y,t)\right] + \frac{1}{2}\partial_y^2 \left[\sigma(y)^2 f(y,t)\right] \tag{II.116}$$

with

$$\mu(y) = (\alpha_0 + \alpha_2) y - (2\beta_0 + \beta_1) y^2 \quad \text{and} \quad \sigma(y)^2 = 2\alpha_2 y - 2(\beta_0 + \beta_1) y^2\,, \tag{II.117}$$

which is equivalent to the Langevin equation for the stochastic variable $Y(t)$:

$$\partial_t Y(t) = \mu(Y(t)) + \sigma(Y(t))\zeta(t) \tag{II.118}$$

where ζ is a Gaussian white noise. Notice that we would have obtained the very same equation for the Doi-Peliti variable ϕ if we had used the *formal* derivation we described in the previous part. This analogy between the Poisson representation and the field-theory approach was first pointed out by Droz and Mc Kane [180].

Therefore, although the subtleties of the proof are hidden in the boundary term, we believe that this derivation and the resulting Langevin equation are plagued with the same inconsistencies as those we highlighted in the previous part, in particular when the reaction scheme is chosen such that $\sigma(Y(t))^2$ becomes negative, therefore yielding complex Langevin equations.

As a conclusion for this part, let us notice that although we derived a new Langevin equation (II.118) that supposedly describes the microscopic dynamics of the initial reaction-diffusion process, we have not explained how the stochastic Langevin variable is connected to the original number of particles $N(t)$ of the reaction-diffusion process. The strength of this formalism stems from the fact that all the moments of the original reaction-diffusion process can in fact be computed via the moments of the auxiliary Langevin variable $Y(t)$ in a simple way:

$$\left\langle N(t)^k \right\rangle_{\mathrm{RD}}^{\mathrm{factorial}} \equiv \langle N(t)(N(t)-1)\cdots(N(t)-k+1)\rangle \tag{II.119}$$

$$= \sum_n P_n(t) n(n-1)\cdots(n-k+1) \tag{II.120}$$

$$= \sum_n \int \mathrm{d}y\, \frac{\mathrm{e}^{-y} y^n}{n!} f(y,t) n(n-1)\cdots(n-k+1) \tag{II.121}$$

$$= \int \mathrm{d}y\, y^k f(y,t) \equiv \left\langle Y(t)^k \right\rangle_{\mathrm{LE}} \tag{II.122}$$

where $\langle\cdot\rangle_{\mathrm{RD}}$ (resp. $\langle\cdot\rangle_{\mathrm{LE}}$) means an average over the reaction-diffusion process (resp. the Langevin process). Therefore, the factorial moments of the number of particles $N(t)$ are equal to the moments of the associated Langevin variable $Y(t)$.

In the next section we derive properly real and exact Langevin equations for reaction-diffusion processes. These equations are obviously stated in a different auxiliary variable that will not have the simple relation (II.122) to be linked to the original reaction-diffusion process. We will have to derive a duality relation to make the correspondence between the two processes.

II.5 Microscopic Langevin equation and duality formalism

In this section we now derive one of the main results of this manuscript [19], and explain how a *real* and *exact* Langevin equation can be obtained starting from a microscopic description [19]. This Langevin equation is obviously not stated in terms of a coarse-grained variable (otherwise we would be performing approximations, for instance valid at large system size), but in terms of a "dual" variable. In order to extract the physics from this Langevin equation on this auxiliary variable, we also prove a duality relation, which links the moments of the auxiliary field to the moments of the particle number of the original reaction-diffusion process.

The section will be organized as follow: we first start by giving the result and write the dual Langevin equation and duality relation, and then we will describe how these equations are derived using two different yet equivalent methods.

II.5.1 Langevin equation in the duality formalism

Langevin equation. Using the procedure that we detail in the following sections, we can give the form of the dual Langevin equation for a generic reaction-diffusion process described by the master equation (II.45) or, equivalently, by its "quantum" version Eq. (II.52). This dual Langevin equation is written in terms of a stochastic variable $Z(t)$ and reads:

$$\partial_t Z(t) = A(Z(t)) + \sqrt{2B(Z(t))}\,\zeta(t), \tag{II.123}$$

where $\zeta(t)$ is a zero mean unit variance Gaussian white noise, and A and B are the functions defined in Eqs. (II.54) and (II.55) [or equivalently in Eqs. (II.109) and (II.110)]. Crucially, due to the form of the drift and diffusion functions $A(z)$ and $B(z)$, the stochastic variable $Z(t)$ always remains (if initially so) in the bounded *real* interval $[\ell, 1]$ where $\sqrt{B(z)} \geq 0$ by definition. This Langevin equation therefore remains *real* at all time.

Notice that the evolution of $Z(t)$ stops when it has reached the absorbing barrier located at 1 (whose fixed location can be traced back to the probability conservation). This implies the existence of a delta-peak term at $z = 1$ in the probability distribution $p(z,t)$ of $Z(t)$[16]. Depending on the values of the α_p, a second delta-peak at $z = \ell$ appears whenever (the otherwise always nonnegative) $A(\ell)$ vanishes. Thus, the general form of $p(z,t)$ reads:

$$p(z,t) = p_c(z,t) + q_1(t)\delta(1-z) + q_\ell(t)\delta(\ell - z) \tag{II.124}$$

where $p_c(z,t)$ is the continuous part of the distribution and q_1, q_ℓ the weights at the boundaries.

Note however that $Z(t)$ is *not* a density and is not simply related to the particle number in the original reaction-diffusion process. We therefore need a relation between these two quantities $Z(t)$ and $N(t)$, and we show in the following that the determination of the statistics of $Z(t)$ suffices to extract "all the physics" of interest for the original reaction-diffusion process. This connection between the two formalisms is called the duality relation.

[16] The appearance of this delta-peak in the distribution is due to the specific form of the noise and drift terms. The shape of these terms may change the nature of the boundary (according to Feller's classification [181], or see for instance [182]).

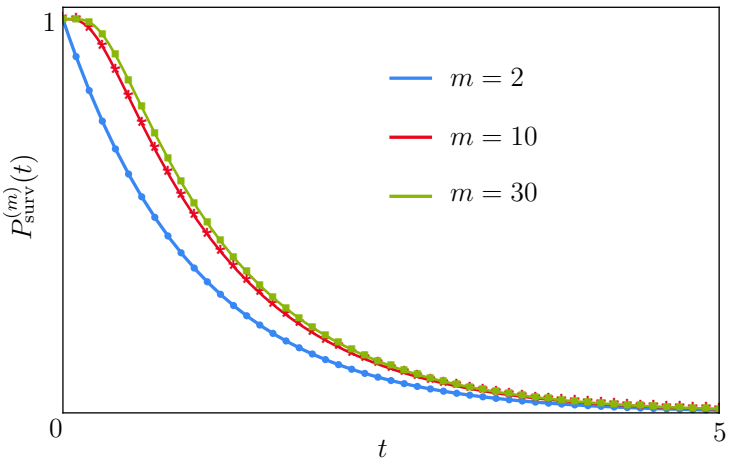

Figure II.5 – *Survival probability $P_{\rm surv}^{(m)}(t)$ in the pure annihilation process $2A \to \emptyset$ with a unit rate. The three curves correspond to different value of m. The solid lines are obtained directly from the reaction-diffusion process, that is $P_{\rm surv}^{(m)}(t) = 1 - P_0(t)$. The symbols are computed through the duality relation: $\langle Z(t)^m \rangle_{\rm LE} = \int_{-1}^{1} {\rm d}z\, p(z,t|0,0) z^m = 1 - P_{\rm surv}^{(m)}(t)$.*

Duality relation. The duality relation, that links the moments of the particle number $N(t)$ in the reaction-diffusion process, and the moments of the Langevin variable $Z(t)$ of the dual process reads:

$$\Big\langle \Big\langle Z(t)^{N(0)} \Big\rangle_{\rm LE} \Big\rangle_{\rm RD} = \Big\langle \Big\langle Z(0)^{N(t)} \Big\rangle_{\rm LE} \Big\rangle_{\rm RD} \tag{II.125}$$

where $\langle \cdot \rangle_{\rm RD}$ (resp. $\langle \cdot \rangle_{\rm LE}$) has to be understood as an averaging over the reaction-diffusion process (resp. the Langevin process). Notice that this relation generalizes an analogous one derived by Doering *et al.* for the reversible coagulation-decoagulation process $A \rightleftharpoons 2A$ [183].

Using the probability distribution $p(z,t)$ of the Langevin variable $Z(t)$, we can rewrite explicitly the duality relation as:

$$\int_\ell^1 {\rm d}z \sum_{n=0}^{\infty} p(z,t) P_n(0) z^n = \int_\ell^1 {\rm d}z \sum_{n=0}^{\infty} p(z,0) P_n(t) z^n \,. \tag{II.126}$$

Notice that on the left-hand side of the duality relation (II.125) appears $N(0)$, which is the initial condition of the reaction-diffusion that one wishes to study, whereas on the right-hand side appears $Z(0)$, the initial condition for the Langevin equation. This initial condition $Z(0)$ is arbitrary, and we will show that choosing it cunningly allows for the computation of various observables of the reaction-diffusion process.

The beauty of the duality relation is that it links in a nontrivial way the two processes, and means that solving one process is equivalent to solving the other. The duality relation (II.125) allows us to trade the very difficult problem of solving the reaction-diffusion process for solving instead a Langevin equation, which, in the numerical as well as theoretical view-point, offers new perspectives for cracking difficult reaction-diffusion processes.

Examples. Before getting into the details of the proof of the duality relation, let us give some examples on how it can be used to compute actual quantities of interest of the reaction-diffusion process, such as the survival probability and the moments of the probability distribution $P_n(t)$.

The survival probability $P_{\rm surv}^{(m)}(t)$ is defined as the probability that, starting at $t = 0$ with $m > 0$ particles, at least one particle survives at time t: $P_{\rm surv}^{(m)}(t) = 1 - P_0(t)$. Using Eq. (II.126)

with $p(z,0)=\delta(z)$ and $P_n(0)=\delta_{mn}$, we obtain

$$1-P^{(m)}_{\rm surv}(t)=\int_\ell^1 \mathrm{d}z\, p(z,t|0,0)z^m=\langle Z(t)^m\rangle_{\rm LE} \tag{II.127}$$

where $p(z,t|z_0,0)$ is the conditional transition probability of the Langevin equation with $p(z,t=0)=\delta(z-z_0)$ as initial condition and the mth-order moment is a readily measurable quantity in a Langevin equation simulation. To give an explicit example, we consider the pure annihilation process in zero dimension. In this case, the probability generating function $G(z,t)$ can be computed exactly as a sum of orthogonal polynomials [184]. The dual probability distribution $p(z,t)$ can be computed exactly as well and it allows us to test on a very simple example the duality relation (see Fig. II.5).

Similarly, the moments of the reaction-diffusion process can be derived from $G(z,t)$ using $p(z,0)=\delta(z-z_0)$ as initial condition; Eq. (II.126) yields[17]:

$$G(z_0,t)=\int_\ell^1 \mathrm{d}z\sum_{n=0}^{\infty} p(z,t|z_0,0)P_n(0)z^n. \tag{II.128}$$

Differentiating $G(z_0,t)$ with respect to z_0 and evaluating it at $z_0=1$ yields the (factorial) moments of the reaction-diffusion process. For instance, the average particle number reads

$$\langle N(t)\rangle=\partial_{z_0}\int_\ell^1 \mathrm{d}z\sum_n p(z,t|z_0,0)P_n(0)z^n\Big|_{z_0=1}. \tag{II.129}$$

All formulas above can be easily generalized to the spatially extended case in the presence of diffusion. For instance, putting m particles at one site i and 0 elsewhere in the reaction-diffusion process and choosing $Z_j(0)=0$ for all sites j for the LE, Eq. (II.127) is replaced by: $P^{(m,i)}_{\rm surv}(t)=1-\langle Z_i(t)^m\rangle_{\rm LE}$[18].

II.5.2 Duality in the field-theoretical context

Our goal in the following is to show a correct proof for the derivation of the dual Langevin equation (II.123) using a field-theory formalism. We will show that the complex-conjugate (coherent states) fields ϕ and ϕ^* can indeed be transformed into a real field $\tilde\psi$ and a purely imaginary field ψ. However, the Wick rotation one has to perform in order to make this transformation cannot be done blindly, to the contrary of what the perturbation theory would suggest, and we take a special care of the convergence of the integrand of $\mathcal{Z}_{\rm RD}$ and of making sure that its leading-order term remains negative to ensure this convergence. For this purpose, we proceed to several contour deformations in the complex plane, and we will see that the price to pay to guarantee the convergence of the integrand is a restriction of the real field $\tilde\psi$ to a bounded interval, instead of living on the whole real axis as the usual proof would suggest.

The starting point of the proof is the Doi-Peliti partition function that we recall here:

$$\mathcal{Z}_{\rm RD}[J,\tilde J]=\int \mathcal{D}\phi\mathcal{D}\phi^*\,\mathrm{e}^{-\mathcal{S}_{\rm RD}[\phi,\phi^*]+\int \mathrm{d}t\,(J\phi+\tilde J\phi^*)}. \tag{II.130}$$

[17] Note that choosing $P_n(0)=\delta_{mn}$ in Eq. (II.128), one recovers that the survival probability Eq. (II.127) is nothing but $1-G(0,t)$.

[18] Notice that because of homogeneity, the mth-order moment at site i can in fact be estimated in a numerical simulation of the Langevin equation as an average over all sites: $1/L^d\sum_i <Z_i(t)^m>_{\rm LE}$.

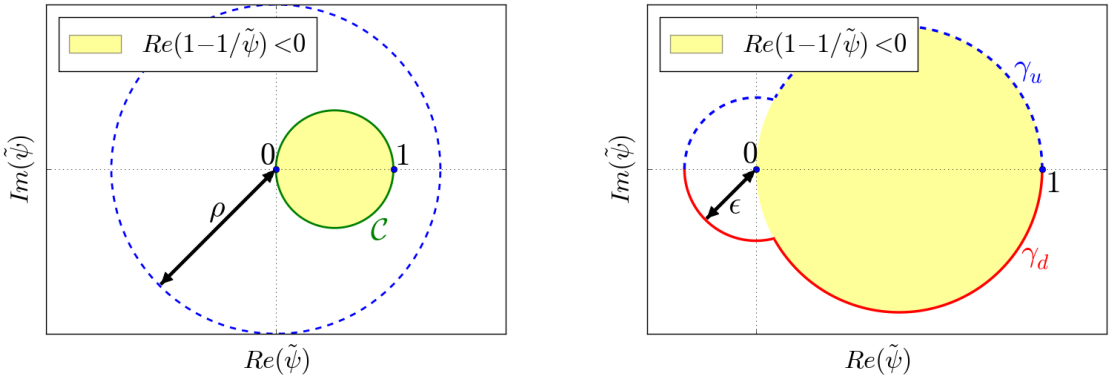

Figure II.6 – ***Left.*** *The initial integration circle $|\tilde{\psi}| = \rho$ (dashed line) and the circle $\mathcal{C}$ in which it is distorted. Inside $\mathcal{C}$ the integral over ρ is not convergent.* ***Right.*** *Deformation of the circle $\mathcal{C}$ including a bump around the origin, where the action S'' in Eq. (II.137) shows an essential singularity. The integration contour is split into γ_u and γ_d which are two (distorted) half-circles, above and below the real axis, respectively.*

II.5.2.a Derivation of the Langevin equation

The proof we show here is directly inspired by appendix A of [185] (in which a different contour deformation was used to make ψ real and $\tilde{\psi}$ purely imaginary). We expose it for simplicity for the reversible coagulation-decoagulation process (without diffusion):

$$A \xrightarrow{\alpha_2} 2A \tag{II.131a}$$

$$2A \xrightarrow{\beta_1} A \tag{II.131b}$$

and we generalize it below to the case with diffusion. It can also be adapted to all the reactions we consider in this chapter, which are summed up in Eq. (II.44) with the extra restriction $q < 2$.

In this simplified zero-dimensional setting and for this specific case of reactions, the corresponding generating functional of correlation and response functions reads (we have dropped the subscript RD to alleviate the notation in the proof):

$$\mathcal{Z} = \int_{\mathbb{C}} \frac{\mathrm{d}\phi\,\mathrm{d}\phi^*}{2i\pi}\, \mathrm{e}^{-S[\phi,\phi^*]+J\phi+\tilde{J}\phi^*} \tag{II.132}$$

where

$$S[\phi,\phi^*] = -\alpha_2\left((\phi^*)^2-\phi^*\right)\phi - \beta_1\left(\phi^*-(\phi^*)^2\right)\phi^2 \tag{II.133}$$

and we recall that $\mathrm{d}\phi\,\mathrm{d}\phi^* = \mathrm{d}\phi_1\,\mathrm{d}\phi_2$ with $\phi = (\phi_1+i\phi_2)/\sqrt{2}$, and that α_2 and β_1 are positive since they are reaction rates. Notice that for clarity we first consider that the time is frozen, and furthermore that $J = \tilde{J} = 0$, the case with sources and with time-dependence will be treated below.

Step 1. The proof begins with a first change of variables and the introduction of polar coordinates:

$$\phi = \rho \mathrm{e}^{i\theta}, \quad \phi^* = \rho \mathrm{e}^{-i\theta}, \tag{II.134}$$

such that we now have:

$$\mathcal{Z} = \int_0^\infty \frac{2\rho\,\mathrm{d}\rho}{2i\pi} \int_0^{2\pi} \mathrm{d}\theta\, \mathrm{e}^{-S'[\rho,\theta]}\,. \tag{II.135}$$

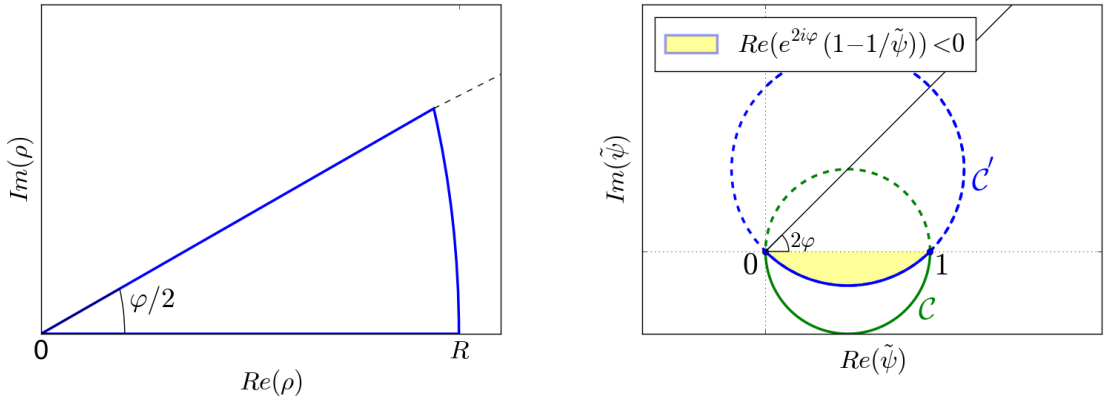

Figure II.7 – ***Left.*** *Wick rotation by angle φ of the integration axis in the complex ρ-plane. The contribution of the integral over the circular arc of radius R vanishes when $R \to \infty$.* ***Right.*** *In the complex $\tilde{\psi}$-plane, the circle $\mathcal{C}$ defined by the convergence condition (II.138) is modified by the Wick rotation and becomes the circle $\mathcal{C}'$. The forbidden region (shaded area) is also modified in consequence.*

Step 2. When ρ is fixed, the integration over the angle θ can be rewritten as a contour integration on the circle of radius ρ over the variable $\tilde{\psi} = \rho \mathrm{e}^{-i\theta}$:

$$\mathcal{Z} = \int_0^\infty \frac{2\rho\,\mathrm{d}\rho}{2\pi} \oint_{|\tilde{\psi}|=\rho} \frac{\mathrm{d}\tilde{\psi}}{\tilde{\psi}}\, \mathrm{e}^{-S''[\rho^2,\tilde{\psi}]} \tag{II.136}$$

with

$$S''[\rho^2,\tilde{\psi}] = \beta_1 \rho^4 \left(1 - \frac{1}{\tilde{\psi}}\right) + \alpha_2 \rho^2 (1-\tilde{\psi}). \tag{II.137}$$

Since at fixed ρ the integrand is holomorphic on $\mathbb{C}^*$ and in anticipation of step 4, we distort the integration contour over $\tilde{\psi}$ on the smallest contour $\mathcal{C}$ such that the integral over ρ remains convergent at large ρ, which is given by the locus of points where the coefficient in front of ρ^4 in the action (II.137) has a positive real part:

$$\mathrm{Re}\left(1 - 1/\tilde{\psi}\right) > 0 \quad \Leftrightarrow \quad |\tilde{\psi}| > \cos(\arg(\tilde{\psi})), \tag{II.138}$$

which defines a circle, see Fig. II.6 (left).

Step 3. The contour over $\tilde{\psi}$ is now deformed, for all ρ, into the circle $\mathcal{C}$ previously defined. Given that the integrand in Eq. (II.136) has an essential singularity at $\tilde{\psi} = 0$, $\mathcal{C}$ is in fact slightly distorted to keep the singularity inside the integration domain, see Fig. II.6 (right).

Remark that along this particular contour, the real part of the leading term in ρ^4 of the action (II.137) vanishes, and the convergence at large ρ of the integral is now determined by the sub-leading term in ρ^2. The convergence is therefore guaranteed whenever

$$\mathrm{Re}\left(\alpha_2 \left(1 - \tilde{\psi}\right)\right) > 0\,, \tag{II.139}$$

which is verified on the half-plane $\mathrm{Re}(\tilde{\psi}) < 1$ since $\alpha_2 > 0$, and in particular all along the previously defined distorted circle $\gamma_u \cup \gamma_d$, see Fig. II.6 (right). The partition function can therefore be rewritten as:

$$\mathcal{Z} = \mathcal{Z}_u + \mathcal{Z}_d = \int_0^\infty \frac{2\rho\,\mathrm{d}\rho}{2\pi} \left(\int_{\gamma_u} + \int_{\gamma_d}\right) \frac{\mathrm{d}\tilde{\psi}}{\tilde{\psi}}\, \mathrm{e}^{-S''[\rho^2,\tilde{\psi}]}. \tag{II.140}$$

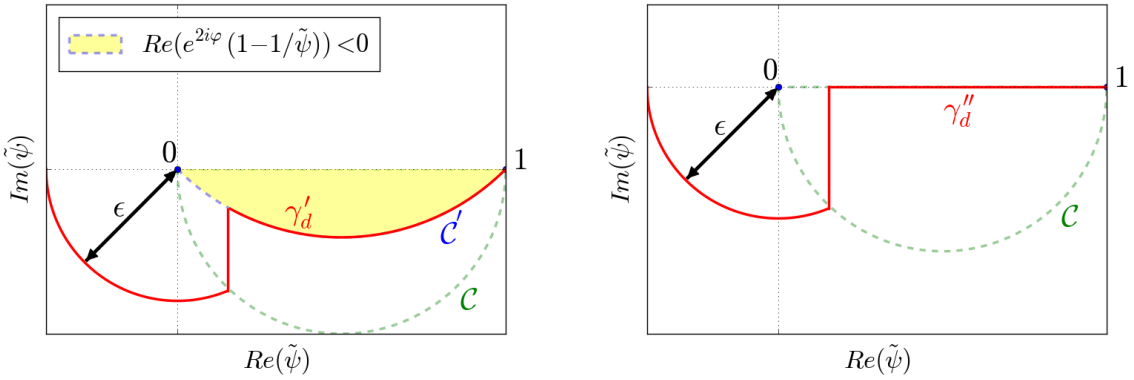

Figure II.8 – ***Left.*** *New contour γ'_d obtained after the Wick rotation.* ***Right.*** *Contour γ''_d obtained by taking the limit $\varphi \to \pi/4$ of γ'_d.*

Step 4. We first consider the integration over the lower contour γ_d. The integration over ρ is Wick-rotated by an angle φ which means that the integration axis is tilted by an angle φ in the complex ρ-plane. This is allowed because no singularity is swept by the integration axis during the rotation and because the integration at infinity does not contribute, see Fig. II.7 (left). Then, $\mathcal{Z}_d$ reads:

$$\mathcal{Z}_d = \int_0^{\infty \mathrm{e}^{i\varphi}} \frac{2\rho\,\mathrm{d}\rho}{2\pi} \int_{\gamma_d} \frac{\mathrm{d}\tilde{\psi}}{\tilde{\psi}}\, \mathrm{e}^{-S''[\rho^2,\tilde{\psi}]} \tag{II.141}$$

and the change of variable $\rho^2 = \rho'^2 \mathrm{e}^{i\varphi}$ yields:

$$\mathcal{Z}_d = \int_0^{\infty} \frac{2\rho'\,\mathrm{d}\rho'}{2\pi} \mathrm{e}^{i\varphi} \int_{\gamma_d} \frac{\mathrm{d}\tilde{\psi}}{\tilde{\psi}}\, \mathrm{e}^{-S''[\rho'^2 \mathrm{e}^{i\varphi},\tilde{\psi}]}\,. \tag{II.142}$$

Step 5. After the Wick rotation, the convergence condition (II.138) becomes:

$$\mathrm{Re}\left(\mathrm{e}^{2i\varphi}\left(1-\frac{1}{\tilde{\psi}}\right)\right) > 0\,, \tag{II.143}$$

which defines a new circle $\mathcal{C}'$ (see Fig. II.7 (right)), and the contour γ_d is modified into a new one γ'_d which follows $\mathcal{C}'$, except for a small detour in order to avoid the singularity, see Fig. II.8 (left).

Step 6. In the limit $\varphi \to \pi/4$, the radius of the circle $\mathcal{C}'$ goes to infinity and the lower part of the circle that we are considering becomes the interval $[0,1]$ and the integration contour becomes γ''_d, see Fig. II.8 (right):

$$\mathcal{Z}_d = \int_0^{\infty} \frac{2\rho'\,\mathrm{d}\rho'}{2\pi} \mathrm{e}^{i\pi/4} \int_{\gamma''_d} \frac{\mathrm{d}\tilde{\psi}}{\tilde{\psi}}\, \mathrm{e}^{-S''[\rho'^2 \mathrm{e}^{i\pi/4},\tilde{\psi}]}. \tag{II.144}$$

The limit $\epsilon \to 0$ is still singular and is therefore not performed yet.

Step 7. A new Wick rotation of angle $\pi/4$ is performed on ρ, as well as a new change of variable $\rho'^2 = \rho''^2 \mathrm{e}^{i\pi/4}$:

$$\mathcal{Z}_d = \int_0^{\infty} \frac{2\rho''\,\mathrm{d}\rho''}{2\pi} \int_{\gamma''_d} \frac{\mathrm{d}\tilde{\psi}}{i\tilde{\psi}}\, \mathrm{e}^{-S''[i\rho''^2,\tilde{\psi}]}. \tag{II.145}$$

Step 8. A last change of variable $\psi = i\rho''^2/\tilde{\psi}$ performed to get back to Cartesian coordinates finally yields:

$$\mathcal{Z}_d = \int_0^{i\infty} \frac{\mathrm{d}\psi}{2\pi} \int_{\gamma_d''} \mathrm{d}\tilde{\psi}\, \mathrm{e}^{-S[\psi,\tilde{\psi}]} \tag{II.146}$$

where S is indeed the very same action as the one we started from in Eq. (II.133). The limit $\epsilon \to 0$ is now trivial because there is no more a singularity when $\tilde{\psi} \to 0$ (the singularity was an artifact coming from the polar variables). Therefore, the integration over the path γ_d'' is simply an integration over the segment $[0,1]$, and $\mathcal{Z}_d$ finally reads:

$$\mathcal{Z}_d = \int_0^{i\infty} \frac{\mathrm{d}\psi}{2\pi} \int_0^1 \mathrm{d}\tilde{\psi}\, \mathrm{e}^{-S[\psi,\tilde{\psi}]}\,. \tag{II.147}$$

Let us insist on the fact that we get a variable $\tilde{\psi}$ that is *bounded*. Although the usual formal replacement that one can find in the literature does not raise such question and assumes that the real field lives on the whole real axis, it should not be so surprising after all: $\tilde{\psi}$ belonging to $[0,1]$ simply reflects the fact that the leading term of the action (II.133) (the one in factor of β_1) must remain negative in order to have convergence of the integrand. This is the case as long as $\phi^* - (\phi^*)^2 > 0$ (since there is a minus sign in front of the action), that is $\phi^* \in [0,1]$. Of course, the usual approach, which is justified by perturbative arguments, misses completely this fact since the series expansion is done in terms of β_1, and the question of the convergence of the integrand is completely overlooked.

The computation of $\mathcal{Z}_u$ follows the same steps as those for $\mathcal{Z}_d$ up to the difference that the lower half-plane is replaced by the upper one. We finally get the expected result, that is, two complex conjugated variables are replaced by two independent variables, one purely imaginary, the other real. The important subtlety is that the real variable $\tilde{\psi}$ is compact with the proper integration boundaries given by the contour deformations, which is *a priori* far from being trivial:

$$\mathcal{Z} = \int_{-i\infty}^{i\infty} \frac{\mathrm{d}\psi}{2\pi} \int_0^1 \mathrm{d}\tilde{\psi}\, \mathrm{e}^{-S[\psi,\tilde{\psi}]}\,. \tag{II.148}$$

The generating functional $\mathcal{Z}$ can now be converted into a Langevin equation using the (reverse) MSRDJ formalism. The quadratic term in ψ of the action S, Eq. (II.133), can now be eliminated by a Hubbard-Stratonovich transformation:

$$\exp\left[\beta_1\left(\tilde{\psi}-\tilde{\psi}^2\right)\psi^2\right] = \int \mathrm{d}\zeta\, \exp\left[-\left(\zeta^2/2 + \sqrt{2\beta_1\left(\tilde{\psi}-\tilde{\psi}^2\right)}\psi\zeta\right)\right]. \tag{II.149}$$

If we now reintroduce the time-dependence in S by adding the term $\psi\partial_t\tilde{\psi}$, the integration over the imaginary variable ψ in Eq. (II.148) yields a Dirac-delta function of the Langevin equation over the real variable $\tilde{\psi}$:

$$\partial_t\tilde{\psi} = \alpha_2\left(\tilde{\psi}^2 - \tilde{\psi}\right) + \sqrt{2\beta_1\left(\tilde{\psi}-\tilde{\psi}^2\right)}\,\zeta \tag{II.150}$$

where ζ is in fact a Gaussian white noise since its probability distribution is given in Eq. (II.149) by $\mathcal{P}(\zeta) = \exp\left(-\zeta^2/2\right)$. Notice now that the fact that $\tilde{\psi} \in [0,1]$ completely makes sense since it therefore guarantees that the square-root terms has a positive argument, and that the Langevin equation remains real.

Remark that taking into account the time-dependence does not invalidate the proof because the extra $\psi\partial_t\tilde{\psi}$ term only adds a sub-leading term (in factor of ρ^2) to the action S'' defined in Eq. (II.137). This sub-leading term is significant only when the contour is exactly on the circle $\mathcal{C}'$.

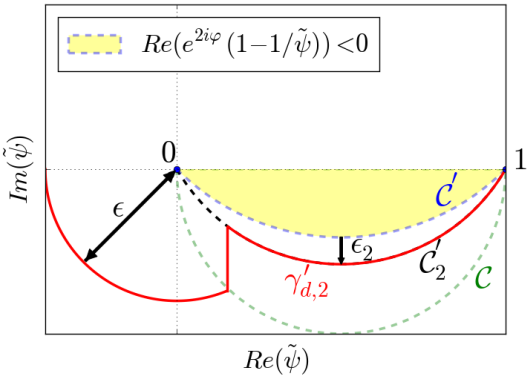

Figure II.9 – *Taking into consideration time and spatial dependence: a new contour $\gamma'_{d,2}$, shifted from the contour γ'_d by a factor ϵ_2, is defined such that the sub-leading terms are never relevant.*

One can therefore slightly shift all the previously defined contours by a factor ϵ_2 in order not to lie on the circle $\mathcal{C}'$, as illustrated on Fig. II.9 in the case of the contour γ'_d. The rest of the proof remains unchanged, except that the limit $\epsilon_2 \to 0$, which is not singular, has to be taken at the end.

The spatially-extended case is treated in the same way since the extra term coming from spatialization also contributes only in a sub-leading way.

Let us now briefly discuss the case with sources, with space and time frozen. In the limit where the sources J and $\tilde{J}$ are infinitesimal, the original partition function (II.132) can be expanded as a power series and reads:

$$\begin{aligned}\mathcal{Z}[J,\tilde{J}] &= \int \frac{\mathrm{d}\phi\,\mathrm{d}\phi^*}{2i\pi}\,\mathrm{e}^{-S[\phi,\phi^*]+J\phi+\tilde{J}\phi^*} \\ &= \int \frac{\mathrm{d}\phi\,\mathrm{d}\phi^*}{2i\pi}\,\mathrm{e}^{-S[\phi,\phi^*]}\left(1+J\phi+\frac{1}{2}J^2\phi^2+\cdots\right)\left(1+\tilde{J}\phi^*+\frac{1}{2}\tilde{J}^2(\phi^*)^2+\cdots\right)\end{aligned} \tag{II.151}$$

and the deformations described above can be applied to all the terms in the sum, which proves that adding infinitesimal sources is not an issue.

Notice that the proof was shown here for the particular choice of reactions (II.131) but is in fact generic for any set of reactions of the form $A \to pA$, $2A \to qA$ with $q < 2$, except that the deformation contours would be different. For instance, if one were to consider the pure annihilation reaction $2A \to \emptyset$, the convergence condition Eq. (II.138) would be modified and would define a lemniscate instead of the circle $\mathcal{C}$.

II.5.2.b Proof of the duality relation

We now prove the duality relation (II.126) using the "quantum" formalism. And for this purpose we first define the bra $\langle\tilde{p}(t)|$:

$$\langle\tilde{p}(t)| \equiv \int_\ell^1 \mathrm{d}z\,\tilde{p}(z,t|z_0,0)\langle z| \equiv \int_\ell^1 \mathrm{d}z\,p_c(z,t)\langle z| + q_1(t)\langle 1| + q_\ell(t)\langle \ell| \tag{II.152}$$

and assume it evolves via:

$$\partial_t\langle\tilde{p}(t)| = \langle\tilde{p}(t)|\mathcal{L}(a^\dagger,a)\,. \tag{II.153}$$

The proof goes as follows: we first show that the bra $\langle\tilde{p}(t)|$ we have just defined is associated with the probability distribution $p(z,t)$ of the dual Langevin equation (II.123), and in a second time we prove the duality relation (II.126).

We have:

$$\left\langle\tilde{p}(t)|z'\right\rangle = \int_\ell^1 \mathrm{d}z\, \tilde{p}(z,t|z_0,0)\mathrm{e}^{izz'} \tag{II.154}$$

$$\text{and thus} \quad \int_{-\infty}^{\infty}\mathrm{d}z'\,\mathrm{e}^{-iyz'}\left\langle\tilde{p}(t)|z'\right\rangle = \int_\ell^1 \mathrm{d}z\, \tilde{p}(z,t|z_0,0)\delta(y-z) \tag{II.155}$$

$$= \tilde{p}(y,t|z_0,0) \tag{II.156}$$

and we can therefore compute the time evolution of $\tilde{p}$:

$$\partial_t\tilde{p}(y,t|z_0,0) = \int_{-\infty}^{\infty}\mathrm{d}z'\,\mathrm{e}^{-iyz'}\left\langle\tilde{p}(t)|\mathcal{L}(a^\dagger,a)|z'\right\rangle \tag{II.157}$$

$$= \int_{-\infty}^{\infty}\mathrm{d}z'\,\mathrm{e}^{-iyz'}\left\{\int_\ell^1 \mathrm{d}z\, p_c(z,t)\underbrace{\mathcal{L}(z,iz')}_{=\mathcal{L}(z,\partial_z)}\mathrm{e}^{izz'} + q_\ell(t)\underbrace{\mathcal{L}(\ell,iz')}_{=A(\ell)}\mathrm{e}^{i\ell z'} + q_1(t)\underbrace{\mathcal{L}(1,iz')}_{=0}\mathrm{e}^{iz'}\right\}. \tag{II.158}$$

Since we have $\mathcal{L}(z,\partial_z) = A(z)\partial_z + B(z)\partial_z^2$, we perform to integrations by parts in the second integral. Taking care of the boundary terms, we get:

$$\partial_t\tilde{p}(y,t) = \int_{-\infty}^{\infty}\mathrm{d}z'\,\mathrm{e}^{-iyz'}\left\{\int_\ell^1 \mathrm{d}z\, \left(-\partial_z(A(z)p_c(z,t)) + \partial_z^2(B(z)p_c(z,t))\right)\mathrm{e}^{izz'}\right.$$
$$\left. + \left[A(z)p_c(z,t)\mathrm{e}^{izz'} + B(z)p_c(z,t)\partial_z\mathrm{e}^{izz'}\right]_\ell^1 - \left[\partial_z(B(z)p_c(z,t))\mathrm{e}^{izz'}\right]_\ell^1 + q_\ell(t)A(\ell)\mathrm{e}^{i\ell z'}\right\}. \tag{II.159}$$

The first boundary term vanishes, and we proceed to the integration over z', which yields Dirac distributions, such that we now have:

$$\begin{aligned}\partial_t\tilde{p}(y,t) = &\underbrace{-\partial_y(A(y)p_c(y,t)) + \partial_y^2(B(y)p_c(y,t))}_{\mathcal{L}^\dagger(y,\partial_y)p_c(y,t)} \underbrace{-\partial_z(B(z)p_c(z,t))|_{z=1}}_{J(1,t)}\delta(y-1)\\ &+\underbrace{(\partial_z(B(z)p_c(z,t))|_{z=\ell} + q_\ell(t)A(\ell))}_{J(\ell,t)}\delta(\ell-y)\end{aligned} \tag{II.160}$$

where we have defined the probability current $J(z,t) = +A(z)p_c(z,t) - \partial_z\left[B(z)p_c(z,t)\right]$. Notice that the currents escaping through the barriers at $y=\ell$ and $y=1$ governs the time evolution of the peaked probability distributions $q_1(t)$ and $q_\ell(t)$, such that the last equality can be rewritten as:

$$\partial_t\tilde{p}(y,t) = \mathcal{L}^\dagger(y,\partial_y)p_c(y,t) + \partial_t q_1(t)\delta(1-y) + \partial_t q_\ell(t)\delta(y-\ell) \tag{II.161}$$

$$= \mathcal{L}^\dagger(y,\partial_y)\tilde{p}(y,t)\,. \tag{II.162}$$

Therefore, $\tilde{p}$ is indeed a probability distribution evolving according to the dual operator $\mathcal{L}^\dagger(y,\partial_y)$ which is a Fokker-Planck operator. The associated dual Langevin equation is Eq. (II.123), which terminates the first point of the proof, that is $\tilde{p}=p$ is indeed the probability distribution of the dual Langevin variable Z.

We now have to prove the duality relation, which is rather simple in this formalism. On the one hand we have:

$$\langle\tilde{p}(t)|P(0)\rangle = \sum_n P_n(0)\int_\ell^1 \mathrm{d}z\,\tilde{p}(z,t|z_0,0)\underbrace{\langle z|n\rangle}_{=z^n}, \tag{II.163}$$

and on the other hand,

$$\langle \tilde{p}(0)|P(t)\rangle = \sum_n P_n(t) \int_\ell^1 \mathrm{d}z\, \tilde{p}(z,t|z_0,0) z^n \,. \tag{II.164}$$

The equality between these two terms, which is the duality relation, is now straightforward from the definition of the evolution of the bra $\langle \tilde{p}(t)|$:

$$\langle \tilde{p}(t)|P(0)\rangle = \left\langle \tilde{p}(0)|\mathrm{e}^{\mathcal{L}(a^\dagger,a)t}|P(0)\right\rangle = \langle \tilde{p}(0)|P(t)\rangle \tag{II.165}$$

which terminates the proof.

II.5.3 Duality in the probability-generating function formalism

Proving the duality relation in the probability-generating function formalism is simpler than in the field-theory formalism. Yet, it was important to prove it using the latter formalism in order to clarify the paradoxical situation pointed out in Sec. II.4.2.a, where we have seen that a supposedly real field was in fact described by a complex Langevin equation. The proof also highlighted the importance of the nature of the fields: the fact that the response-field is imaginary, and more interestingly that the real field $\tilde{\psi}$ is in fact bounded is often overlooked in the literature.

First, notice that the probability-generating function $G(z,t)$ associated with the reaction-diffusion process and the probability distribution $P_n(t)$ evolves according to Eq. (II.107):

$$\partial_t G(z,t) = \mathcal{L} G(z,t) \tag{II.166}$$

where $\mathcal{L}$ is the second-order differential operator defined in Eq. (II.108). Although it is *not* a Fokker-Planck operator, its adjoint – or dual – operator $\mathcal{L}^\dagger$ defines a Fokker-Planck operator for the dual probability distribution $p(z,t)$ that we *define* as evolving according to the following equation:

$$\partial_t p(z,t) = \mathcal{L}^\dagger p(z,t) \tag{II.167}$$

and to which is associated the dual Langevin equation (II.123):

$$\partial_t Z(t) = A(Z(t)) + \sqrt{2B(Z(t))}\,\zeta(t), \tag{II.168}$$

where $Z(t)$ is the dual variable.

To prove the duality relation, we first need to compute the time evolution of the m^{th} moment of $Z(t)$, which is done by performing a change of variable in the previous Langevin equation. Using the Itō formula (see App. B.1), we thus obtain:

$$\partial_t Z(t)^m = \sum_n L_{nm} Z(t)^n + m Z(t)^{m-1} \sqrt{2B(Z(t))}\,\zeta(t) \tag{II.169}$$

where L_{nm} is the transition matrix defined in Eq. (II.45). Taking the average of the previous equation, we finally get:

$$\partial_t \left\langle Z(t)^m \right\rangle_{\text{LE}} = \sum_n L_{nm} \left\langle Z(t)^n \right\rangle_{\text{LE}} \,. \tag{II.170}$$

Indeed, the last term of the right-hand side of Eq. (II.169) has a vanishing average since the noise ζ is independent of the stochastic variable $Z(t)$.

Notice now that the process $\mathcal{M}(t) = \sum_m Z(t)^m P_m(T-t)$ with $0 \leq t \leq T$ is a martingale, that means that its average value is independent of the time t at which it is evaluated. The proof is direct by showing that $\partial_t \left\langle \mathcal{M}(t)\right\rangle_{\text{RD}} = 0$. Then, evaluating the average of $\mathcal{M}$ at $t=0$ and $t=T$, we obtain the duality relation (II.126). The spatially-extended case is treated in App. B.3.

II.6 Conclusion

In this chapter we have introduced two formalisms to obtain a field-theoretical description of a nonequilibrium phenomenon. The MSRDJ formalism starts from a Langevin description of the system, whereas the Doi-Peliti approach stems from the microscopic description of a reaction-diffusion process in terms of a master equation. The MSRDJ formalism will be the starting point of the NPRG studies in Chaps. III and IV.

More importantly, we have shown that for single species reaction-diffusion processes, the Doi-Peliti path integral can be interpreted as a MSRDJ path integral and therefore yields an exact Langevin equation that is dual to the initial reaction-diffusion process. The derivation of this result, although known in the literature for a long time, is plagued with inconsistencies and produces complex Langevin equations if not conducted with some care. The first main result of this manuscript was therefore to show properly how one can derive an *exact* and *real* Langevin equation starting from the reaction-diffusion description.

The very fact that one could obtain *real* Langevin equation for the description of some of these systems was not obvious. Indeed, in the literature, the appearance of an imaginary noise was associated with the fact of having anti-correlations in the system and an imaginary noise is the only mean of getting a narrowing of the probability distribution which is the hallmark of these anti-correlations. How, in this condition, could one get anti-correlations while having a real Langevin dynamics? The answer lies in the duality relation (II.125): the real Langevin equation that we have derived does not describe the evolution of the reaction-diffusion particle number $N(t)$ but that of a dual variable $Z(t)$. This dual variable Z can be seen in a sense as describing some kind of "time-reversed" dynamics [in the path-integral derivation, this is made clear by the fact that $Z(t) = \tilde{\psi}(-t)$, whereas in the probability generating formulation, we have seen that the evolution of $N(t)$ is coupled to that of $Z(T-t)$]. Therefore, the broadening of the probability distribution of $Z(t)$ under the real Langevin dynamics indeed corresponds to a narrowing of the probability distribution of $N(t)$, and the paradox is resolved.

However, it happens that this remarkable formalism only seems to hold for a single species of particles and we were not able to extend the derivation to several species reaction-diffusion processes. When several particles are involved, we cannot perform contour deformations that guarantee the convergence of the integrand at all time and we systematically get imaginary-noise Langevin equations. This problem may be solved if we were able to find the "right" variables: in the one species problem, the right variable on which is stated the Langevin equation appears naturally as the "response field" $\tilde{\psi}$. In the case of several species, this miraculous variable yielding real equations may be a non trivial combination of the fields describing each species.

Finally, we argued in this chapter that real Langevin equation would prove very useful for the numerical study of some controversial reaction-diffusion processes near their critical point. Let us mention that Al Hammal *et al.* already studied the parity conserving generalized voter (PCGV) universality class through a phenomenologically derived Langevin equation [152] which turns out to be indeed the dual Langevin equation one would have obtained starting with set of reactions $A \xrightarrow{\alpha_3} 3A$, $A \xrightarrow{\alpha_5} 5A$, $2A \xrightarrow{\beta_0} \emptyset$ that indeed belongs to the PCGV class.

Method	Langevin equation	Example: $A \xrightarrow{\alpha_2} 2A$ and $2A \xrightarrow{\beta_0} \emptyset$	Connection between the moments	Comments
van Kampen	Eq. (II.92)	$\partial_t y = (\alpha_2 - 2\beta_0(2\phi - 1))\, y + \sqrt{\alpha_2\phi + 4\beta_0\phi(\phi-1)}\,\zeta$	$\left\langle N^k \right\rangle_{\text{RD}} = \left\langle (\Omega\phi + \Omega^{1/2} y)^k) \right\rangle_{\text{LE}}$	**Approximate** method valid in the large density and small noise limit. Can be applied to any reaction-diffusion process, even involving several species.
Gillespie	Eq. (II.91)	$\partial_t x = \alpha_2 x - 2\beta_0 x(x-1) + \sqrt{\alpha_2 x + 4\beta_0 x(x-1)}\,\zeta$	$\left\langle N^k \right\rangle_{\text{RD}} = \left\langle x^k \right\rangle_{\text{LE}}$	**Approximate** method valid in the large density limit. Can be applied to any reaction-diffusion process, even involving several species.
Poisson representation	Eq. (II.118)	$\partial_t Y = Y(\alpha_2 - 2\beta_0 Y) + \sqrt{2Y(\alpha_2 - \beta_0 Y)}\,\zeta$	$\left\langle N^k \right\rangle_{\text{RD}}^{\text{factorial}} = \left\langle Y^k \right\rangle_{\text{LE}}$	Inconsistencies in the proof. Yield complex Langevin equations. Valid for a restricted set of reactions, Eq. (II.44).
Formal field-theoretical method	Eq. (II.118)	$\partial_t \phi = \phi(\alpha_2 - 2\beta_0\phi) + \sqrt{2\phi(\alpha_2 - \beta_0\phi)}\,\zeta$	$\left\langle N^k \right\rangle_{\text{RD}}^{\text{factorial}} = \left\langle \phi^k \right\rangle_{\text{LE}}$	Inconsistencies in the proof. Yield same complex Langevin equations as the previous method. Valid for a restricted set of reactions, Eq. (II.44).
Duality	Eq. (II.123)	$\partial_t Z = -\alpha_2 Z(1-Z) + \sqrt{2\beta_0(1-Z^2)}\,\zeta$	$\left\langle \left\langle Z(t)^{N(0)} \right\rangle_{\text{LE}} \right\rangle_{\text{RD}} = \left\langle \left\langle Z(0)^{N(t)} \right\rangle_{\text{LE}} \right\rangle_{\text{RD}}$	**Exact** method, yield real Langevin equations. Valid for a restricted set of reactions, Eq. (II.44).

Table II.1 – *Comparison of the different Langevin equations obtained from a microscopic reaction-diffusion process. Note that the example is given for a zero-dimensional system for simplicity, although all the methods can be generalized to any spatially-extended system.*

Chapter III

Frequency regulator

Contents

In the previous chapter, we have seen how generic out-of-equilibrium processes can be cast into a path-integral formulation, which is the starting point of RG methods. The aim of this chapter will therefore be twofold: (i) detail how the NPRG approach can be extended from equilibrium critical systems to their nonequilibrium counterpart and (ii) explain how the regulator term of the NPRG approach must be modified in order to take care of the temporal fluctuations that arise in nonequilibrium critical phenomena. The implementation of the NPRG in an out-of-equilibrium context has been developed more than ten years ago [35, 54, 144] and have proved to be a very powerful and versatile tool for models where the usual RG approach was often ineffective. Examples are the reaction-diffusion processes and in particular the directed percolation transition [144], the Kardar-Parisi-Zhang equation [16, 91, 186, 187] and more recently the Navier-Stokes equation [15, 92, 93]. It has also proven useful for the study of the kinetic Ising model [21, 188] (on which we give more details in the following) and its universal dynamics after a quench to the critical temperature [53]. On the other hand, the design of a frequency regulator that takes care of the growing temporal fluctuations near a nonequilibrium critical point has never been studied and represents the second main result of this manuscript [22].

As we have seen in the first chapter, the key to the success of the NPRG approach in equilibrium physics is its ability to take care of growing fluctuations near criticality by integrating them out in a controlled way. This is achieved by coarse-graining the spatial fluctuations using a regulator function $R_k(|x-y|)$ in the action of the model which has a typical range $|q| \lesssim k$ in momentum space. This key feature of the NPRG, reminiscent of the block-spin idea, is probably not sufficient in many nonequilibrium problems, where temporal fluctuations also play a major role. The introduction of a regulator that would also take care of these temporal fluctuations therefore seems essential, and designing such a regulator is the aim of this chapter.

The most used approximation in the NPRG context is the derivative expansion (DE). In this approximation, we have explained in Sec. I.4.3 that the contributions of all the correlation

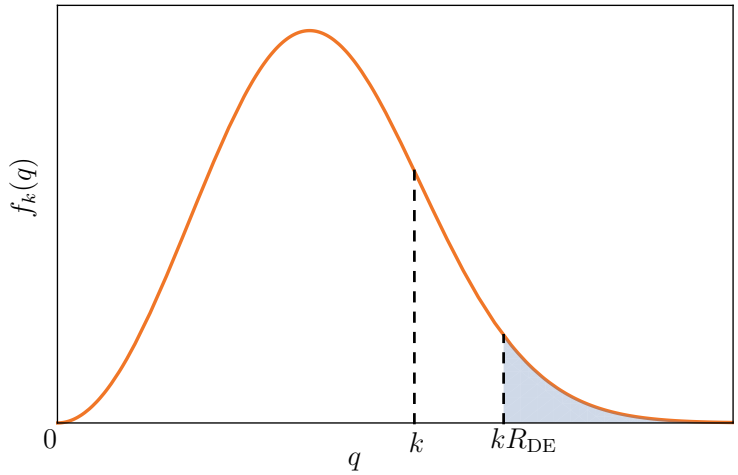

Figure III.1 – *Typical shape of the integrand $f_k(q)$ inside the integral in Eq. (III.1). Because of the regulator function $R_k(q)$, the integrand is peaked around $q = k$. Since the derivative expansion has a finite radius of convergence $R_{\rm DE}$, all the contributions to the integral for $q > R_{\rm DE}k$ will be wrong. Fortunately, the regulator ensures that this contribution is very small (blue shaded area), ensuring that these wrong terms do not contribute too much to the computation of the flow equations.*

functions to the RG flow are retained, but their momentum/frequency dependence is replaced by a Taylor expansion. The role of the regulator R_k is to ensure that the momentum region where this approximation is not valid is effectively cut off. To be more specific, within the NPRG formalism, one has to compute the flow of the vertices $\Gamma_k^{(i)}(\{p_j\})$, which are composed of terms involving a product of the propagator $G_k(q) \equiv [R_k(q) + \Gamma_k^{(2)}(q)]^{-1}$ to some power, and of the vertices $\Gamma_k^{(m)}$ (with $m \leq i+2$) both evaluated at some combination of the internal and external momenta q and $\{p_j\}$. For instance, in the case of the Ising model, the flow of the second derivative of the effective average action reads [c.f. Eq. (I.47)]:

$$\partial_k \Gamma_k^{(2)}(p) = \int_q \partial_k R_k(q) G_k(q) \Big[\Gamma_k^{(3)}(q, -q-p, p) G_k(p+q) \Gamma_k^{(3)}(p+q, -q, -p) - \frac{1}{2} \Gamma_k^{(4)}(q, -q, p, -p) \Big] G_k(q) \,. \tag{III.1}$$

In the spirit of the derivative expansion – that is a series expansion in terms of the momentum –, the flow of these vertices are evaluated at vanishing external momenta $\{p_j = 0\}$ and in addition each term under the integral is replaced by its series expansion in q. For instance the propagator, at the second-order of the derivative expansion reads:

$$G_k(q)^{-1} - R_k(q) \underset{q\to 0}{=} U_k''(\psi) + q^2 Z_k(\psi) + O(q^4) \,. \tag{III.2}$$

The obvious problem of this approximation is that the integration over the internal momentum q in Eq. (III.1) runs up to $|q| \to \infty$, where the series expansion (III.2) is clearly no longer valid. In fact, the NPRG tackles this problem using a regulator function. Indeed, in the presence of the regulator R_k, the typical shape of the integrand appearing in the right-hand side of Eq.(III.1) is shown in Fig. III.1 and one sees that the momenta $|q| \gtrsim k$ are simply discarded from the integral. Therefore, the derivative expansion is valid and accurate provided that the radius of convergence $R_{\rm DE}$ of this Taylor expansion is larger than the range of the integrals over the momentum and frequency in the RG flow equations.

One can thus wonder what the radius of convergence of the derivative expansion is. This question is of course very delicate, and its value depends on the particular choice of the regulator R_k, but we can however try to give an estimate of this value. For the $O(N)$ model, it is known

that the series expansion of $\Gamma^{(2)}_{k=0}(p)$ of the massive theory (that is at a finite distance from the critical point), which reads

$$\Gamma^{(2)}_{k=0}(p) \underset{p\to 0}{=} m^2 \left(c_1 + c_2 \frac{p^2}{m^2} + O\left[(p/m)^4\right] \right), \tag{III.3}$$

where c_1 and c_2 are constants and m is the mass, has a radius of convergence $R_{\rm LT} = 2$ in the low-temperature phase, and $R_{\rm HT} = 3$ in the high-temperature phase [189–191]. Therefore, since we have argued in Chap. I that in the NPRG formalism the scale k plays the role of a mass, we can infer that the series expansion of Γ_k at the critical point will take the form of a series expansion in p/k:

$$\Gamma^{(2)}_{k}(p) \underset{p\to 0}{=} m^2 \left(c'_1 + c'_2 \frac{p^2}{k^2} + O\left[(p/k)^4\right] \right), \tag{III.4}$$

with a radius of convergence $R_{\rm DE}$ that we can guess to be $R_{\rm DE} \simeq$ 2-3 by analogy with the previous result. At equilibrium, the role of the regulator $R_k(q)$ introduced within the NPRG framework is therefore paramount, since it has to effectively cut off the momentum integration from $|q| \in [0, \infty[$ to $0 \leq |q| \lesssim R_{\rm DE} k$ in order to allow for the replacement of the correlation functions and the propagator by their Taylor expansion in the integrals of the flow equations. This efficient cut-off function R_k probably explains the success of the derivative expansion [23, 192].

For nonequilibrium systems, this issue is subtler because the RG flow equations involve also a frequency integral. This integral is convergent without any regularization[1] which means that the integrand decreases sufficiently rapidly for the region of large frequencies to contribute a finite amount. However, the fact that the frequency integral is convergent does not guarantee that it is accurately computed when the correlation functions are replaced in the integrand by their frequency-expansion. Therefore, this integral must also be cut off by a regulator to avoid summing contributions at large frequencies corresponding to a region where the Taylor expansion of the correlation functions is not valid.

Examples where such a frequency regulator could be needed are numerous: a first example is the parity conserving generalized voter model, that we already met in Sec. II.3.1.c, and which is a one-species reaction-diffusion system where the parity of the number of particles is conserved by the dynamics [151, 153]. As we already emphasized, some approximate results obtained with the NPRG [95] for this model disagree qualitatively with exact ones [96], indicating that the fluctuations are not properly taken into account, at least within this level of approximation (the local potential approximation), which has proven to be very efficient in equilibrium problems.

Our goal in this chapter is to design frequency regulators that generalize the role played by the regulators in the usual equilibrium NPRG settings to nonequilibrium cases. We therefore start in the following by explaining how the NPRG is implemented in a general context of out-of-equilibrium statistical physics. We then discuss the general theoretical properties a frequency regulator must fulfill. These requirements are then refined when testing our regulators on benchmark models: the model A (also called the kinetic Ising model), and its multidimensional-spin counterpart (the kinetic $O(N)$ model) [193]. For these models, we will see that enforcing important physical constraints such as causality and the fluctuation-dissipation theorem is especially important.

[1] This is true at order two of the derivative expansion, but depending on the approximations performed, the integral over the frequencies could diverge, in which case regularization would of course be necessary.

III.1 NPRG approach to nonequilibrium

III.1.1 Effective average action and exact flow equation

As in equilibrium statistical physics, the starting point of the NPRG is a field-theoretical description of the system, usually derived either starting from a coarse-grained description involving a Langevin equation and using the MSRDJ formalism, or starting from a microscopic description using a master equation and applying the Doi-Peliti formalism (see Chap. II for a description of these two formalisms). In both cases, one can derive the analog of the partition function which has the general form[2]:

$$\mathcal{Z}[j,\tilde{j}] = \int \mathcal{D}\phi\mathcal{D}\tilde{\phi}\, \mathrm{e}^{-\mathcal{S}[\Phi]+\int_{\boldsymbol{x}} J(\boldsymbol{x})^T\cdot\Phi(\boldsymbol{x})} \tag{III.5}$$

where $\boldsymbol{x} \equiv (\vec{x},t)$ and $\int_{\boldsymbol{x}} \equiv \int \mathrm{d}^d\vec{x}\,\mathrm{d}t$, and we now use a matrix notation and define the following vectors

$$\Phi(\boldsymbol{x}) = \begin{pmatrix} \phi(\boldsymbol{x}) \\ \tilde{\phi}(\boldsymbol{x}) \end{pmatrix} \quad \text{and} \quad J(\boldsymbol{x}) = \begin{pmatrix} j(\boldsymbol{x}) \\ \tilde{j}(\boldsymbol{x}) \end{pmatrix}. \tag{III.6}$$

As in equilibrium, the generating functional of the connected correlation and response functions is $\mathcal{W}[J] = \log \mathcal{Z}[J]$. We also introduce its Legendre transform, the generating functional of the one-particle irreducible correlation functions $\Gamma[\Psi]$, where $\Psi = \langle\Phi\rangle$.

In order to determine the effective action Γ, we apply the NPRG formalism and write a functional differential equation which interpolates between the microscopic action $\mathcal{S}$ and the effective action Γ. As explained in Chap. I, the interpolation is performed through a momentum scale k and by integrating over all the fluctuations with momenta $|q| > k$, while those with momenta $|q| < k$ are frozen. At scale $k = \Lambda$, where Λ is the ultra-violet cutoff imposed by the (inverse) microscopic scale of the model (e.g. the lattice spacing), all fluctuations are frozen and the mean-field approximation becomes exact; at scale $k \to 0$, all the fluctuations are integrated over and the original functional $\mathcal{Z}$ is recovered. The interpolation between these scales is made possible by using a regulator $\mathcal{R}_k(\boldsymbol{x})$, whose role is to freeze out all the fluctuations with momenta $|q| < k$. This regulator is introduced via an extra term to the action and thus defining a new partition function $\mathcal{Z}_k$:

$$\mathcal{Z}_k[j,\tilde{j}] = \int \mathcal{D}\phi\mathcal{D}\tilde{\phi}\, \mathrm{e}^{-\mathcal{S}-\Delta\mathcal{S}_k+\int_{\boldsymbol{x}} J(\boldsymbol{x})^T\cdot\Phi(\boldsymbol{x})}\,, \tag{III.7}$$

with

$$\Delta\mathcal{S}_k = \frac{1}{2}\int_{\boldsymbol{x},\boldsymbol{x'}} \Phi(\boldsymbol{x})^T\cdot\mathcal{R}_k(\boldsymbol{x}-\boldsymbol{x'})\cdot\Phi(\boldsymbol{x'})\,, \tag{III.8}$$

where $\mathcal{R}_k$ is a 2×2 regulator matrix, depending both on space and time, and whose task is to cancel slow-mode fluctuations. We shall see in the following sections that the regulator form (and especially its frequency part) is constrained by causality and by symmetry considerations. We also define the effective average action Γ_k as a modified Legendre transform of $\mathcal{W}_k[J] = \log\mathcal{Z}_k[J]$:

$$\Gamma_k[\Psi] + \mathcal{W}_k[J] = \int_{\boldsymbol{x}} J^T\cdot\Psi - \frac{1}{2}\int_{\boldsymbol{x},\boldsymbol{x'}} \Psi(\boldsymbol{x})^T\cdot\mathcal{R}_k(\boldsymbol{x}-\boldsymbol{x'})\cdot\Psi(\boldsymbol{x'}) \tag{III.9}$$

[2]Notice however that depending on the formalism from which it stems from, the fields ϕ and $\tilde{\phi}$ have a different nature. In the Doi-Peliti formalism they are complex conjugated, whereas one is real (and may be bounded) and the other imaginary in the MSRDJ context.

in such a way that Γ_k coincides with the action at the microscopic scale ($\Gamma_{k=\Lambda} = \mathcal{S}$) and with Γ at $k = 0$ ($\Gamma_{k=0} = \Gamma$), when all fluctuations have been integrated over. The evolution of the interpolating functional Γ_k between these two scales is given by the Wetterich equation [36, 37]:

$$\partial_k \Gamma_k[\Psi] = \frac{1}{2}\mathrm{Tr}\int_{\boldsymbol{x},\boldsymbol{x'}} \partial_k \mathcal{R}_k(\boldsymbol{x}-\boldsymbol{x'})\cdot G_k[\boldsymbol{x},\boldsymbol{x'};\Psi] \tag{III.10}$$

where $G_k[\boldsymbol{x},\boldsymbol{x'};\Psi] \equiv [\Gamma_k^{(2)} + \mathcal{R}_k]^{-1}$ is the full, field-dependent, propagator and $\Gamma_k^{(2)}$ is the 2×2 matrix whose elements are the $\Gamma^{(2)}_{k,ij}$ defined such that:

$$\Gamma^{(n)}_{k,i_1,\cdots,i_n}[\boldsymbol{x}_i;\Psi] = \frac{\delta^n \Gamma_k[\Psi]}{\delta\Psi_{i_1}(\boldsymbol{x}_1)\cdots\delta\Psi_{i_n}(\boldsymbol{x}_n)}\,. \tag{III.11}$$

The Wetterich equation (III.10) represents an exact flow equation for the effective average action Γ_k, which is of course too complicated to be solved without approximations. In the following, we will use the derivative expansion (DE), which will restrict the functional form of Γ_k. Instead of following the full Γ_k along the flow, only the first terms of its series expansion in space and time derivatives of Ψ are considered. These terms have to be consistent with the symmetries of the action $\mathcal{S}$, and we will therefore discuss them when we will consider a specific model.

III.1.2 Some general properties of the out-of-equilibrium regulator

Before focusing on a specific out-of-equilibrium model, we would like to stress out some important properties that the regulator matrix $\mathcal{R}_k(\boldsymbol{x})$ must fulfill. First of all and for the whole consistency of the NPRG approach, we recall that the regulator must have a large value when $k \to \Lambda$ in order to retrieve $\Gamma_{k=\Lambda} = \mathcal{S}$. Second, the regulator must vanish when $k \to 0$ in order to have $\Gamma_{k=0} = \Gamma$ when all fluctuations have been integrated over. The minimal requirements for the k-dependence of $\mathcal{R}_k(\boldsymbol{x})$ therefore read:

$$\begin{cases} \mathcal{R}_k(\boldsymbol{x}) & \xrightarrow[k\to\Lambda]{} \infty \\ \mathcal{R}_k(\boldsymbol{x}) & \xrightarrow[k\to 0]{} 0 \end{cases} \tag{III.12}$$

Out of equilibrium, the dependence of the regulator on $\vec{x}$ and t is also constrained, and it is crucial to have an intuitive idea of the meaning of the regulator for the underlying physical model. We will therefore describe how this regulator term modifies the underlying model, and how it implies new specifications for its behaviour.

III.1.2.a Properties for a field theory stemming from a Langevin equation

In this part we consider that the field theory stems from a coarse-grained Langevin equation which reads:

$$\partial_t \phi(\boldsymbol{x}) = F[\phi] + \xi(\boldsymbol{x}) \tag{III.13}$$

where $F[\phi]$ is a macroscopic force and ξ is some (non-necessarily white) noise. Let us first notice that the MSRDJ formalism together with Itō's prescription does not allow for a term in the action not proportional to the response field $\tilde{\phi}$, see Sec. II.2.3. This implies that there is no cut-off term in the ϕ^2 direction if we wish to preserve this property, and the regulator matrix $\mathcal{R}_k(\boldsymbol{x})$ can be written in full generality as:

$$\mathcal{R}_k(\boldsymbol{x}) = \begin{pmatrix} 0 & R_{1,k}(x,t) \\ R_{1,k}(x,-t) & 2R_{2,k}(x,t) \end{pmatrix} \tag{III.14}$$

where the minus sign in $R_{1,k}(x,-t)$ is a consequence of $\Delta\mathcal{S}_k$ being written in a matrix form and the factor 2 in front of $R_{2,k}$ has been included for convenience. Notice that these two regulator terms have a meaning for the underlying Langevin equation. Indeed, adding a regulator $R_{1,k}$ means changing the external force in the Langevin equation:

$$F \;\to\; F + \Delta F_k \tag{III.15}$$

where $\Delta F_k(\boldsymbol{x}) = -\int_{\boldsymbol{u}} R_{1,k}(\boldsymbol{u}-\boldsymbol{x})\phi(\boldsymbol{u})$. The regulator $R_{1,k}$ is thus similar to the usual mass-like regulator used at equilibrium. We restrict ourselves in the following to additional forces ΔF_k which are *causal*. This implies $R_{1,k}(x,t>0)=0$, which translates to $R_{1,k}(x,t)\propto\Theta(-t)$ (Θ being the Heaviside step function).

On the other hand, adding a regulator $R_{2,k}$ is equivalent to modifying the distribution of the noise. The noise correlations are therefore shifted as:

$$C(\boldsymbol{x},\boldsymbol{x}') \equiv \big\langle \xi(\boldsymbol{x})\xi(\boldsymbol{x}')\big\rangle \;\to\; C(\boldsymbol{x},\boldsymbol{x}') - R_{2,k}(\boldsymbol{x}-\boldsymbol{x}')\,. \tag{III.16}$$

In particular, if the initial noise is white: $C(\boldsymbol{x},\boldsymbol{x}')=\delta(\boldsymbol{x}-\boldsymbol{x}')$, it becomes "colored" by the regulator along the flow and the δ-correlations are recovered only at $k=0$, where $R_{2,k}$ must identically vanish (according to Eq.(III.12)).

As we will see in the following, dependent on the specific system that is studied, extra specifications can be added. In the case of the model A, the fluctuation-dissipation theorem will for instance enforce a relation between $R_{1,k}$ and $R_{2,k}$.

III.1.2.b Properties for field-theories stemming from a master equation

Giving an interpretation of the regulators $R_{1,k}$ and $R_{2,k}$ for a field theory stemming from a reaction-diffusion process is less obvious. The $R_{1,k}$ can be interpreted as a modification of the reactions involving a single reacting particle, it modifies in particular the diffusion. If $R_{1,k}$ modifies the diffusion coefficient, a very large $R_{1,k}$ for $q>k$ means that the system is well-mixed for $q>k$, and can be treated as a mean-field system. We retrieve the usual interpretation of the regulator term.

The $R_{2,k}$ on the other hand is more difficult to handle, since it would account for reactions of the form:

$$\emptyset \to 2A \tag{III.17}$$

with a rate $R_{2,k}$ and therefore depending on space and time. Near a transition to an absorbing state, having a production of particles by the means of the regulator $R_{2,k}$ could thus place the system out of the critical regime.

III.2 The model A as a benchmark

Now that we have introduced the NPRG formalism for out-of-equilibrium systems, and that we have given some basic properties that the regulators must fulfill, we focus on the specific example of the model A, which will be our benchmark to design and try out a frequency regulator.

III.2.1 Model A, field theory and fluctuation-dissipation theorem

III.2.1.a Model and field theory formalism

The model A or kinetic Ising model is one of the simplest models one can think of to describe out-of-equilibrium critical phenomena. It is a coarse-grained description of Glauber dynamics

for Ising spins [7, 193]. On a d-dimensional lattice, Ising spins are allowed to flip with transition rates that depend on the orientation of their neighbours and satisfy the detailed-balance condition, guaranteeing the system relaxes toward equilibrium at large time. The model A uses a Langevin description of the spins dynamics, and it is therefore stated in terms of a coarse-grained local spin variable $\phi(x,t)$ following the stochastic equation (in the Itō sense)[3]:

$$\partial_t \phi(x,t) = -\frac{\delta H}{\delta \phi} + \zeta(x,t)\,, \tag{III.18}$$

where $H = H[\phi]$ is the usual Ginzburg-Landau Hamiltonian:

$$H[\phi] = \int_{\boldsymbol{x}} \left(\frac{1}{2} (\nabla \phi)^2 + V(\phi) \right) \tag{III.19}$$

with $\boldsymbol{x} \equiv (x,t)$, $\int_{\boldsymbol{x}} \equiv \int \mathrm{d}^d x \,\mathrm{d}t$, $V(\phi) = r/2\,\phi^2 + u/4!\,\phi^4$, and $\zeta(\boldsymbol{x})$ is a Gaussian white noise taking into account the fluctuations of the order parameter coming from its coarse-grained nature. The noise probability distribution $P(\zeta)$ is consequently:

$$P(\zeta) \propto \mathrm{e}^{-\frac{1}{4}\int_{\boldsymbol{x}} \zeta(\boldsymbol{x})^2} \tag{III.20}$$

yielding in particular

$$\left\langle \zeta(\boldsymbol{x}) \zeta(\boldsymbol{x'}) \right\rangle = 2\,\delta(t-t')\delta^d(x-x')\,, \tag{III.21}$$

where we have rescaled the time and the field such that the variance of the noise is 2. At long time, the system relaxes toward the equilibrium state associated to the Ginzburg-Landau Hamiltonian (III.19), and such a system is called "relaxational" for this reason. The relaxational models are usually the simplest nonequilibrium systems to study, since they present extra properties (such as the fluctuation-dissipation theorem (FDT) that we will detail in the following) and reach at long time a known equilibrium state.

From the Langevin equation (III.18) a field-theoretical approach can be derived using the Martin-Siggia-Rose-de Dominicis-Janssen (MSRDJ) approach as explained in Sec. II.2.3. We recall that within this formalism, the mean value (over the realizations of the noise) of a given observable $\mathcal{O}[\phi]$ is given by:

$$\langle \mathcal{O}[\phi] \rangle_\zeta = \int \mathcal{D}\phi \mathcal{D}\tilde{\phi}\, \mathrm{e}^{-\mathcal{S}[\phi,\tilde{\phi}]} \mathcal{O}[\phi] \tag{III.22}$$

with the action

$$\mathcal{S}[\phi,\tilde{\phi}] = \int_{\boldsymbol{x}} \tilde{\phi} \left(\partial_t \phi - \tilde{\phi} + \frac{\delta H}{\delta \phi} \right)\,. \tag{III.23}$$

III.2.1.b Fluctuation-dissipation theorem

Let us recall that in the MSRDJ formulation of a Langevin equation, the linear response function $\chi(\boldsymbol{x},\boldsymbol{x}')$, defined as:

$$\chi(\boldsymbol{x},\boldsymbol{x}') \equiv \frac{\langle \delta\phi(\boldsymbol{x}) \rangle}{\delta J(\boldsymbol{x}')}|_{J\to 0}\,, \tag{III.24}$$

[3] Notice that in this description, the order parameter (the magnetization M) is *not* conserved by the dynamics. An alternative version, the model B, describes the relaxation to equilibrium in the case of conservative dynamics for the order parameter [193].

can be computed directly from the two-point correlation function

$$\chi(\boldsymbol{x},\boldsymbol{x}') = \left\langle \tilde{\phi}(\boldsymbol{x}')\phi(\boldsymbol{x}) \right\rangle . \tag{III.25}$$

This property will be used to find how the time-reversal symmetry is encoded within the MSRDJ formalism.

After the initial conditions have been washed out by the dynamics, the model A relax at long time toward its equilibrium (Ising) state. This relaxation toward equilibrium is related to a time-reversal symmetry of the system, which implies in turn that the action $\mathcal{S}$ [c.f. Eq. (III.23)] must be invariant under the following transformation [194, 195]:

$$\begin{cases} \phi'(x,t) &= \phi(x,-t) \\ \tilde{\phi}'(x,t) &= \tilde{\phi}(x,-t) - \dot{\phi}(x,-t) \end{cases} \tag{III.26}$$

where $\dot{f}(t) \equiv \partial_t f(t)$. Indeed, the correlation functions of ϕ are invariant under this field transformation, whereas the application of the transformation (III.26) to the response functions $\left\langle \phi(x,t)\tilde{\phi}(x',t') \right\rangle$ yields:

$$\left\langle \phi(x,t)\tilde{\phi}(x',t') \right\rangle = \left\langle \phi(x,t')\tilde{\phi}(x',t) \right\rangle - \left\langle \phi(x,t')\dot{\phi}(x',t) \right\rangle . \tag{III.27}$$

If $t > t'$ then the first term in the right-hand side of the previous equation vanishes because of causality, and we get the fluctuation-dissipation theorem:

$$\left\langle \phi(x,t)\tilde{\phi}(x',t') \right\rangle = -\left\langle \phi(x,t')\dot{\phi}(x',t) \right\rangle , \tag{III.28}$$

which is the hallmark of time-reversal symmetry and links the correlation function (the fluctuations, in the right-hand side of the previous equation) to the response function (the dissipation, in the left-hand side) in equilibrium dynamics.

III.2.2 NPRG formulation

III.2.2.a Ansatz for the effective average action

We study the model A using the derivative expansion (DE) approximation, which means that we propose an ansatz for the effective average action Γ_k built as a Taylor expansion in terms of the time and space derivatives of the fields. To construct this ansatz we use the symmetries of our model, and in particular the fluctuation-dissipation theorem, encoded in the transformation (III.26). This allows us to write the following ansatz for Γ_k, at first order in time derivative, and second order in space derivative [21]:

$$\begin{aligned} \Gamma_k[\psi,\tilde{\psi}] &= \int_{\boldsymbol{x}} \tilde{\psi}\left[X_k(\psi)\left(\partial_t\psi - \tilde{\psi}\right) + \frac{\delta\gamma_{\mathrm{eq},k}}{\delta\psi(\boldsymbol{x})} \right] \\ &= \int_{\boldsymbol{x}} \tilde{\psi}\left[X_k(\psi)\left(\partial_t\psi - \tilde{\psi}\right) + U_k'(\psi) - Z_k(\psi)\nabla^2\psi - \frac{1}{2}Z_k'(\psi)(\nabla\psi)^2 \right] \end{aligned} \tag{III.29}$$

where, at equilibrium:

$$\Gamma_{\mathrm{eq},k}[\psi] = \int \mathrm{d}^d x\, \gamma_{\mathrm{eq},k}(\psi(x,t)) \tag{III.30}$$

$$= \int \mathrm{d}^d x \left[\frac{1}{2}Z_k(\psi)(\nabla\psi)^2 + U_k(\psi) \right] . \tag{III.31}$$

Let us briefly justify the form of Γ_k. It is natural to choose it invariant under transformation (III.26) so that the fluctuation-dissipation theorem holds at all k. This implies that terms proportional to $\tilde{\psi}^2$ and $\tilde{\psi}\partial_t\psi$ renormalize in the same way and therefore depend on a single function X_k, which is a tremendous simplification of the RG flow. The second part of the ansatz, $\tilde{\psi}\,\partial\gamma_{\mathrm{eq},k}/\partial\psi(x,t)$ is linear in $\tilde{\psi}$ and therefore invariant on its own since the transformation (III.26) generates a term proportional to $\partial_t\psi\,\partial\gamma_{\mathrm{eq},k}/\partial\psi(x,t) = \partial_t\gamma_{\mathrm{eq},k}(\psi)$ that vanishes after time integration in the stationary regime. Notice that because of the fluctuation-dissipation theorem, higher-order terms in $\tilde{\psi}$ are not allowed at this order of the derivative expansion, and thus U_k, Z_k, and X_k are functions of ψ only (see also [188] for further explanations).

Choosing ansatz (III.29) implies to use only regulators compatible with (III.26) and we show in the following that it is indeed possible to devise such regulators even when they depend on frequencies. Of course, it is possible to consider regulators that are incompatible with (III.26) at the price of giving up the fluctuation-dissipation theorem for $k > 0$. This implies that in Γ_k the two terms $\tilde{\psi}^2$ and $\tilde{\psi}\partial_t\psi$ do no longer renormalize in the same way. In this case, the ansatz (III.29) becomes

$$\Gamma_k[\psi,\tilde{\psi}] = \int_{\boldsymbol{x}} \tilde{\psi}\left[X_k(\psi)\partial_t\psi + W_k(\psi)\tilde{\psi} + \frac{\delta\gamma_{\mathrm{eq},k}}{\delta\psi(\boldsymbol{x})}\right]. \tag{III.32}$$

Notice that when the field dependence of $X_k(\psi)$ and $W_k(\psi)$ is neglected ($X_k(\psi) \to \bar{X}_k$ and $W_k(\psi) \to \bar{W}_k$) and that the regulator is frequency-independent the flows of $\bar{X}_k$ and $\bar{W}_k$ are identical (see for instance [53]). This incidental property is however lost when the field dependence of these functions is kept.

Using ansatz (III.29) drastically simplifies the resolution of the Wetterich equation since a functional differential equation is converted into a set of partial differential equations over the functions U_k, Z_k and X_k. The role of the regulator is essential for the validity of this approximation, and we therefore discuss its properties in more details in the following section.

III.2.2.b Derivation of the flow equation

In Sec. III.1 we introduced the NPRG formalism for an out-of-equilibrium system in a formal way and we now give more details and explain how to derive the flow equations. Since the formalism is the same for the multidimensional-spin counterpart of the model A, the kinetic $O(N)$ model, we focus in the following on the general case where the coarse-grained spin variable ϕ is now a N-dimensional vector, denoted $\underline{\phi}$. We therefore modify the ansatz for the effective average action Γ_k to be

$$\begin{aligned}\Gamma_k[\underline{\psi},\underline{\tilde{\psi}}] = \int_{\boldsymbol{x}}\sum_i \tilde{\psi}_i\Big[&X_k(\rho)\left(\partial_t\psi_i - \tilde{\psi}_i\right) + \psi_i U_k'(\rho)\\ &+ \frac{\psi_i}{2}Z_k'(\rho)(\nabla\underline{\psi})^2 - Z_k(\rho)\nabla^2\psi_i - Z_k'(\rho)\nabla\psi_i(\underline{\psi}\cdot\nabla\underline{\psi})\\ &+ \frac{\psi_i}{4}Y_k'(\rho)(\nabla\rho)^2 + \frac{1}{2}Y_k(\rho)\nabla\rho\nabla\psi_i\Big],\end{aligned} \tag{III.33}$$

where $\rho = \underline{\psi}^2/2$. In order to compute the RG flow of the functions involved in Eq. (III.29), we define them in the following way:

$$U_k'(\rho) = \frac{1}{\psi}\,\mathrm{FT}\left(\frac{\delta\,\Gamma_k}{\delta\tilde{\psi}_1(\boldsymbol{x})}\bigg|_{\underline{\Psi}=(\psi,\underline{0})}\right)\bigg|_{\nu=0,p=0} \tag{III.34}$$

$$Z_k(\rho) = \left[\partial_{p^2}\,\mathrm{FT}\left(\frac{\delta^2\Gamma_k}{\delta\tilde{\psi}_2(\boldsymbol{x})\delta\psi_2(\boldsymbol{y})}\bigg|_{\underline{\Psi}=(\psi,\underline{0})}\right)\right]\bigg|_{\nu=0,p=0} \tag{III.35}$$

$$X_k(\rho) = \left[\partial_{i\nu}\,\mathrm{FT}\left(\frac{\delta^2\Gamma_k}{\delta\tilde{\psi}_2(\boldsymbol{x})\delta\psi_2(\boldsymbol{y})}\bigg|_{\underline{\Psi}=(\psi,\underline{0})}\right)\right]\bigg|_{\nu=0,p=0} \tag{III.36}$$

where $\underline{\Psi} = (\psi, \underline{0})$ is a $2N$ constant vector where $\Psi_1 = \psi_1 = \psi$ is a constant field and $\Psi_2 = \cdots = \Psi_{2N} = 0$, where $\mathrm{FT}(\cdot)$ means the Fourier transform as defined in Eq. (1) and p and ν are the momentum and frequency associated to this transform. Notice that in the case of the model A, the function Y_k does not appear in the ansatz for Γ_k, and that the functions Z_k and X_k are evaluated in the $\psi_1 = \psi$, $\tilde{\psi}_1 = \tilde{\psi}$ direction. In the spirit of the derivative expansion, we evaluate the renormalization functions at zero external momentum and frequency since it is in this limit that the approximation is valid. The flow of these functions is then computed using the Wetterich equation (III.10) with the initial conditions $U_\Lambda' = V'$, $Z_\Lambda = 1 = X_\Lambda$.

As an example, the flow of U_k' for the model A ($N = 1$) is given by

$$\partial_k U_k'(\rho) = \frac{1}{\psi}\mathrm{FT}\left(\frac{\delta}{\delta\tilde{\psi}}\partial_k\Gamma_k\bigg|_{\Psi=(\psi,0)}\right) \tag{III.37}$$

$$= \frac{1}{\psi}\mathrm{FT}\left(\frac{1}{2}\tilde{\partial}_k\mathrm{Tr}\left[\int_{t_i,x_i}\Gamma^{(3)}_{k,\tilde{\psi}}\cdot G_k\right]\bigg|_{\Psi=(\psi,0)}\right) \tag{III.38}$$

where $\Gamma^{(3)}_{k,\tilde{\psi}} \equiv \delta\Gamma^{(2)}_k/\delta\tilde{\psi}$ and $\tilde{\partial}_k \equiv \partial_k R_k\,\partial/\partial R_k$. Taking the appropriate functional derivatives of (III.29) and evaluating the result at the uniform and stationary field configuration $\Psi(x,t) = (\psi, 0)$, one finds in Fourier space:

$$\Gamma^{(3)}_{k,\tilde{\psi}}(p,\nu;q,\omega;\psi) = \psi\begin{pmatrix} h_3(p,\nu;q,\omega;\rho) & -2X_k'(\rho) \\ -2X_k'(\rho) & 0\end{pmatrix} \tag{III.39}$$

with $h_3 = 2\rho\,U_k^{(3)} + 3U_k'' + Z_k'(p^2+q^2+p\cdot q) - i\nu X_k'$, which is a function of ρ. The propagator G_k in Eq. (III.38) is obtained by inverting the 2×2 matrix $(\Gamma^{(2)}_k + \mathcal{R}_k)$ evaluated at $\Psi(x,t) = (\psi, 0)$. One finds:

$$G_k(q,\omega;\rho) = \begin{pmatrix} \frac{-R_{2,k}(q^2,\omega)+2X_k}{P(q^2,\omega)P(q^2,-\omega)} & \frac{1}{P(q^2,-\omega)} \\ \frac{1}{P(q^2,\omega)} & 0\end{pmatrix} \tag{III.40}$$

where $P(q^2,\omega) = h(q^2,\omega) + i\omega X_k$ with $h(q^2,\omega) = Z_k(\rho)q^2 + R_{1,k}(q^2,\omega) + U_k'(\rho) + 2\rho U_k''(\rho)$.

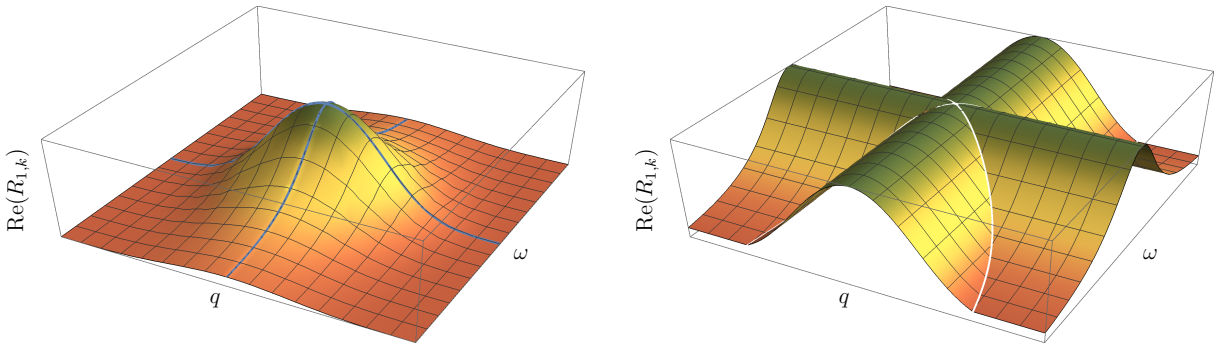

Figure III.2 – *Typical shape of the real part of the regulator $R_{1,k}(q,\omega)$ in the case where the frequency and momentum contributions can be factorized as in Eq. (III.42). Only the region where both $|q| \lesssim k$ and $|\omega| \lesssim k$ acquire a large mass* ***(left)****. An alternative regulator* ***(right)*** *could give a large mass to the system both when $|q| \lesssim k$ or $|\omega| \lesssim k$. It is however difficult to design a non-factorized regulator which fulfills causality.*

III.2.2.c Definition of the dimensionless variables and functions

Since we are interested in the scale-invariant regime, we introduce the dimensionless and renormalized variables, fields and functions:

$$\hat{x} = k\,x \tag{III.41a}$$
$$\hat{t} = \bar{Z}_k \bar{X}_k^{-1} k^2\, t \tag{III.41b}$$
$$s = \log(k/\Lambda) \tag{III.41c}$$
$$\hat{\underline{\psi}}(\hat{x},\hat{t}\,) = k^{(2-d)/2} \bar{Z}_k^{1/2} \underline{\tilde{\psi}}(x,t) \tag{III.41d}$$
$$\hat{\underline{\psi}}(\hat{x},\hat{t}\,) = k^{(2-d)/2} \bar{Z}_k^{1/2} \underline{\psi}(x,t) \tag{III.41e}$$
$$\hat{\rho}(\hat{x},\hat{t}\,) = k^{2-d} \bar{Z}_k \rho(x,t) \tag{III.41f}$$
$$\hat{U}(\hat{\rho}) = k^{-d} U_k(\rho) \tag{III.41g}$$
$$\hat{Z}(\hat{\rho}) = \bar{Z}_k^{-1} Z_k(\rho) \tag{III.41h}$$
$$\hat{X}(\hat{\rho}) = \bar{X}_k^{-1} X_k(\rho) \tag{III.41i}$$

where the running coefficients $\bar{Z}_k \equiv Z_k(\rho_0)$ and $\bar{X}_k \equiv X_k(\rho_0)$ are defined at a fixed normalization point ρ_0, and we have defined s the (negative) RG time. In the critical regime, these running coefficients are expected to behave as power laws $\bar{Z}_k \sim k^{-\eta(k)}$ and $\bar{X}_k \sim k^{-\eta_X(k)}$ with $\eta(k) = -k\partial_k \ln \bar{Z}_k$ and similarly for $\eta_X(k)$. The anomalous dimension η and the dynamical exponent z can be expressed in terms of the fixed-point values of $\eta(k)$ and $\eta_X(k)$ as $\eta \equiv \eta^*$ and $z \equiv 2 - \eta^* + \eta_X^*$.

We furthermore define the dimensionless regulators r_1 and r_2 such that:

$$\begin{aligned} R_{1,k}(q,\omega) &= y \bar{Z}_k k^2 r_1(y,\hat{\omega}) \\ &= y \bar{Z}_k k^2 \rho_1(\hat{\omega}) r(y) \end{aligned} \tag{III.42}$$
$$\begin{aligned} R_{2,k}(q,\omega) &= \bar{X}_k r_2(y,\hat{\omega}) \\ &= y \bar{X}_k \rho_2(\hat{\omega}) r(y) \end{aligned} \tag{III.43}$$

with $y = \hat{q}^2$ and $\hat{\omega} = \bar{X}_k \bar{Z}_k^{-1} k^{-2} \omega$ and where we have assumed for simplicity that the spatial and frequency parts of the regulators can be factorized, and where $r(y)$ is the usual momentum regulator, for example an exponential regulator:

$$r(y) = \frac{a}{\mathrm{e}^y - 1} \tag{III.44}$$

where a is a free parameter. The frequency part of the regulators, ρ_1 and ρ_2, also have to satisfy condition (III.55), and we give explicit examples in the following.

Notice that we have assumed that the spatial and frequency parts of the regulators can be factorized, for the causality condition of the regulator can be simply enforced in this case. However, having a factorized form means that only the region where both $|q| \lesssim k$ and $|\omega| \lesssim k$ will efficiently be cut off, although it might be more sensible to cut off regions where either $|q| \lesssim k$ or $|\omega| \lesssim k$, see Fig. III.2. In the latter case, it is however difficult to enforce causality and we have thus only focused on factorized regulators as in Eqs. (III.42) and (III.43).

From the previous definitions we deduce the regulator derivatives with respect to k:

$$\partial_s R_{1,k}(q,\omega) = -k^2 \bar{Z}_k y(\eta r_1 + 2y\partial_y r_1 + (2-\eta+\eta_X)\hat{\omega}\partial_{\hat{\omega}} r_1) \tag{III.45}$$

$$\partial_s R_{2,k}(q,\omega) = -\bar{X}_k(\eta_X r_2 + 2y\partial_y r_2 + (2-\eta+\eta_X)\hat{\omega}\partial_{\hat{\omega}} r_2)\,. \tag{III.46}$$

Finally, applying the Wetterich equation (III.10) on the definitions (III.34),(III.35) and (III.36) of the functions $\hat{U}'$, $\hat{Z}$ and $\hat{X}$, we can derive their flow equation as the sum of a dimensional part and a dynamical part:

$$\partial_s \hat{U}' = \partial_s \hat{U}'|_{\rm dim} + \partial_s \hat{U}'|_{\rm dyn} \tag{III.47}$$

$$\partial_s \hat{Z} = \partial_s \hat{Z}|_{\rm dim} + \partial_s \hat{Z}|_{\rm dyn} \tag{III.48}$$

$$\partial_s \hat{X} = \partial_s \hat{X}|_{\rm dim} + \partial_s \hat{X}|_{\rm dyn} \tag{III.49}$$

The definition of the dimensionless variables yields the following dimensional parts:

$$\partial_s \hat{U}'|_{\rm dim} = (\eta-2)\,\hat{U}' + (d+\eta-2)\,\hat{\rho}\,\hat{U}'' \tag{III.50}$$

$$\partial_s \hat{Z}|_{\rm dim} = \eta\,\hat{Z} + (d+\eta-2)\hat{\rho}\,\hat{Z}' \tag{III.51}$$

$$\partial_s \hat{X}|_{\rm dim} = \eta_X\,\hat{X} + (d+\eta-2)\hat{\rho}\,\hat{X}' \tag{III.52}$$

whereas the dynamical part depends on the frequency regulator and we discuss it in the following.

III.2.3 NPRG results without a frequency regulator

In a first step, we consider frequency-independent regulators, which means $R_{2,k} = 0$ and $R_{1,k}(q,\omega) = R_{1,k}(q)$. In this case, the calculation of the flow equations is much simpler since the integration over frequency can be done analytically using residues. We show the explicit expression of the flow equations in the case not regularized in frequencies in App. C.1.

In the kinetic Ising case, we keep the full ρ-dependence of the functions U_k, Z_k and X_k and derive the flow equation for the derivative expansion (DE) at the first order in time derivative and second order in space derivative. On the other hand, we perform in the kinetic $O(N)$ case, on top of the derivative expansion, a field expansion usually called the local potential approximation prime (LPA') which consists in discarding the function $Y_k(\rho)$ and neglecting the field dependence of $Z_k(\rho)$ and $X_k(\rho)$: $Z_k(\rho) \to \bar{Z}_k$ and $X_k(\rho) \to \bar{X}_k$.

In both cases, notice that the flows of $\hat{U}'(\hat{\rho})$ and $\hat{Z}(\hat{\rho})$ do not depend on $\hat{X}(\hat{\rho})$ and are the standard equilibrium flow equations of the Ising model (respectively the $O(N)$ model). This is not surprising because with the regulators chosen above, the model A satisfies for any k the fluctuation-dissipation theorem which is the hallmark of thermal equilibrium. Consequently, the critical exponents ν and η for the model A (resp. the kinetic $O(N)$ model) are the same as in the static Ising model (resp. $O(N)$ model).

Our results are optimized with respect to the parameter a of the regulator using the principle of minimum sensitivity (PMS) [104] (see the App. C.2 for a more detailed explanation about the

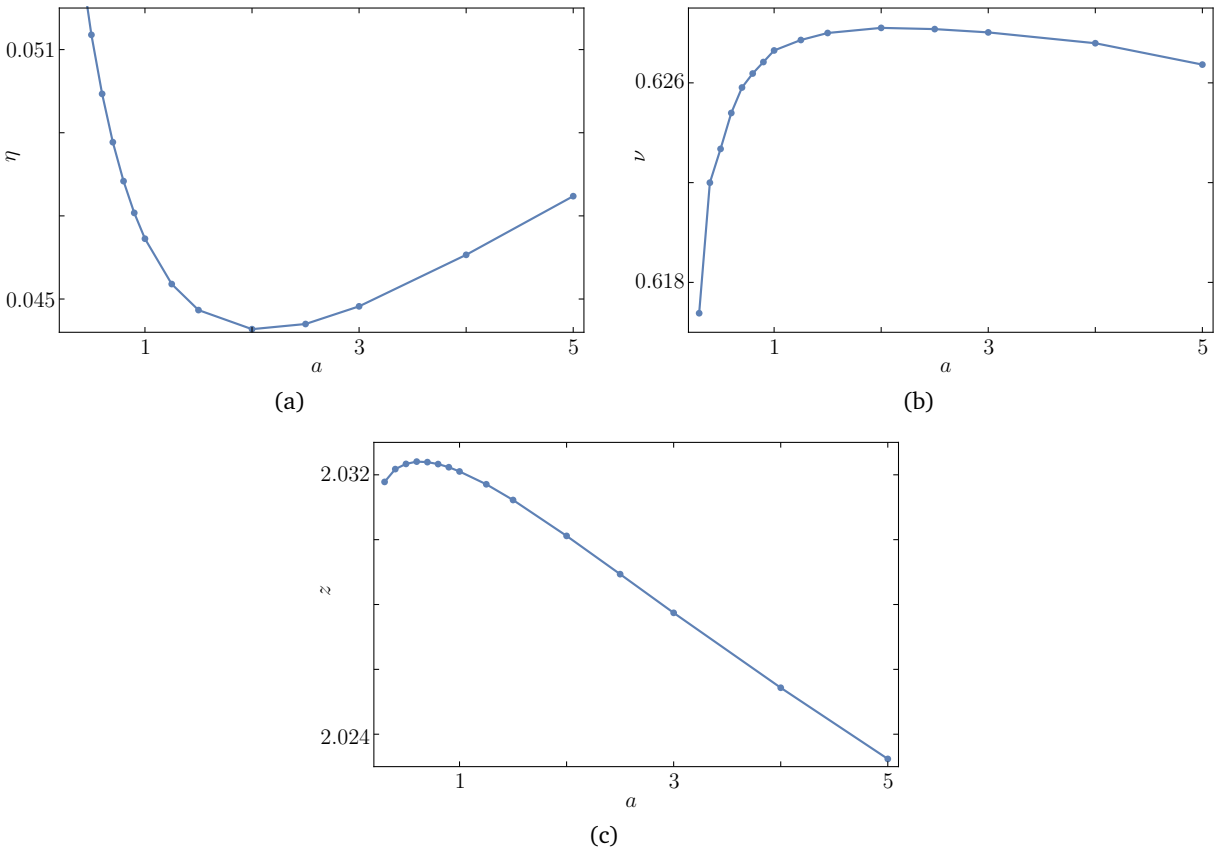

Figure III.3 – *Values of the critical exponents η (a), ν (b) and the dynamical exponent $z = 2+\eta_X-\eta$ (c) in $d = 3$ for the frequency-independent regulator $R_{1,k}(q,\omega) = R_{1,k}(q)$, $R_{2,k}(q,\omega) = 0$ and different values of the regulator parameter a in Eq. (III.44). The PMS value is reached for $a \simeq 2$ for the two static exponents η and ν and for $a \simeq 0.6$ for the dynamical exponent z.*

PMS). According to this principle, the critical exponents do not depend on the unphysical parameter a if no approximation is performed, and we therefore select the values of this parameter where the exponents are stationary (see Fig. (III.3) for model A in $d = 3$).

The numerical integration of the flow equations (C.1)-(C.3) for the model A yields the results displayed in Table III.1 for $d = 3$ together with the results coming from perturbative field theory (PFT), Monte Carlo (MC) simulations and previous NPRG works where the field-dependence of the functions Z_k and X_k was neglected. For $d = 2$, the results are given in Table III.2.

Similarly, for $N = 2$ and $N = 3$, the integration of the equations (C.4)-(C.6) yields the results displayed in Table III.3. Note that an expansion of these equations in $\epsilon' = d - 2$ yields $\eta = \eta_X = \epsilon'/(N-2)$ and therefore a trivial dynamical exponent $z = 2$ in $d = 2$ for $N > 2$.

Finally, notice in the plots of Fig. III.3 that stationarity yields values of a that are close to each other for both η and ν: $a_\eta^{\rm PMS} \simeq a_\nu^{\rm PMS} \simeq 2$, whereas the PMS for z is obtained when $a_z^{\rm PMS} \simeq 0.6$. The internal consistency of the PMS relies on the fact that the values of an exponent computed either at its stationary point or at the stationary points of the other exponents remain close. This is not the case here since we find for instance that $\eta(a = a_z^{\rm PMS}) = 0.0499$ which differs by about 13% from its PMS value whereas $\eta(a = a_\nu^{\rm PMS})$ and $\nu(a = a_\eta^{\rm PMS})$ differ from their PMS values by less than 1%. This is a signal that the exponent z is poorly determined and it is therefore mandatory to study the impact of the frequency-dependence of the regulator on this exponent.

Reference	ν	η	z	
This work	0.628	0.0443	(a): 2.032	(b): 2.024
			(c): 2.024	(d): 2.023
NPRG	0.6281 [95]	0.0443 [95]	2.14 [188]	
PFT [196]	0.6304(13)	0.0335(25)		
MC [77]	0.63002(10)	0.03627(10)		
CBS [81]	0.629971(4)	0.036298(2)		
PFT [84]			2.0237(55)	
MC [85]			2.032(4)	

Table III.1 – *Critical exponents of model A in $d = 3$ from different methods. In the first row, (a): without frequency regulator, (b): using the first frequency regulator defined by Eq. (III.56), (c): second regulator (III.59) and (d): third regulator (III.60). All these results are obtained at the stationary points, a^{PMS}. The exponent z in the NPRG row was obtained in [188], where the field-dependence of the functions Z_k and X_k was neglected. PFT stands for perturbative field theory methods, MC for Monte Carlo simulations, and CBS for conformal bootstrap methods.*

III.2.4 NPRG results with a frequency regulator

We now focus on regulating the frequencies in the flow equations and show how it modifies the NPRG results.

III.2.4.a Fluctuation-dissipation theorem for the frequency regulator

In addition to the properties we discussed before, the regularization of frequencies for the model A necessitates an extra property which is to fulfill the fluctuation-dissipation theorem for all k. Indeed, because we choose the ansatz (III.29) to be invariant under the fluctuation-dissipation theorem transformation (III.26), the regulator terms must also satisfy this symmetry along the flow. We show in App. C.3 that this implies that $R_{1,k}$ and $R_{2,k}$ satisfy the following relation:

$$R_{1,k}(\boldsymbol{x}) - R_{1,k}(x,-t) + \dot{R}_{2,k}(\boldsymbol{x}) - \dot{R}_{2,k}(x,-t) = 0\,. \tag{III.53}$$

The above condition, together with the facts that we choose $R_{1,k}$ to be causal and $R_{2,k}$ even in time [since it comes in $\int_{\boldsymbol{x},\boldsymbol{x}'} \tilde{\phi}(\boldsymbol{x}) R_{2,k}(\boldsymbol{x}-\boldsymbol{x}')\tilde{\phi}(\boldsymbol{x}')$], lead to the following relation:

$$R_{1,k}(\boldsymbol{x}) = 2\Theta(-t)\,\dot{R}_{2,k}(\boldsymbol{x})\,. \tag{III.54}$$

Notice that the case $R_{2,k}(\boldsymbol{x}) = 0$ which implies that $R_{1,k}(|x|,t) \propto \delta(t)$ is not included in the solutions of (III.54) which holds only for $t \neq 0$. Eq. (III.54) becomes in Fourier space:

$$R_{2,k}(q,\omega) = \frac{R_{1,k}(q,-\omega) - R_{1,k}(q,\omega)}{2i\omega} \tag{III.55}$$

where the Fourier transform is defined in Eq. (1). Notice that the particular case $R_{2,k} = 0$ and $R_{1,k}(q,\omega)$ independent of ω is a solution of (III.55).

III.2.4.b Specific choices of frequency regulators

We now have determined all the constraints a frequency regulator for the model A must fulfill, and we present here the three specific regulators – all suited for regulating large frequencies but not equally efficient – we use for computing the dynamical exponent z.

Reference	ν	η	z			
This work	1.13	0.29	(a): 2.28	(b): 2.16	(c): 2.15	(d): 2.14
Exact	1	0.25				
PFT [197]			2.093			
MC [198]			2.1667(5)			

Table III.2 – *Critical exponents of model A in $d = 2$ from different methods. In the first row, (a): without frequency regulator, (b): using the frequency regulator defined by Eq. (III.56), (c): second regulator (III.59) and (d): third regulator (III.60). All these results are obtained at the stationary points, a^{PMS}. We also display results for the dynamical exponent z coming from perturbative field theory (PFT) and Monte Carlo (MC) simulations.*

Reference	ν	η	z		
This work ($N = 2$)	0.70	0.039	(a): 2.029	(b): 2.024	(c): 2.023
This work ($N = 3$)	0.75	0.037	(a): 2.025	(b): 2.021	(c): 2.021
PFT ($N = 2$)	0.6704(7)	0.0349(8)	2.026		
PFT ($N = 3$)	0.7062(7)	0.0350(8)	2.026		

Table III.3 – *Critical exponents of the kinetic $O(N)$ model in $d = 3$ for different values of N and from different methods. The exponents η and z have been computed in this work using the LPA' (see Sec. III.2.3 in the main text for a definition). In the two first row, (a): without frequency regulator, (b): using the frequency regulator defined by Eq. (III.56) and (c): second regulator (III.59). All these results are obtained at the stationary points, a^{PMS}. The static exponents η and ν for the perturbative field theory (PFT) comes from [87], the dynamic exponent z is computed using the value of η from [87] and the relation $z = 2 + c\eta$ from [86], which is a relation obtained perturbatively at order ϵ^4, with $\epsilon = 4 - d$. Very few MC studies exist for the determination of z. More details on the determination of this exponent can be found in [88] (see also reference [199] for a review of the determination of the static exponents).*

A first convenient choice for the regulator in direct space is the following:

$$R_{1,k}(x,t) = \frac{1}{\tau_k}\Theta(-t)\,\mathrm{e}^{t/\tau_k} r_k(x)\,, \tag{III.56}$$

where $r_k(x)$ is the space regulator (usually exponential) whose Fourier transform is given by Eq. (III.44), and $\tau_k = \beta\,\bar{X}_k\bar{Z}_k^{-1}k^{-2}$ with β a dimensionless free parameter that we use for optimization. We display the time-dependent part $\rho_1(t)$ of this regulator in Fig. III.4. The choice of this first regulator is motivated by three main reasons: (i) it is causal and satisfies relation (III.54), (ii) it decays sufficiently fast in time so that the noise correlations (III.16) are not modified too drastically, (iii) its Fourier transform can be computed analytically and is a simple rational fraction. Indeed, using dimensionless frequencies, the Fourier transforms of their frequency part read:

$$\rho_1(\hat{\omega}) = \frac{i}{i - \beta\hat{\omega}}\,, \tag{III.57}$$

$$\rho_2(\hat{\omega}) = \frac{\beta}{1 + \beta^2\hat{\omega}^2}\,. \tag{III.58}$$

When $\beta \to 0$, we retrieve the usual non-regulated in time theory. Now that we have specified the frequency and space parts of the regulators, we check that they both fulfill NPRG requirements: in addition to a sufficiently fast decay, they must also satisfy some limits when $k \to 0$ and $k \to \Lambda$: $R_{1,k}(q,\omega)$ and $R_{2,k}(q,\omega)$ must both vanish when $k \to 0$ in order to retrieve the original theory. In the limit $k \to \Lambda$, we design $R_{1,k}$ such that $R_{1,k}(q,\omega) \underset{k\to\Lambda}{\sim} \Lambda^2 \gg 1$: the system acquires a large

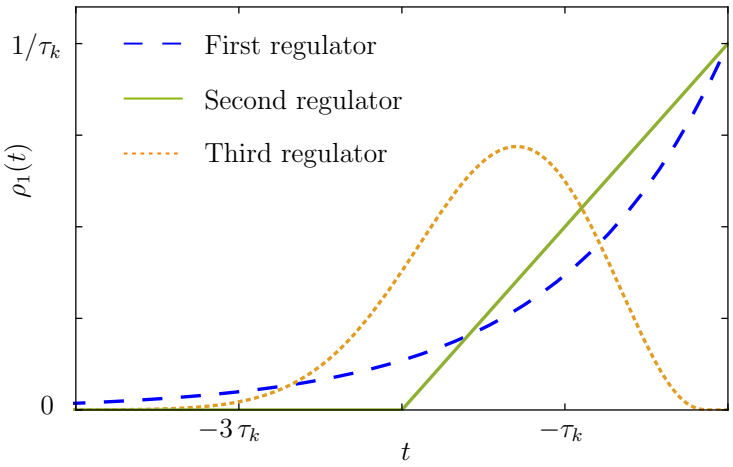

Figure III.4 – *Typical shape of the time-dependent part $\rho_1(t)$ of the three regulators studied: the first regulator is defined in Eq. (III.56), the second in (III.59) and the third in (III.60).*

"mass" that freezes the fluctuations. Finally, one finds $R_{2,k}(q,\omega) \underset{k\to\Lambda}{\sim} a\beta$, which means the initial noise correlation is modified which is harmless for the computation of universal quantities.

In order to compare the results obtained with different frequency regulators, we have engineered two other regulators in addition to this simple first one (see Fig. III.4 for a plot of their time-dependent part). The second regulator we propose is defined as:

$$R_{1,k}(x,t) = \frac{r_k(x)}{2\tau_k} \times \begin{cases} (t+2\tau_k)/\tau_k & \text{if } -2\tau_k \le t \le 0, \\ 0 & \text{otherwise.} \end{cases} \tag{III.59}$$

Notice that its Fourier transform can also be computed analytically. Since singularity in the time domain means slow decay in the frequency domain, the more singular in t the slower the decay of $\rho_1(\hat{\omega})$ at large $\hat{\omega}$. This second regulator is discontinuous at $t = 0$ and $t = -2\tau_k$ and we therefore expect it to be less effective than the first one.

Finally, the third frequency regulator we consider is the following:

$$R_{1,k}(x,t) = \frac{A}{\tau_k}\Theta(-t)\,\mathrm{e}^{-(1+t/\tau_k)^2+\tau_k/t} r_k(x) \tag{III.60}$$

where A is a constant such that the area under its curve is one, in order to retrieve a Dirac function as $\beta \to 0$. This third regulator is infinitely differentiable at $t = 0$ and we therefore expect it to be sharper than the two previous regulators in the frequency domain. On the other hand, the computation of its Fourier transform has to be done numerically.

Finally, we insist on the fact that enforcing causality along the flow is not an obvious task: although choosing a regulator that is causal [$R_{1,k}(x,t) \propto \Theta(-t)$] seems at least necessary to preserve causality, one must check that it also preserves causality all along the flow [21]. As we explain in App. C.4, causality means that the poles of the response function

$$\chi(\omega) = \frac{1}{P(q^2,-\omega)} = \frac{1}{h(q^2,-\omega) - i\omega X_k}, \tag{III.61}$$

where $h(q^2,\omega) = Z_k(\rho)q^2 + R_{1,k}(q^2,\omega) + U_k'(\rho) + 2\rho U_k''(\rho)$, must lie in the lower-half of the complex ω-plane. When $R_{1,k}(q^2,\omega)$ is a (simple) rational fraction as it is the case for the first regulator defined by Eq. (III.56), it is easy to check that the causality of the response function is enforced all along the flow. For the second regulator (III.59) and the third regulator (III.60), we only checked it for the initial condition, and at the fixed point of the flow.

We also stress that if $R_{1,k}(q^2,\omega)$ is a rational fraction, one can hope to design "by hand" a regulator for which all the poles of the response function have a negative imaginary part.

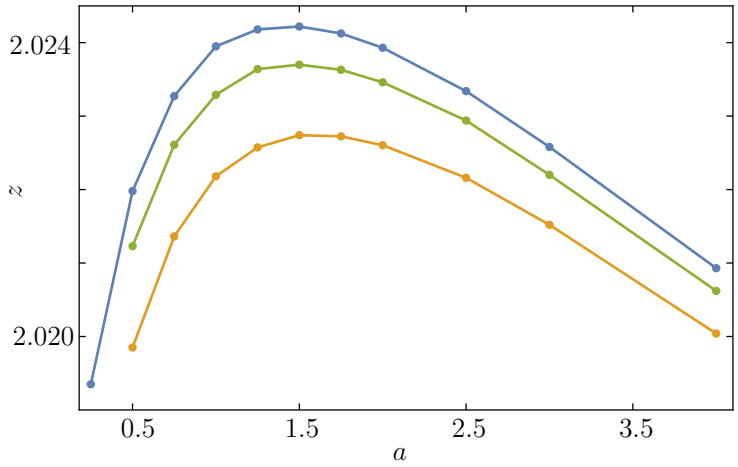

Figure III.5 – *Values of the critical exponent z in $d = 3$ for the flow regulated in frequencies for different values of the regulator parameter a. For each value of a, the value of β has been chosen such that z is extremal. The three curves are obtained from top to bottom by the regulators defined in Eqs. (III.56), (III.59) and (III.60). The PMS value is reached for $a \simeq 1.5$ for the three regulators.*

However, if one wishes to build a regulator that decays faster than a power law, then the only remaining option is to construct it in direct space and afterwards check the decay in Fourier space.

III.2.4.c Results with a frequency regulator

In the presence of the three regulators defined respectively in Eqs. (III.56,III.59,III.60), the flow equations of $\hat{U}'$ and $\hat{Z}$ remain identical to those at equilibrium (C.1)-(C.2) since the fluctuation-dissipation theorem is valid all along the flow. On the other hand, the flow of $\hat{X}$ now depends on β and is more complicated than without a frequency regulator. For the first regulator defined by Eq. (III.56), the integrals over the frequencies in the flow equation can still be performed analytically since its Fourier transform is a simple rational fraction in $\hat{\omega}$. For the two other regulators, the integrals over frequencies must be computed numerically.

We have numerically integrated the new flow equations for different values of a and β in order to compute the critical exponents at the stationary point in the (a, β)-plane. For each value of β, we find a value of a where z is extremal. This yields a curve $z(a)$, see Fig. III.5, that shows a maximum which is therefore the stationary point in the (a, β)-plane. One notices that the PMS value is now obtained for $a_z^{\rm PMS} \simeq 1.5$ (instead of 0.6 in the case without a frequency regulator), which is closer to the PMS value of η and ν (obtained at $a \simeq 2$). More precisely, we find for instance for the model A in $d = 3$ that $\eta(a = a_z^{\rm PMS})$ differs by about 1% from its PMS value, and $\nu(a = a_z^{\rm PMS})$ and $z(a = a_\nu^{\rm PMS})$ differ from their PMS values by less than 1%.

In the light of the above, it is clear that the frequency-independent regulators are simply a particular class of regulators. In our examples, they correspond to the limit $\beta \to 0$ of the three frequency regulators studied. Their main advantage is their simplicity since there is only one regulator which lies in the $\tilde{\phi} - \phi$ direction and also because the frequency integrals can be performed analytically in the flow equations. However, we can see in Fig. III.6 that from the point of view of the PMS, the class of regulators with $\beta = 0$ does not correspond at all to an extremum in the β-direction, even for the value $a = 0.6$, which is optimal at $\beta = 0$. Moreover, the difference between $a_z^{\rm PMS} \simeq 1.5$ and $a = 0.6$ is not only quantitatively important, it is also qualitatively important because it makes the PMS a self-consistent criterion for optimizing the critical exponents. It is remarkable and reassuring that this latter value of $a_z^{\rm PMS}$, which has a meaning *per se* because it can be compared to $a_\eta^{\rm PMS} \simeq a_\nu^{\rm PMS} \simeq 2$, is extremely stable when

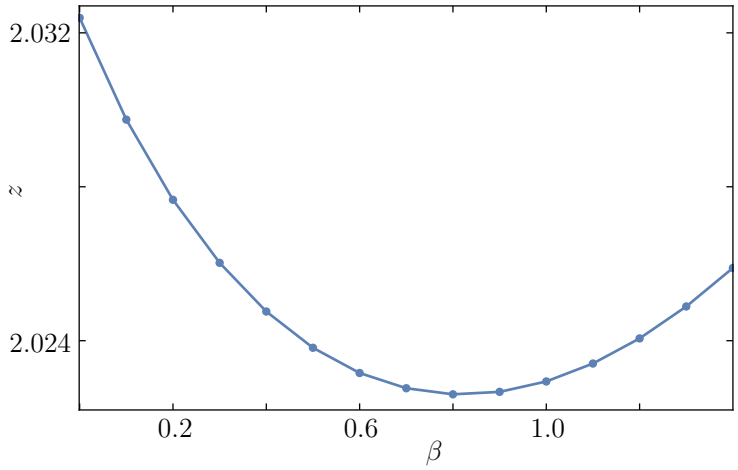

Figure III.6 – *Exponent z for $N = 1$ in $d = 3$ as function of the parameter β of the regulator (III.56). This curve is obtained for $a = 0.6$ which corresponds to the stationary point of z at $\beta = 0$.*

changing the shape of the regulator, see Figs. III.4 and III.5. Finally, we find as expected that the accuracy of the optimized value of $z-2$ found in this work compared to the average of the other estimates, $z-2 \simeq 0.028$, is comparable to the accuracy of the optimized value of η compared to the world's best value, that is, is around 15%, see Table. III.1. Together with the stability of our results, this is a strong indication that the regulators we study here are almost optimal at this order of the derivative expansion.

III.3 Conclusion

We have shown in this chapter how to engineer regulators of the NPRG flow equations acting on frequencies, a feature that is believed to be of tremendous importance when solving generic out-of-equilibrium problems with the derivative expansion, since the regulator guarantees the validity of this approximation. Causality, of course, has to be taken care of and is the main preoccupation when designing such a regulator. Therefore, to the contrary of the space regulator which can be engineered directly in Fourier space, it is convenient to think first in direct space for a frequency regulator to enforce causality. For systems that relax toward equilibrium, introducing a second regulator in the $\tilde{\phi}-\tilde{\phi}$ direction connected to the other one in the $\tilde{\phi}-\phi$ direction is mandatory to preserve the time-reversal symmetry all along the flow, a feature that is surely desirable and that, at least, simplifies the formalism. The status and whether or not a regulator in the $\tilde{\phi}-\tilde{\phi}$ is mandatory for non-relaxational models depend on the precise symmetries of these models.

Moreover, to discriminate between the functions that are candidates for regularizing the frequencies, a deeper study could be carried out: either by testing the convergence of the approximation schemes when different regulator are used in the following of [67], or by comparing their effect on the trajectories of the flow in the spirit of [106].

The next step will be to implement frequency regulators for generic out-of-equilibrium models not displaying such a strong constraint as the fluctuation-dissipation theorem. For instance, in the previous NPRG studies of the directed percolation universality class, only results at the LPA' were reported [98, 144]. Improving these results by going at order two of the derivative expansion surely requires the use of a frequency regulator. The parity conserving generalized voter model is another candidate since the NPRG results are not fully satisfactory for this model; see [96] for an exact result that disagrees with the conclusions of [95] obtained within the LPA without frequency regulators.

Chapter IV

Landscape erosion

Contents

Scale invariance is ubiquitous in natural landscapes: mountain ranges, river networks, coastlines [9, 200]. All have portions of their features that can be considered as a reduced-scale image of the whole. Coastlines are especially famous for being self-similar since Mandelbrot entitled his seminal paper about fractals "How long is the coast of Britain?" [201], underlining the fact that the length of a fractal object depends on the length scale. Indeed, measuring the length of the coastline of Britain (following all the bays and peninsulas) with a one-kilometer ruler yields some (finite) result. Start again taking now a one-meter ruler: you will realize that the bays and peninsulas you were measuring contain in fact more sub-bays and sub-peninsulas, and the resulting length will be much larger than the previous one. Measure again with a one-millimeter ruler: the final length will still be growing. Such a puzzling result – that the length of an object may depend on the length scale and may therefore grow to infinity as the length scale is reduced – is simply the signature of a fractal (or scale-invariant) property. Such objects do not have an intrinsic length scale (except of course the microscopic length of the smallest part composing it), and a measure of their length relative to a given scale does not really make sense. How fast grows the length when the measuring scale is reduced, however, has a meaning and yields the definition of the fractal dimension introduced by Mandelbrot [202].

This kind of self-similar behaviour is found everywhere when studying landscapes: the self-similarity of branching rivers networks – with brooks merging into creeks that become streams flowing to form rivers – is also a well-known fact in geomorphology and was studied extensively (see [24, 200] and references therein). As an example, the length ℓ of a river (or any stream) is found to be related to the drainage basin area a – that is the area of all the streams

flowing to this river – by a scaling law which reads:

$$\ell \propto a^{\theta} \tag{IV.1}$$

where $\theta \simeq 0.5 - 0.6$ according to experimental data. This scaling behaviour, first noticed by Hack in 1957 [203] is verified experimentally for most river networks across the Earth (see for example Fig. IV.1). Many other experimental scaling laws exist concerning rivers that highlight their intrinsic scale invariance, and one may therefore wonder where this self similarity comes from.

Being familiar with phase transitions, we could be tempted to notice that scale invariance is a feature that arises naturally at criticality where the only characteristic length of the system – the correlation length ξ – diverges, hence leading to a self-similar regime. However, as far as equilibrium phase transitions are concerned, this critical behaviour demands the fine tuning of a parameter, usually the temperature, which has to be set precisely to $T = T_c$ in order to observe the scale-invariant regime. Which parameter is then fine-tuned in natural landscapes that makes them display this critical behaviour?

To answer this question, the so-called self-organized criticality (see for instance [10, 11] and reference therein) was very appealing and has been thought to be a good candidate for explaining and understanding this fine-tuning to criticality. However, the ambiguity for defining precisely the self-organized criticality and the difficulty to link the theory to the natural data decreased its attractiveness, at least on the theoretical point-of-view.

On the other hand, some other out-of-equilibrium systems (such as the Navier-Stokes equation in its turbulent regime, or the Kardar-Parisi-Zhang equation) are known to display generic scaling, that is to be critical without fine-tuning. For this reason, we are interested in this chapter in finding a coarse-grained description of the phenomena leading to the formation of scale-invariant landscapes, having in mind to find equations that would display generic scaling. More precisely, we will not be interested in coastlines or river networks but rather in the erosion of landscapes.

The characterization of the scale invariance of erosional landscapes is not as obvious as the fractal behaviour of river networks. However, given the topographic map of an area, one can easily deduce the associated river network since water flows according to the steepest slope. Therefore, if river networks display scale invariance, it seems sensible that the topographic map itself also exhibit some scaling, and we will see in the following that it is indeed the case.

IV.1 Experimental facts and models

IV.1.1 Experimental data

In this chapter we are mainly interested in erosional landscapes, such as mountain ranges, that also display scale invariance [204]. This scale invariance – less obvious than for other geophysics phenomena – is unraveled by computing the roughness of the landscape, given by the height-height correlation function:

$$C(\vec{r}) = \sqrt{\langle |h(\vec{x}+\vec{r}) - h(\vec{x})|^2 \rangle_{\vec{x}}} \quad , \tag{IV.2}$$

where $\langle \cdot \rangle_{\vec{x}}$ denotes a spatial averaging (over $\vec{x}$). This correlation function is shown in various empirical measurements to scale as $C(\vec{r}) \sim |\vec{r}|^{\alpha}$, where α is known as the roughness exponent. Although the scaling behaviour of erosional landscapes is a well-documented fact [26, 205–212], an unambiguous and unique value of the roughness exponent α remains elusive as we will explain in the following. We briefly review the different methods that exist for computing the roughness exponent α, and that have been used to gain insights about the erosion mechanisms.

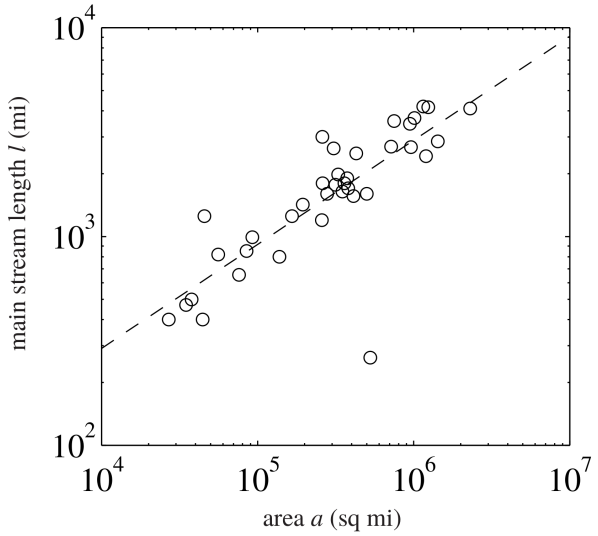

Figure IV.1 – *Figure from [200]. Main stream length ℓ versus the area a of the drainage basin for 37 of the world's largest basins. Hack's exponent θ appearing in Eq. (IV.1) is estimated to be $\theta \simeq 0.50$ in this case.*

IV.1.1.a Field measurements

Deeper insight into the structure and scale invariance of landscapes has been gained after the introduction of digital elevation maps (DEMs). Usually, these DEMs consist of elevations, obtained by topography from space, in a grid whose spacing is of the order of $10 - 90$ m. Using this grid of digital elevations, various methods can be used to compute the roughness exponent α, such as variograms, box-counting, power-spectrum, etc. (see for instance [24] for details about these methods). We should however warn that these different methods may yield different values of the roughness exponent, mostly because of the finite range of available data [9, 213, 214]. One should at least make sure that the same method is used when computing α for different areas in order to compare their roughness [214]. Notice that in the geophysics literature one can also find, instead of the roughness exponent, the fractal dimension D. The relation between the two quantities is $\alpha = d + 1 - D$, where d is the spatial dimension [9].

Let us briefly explain one of the existing method to compute the roughness of a landscape: the variogram technique (see for instance [206]), which simply relies on the computation of the height-height correlation function (IV.2). The variogram is constructed by considering the variance of the elevation as a function of the horizontal distance: for a pair of point (x_1, y_1, z_1) and (x_2, y_2, z_2), the contribution to the variance is $(\Delta z)^2 = (z_1 - z_2)^2$ and the horizontal distance is $\Delta x = \sqrt{(x_1 - x_2)^2 + (y_1 - y_2)^2}$ (see Fig. IV.2 for an illustration). These quantities are then computed for every pair of points on the grid, and the slope of the logarithmic plot of the standard deviation against the logarithm of the distance yields the roughness exponent.

IV.1.1.b Laboratory experiments

In addition to the natural data available through digital elevation models, laboratory experiments that mimic natural erosion of landscapes have flourished in the recent years (see [208] and references therein for a review). Although imperfect and in spite of differences of spatial scale, material properties and the simplicity of the settings, these experiments produce spatial structure and kinematics that compare quite well with natural systems. The fact that despite a clear understanding of the underlying erosional mechanisms, very simple experimental models still resemble strikingly to natural landscapes probably arises from the scale-invariant property

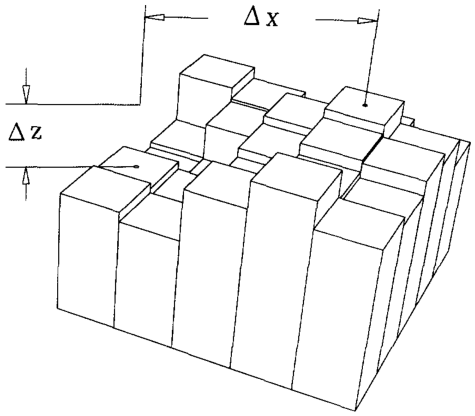

Figure IV.2 – *Schematic illustration from [206] of the computation of variograms. The variance of the elevation difference Δz is the height-height correlation function (IV.2) from which the roughness exponent can be computed.*

of the natural systems, and is probably the signature of some universality in these phenomena.

Unfortunately, and despite the large number of such experiments, it seems that none of them focused on the scale invariance of the topography itself, and there is no available results for the roughness exponent α from these laboratory experiments.

IV.1.1.c Numerical studies

Numerical studies have a long history in the geophysics of erosion, and more precisely in trying to understand the formation of river networks in landscapes (see for instance [24] and references therein). Many of these numerical models are based on discrete models, where erosion is simulated by following the flow of discrete units of raindrop down the steepest slope and eroding the hillslope with some phenomenological dependence between the erosion process and the slope (see for instance [206, 209, 210]). Some other numerical studies rely on continuous descriptions based on partial differential equations, such as the Kardar-Parisi-Zhang equation (that we will describe in more details in the following) or on various other equations, focusing on different features of the landscape erosion [211, 212].

Most of the time, these numerical procedures are run to produce a given landscape topography, which is in turn used to create an associated river networks. Although these models are usually able to reproduce some of the fractal properties of the river networks[1], they often miss some other scaling properties depending on the precise model that is considered [216].

Since most of these simulations are rather focused on the river network than on the topography itself, these numerical studies do not pay a particular attention on the roughness exponent and are therefore of little use in our case, although these extensive numerical studies have widely contributed to the understanding of landscape formation.

IV.1.1.d Some facts about the roughness exponent

Despite an important effort made for computing the roughness of landscapes using the different methods that have quickly been presented above, finding a unique value for the roughness exponent α has been inconclusive. However, from the large amount of experimental data available, at least two features can be extracted: (i) The roughness exponent has a large variability, and it seems to span the whole range between $\alpha \simeq 0.2$ and $\alpha \simeq 1$, (ii) There is a tendency to find larger

[1] Such as the Horton's law [215] which finds scale invariance in the way stream networks are organized. See for instance [24] for more details about it.

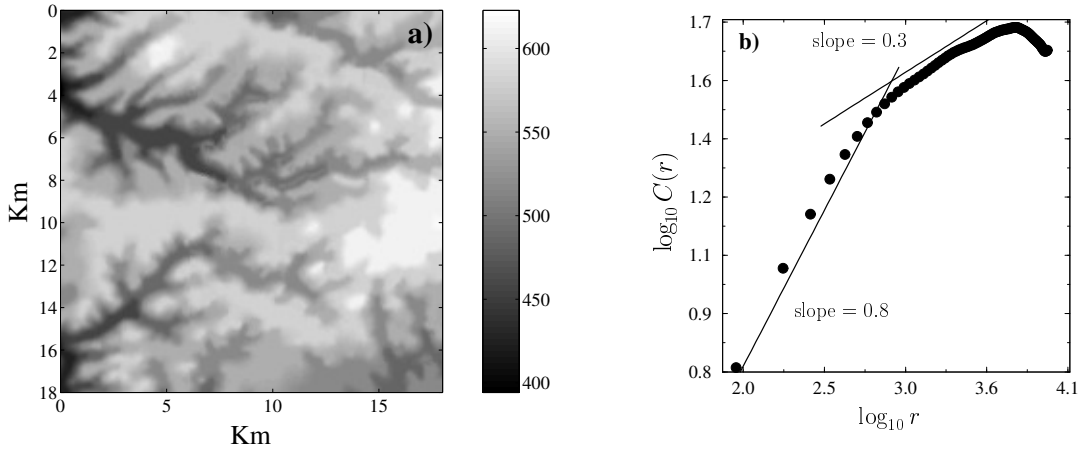

Figure IV.3 – *Figures extracted from [217]. **(Left)** Digital elevation map of an area of the Appalachian Plateau, in Northwest Pennsylvania. Elevations are given in meters. The spatial resolution is 90 m. **(Right)** Averaged height-height correlation function $C(r)$ for the landscape displayed on the left, and where r is oriented in the vertical direction of the elevation map. A plot of similar shape, but with smaller values of $C(r)$, is obtained in the horizontal case. Logarithms are computed from quantities measured in units of meters.*

values of the roughness exponent ($0.70 \lesssim \alpha \lesssim 0.85$) at intermediate length scales ($\lesssim 2$ km), and smaller values ($0.30 \lesssim \alpha \lesssim 0.55$) at larger length scales [26, 205–207]. This second feature is made particularly clear on Fig. IV.3. This suggests that two different regimes exist in the erosion of landscapes, which therefore require two different mechanisms to be described.

Notice however that this assumption of two different regimes characterized by two different scaling exponents should be treated with caution, since this scaling behaviour is only observed for one or two logarithmic decades at most, and more experimental evidence stemming from laboratory experiments (or maybe geophysical data from other planets) would probably be necessary to make a definitive statement about this crossover. We will nonetheless make the assumption that this crossover has a physical meaning and is indeed the signature of a first mechanism at small scale which is then taken over by a different erosion mechanism at larger scale. We will argue in details in the following that at large length scale an isotropic and non-conservative Kardar-Parisi-Zhang description of the erosion is satisfactory, whereas at smaller length scale, the intrinsic anisotropy of the process (due to a preferred direction, that of the slope of the mountain) requires an alternative description.

In the following we explain in details these two models and, before that, we present the minimal ingredients to reproduce landscape formation and scale invariance, that have been identified thanks to the different experimental and numerical methods we presented above.

IV.1.2 Minimal ingredients for an erosion model

The physical phenomena involved in the erosion of landscapes are numerous (rainfalls and storms, freezing events and changes in temperature, chemical erosion, landslides and avalanches, etc. [218]). Because of the complexity and variety of these erosion mechanisms, a model stemming directly from them seems out of reach. However, the scale invariance displayed by these systems suggests that the intermediate and large-scale physics of these systems is, at least to a large extent, independent of the smallest scale details. A simple phenomenological model that would capture the relevant elements could thus be sufficient to reproduce this power-law behaviour and predict the value of the roughness exponent. So far, some necessary elements for this self-similarity to emerge have already been identified [25] and we now discuss them.

First, at the simplest level of description, the flowing of eroded material by diffusion of the

soil has of course to be considered, and the evolution of the height profile $h(\vec{x},t)$ is given by simple diffusion:

$$\partial_t h(\vec{x},t) = D\nabla^2 h(\vec{x},t) \tag{IV.3}$$

which accounts for the smoothing of the irregularities of the landscape. In some simple cases such as river deltas formation, diffusion in itself can be sufficient to explain the delta front profile [219]. However, the nontrivial scaling property of the correlation function $C(r)$ in eroding landscapes is not reproduced with this sole ingredient. One can moreover notice that diffusion is a smoothing mechanism, and we should look for an ingredient that would instead have a roughening contribution.

This second ingredient is a noise term [25, 212] that takes into account the roughening mechanisms that occur at small scale: rainfalls, variability in the erodibility of the soil (which may depend both on the position $\vec{x}$ and the height h itself), randomness of tectonic events etc. In full generality, this noise term may depend on $\vec{x}$, t and h, and we will see in the following that the choice of the noise distribution can indeed lead to different predictions for the model [209]. In the simplest case of an additive noise[2] – on which we focus in the following –, the evolution of the height through the combined action of diffusion and noise is known as the Edwards-Wilkinson model of noisy diffusion. However, this model is known for displaying scale invariance only in dimension $d = 1$, with a nonvanishing value of α. In $d = 2$ however, which is the dimension of physical interest for the erosion of landscape, one finds $h \sim \log x$ which means an effective roughness exponent $\alpha = 0$ and a smooth landscape [220].

Therefore, a third ingredient is requested: a nonlinear term, that counterbalances the smoothing effect of diffusion and creates a rough landscape [204, 221]. As we will see in the following, this nonlinear term can take different forms that also lead to different predictions for the value of the roughness exponent. The combination of these three elements is minimal to get scaling features in an erosive model, and we now proceed to a more precise description of models that were proposed to describe the erosion of landscapes.

IV.1.3 Large length scale: the Kardar-Parisi-Zhang equation

Amongst the equations displaying the features highlighted above, the Kardar-Parisi-Zhang (KPZ) equation stands out of the crowd [13]. First derived and famous in the context of surface growth, Sornette and Zhang suggested that the KPZ equation is also a plausible model to describe isotropic erosion of landscapes at large length scale [25].

It is not so surprising that this equation, although derived in a different context, still remains a good candidate for an erosion model: in addition to possessing the three ingredients we discussed above (diffusion, nonlinearity and noise) that are minimal for finding a scaling-behaviour, the KPZ equation is in fact the simplest nonlinear equation for an isotropic, independent of the absolute height, noisy diffusion problem.

To derive this equation, we consider the erosion of an initially flat surface, which we take as the origin for computing the height $h(\vec{x},t)$, and the positive axis for h is taken to point downward. The simplest erosion mechanism can be written as [25]:

$$\partial_t h(\vec{x},t) = D\nabla^2 h + v(h) \tag{IV.4}$$

with $D > 0$ and the first term $D\nabla^2 h$ accounts for the smoothing effect due to gravity. Indeed, a negative local curvature $\nabla^2 h < 0$ (that is, a bump), has a negative contribution to $\partial_t h$ and will therefore decrease and be smoothed out. To the contrary, a positive local curvature $\nabla^2 h > 0$ (a well) will grow since it yields a positive contribution to $\partial_t h$, which also has the effect of making the surface smoother (see Fig. IV.4 for an illustration). The velocity term $v(h)$ is the local

[2] That is, a noise noise independent of the height h.

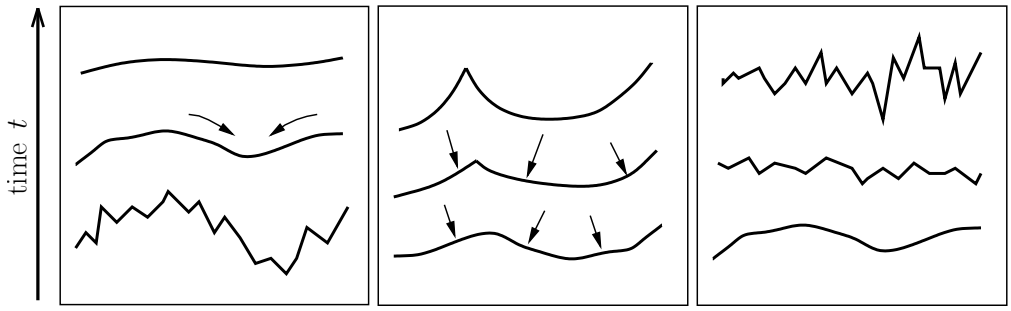

(a) diffusion (b) nonlinearity (c) noise

Figure IV.4 – *Cartoon representation of the different terms appearing in the KPZ equation (IV.6).* ***(a)****: diffusive term $\nabla^2 h$. Diffusion of the material has a smoothing effect: bumps shrinks while wells are filled by the eroding material (symbolized by the arrows).* ***(b)****: nonlinear term $(\nabla h)^2$. This term accounts for an erosion proportional to the surface of exposed material, and takes place in a direction orthogonal to the slope (symbolized by the arrows). As a consequence, the irregularities of the surface are increased by this term which therefore makes the surface rougher.* ***(c)****: noise term $\eta(\vec{x}, t)$. The noise is used to model the wealth of events that contributes to erosion and to rough landscapes: showers, storms, inhomogeneities in the erodibility of the soil.*

effective rate of material removal per unit area and since we are interested in the fluctuations of the height around a surface that is flat on average, we can assume that the slope is small and perform an expansion in term of ∇h of the velocity term:

$$v(h) = v_0 + \nabla h \frac{\partial v}{\partial(\nabla h)} + \frac{1}{2}(\nabla h)^2 \frac{\partial^2 v}{\partial(\nabla h)^2} + O\left[(\nabla h)^3\right] . \tag{IV.5}$$

The first term v_0 accounts for a systematic global erosion process and can be removed by going in the co-moving frame $h \to h - v_0 t$. The second term linear in ∇h can be removed as well by a Galilean transformation: $\vec{x} \to \vec{x} - t\, \partial v/\partial(\nabla h)$. Finally, the third term $(\nabla h)^2$ admits a geometrical interpretation: if the local slope is ∇h, then the local exposed surface is proportional to $\sqrt{1 + (\nabla h)^2}$ and this third term therefore accounts for an erosion proportional to the local exposed surface (see Fig. IV.4 for an illustration).

Finally, and as we argued before, a noise term is added to the diffusion and nonlinear terms, and we obtain the celebrated KPZ equation [13]:

$$\partial_t h(\vec{x}, t) = D\nabla^2 h + \lambda(\nabla h)^2 + \eta(\vec{x}, t) . \tag{IV.6}$$

The noise term, in addition to being necessary for having an erosion model displaying scale invariance, also accounts for the other erosion mechanisms that cannot be described by a geometric term. For instance it describes the erosion due to showers and storms, that are erratic in time, space and intensity. A "quenched"/static noise term can also account for the heterogeneity of the materials that are being eroded (different kinds of rocks and soil). Notice that similarly to the nonlinear term, the noise has the tendency of making the eroding surface rougher and rougher (see Fig. IV.4 for an illustration).

The KPZ equation has been extensively studied in the literature, experimentally, numerically and theoretically, mainly because it is the representative of a very broad universality class which describes or can be mapped to a wealth of problems, such as propagation and kinetic roughening phenomena (for instance the front of a forest fire, or coffee particles accumulating at the edge of a coffee drop), randomly stirred fluid (Burgers' equation), directed polymers in random media, etc. [109]. The KPZ equation is also famous for causing troubles to the perturbative RG: although exacts results exist in $d = 1$ thanks to extra symmetries in this case (and a mapping

to random matrices theory [41, 89]), the perturbative expansion has failed to accurately describe the KPZ fixed point in dimension $d > 1$, because the KPZ "strong-coupling" fixed point is genuinely nonperturbative in $d > 1$ and therefore cannot be reached from an ε expansion near $d = 1$. By contrast, the NPRG and its nonperturbative approach has proved very well suited for studying this equation and its critical properties in $d = 2$[3] [16, 91, 186, 187].

Numerical simulations [222] and NPRG approach [16] predict a roughness exponent $\alpha \simeq 0.4$ in $d = 2$. However, although a description of erosion by the KPZ equation seems satisfactory for large scale landscapes, where erosion is indeed isotropic and where the KPZ prediction for the roughness exponent α seems to meet the experimental data (for which $0.30 \lesssim \alpha \lesssim 0.55$), it is not the case for intermediate length scales, where erosion occurs along a preferred direction (the slope of the mountain), and the KPZ equation – which is isotropic – fails to capture this important additional ingredient and underestimate the roughness exponent (which is of order $0.70 \lesssim \alpha \lesssim 0.85$) [200]. In addition, the KPZ equation is also nonconservative, a feature that is not realistic for smaller scale erosion [212]. Notice finally that the breakdown of a description by the KPZ equation at small length scale is not completely surprising since the KPZ equation can be seen as a gradient expansion, and should therefore be valid in the low-momentum limit $|q| \to 0$, that is at large length scale. We therefore present in the following a different approach to describe erosion at this smaller scale.

IV.1.4 Small length scale: an anisotropic model

IV.1.4.a Controversy

As discussed before, the KPZ equation does not provide a satisfactory description of the erosion of landscapes at small length scale, for it predicts a roughness exponent which is too small compared to the field measurements. To bridge this gap, Pastor-Satorras and Rothman suggested a nonlinear yet conservative description, and to add anisotropy on top of the three main ingredients discussed above [26, 217]. Their perturbative renormalization group (RG) analysis that retains only one coupling constant yields exponents in surprisingly good agreement with field measurements. Unfortunately, a recent paper by Antonov and Kakin [27] revealed a mistake in their analysis, showing that there is not a single but infinitely many relevant coupling constants in the theory, which invalidates their results. Antonov and Kakin are however unable to predict the value of the roughness exponent α, but they suggest that the correct model has a line of fixed points, and therefore possibly a continuous range of values for α if this line is attractive, which they cannot show. Moreover, Antonov and Kakin's paper focus only on a single type of noise (the isotropic noise, which we describe in more details in the following), while Pastor-Satorras and Rothman studied in addition a more interesting model involving a static noise. In this second model, it is not known whether a line of fixed points also exists.

In the following of the chapter, and this is the last result of this manuscript [28], we tackle this anisotropic erosion model with two different kinds of noise using again the NPRG formalism, which is perfectly suited for studying a model involving infinitely many coupling constants, since the NPRG is functional in essence. We do agree with Antonov and Kakin about the infinite number of coupling constants involved in the model and with the fact that any truncation retaining only a finite number of them yields wrong predictions in the case of the isotropic noise. We show in addition that this conclusion holds for the two types of noise.

Furthermore, we are able to integrate numerically the flow equation, and find that in the case of the static noise, there indeed exists for this model an interval of stable fixed points in the case of physical interest $d = 2$. This interval shrinks to a single fixed point, the trivial Edwards-Wilkinson fixed point, in the case of an isotropic noise. This results is of course in marked

[3] We recall that the NPRG approach breaks down in $d > 3.5$, and yields poor roughness exponent in $d > 2$ [16].

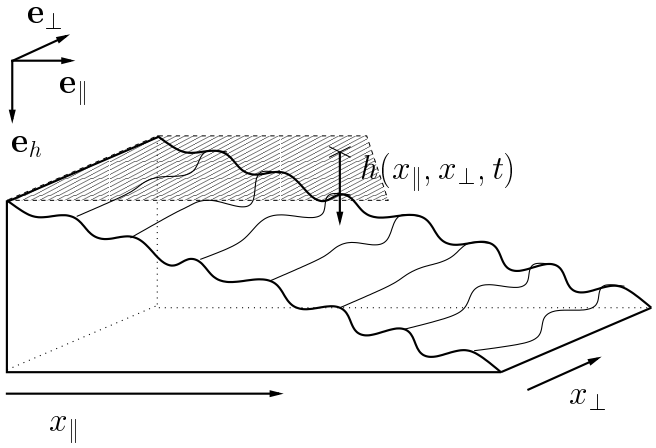

Figure IV.5 – *Figure from [217], illustrating the settings for an anisotropic erosion model.*

disagreement with those of [26, 217] and in partial disagreement with those of [27] in which it is argued that the isotropic noise case could yield nontrivial exponents.

Moreover, although we are not able to predict whether the whole line of fixed points can be reached from realistic initial conditions, the very existence of this line of fixed points could be a first step to explain the large variability observed in the experimental values of the roughness exponent α.

IV.1.4.b Anisotropic model

We now present the anisotropic erosion model as originally proposed by Pastor-Satorras and Rothman [217]. Their idea is that at smaller length scale the erosion takes place in a preferred, downhill direction, that is the direction of the slope of the mountain. Notice that an anisotropic version of the KPZ equation had already been suggested by Hwa and Kardar in [223, 224], but their approach was mostly based on symmetry considerations, whereas Pastor-Satorras and Rothman's model relies on the underlying erosion mechanisms.

To describe the erosion of a surface with a fixed mean tilt which introduces an intrinsic anisotropy in the model, the preferred direction is identified by a unit vector that we denote $\vec{e}_\parallel$ (see Fig. IV.5). Thus, the d-dimensional horizontal position $\vec{x}$ can be decomposed as $\vec{x} = \vec{x}_\perp + x_\parallel \vec{e}_\parallel$ with $\vec{x}_\perp \cdot \vec{e}_\parallel = 0$, and $\vec{x}_\perp$ is therefore a $(d-1)$-dimensional vector. We also define the derivative in the slope direction as $\partial_\parallel \equiv \partial/\partial x_\parallel$ and in the transverse direction as $\nabla_\perp \equiv (\partial/\partial x_{\perp,i})$ with $i = 1 \dots (d-1)$. Note that similarly to the KPZ description, the height $h(\vec{x}, t)$ is positive in the downward direction.

By contrast to the KPZ equation which is isotropic but nonconservative, Pastor-Satorras and Rothman suggested a locally conservative dynamics such that one can write:

$$\partial_t h = -\nabla \cdot \vec{J} + \xi \tag{IV.7}$$

where ξ is a stochastic noise term that we discuss in the following, and $\vec{J}$ is the current of soil per unit length. This current represents two effects: (i) an isotropic diffusion term similar to the one appearing in the KPZ equation and that we already discussed in the previous section and (ii) an anisotropic contribution due to a global flow of dragged soil in the downhill direction. We can therefore write the current as:

$$\vec{J} = -\nu \nabla h - \gamma \nabla_\parallel h \tag{IV.8}$$

where the first term corresponds to Fick's law for diffusion, and the second term represents the anisotropic contribution, with γ playing the role of an anisotropic diffusivity. Consider that this term stems from the flow of overland water: the greater this flow, the stronger the stress exerted on the soil. Because of the anisotropy, the flow increases with the distance downhill $x_\parallel$, but since the height h increases with $x_\parallel$, we can as well parameterize the anisotropic diffusivity as a function of h and write $\gamma \equiv \gamma(h)$. For notational convenience, we write $\gamma(h) = \nu_0 + b(h)$ with $b(0) = 0$, and we moreover define $B(h) = \int \mathrm{d}h\, b(h)$ in order to have:

$$b(h)\partial_\parallel h = \frac{\mathrm{d}B}{\mathrm{d}h}\partial_\parallel h = \partial_\parallel B(h)\,. \tag{IV.9}$$

Finally, substituting the current (IV.8) into Eq. (IV.7) we get the equation derived by Pastor-Satorras and Rothman in [26, 217] to describe the evolution of the height profile as a minimal Langevin equation that takes into account diffusion, nonlinearity, noise, conservation of matter, and anisotropy. It reads:

$$\partial_t h(\boldsymbol{x}) = \nu_\parallel \partial_\parallel^2 h(\boldsymbol{x}) + \nu_\perp \nabla_\perp^2 h(\boldsymbol{x}) + \partial_\parallel^2 B(h(\boldsymbol{x})) + \xi(\boldsymbol{x}) \tag{IV.10}$$

where $\boldsymbol{x} \equiv (\vec{x}, t)$, $\nu_\perp = \nu$, $\nu_\parallel = \nu + \nu_0$. Notice that to preserve the symmetry $h \to -h$, $\vec{J} \to -\vec{J}$ of Eq. (IV.7), the function $B(h)$ must be an odd function of the height. As usual, the above Langevin equation has to be understood in the Itō sense.

Let us now discuss the noise term. Its probability distribution $P(\xi)$ reads:

$$P(\xi) \propto \mathrm{e}^{-\frac{1}{4D}\int_{\boldsymbol{x},t'} W(t-t')^{-1}\xi(x,t)\xi(x,t')} \tag{IV.11}$$

with $\int_{\boldsymbol{x}} \equiv \int \mathrm{d}^d x\, \mathrm{d}t$ (notice that we now drop the arrow above the spatial vector $\vec{x}$ to alleviate the notation), and the noise correlations are:

$$\left\langle \xi(\boldsymbol{x})\xi(\boldsymbol{x'})\right\rangle = 2D\, W(t-t')\delta^d(x-x')\,, \tag{IV.12}$$

where $W(t-t') = 1$ for a static noise, and $W(t-t') = \delta(t-t')$ for an isotropic noise. In this model, the choice of the noise is paramount [212], since different noises will lead to different universality classes, different critical dimensions, and therefore either to a trivial ($\alpha = 0$), or nontrivial roughness exponent in $d = 2$ as we will see in the following. As we already argued in the previous section, a static/quenched noise $W(t-t') = 1$ expresses the fact that different types of soil (with various erodibility) can be originally present, whereas a thermal/isotropic noise $W(t-t') = \delta(t-t')$ is more suited for mimicking the action of rainfalls over the eroding land. As will be shown in the following, the former leads to a nontrivial roughness exponent in $d = 2$, whereas the latter results in smooth landscapes.

From the Langevin equation (IV.10), an equivalent field theory can be derived using the Martin-Siggia-Rose-de Dominicis-Janssen (MSRDJ) approach as explained in Sec. II.2.3. In this formalism, the mean value (over the different realizations of the noise) of a given observable $\mathcal{O}[h]$ is given by:

$$\langle \mathcal{O}[h]\rangle_\xi = \int \mathcal{D}h\mathcal{D}\tilde{h}\, \mathrm{e}^{-\mathcal{S}[h,\tilde{h}]}\mathcal{O}[h] \tag{IV.13}$$

with the action

$$\begin{aligned}\mathcal{S}[h,\tilde{h}] = \int_{\boldsymbol{x}} \tilde{h}(\boldsymbol{x})\left[\partial_t h(\boldsymbol{x}) - \nu_\parallel\partial_\parallel^2 h(\boldsymbol{x}) - \nu_\perp\nabla_\perp^2 h(\boldsymbol{x}) - \partial_\parallel^2 B(h(\boldsymbol{x}))\right] \\ - \int_{x,t,t'} W(t-t')\tilde{h}(x,t)\tilde{h}(x,t')\,.\end{aligned} \tag{IV.14}$$

where we recall that $\tilde{h}$ is an extra field introduced by the MSRDJ formalism, called the "response" field. Notice that up to a rescaling of the time t, the longitudinal direction $x_\parallel$, and of the fields $\tilde{h}$ and h, one can set $\nu_\parallel = \nu_\perp = D = 1$, which is the normalization we keep in the following and which simplifies the symmetry analysis.

IV.2 NPRG approach for erosion

In this section we describe briefly the implementation of the NPRG formalism for the anisotropic erosion model. We have already seen in Chap. III how the NPRG is built for nonequilibrium models, and we will therefore be very concise. We define the generating functional at scale k:

$$\mathcal{Z}_k[j,\tilde{j}] = \int \mathcal{D}h\mathcal{D}\tilde{h}\, \mathrm{e}^{-\mathcal{S}-\Delta\mathcal{S}_k+\int_{\boldsymbol{x}} J(\boldsymbol{x})^T\cdot H(\boldsymbol{x})} \tag{IV.15}$$

where we use a matrix notation and define the following vectors

$$H(\boldsymbol{x}) = \begin{pmatrix} h(\boldsymbol{x}) \\ \tilde{h}(\boldsymbol{x}) \end{pmatrix} \quad \text{and} \quad J(\boldsymbol{x}) = \begin{pmatrix} j(\boldsymbol{x}) \\ \tilde{j}(\boldsymbol{x}) \end{pmatrix}. \tag{IV.16}$$

The regulator term $\Delta\mathcal{S}_k$ reads

$$\Delta\mathcal{S}_k = \frac{1}{2}\int_{\boldsymbol{x},\boldsymbol{x'}} H(\boldsymbol{x})^T\cdot\mathcal{R}_k(\boldsymbol{x}-\boldsymbol{x'})\cdot H(\boldsymbol{x'}) \tag{IV.17}$$

where $\mathcal{R}_k$ is a 2×2 regulator matrix, depending both on space and time, and whose task is to decouple slow-mode fluctuations. In the following, we only consider a space regulator, that is, a regulator which is trivial in the time direction, such that

$$\mathcal{R}_k(\boldsymbol{x}) = \begin{pmatrix} 0 & R_k(x)\delta(t) \\ R_k(x)\delta(t) & 0 \end{pmatrix}. \tag{IV.18}$$

In this paper we use the Θ-regulator which allows for an analytical computation of the integrals over momentum, and which is defined in Fourier space as:

$$R_k(q) = (k^2-q^2)\Theta(k^2-q^2) \tag{IV.19}$$

where $\Theta(q)$ is the Heavyside step-function ($\Theta(q<0)=0$ and $\Theta(q\geq 0)=1$). We also define the effective average action Γ_k as a modified Legendre transform of $\mathcal{W}_k[J]=\log\mathcal{Z}_k[J]$:

$$\Gamma_k[\Phi]+\mathcal{W}_k[J] = \int_{\boldsymbol{x}} J^T\cdot\Phi - \frac{1}{2}\int_{\boldsymbol{x},\boldsymbol{x'}}\Phi(\boldsymbol{x})^T\cdot\mathcal{R}_k(\boldsymbol{x}-\boldsymbol{x'})\cdot\Phi(\boldsymbol{x'}) \tag{IV.20}$$

where $\Phi=\langle H\rangle$. We remind that Γ_k coincides with the action at the microscopic scale ($\Gamma_{k=\Lambda}=\mathcal{S}$) and with Γ at $k=0$ ($\Gamma_{k=0}=\Gamma$), when all fluctuations have been integrated over. The evolution of the interpolating functional Γ_k between these two scales is given by the Wetterich equation that we recall here:

$$\partial_k\Gamma_k[\Phi] = \frac{1}{2}\mathrm{Tr}\int_{\boldsymbol{x},\boldsymbol{x'}}\partial_k\mathcal{R}_k(\boldsymbol{x}-\boldsymbol{x'})\cdot G_k[\boldsymbol{x},\boldsymbol{x'};\Phi] \tag{IV.21}$$

where $G_k[\boldsymbol{x},\boldsymbol{x'};\Phi]\equiv[\Gamma_k^{(2)}+\mathcal{R}_k]^{-1}[\boldsymbol{x},\boldsymbol{x'};\Phi]$ is the full, field-dependent, propagator and $\Gamma_k^{(2)}$ is the 2×2 matrix whose elements are the $\Gamma^{(2)}_{k,ij}$ defined such that:

$$\Gamma^{(n)}_{k,i_1,\cdots,i_n}[\boldsymbol{x}_i;\Phi] = \frac{\delta^n\Gamma_k[\Phi]}{\delta\Phi_{i_1}(\boldsymbol{x}_1)\cdots\delta\Phi_{i_n}(\boldsymbol{x}_n)}. \tag{IV.22}$$

We finally recall that the Wetterich equation (IV.21) represents an exact flow equation for the effective average action Γ_k, which we solve approximately by restricting its functional form. We use in the following the derivative expansion (DE), stating that instead of following the full Γ_k along the flow, only the first terms of its series expansion in space and time derivatives of Φ are considered. The terms retained in this derivative expansion have to be consistent with the symmetries of the action $\mathcal{S}$, and we therefore discuss them before giving an explicit ansatz for Γ_k.

IV.2.1 Approximation and symmetries

IV.2.1.a Symmetries

In order to find a meaningful and simple ansatz for the effective average action Γ_k, we start by studying the symmetries of the action. We consider the following shift-gauged symmetry:

$$\tilde{h}'(\boldsymbol{x}) = \tilde{h}(\boldsymbol{x}) + \varepsilon(x_\perp, t) \tag{IV.23}$$

where ε is an arbitrary infinitesimal function. The action (IV.14) is not strictly invariant under the transformation (IV.23), but since the variations of the action following this transformation are linear in the fields, it also yields useful Ward identities [91, 93]. Under transformation (IV.23), the integral (IV.15) remains unchanged, which yields:

$$\int_{\boldsymbol{x}} \left[\tilde{j}(\boldsymbol{x})\varepsilon(x_\perp,t) - \varepsilon(x_\perp,t)\partial_t \langle h(\boldsymbol{x})\rangle + \varepsilon(x_\perp,t)\nabla_\perp^2 \langle h(\boldsymbol{x})\rangle - \int_{\boldsymbol{x}'} \varepsilon(x_\perp,t) R_k(\boldsymbol{x}-\boldsymbol{x}') \langle h(\boldsymbol{x}')\rangle \right] + 2\int_{\boldsymbol{x},t'} W(t-t')\,\varepsilon(x_\perp,t) \left\langle \tilde{h}(x,t') \right\rangle = 0\,. \tag{IV.24}$$

Notice that we have integrated by parts the terms involving a derivation with respect to $x_\parallel$, and that the boundary terms that result from this integration by parts vanish because of the symmetry $x_\parallel \to -x_\parallel$.

Then, using the definition (IV.20) of the modified Legendre transform to eliminate the external field $\tilde{j}$, and using the fact that, by definition, $\langle h\rangle = \phi$ and $\langle \tilde{h}\rangle = \tilde{\phi}$, the previous expression becomes:

$$\int_{\boldsymbol{x}} \left[\frac{\delta\Gamma_k}{\delta\tilde{\phi}} - \partial_t\phi + \nabla_\perp^2\phi + 2\int_{t'} W(t-t')\tilde{\phi}(x,t') \right] \varepsilon(x_\perp,t) = 0\,. \tag{IV.25}$$

Since this equality is true for any function $\varepsilon(x_\perp,t)$, it means that the Fourier transform [defined in Eq. (1)] of the term inside the brackets vanishes at $q_\parallel = 0$. Consequently, at $q_\parallel = 0$, the functional

$$\Gamma_k - \int_{\boldsymbol{q}} \tilde{\phi}(-\boldsymbol{q}) \left[-i\omega + q_\perp^2 \right] \phi(\boldsymbol{q}) + \int_{\boldsymbol{q}} W(\omega)\tilde{\phi}(-\boldsymbol{q})\tilde{\phi}(\boldsymbol{q}) \tag{IV.26}$$

vanishes under transformation (IV.23). It finally means that only the terms $\partial_\parallel h$ and $\partial_\parallel B(h)$ [which are invariant under (IV.23)] are renormalized, while the terms $\int \tilde{\phi}\partial_t\phi$, $\int \tilde{\phi}\nabla_\perp^2\phi$ and $\int W(t-t')\tilde{\phi}(x,t)\tilde{\phi}(x,t')$ are not. Thus, at lowest order in the space and time derivatives, the most general ansatz for the effective average action $\Gamma_k[\phi,\tilde{\phi}]$ reads:

$$\Gamma_k[\phi,\tilde{\phi}] = \int_{x,t} \tilde{\phi}(x,t) \left[\partial_t\phi - \nabla_\perp^2\phi - \partial_\parallel^2 A_k(\phi) \right] - \int_{x,t,t'} W(t-t')\tilde{\phi}(x,t)\tilde{\phi}(x,t')\,. \tag{IV.27}$$

We conclude that at this order only one function, $A_k(\phi)$, has a nontrivial renormalization flow that we derive in the following.

IV.2.1.b Upper critical dimension

Before deriving the flow equation and giving the results using the NPRG, we discuss here the upper critical dimension of this model, and try to clarify the misunderstanding about the relevance of some operators. First, depending on the nature of the noise, isotropic or static, the model has different upper critical dimensions. This upper critical dimension is $d_c^{\text{stat}} = 4$ in the case of a static noise, and $d_c^{\text{iso}} = 2$ in the case of an isotropic noise.

Indeed, the computation of the upper critical dimension is made very simple once the model has been cast into its simplest form (IV.27) using symmetry considerations. From this equation, we find that the engineering dimension of the field ϕ (expressed in momentum scale) is:

$$[\phi] = \frac{d - 2\kappa}{2} \tag{IV.28}$$

where $\kappa = 1$ for an isotropic noise, and $\kappa = 2$ for a static noise. Therefore, a coupling constant in front of a ϕ^n term is irrelevant for $d > d_c = 2\kappa$, which indeed yields the previous upper critical dimensions.

However, the important and surprising feature of this model is that exactly at the upper critical dimension $d = d_c^{\text{stat}}$ or $d = d_c^{\text{iso}}$, the dimension of the field ϕ vanishes, meaning that all terms $\int_{\boldsymbol{x}} \tilde{\phi}\, \partial_{\parallel}^2 \phi^n$ coming from the expansion of the function $A_k(\phi)$ in Eq. (IV.27) are equally relevant, as pointed out in [27, 225] in the isotropic case. It therefore invalidates the whole approach of [26, 217] since infinitely many coupling constants were discarded. We indeed show in the following that truncating the function A_k greatly modifies the physics and the computation of the critical exponent of the model.

IV.2.2 Flow equation

We now compute the flow of the function $A_k(\phi)$, which we define as:

$$A_k(\phi) = \frac{1}{\Omega} \left(\partial_{p_{\parallel}^2} \mathrm{FT} \left(\frac{\delta \Gamma_k}{\delta \tilde{\phi}(z)} \right) (\boldsymbol{p}) \right) \Big|_{\phi(x,t)=\phi, \boldsymbol{p}=0} \tag{IV.29}$$

where Ω is the volume of the system, and $\mathrm{FT}(f)(\boldsymbol{q})$ refers to the Fourier transform of the function $f(\boldsymbol{x})$ with the convention (1). Notice that one has to evaluate it at constant field *after* having performed the momentum derivation. This is unusual in the NPRG context, and we therefore give slightly more details of the derivation of the flow in the App. D.1. In order to find a fixed point of the RG flow, one has to write the flow equation in terms of dimensionless variables. We define them in the following way:

$$\hat{x}_{\perp} = k\, x_{\perp} \tag{IV.30a}$$
$$\hat{t} = k^2\, t \tag{IV.30b}$$
$$s = \log(k/\lambda) \tag{IV.30c}$$
$$\hat{A}(\hat{\phi}) = \bar{A}_k^{-1} A_k(\phi) \tag{IV.30d}$$
$$\hat{x}_{\parallel} = k^{1+(d-2\kappa)/3} \bar{A}_k^{-2/3}\, x_{\parallel} \tag{IV.30e}$$
$$\hat{\phi} = k^{(4\kappa-2d)/3} \bar{A}_k^{1/3}\, \phi \tag{IV.30f}$$
$$\hat{\tilde{\phi}} = k^{2(\kappa-d)/3} \bar{A}_k^{1/3}\, \tilde{\phi} \tag{IV.30g}$$

where we define the running coefficient $\bar{A}_k$ such that $\hat{A}'(\hat{\phi} = 0) \equiv 1$ where the prime means derivation with respect to ϕ, and we defined the (negative RG time s). In the critical regime and at small k, this running coefficient is expected to behave as a power law $\bar{A}_k \sim k^{-\eta_A^*}$, and we therefore define a running exponent $\eta_A(k) = -\partial_s \ln \bar{A}_k$ such that $\eta_A(k = 0) \equiv \eta_A^*$. The roughness exponent α and the anisotropy exponent ζ correspond respectively to the anomalous dimension of the field ϕ and to the anomalous dimension of the longitudinal direction $x_{\parallel}$. They can thus be expressed in terms of the fixed point value of η_A^* as:

$$\alpha \equiv (4\kappa - 2d - \eta_A^*)/3\,, \tag{IV.31}$$
$$\zeta \equiv 1 + (d + 2\eta_A^* - 2\kappa)/3\,. \tag{IV.32}$$

The flow of the function $\hat{A}(\hat{\phi})$ can be split into two parts:

$$\partial_s \hat{A}(\hat{\phi}) = \partial_s \hat{A}(\hat{\phi})|_{\rm dim} + \partial_s \hat{A}(\hat{\phi})|_{\rm dyn} \tag{IV.33}$$

where the dimensional part of the flow $\partial_s \hat{A}(\hat{\phi})|_{\rm dim}$ directly follows from the previous definitions (IV.30) and reads:

$$\partial_s \hat{A}(\hat{\phi})|_{\rm dim} = \eta_A \hat{A}(\hat{\phi}) + \frac{2d + \eta_A - 4\kappa}{3} \hat{\phi} \hat{A}'(\hat{\phi}) \,, \tag{IV.34}$$

while the dynamical part of the flow is derived in App. D.1 and reads:

$$\partial_s \hat{A}(\hat{\phi})|_{\rm dyn} = \frac{(3\kappa - 2) K_d}{2} \int_{y=0}^{\infty} \int_{\theta=0}^{\pi} \frac{y^{d/2-\kappa} \sin(\theta)^{d-2} r'(y) \hat{A}''(\hat{\phi})}{\Big(r(y) + \sin^2\theta + \hat{A}'(\hat{\phi}) \cos^2\theta \Big)^{1+\kappa}} \tag{IV.35}$$

where $K_d = (2^{d-1}\pi^{d/2}\Gamma(d/2))^{-1} = S_{d-1}/(2\pi)^d$ with S_d the surface of the d-dimensional unit hypersphere. Moreover, the definition of the running anomalous dimension $\eta_A(k)$ provides us with the additional equation $\partial_s \hat{A}'(0) = 0$, which yields:

$$\eta_A = \kappa - d/2 - \frac{3(3\kappa - 2) K_d}{8 \hat{A}'(0)} \int_{y=0}^{\infty} \int_{\theta=0}^{\pi} \frac{y^{d/2-\kappa} \sin(\theta)^{d-2} r'(y) \hat{A}'''(0)}{\Big(r(y) + \sin^2\theta + \hat{A}'(0) \cos^2\theta \Big)^{1+\kappa}} \,. \tag{IV.36}$$

Notice that in Eqs. (IV.33) and (IV.36) the dimension d, as well as the nature of the noise κ are real parameters that can be chosen at will. Starting from the flow equations (IV.33) to (IV.36), one can easily retrieve the one-loop perturbative results obtained in [27], and the truncated results of [26, 217]; this is explained in App. D.2.

Notice that in the case of static noise, in $d = 2$ and with the Θ-regulator (IV.19), the flow equation (IV.33) can be rewritten in a much simpler form:

$$\partial_s \hat{A} = \eta_A \hat{A} + \frac{\eta_A - 4}{3} \hat{\phi} \hat{A}' - \frac{(1 + 3\hat{A}')\hat{A}''}{4(\hat{A}')^{3/2}} \tag{IV.37}$$

where we have omitted the argument of $\hat{A}$ and its s-dependence for convenience.

IV.2.3 A line of fixed points

We now study the properties of the flow equation (IV.33). Notice that at the fixed point (namely when $\hat{A}(\hat{\phi}) = \hat{A}^*(\hat{\phi})$ such that $\partial_s \hat{A}^*(\hat{\phi}) = 0$), the flow equation provides us with an iterative scheme for computing the derivatives $\hat{A}^{*(j)}(0) \equiv \hat{a}_j$ for all j. Indeed, at the fixed point and evaluated at $\hat{\phi} = 0$, the derivatives of Eq.(IV.33) can be rewritten as:

$$f_3(\eta_A^*, \hat{a}_3) = 0 \tag{IV.38a}$$
$$f_5(\eta_A^*, \hat{a}_3, \hat{a}_5) = 0 \tag{IV.38b}$$
$$f_7(\eta_A^*, \hat{a}_3, \hat{a}_5, \hat{a}_7) = 0 \tag{IV.38c}$$
$$\vdots$$

where the f_i are linear functions of their last argument. For instance, for the static noise in $d = 2$ and with the Θ-regulator (IV.19), the previous equations yield:

$$\hat{a}_3 = \frac{4}{3}(\eta_A^* - 1) \tag{IV.39a}$$
$$\hat{a}_5 = \frac{4}{3}(\eta_A^* - 1)(5\eta_A^* - 7) \tag{IV.39b}$$
$$\vdots$$

Therefore, provided that the Taylor expansion of $\hat{A}^*(\hat{\phi})$ around $\hat{\phi} = 0$ can be analytically continued on the whole real axis then a line of fixed points parametrized by the values of η_A^* exists, as claimed in [27]. On the other hand, notice that a truncation of $\hat{A}$ at any finite order will *not* yield a line of fixed points. For instance, writing $\hat{A} = \hat{\phi} + \hat{a}_3/3!\,\hat{\phi}^3$ means that the coefficient $\hat{a}_5$ vanishes and thus yields $\eta_A^* = 1$ or $\eta_A^* = 7/5$ according to Eq. (IV.39b). Instead of improving the accuracy of η_A^*, increasing the rank of the truncation will rather yield more and more (different) fixed points, with some stable and some unstable. The correct picture is therefore only accessible when the problem is tackled functionally, that is with the full function $\hat{A}(\hat{\phi})$.

Studying numerically these fixed points as well as their stability is nontrivial as we show in the following but simple physical arguments already allow us some comments: (i) the line of fixed points is upper-bounded in all dimensions because the roughness exponent α is positive, and we therefore deduce from Eq. (IV.31) that $\eta_A^* \leq 2(2\kappa - d)$; (ii) the anisotropy exponent ζ characterizes the ratio between the roughness exponent in the transverse direction, $\alpha_\perp \equiv \alpha$, and the roughness exponent in the parallel direction $\alpha_\parallel$ [26, 217]. In our anisotropic model, we expect this ratio to be larger than 1, i.e. $\zeta \geq 1$, which translates for η_A^* as [using Eq. (IV.32)]: $\eta_A^* \geq (2\kappa - d)/2$.

The first inequality is directly encoded in the flow equation since there exists no scaling solution (of the form $\hat{A}^*(\hat{\phi}) \sim \hat{\phi}^\gamma$ at large field) of the fixed point equation (IV.33) when η_A^* is such that $\alpha < 0$. The second inequality also has a signature in the flow equation, more precisely on the scaling form of the fixed point function $\hat{A}^*(\hat{\phi})$: indeed, studying Eq. (IV.33) at large fields, one finds that the fixed-point function should scale as:

$$\hat{A}^*(\hat{\phi}) \underset{\hat{\phi}\to\infty}{\sim} \hat{\phi}^\gamma \quad \text{with} \quad \gamma = \frac{3\eta_A^*}{4\kappa - 2d - \eta_A^*} \tag{IV.40}$$

and the inequality $\zeta \geq 1$ is equivalent to saying that $\hat{A}^*(\hat{\phi})$ is sub-linear at large field, which is not unphysical, but simply does not correspond to the model that we study where we expect nonlinearity and a power-law behaviour at large field. These considerations allow us to discard the isotropic noise ($\kappa = 1$) since in dimension $d = 2 = d_c^{\text{iso}}$ (the physical dimension of our problem), the only value of α that satisfies both inequalities is the trivial Edwards-Wilkinson exponent $\alpha = 0$. Within this erosion model, an isotropic noise can therefore not explain the observed landscapes roughness, see Fig. IV.6.

IV.2.4 Stability of the fixed points and numerical solution

IV.2.4.a Line of fixed points

We are now interested in confirming the existence of the line of fixed points found above from a Taylor expansion around $\hat{\phi} = 0$ and studying their stability. We focus on the case of a static noise, in $d = 2$ and with the Θ-regulator (IV.19), although the method we present remains true for a different noise, dimension or regulator. The flow equation in this case is given by Eq. (IV.37).

We thus solve numerically the fixed point equation: $\partial_s \hat{A}^*(\hat{\phi}) = 0$ together with the two boundary conditions $\hat{A}^*(0) = 0$ coming from the fact that $A(\phi)$ is odd and $\hat{A}^{*\prime}(0) = 1$ which defines $\eta_A(k)$. The numerical integration is performed on a finite grid $\hat{\phi} \in [0, \hat{\phi}_{\max}]$. The derivatives of $\hat{A}^*$ are then computed on this grid using the usual "five-point stencil" method. At the leftmost part of the grid ($\hat{\phi} = 0$), we use the fact that $\hat{A}^*(-\hat{\phi}) = -\hat{A}^*(\hat{\phi})$. On the rightmost part of the grid, we do not impose any boundary condition and the derivatives are computed using only points inside the grid. This simple scheme confirms the existence of a line of fixed points: for any given η_A^* (such that $\alpha \geq 0$) we find a fixed point function $\hat{A}^*$ solution of Eq. (IV.37). The precision of each of these solutions is refined when the size of the box $\hat{\phi}_{\max}$ or the number of discretization points is increased. In particular, the scaling at large field, Eq. (IV.40), is very well reproduced (at least when $\hat{\phi}_{\max}$ is large enough) which confirms the global existence of

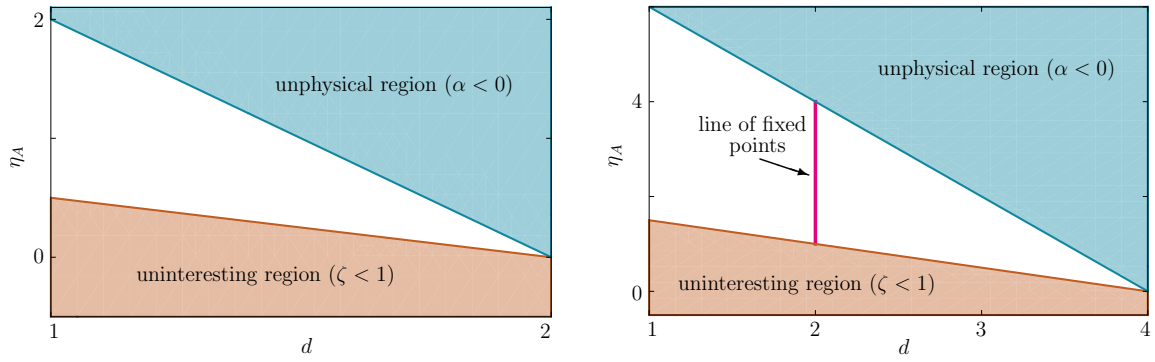

(a) isotropic noise (b) static noise

Figure IV.6 – *Critical exponent η_A for isotropic (a) and static (b) noises as a function of the physical space dimension d. Recall that for landscape erosion, the dimension of interest is $d = 2$. The upper colored region is unphysical($\alpha < 0$). Its lower boundary is the Edwards-Wilkinson fixed point with $\alpha = 0$. The bottom region is the physical yet uninteresting region for which the anisotropy exponent ζ is lower than 1. In this region, the function behaves like $\hat{A}_k^* \sim \hat{\phi}^\gamma$ as $\hat{\phi} \to \infty$, with $\gamma < 1$, and the system does not display the kind of nonlinearity we were looking for. The blank region in between is therefore the interesting region for our model, it ends up in a single point at the upper critical dimension, $d_c^{\text{iso}} = 2$ (a), or $d_c^{\text{stat}} = 4$ (b). In the case of the anisotropic noise (b), we see that there is an interval of fixed points (red line) in $d = 2$.*

the fixed points. Notice that an exact solution of the fixed point equation (IV.37) for $\eta_A^* = 0$ is available (see App. D.3) which allows for a check of our numerical solution in this particular case.

The stability of these fixed points is a subtler issue. Usually, the stability analysis is simply performed by linearizing the flow around the fixed point, that is, by computing the (discretized) stability matrix and evaluating its eigenvalues. The sign of these eigenvalues then provides the stability of each fixed point. An alternative path consists in perturbing the fixed point solution: $\hat{A}(\hat{\phi}) = \hat{A}^*(\hat{\phi}) + \varepsilon e^{\lambda s} g(\hat{\phi})$ (where s is the (negative) RG time and $\varepsilon \ll 1$ a small parameter) and then solving the differential equation for g while using a shooting method to find the eigenvalues [61, 62, 226]. In this model however, none of these methods yield reliable results since we do not observe any convergence of the eigenvalues when the size of the box or the number of discretization points is increased.

To tackle this issue, we perform a numerical integration of the flow equation (IV.37) starting with different initial conditions $\hat{A}^{\text{init}}(\hat{\phi})$. We use a Runge-Kutta scheme and the same discretization for the field $\hat{\phi}$ as explained above for the fixed point equation, up to a minor modification of the computation of the derivatives at the rightmost side of the grid, that we explain and detail in the following. For each different initial conditions, we observe that $\eta_A(s)$ reaches a different, fully attractive, fixed point (see Fig. IV.7). Changing the initial conditions, we can virtually obtain any value of η_A^* such that $\alpha \in [0, 1]$. We conclude from this numerical study that the whole interval of fixed points is stable, and we show in the following that the convergence to one of this fixed point is determined by the large-field behaviour of the initial condition. This crucial dependence over the initial condition signs the breakdown of universality for this model.

IV.2.4.b Numerical difficulties and solution

In the previous part, we gave the answer to the stability issue through the numerical integration of the flow, using slightly modified derivatives near $\hat{\phi}_{\max}$. Let us now detail why and how we modified the numerical scheme to obtain the correct results, and let us show some numerical

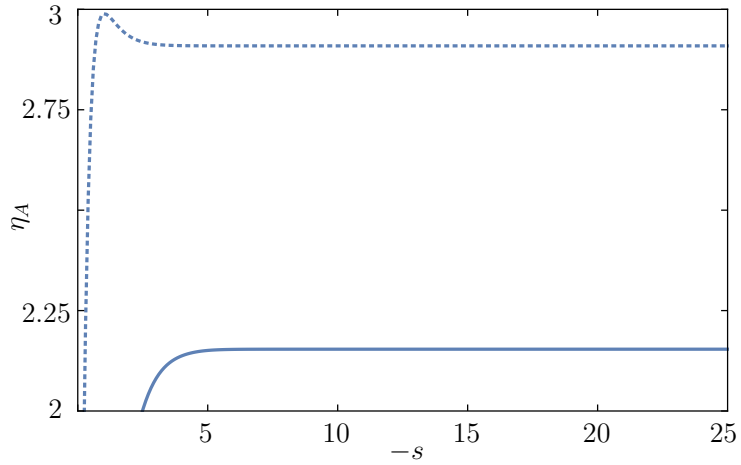

Figure IV.7 – *RG flows ($s = \log(k/\Lambda)$ is the RG time) of the exponent η_A for two different initial conditions, obtained by integrating numerically the flow equation (IV.37), with improved computation of the derivatives of $\hat{A}$ around $\hat{\phi}_{\max}$ (see main text). Dotted line: initial condition with a large field behaviour $\hat{A}^{\rm init}(\hat{\phi}) \sim \hat{\phi}^8$ for which we expect from Eq. (IV.40) an exponent $\eta_A^* \simeq 2.91$ which is indeed what is observed on the plateau. Solid line: same as above with $\hat{A}^{\rm init}(\hat{\phi}) \sim \hat{\phi}^{3.5}$ and $\eta_A^* \simeq 2.15$ which is observed on the plateau.*

subtleties that this model is hiding.

Usually (for instance in the case of the $O(N)$ model), the numerical integration of the flow is performed by discretizing the field $\hat{\phi}$ in a box $[0, \hat{\phi}_{\max}]$. The derivatives of the potential $\hat{A}(\hat{\phi})$ are then computed using a "five-point stencil" method, that is a finite-difference approximation that uses the point $\hat{\phi}_i$ and its four neighbours on the grid to compute the derivatives in $\hat{\phi}_i$. On the left-side of the discretization box (in $\hat{\phi} = 0$), we use the fact that $\hat{A}(-\hat{\phi}) = -\hat{A}(\hat{\phi})$ to compute the derivatives in the same way as they are computed in the bulk of the box. On the right-side of the box (in $\hat{\phi} = \hat{\phi}_{\max}$), the computation of the derivatives is made using only the points to the left of $\hat{\phi}_{\max}$ (inside the box). Using this rather simple scheme (and a Runge-Kutta routine), one usually obtains well-behaved flows (similar to those displayed in Chap. I). As requested for the consistency of the numerical scheme, these flows do not depend on the value of $\hat{\phi}_{\max}$, provided that $\hat{\phi}_{\max}$ is sufficiently large so that the large-field behaviour (the scaling regime) is captured.

The peculiarity of the flow equation (IV.33) of this model, which caused our difficulties, is a dramatic dependence of the flow on the value of $\hat{\phi}_{\max}$, even though this value is already large enough so that the scaling regime is captured (in particular, $\hat{\phi}_{\max}$ is large enough so that the large-field behaviour (IV.40) is obtained). More precisely, we will see that the numerical difficulties come from the inaccurate computation of the derivatives at the rightmost side of the grid.

Let us now detail the numerical issues and the results we obtain if we integrate the flow naively. For various initial conditions, we observe in fact that $\eta_A(s)$ reaches a first plateau (see Fig. IV.8) which depends on the initial condition, and which is left after a finite RG time. Then, the flows (regardless of the initial condition) reach a second plateau where they stay forever. Whereas the position of the first plateaus depends on the initial condition, the second plateau is the same for all initial conditions; this seems to indicate the existence of a unique fully attractive fixed point, for which $\eta_A^* \simeq 2.29$, whereas all the other fixed points (corresponding to the first plateaus) are unstable. However, increasing the size of the box $\hat{\phi}_{\max}$ increases the length of the first plateaus (see Fig. IV.8) and it seems that except for numerical stability issues[4], we could virtually extend these plateaus for an arbitrary long RG time by increasing $\hat{\phi}_{\max}$.

[4]The numerical difficulty comes in particular from the fact that at large field the power-law behaviour of $\hat{A}$ generates very large numbers that are difficult to manipulate numerically.

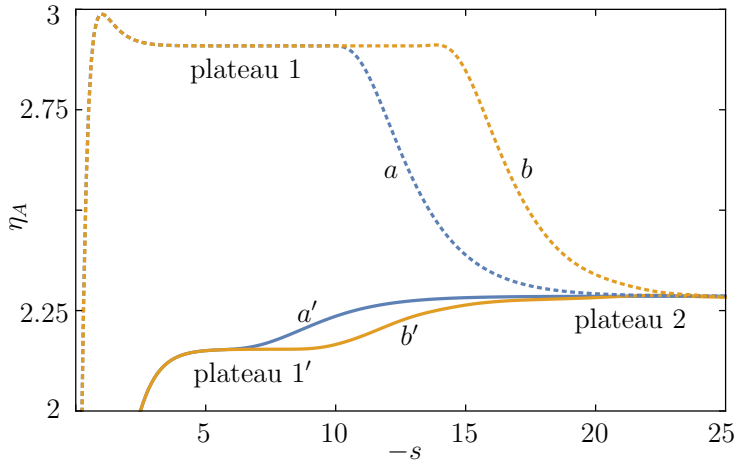

Figure IV.8 – *RG flows ($s = \log(k/\Lambda)$ is the RG time) of the exponent η_A for two different initial conditions, obtained by integrating numerically the flow equation (IV.37). Dotted lines a and b: same initial condition as for the dotted line in Fig IV.7, for which we expect from Eq. (IV.40) an exponent $\eta_A^* \simeq 2.91$ which is indeed what is observed on the plateau 1. Solid lines a' and b': same initial condition as for the solid line in Fig IV.7, for which we expect $\eta_A^* \simeq 2.15$ which is observed on the plateau $1'$. At large s, both flows end on the plateau 2. The curves b and b' are obtained by increasing the size of the box $\hat{\phi}_{\max}$, which increases the length of the plateaus 1 and $1'$.*

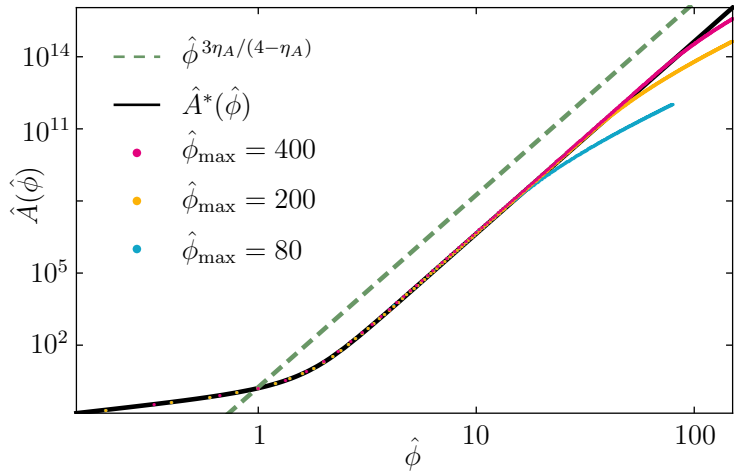

Figure IV.9 – *Solid line: fixed point solution $\hat{A}^*(\hat{\phi})$ of Eq. (IV.33) for $\eta_A = \eta_A^{\text{plateau}} \simeq 2.91$. Dashed line: asymptotic behaviour in $\hat{\phi}^{3\eta_A/(4-\eta_A)}$ with $\eta_A = \eta_A^{\text{plateau}}$. Dots: plateau solution $\hat{A}^{\text{plateau}}(\hat{\phi})$ for $\hat{\phi}_{\max} = 80$ (blue), 200 (yellow) and 400 (red) taken from the numerical solution of Eq. (IV.33) at RG time $s = -5$. The plateau solution converges toward the true fixed point solution as $\hat{\phi}_{\max}$ is increased.*

Furthermore, we notice that all the plateau functions $\hat{A}^{\text{plateau}}(\hat{\phi})$ match with the fixed point solutions found by integrating Eq. (IV.37) directly at the fixed point and for $\eta_A = \eta_A^{\text{plateau}}$ (see Fig. IV.9). This indicates that the first plateaus do correspond to fixed points of Eq. (IV.37), but they are (numerically) unstable. Figure IV.9 also highlights the fact that the scaling behaviour is reached, and yet the large-field behaviour continues to drive the flow. The inaccurate computation of the derivatives creates the drift that eventually leads the flow to leave plateaus 1 and $1'$ of Fig. IV.8.

A first idea to tame this dramatic dependence in the size of the box $\hat{\phi}_{\max}$ is therefore to compactify the field $\hat{\phi}$. Indeed, the numerical problems come from the fact that we can only reach finite $\hat{\phi}_{\max}$ and could therefore be solved if we had an infinite-size box. The aim of this

compactification is therefore to map the whole interval $\hat{\phi} \in [0, \infty[$ onto a compactified variable $\hat{y} \in [0, 1]$ that can be discretized. We also have to give a compactified form to the function $\hat{A}$, and we proceed in the following way. We define a first function $\hat{C}_1$ such that:

$$\hat{A}(\hat{\phi}) = \sqrt{\hat{x}}\, \hat{C}_1(\hat{x}) \,, \tag{IV.41}$$

with $\hat{x} = \hat{\phi}^2$ and such that we do not require $\hat{C}_1(\hat{x})$ to be even or odd. We then define a second function $\hat{C}_2$ as:

$$\hat{C}_2(\hat{x}) = \frac{\log(\hat{C}_1(\hat{x}))}{\log(2 + \hat{x})} \,, \tag{IV.42}$$

and such that $\hat{C}_2$ is finite when $\hat{x} \to \infty$. We finally define the compactified variable $\hat{y} = \hat{x}/(m + \hat{x})$, with $m > 0$ a free parameter and $\hat{y} \in [0, 1]$. This defines a last function $\hat{D}$, such that:

$$\hat{D}(\hat{y}) = \hat{C}_2 \left(\frac{m\hat{y}}{1 - \hat{y}} \right) . \tag{IV.43}$$

The whole interval $\hat{\phi} \in [0, \infty[$ is mapped onto $\hat{y} \in [0, 1]$ as requested, and the function $\hat{A}$ now has a compactified form: $\hat{D}(\hat{y}) \in [0, \gamma/2 - 1/2]$, where the value of $\hat{D}(\hat{y} = 1)$ comes from the scaling behaviour (IV.40) of $\hat{A}$ at large field.

In this compactified version, the flow of $\hat{D}$ provides us with a boundary condition at the rightmost side of the new box, $\hat{y} = 1$. The numerical integration of this compactified version reveals that each initial condition converges toward a different fixed point, that is, to a single plateau (reminiscent of the plateaus 1 and 1′ (see Fig. IV.8) in the noncompactified version), different for each initial condition. This qualitative feature is not modified when the number of discretization points is increased or when m is varied. This therefore highlights the fact that the previous stable fixed point, reached at large RG time and observed in Fig. IV.8 on the unique plateau 2, is a numerical artifact. However, the quantitative picture, that is, the precise positions of the plateaus analogous to the plateaus 1 and 1′ in Fig. IV.8, is modified when the number of discretization points is increased, which is of course problematic for the consistency of this numerical procedure. We have not been able to obtain fully converged results by increasing the number of points in the grid which indicates that the behaviour of $\hat{D}$ in the vicinity of $\hat{y} \simeq 1$ is not well captured by our numerical scheme in the compactified version.

The final remedy to these numerical hurdles is the following: going back to the noncompact formulation in terms of $\hat{\phi}$ and $\hat{A}$, we modify the way the derivatives of $\hat{A}$ are computed around $\hat{\phi}_{\max}$. Instead of using the "five-point stencil" method, we now fit the large-field region by a function $b\,\hat{\phi}^\gamma$ [where γ is given by Eq. (IV.40)], and compute the derivatives at the boundary using this fitting function. This fit prevents the numerical drift (coming from the inaccurate computation of the derivatives at $\hat{\phi}_{\max}$) that eventually leads the flows to leave the plateaus 1 or 1′, and confirms that the convergence at large RG time toward the fixed point $\eta_A^* \simeq 2.29$ is only a numerical artifact. Using this method, we get the correct picture that we presented in the first place, see Fig. IV.7. Notice that the beginning of the flow is not modified whatsoever between the "five-point stencil" method or the fitting method we used to cure the numerical issues. The fitting method only prevents the numerical drift that eventually leads the flows to leave their true fixed-point value.

Finally, let us emphasize the subtlety of these numerical issues: notice that the size of the grid is sufficiently large so that the function $\hat{A}$ is already in its scaling regime at large $\hat{\phi}$ when the first plateau 1 or 1′ is reached (see Fig. IV.9). However, the flow still leaves the plateau because the very last values of $\hat{A}$ are not computed correctly, meaning that the very last points of the grid drives the flow in the large (negative) RG-time regime. Since we are interested in the fixed point solutions, this is exactly the regime we are looking for. Even more dramatic, if one takes a too small value for $\hat{\phi}_{\max}$, the intermediary plateau 1 or 1′ may be missed, and the flow directly reaches the plateau 2, which is a numerical artifact. This could – erroneously – lead to the conclusion that there exists a single stable fixed point.

IV.3 Conclusion

In this chapter we have seen that despite the obvious scaling behaviour of natural erosional landscapes, characterized by a nonvanishing value of the roughness exponent, a clear understanding of the underlying mechanisms leading to this power-law behaviour is still missing.

Let us emphasize again some limitations coming from the data available for natural landscapes: the scale-invariant regime with a power-law behaviour and a clearly defined exponent α is often limited only to a few decades in log-scale, and sometimes even a single decade for the small length scale regime that has been the focus of this chapter. Second, the way the computation of the exponent α is carried out sometimes varies from one author to the other; although this method (box-counting, variograms, etc.) should not matter for an infinite-size system and an infinitely precise resolution, the finite range accessible in data may lead to discrepancies in the value of the exponents between different methods [213]. At least, when comparing different values of α from different datasets, one should make sure that they were computed using the same method [214].

These caveats being made, experimental measurements indicate a tendency to have large values of α at small length scale, and small values at large length scale. The large length scale seems to be rather well described by the KPZ equation, which predicts $\alpha \simeq 0.4$ in $d = 2$, while experimental data agrees on $0.30 \lesssim \alpha \lesssim 0.55$. On the other hand, the KPZ equation breaks down for larger length scale where $0.70 \lesssim \alpha \lesssim 0.85$ and an anisotropic model was proposed to explain this different regime. What we showed however in this chapter is that this model displays a line of attractive fixed points, leading to a continuous range for the values of α. In the light of this result, it is needless to say that the discussion about the origin of the scaling in erosional landscapes is not completely closed. However, some new elements are now available: anisotropy is indeed a relevant feature in this context, and should not be overlooked when proposing a model for erosion at short length scale. The nature of the noise is also a main characteristic and drastically modifies the scaling behaviour of the model, since it changes its universality class.[5] Moreover, we believe that the results presented in this chapter may give some insights for the wide dispersion of the values of the roughness exponent α when looking at different in situ measurements: if this model is valid (or at least the fact that an interval of fixed points may be generic in more realistic erosion models), then the dispersion of the roughness exponent is likely to be a signature of this line of fixed points, each of them corresponding to a different value of the exponent due to the difference in the initial conditions, i.e. differences in the geological context in the case of real landscapes.

Finally, we can hope that extra data coming either from laboratory experiments or different natural settings (Mars or other planets topography for instance) may help to elucidate the status of the small scale erosion, but the study in itself of this anisotropic model is rather surprising and interesting: although this model is quite simple (there is only one renormalized function), it yields a very nontrivial RG physics, functional in essence and displaying a line of fully attractive fixed points.

[5] As a remark, notice that within the NPRG formalism, the noise term could be studied for noninteger values of κ between 1 and 2, therefore giving rise to a smaller range of accessible α. The status of a noninteger value of κ is not mathematically clear, but one can see it as an interpolation between the two meaningful values $\kappa = 1$ (isotropic noise) and $\kappa = 2$ (static noise).

Conclusion

The guiding thread throughout this manuscript has been the study of critical phenomena in a nonequilibrium context. To understand these phenomena theoretically and beyond the mean-field level, the renormalization group is usually the most versatile tool, capable of tackling generic critical problems and capable of handling the large number of correlated degrees of freedom present at the critical point. In this work, the focus was set on the nonperturbative version of the renormalization group: following the idea of a systematic reduction of the number of correlated variables through coarse-graining, the nonperturbative renormalization group (NPRG) conducts this coarse-graining of the fluctuations with the help of a regulator function which plays a pivotal role in controlling the approximations and thus in the success of the NPRG techniques to handle critical systems.

We have therefore shown in this manuscript that an improvement of the regulator function is necessary in the nonequilibrium context in order to take care of the temporal part of the critical fluctuations, which are not regularized by the usual equilibrium regulator. Without this upgrade, the approximations made within the NPRG formalism are jeopardized since they crucially rely on the regulator function to be justified. The benchmark study we carried out on the kinetic Ising and $O(N)$ models of this frequency regulator showed indeed an improvement of the quantitative results for the computation of the dynamical exponent. The step forward would be to make a concrete use of this frequency regulator to study genuinely nonequilibrium models. Two paths have to be investigated: (i) does a frequency regulator systematically improve the quantitative results (for instance the values of the computed critical exponents) obtained up to now for nonequilibrium systems? (ii) Can a frequency regulator be used to cure inconclusive attempts of the NPRG in some models such as the Kardar–Parisi–Zhang (KPZ) equation in $d > 2$, the parity conserving generalized voter (PCGV) and the pair-contact process with diffusion (PCPD) universality classes, etc? Finally, we have seen that similarly to the equilibrium situation, many frequency regulators are candidates. Finding some criteria to discriminate the most suitable one for a given model and within a given approximation scheme should also be investigated in more details.

In the case of reaction-diffusion processes, we have seen in Chap. II of this manuscript that some of the difficulties that arise in this context can be cured by a nonperturbative approach as well. Indeed, we recall that for reaction-diffusion processes, a microscopic Langevin equation can be derived from the microscopic description of the system stated in terms of a master equation. The variable of this Langevin equation is therefore not coarse-grained (as it is usually the case for Langevin equations), but describes the exact dynamics. This variable is not the density itself (which evolution is described by the master equation), but an auxiliary field[6] whose moments are simply linked to those of the density. In this context, a longstanding issue was the appearance of imaginary-noise Langevin equations whose numerical and theoretical handling was facing major difficulties. This paradoxical situation remained and no definitive statement about it was made: these complex Langevin equations were simply overlooked because intractable. In this manuscript, I have shown that this situation can be resolved: the Langevin equations that have been derived are simply not correct and their derivation relied on

[6] Abusively called "density field" in the literature.

an erroneous argument, although valid at all orders of the perturbative expansion.

A more rigorous approach, nonperturbative in spirit and relying on contour deformations shows that exact, real Langevin equations can in fact be derived. The real Langevin variable introduced in this formalism is clearly not the same auxiliary field as in the previous approach, but it can still be linked to the initial reaction-diffusion process via a duality relation. These real Langevin equations overcome the hurdles of complex stochastic variables and can in particular be solved numerically: in fact, such a dual Langevin equation had already been *intuited* in the literature [152], providing results for the PCGV universality class. The path forward is now to further investigate reaction-diffusion processes near their critical point using these well-behaved Langevin equations. A major step forward would be made if this exact derivation of real Langevin equations could be generalized to multi-species reaction-diffusion processes. However, and despite our efforts, this generalization remains elusive.

Finally, the last part of this manuscript was dedicated to the study of the erosion of landscapes. More precisely, erosional landscapes are known to present a scaling behaviour, characterized by a power-law behaviour of the height-height correlation function. The scaling exponent of this correlation function is called the roughness exponent α and is found to match the one of the KPZ equation for erosion at large length scale. For smaller length scale, however, the roughness exponent is much larger and does not agree with the KPZ prediction. This mismatch urged for the introduction of a different model to capture the physics at small length scale. It was done by the suggestion of an anisotropic erosion model that takes care of the intrinsic anisotropy (the slope of the mountain) at these scales. The initial study of this model by the perturbative renormalization group however yielded false predictions. In this manuscript, I have applied the NPRG techniques to tackle this model, and the results are quite surprising since this model happens to display a line of fixed points. This line of fixed points is consistent with the generic scaling observed in natural landscapes, but means also nonuniversality: each initial condition (i.e. each soil particularities, climate properties, etc.) leads to a different topography and roughness exponent. Although perturbing, this scenario could explain the large variability of the roughness exponent observed in experimental data.

Let us however temper this statement by emphasizing the fact that the data available at small length scale is limited: only one decade in log-scale is accessible to support the existence of this scaling. In any case, the theoretical study of this model already shows that generic scaling and nonuniversality can arise from a rather simple nonequilibrium model and such results are probably worth noticing in themselves.

Furthermore, although this last chapter was focused on the erosion of landscapes and on the topography itself, continuum models have also been devised and applied to river landscapes [227, 228]. Numerical studies stemming from these models have been carried out but they still lack a theoretical study. The NPRG framework could be applied successfully to these models.

The perspectives in the physics of nonequilibrium critical phenomena are countless. In addition to the further investigations suggested above, many more open problems exist that could be treated using nonperturbative approaches.

For instance, in the following of [53], the NPRG techniques can be adapted to handle initial conditions and capture the universal scaling associated to quenches to the critical point. This study of the quench dynamics was performed within a derivative expansion approximation in [53], and it is reasonable to believe that further results could be obtained for such quenches using the BMW approximation, that allows for the computation of momentum/frequency dependent quantities. So far, the BMW approximation has been very sparsely used in a nonequilibrium setting and implementing it on a rather simple model is surely valuable.

Many other nonequilibrium models could use a NPRG approach: for instance, a chemotactic model where cells diffuse, die, divide and interact at long-range through concentration fields

has recently been studied by Gelimson *et al.* [229] using a perturbative renormalization group approach. However, they used an approximate Langevin equation to describe the birth and death process, which breaks down at low concentrations where an interesting behaviour could arise. Using rather an exact Langevin equation that we have derived in this manuscript could yield a different picture. Furthermore, they reported the existence of a nonperturbative fixed point that was out-of-reach of their approach and could therefore be studied using NPRG techniques.

Another challenging domain in nowadays nonequilibrium physics is the transition to collective motion: many models exist in the literature to describe and understand the "flocking" behaviour of animals (birds, fishes, bacteria...), the most famous one being probably the Vicsek model [230], which captures a rich dynamic behaviour with minimal ingredients. However, despite intensive numerical and experimental works on these models, a theoretical description of the associated phase transition is still lacking. An alternative model was proposed by Toner and Tu [231] that is more suited for field-theoretical approaches. It has been studied through the perturbative renormalization group, but an alternative nonperturbative approach could there again prove useful.

Appendix A

Scale invariance, universality and renormalization group

A.1 Probability distribution of the effective potential

In this appendix, we recall how the thermodynamic potential $U(\sigma)$ is directly related to the probability distribution of the mean spin σ. Following [31], we consider the Ising model on a d-dimensional cubic lattice and define the mean spin $\sigma \equiv L^{-d}\sum_j S_j$, with L the length of the lattice. The mean spin is a stochastic variable (whose mean $\langle\sigma\rangle = M$ is the magnetization) and we would like to compute its probability distribution $p(\sigma)$.

Since $\left\langle \mathrm{e}^{-iq\sum_j S_j} \right\rangle$ is the characteristic function of the random variable $L^d\sum_j S_j$, the probability distribution of the mean spin $p(\sigma)$ is given by its Fourier transform as:

$$p(\sigma) = L^d \int_q \mathrm{e}^{iqL^d\sigma} \left\langle \mathrm{e}^{-iq\sum_j S_j} \right\rangle . \tag{A.1}$$

Moreover, the characteristic function $\left\langle \mathrm{e}^{-iq\sum_j S_j} \right\rangle$ has in fact a simple relation to the analytic continuation of the partition function in the presence of an imaginary external field $h = -iq$:

$$\left\langle \mathrm{e}^{-iq\sum_j S_j} \right\rangle = \frac{\mathcal{Z}[h=-iq]}{\mathcal{Z}[h=0]} . \tag{A.2}$$

Using this equality and defining $W[h] \equiv \log \mathcal{Z}[h]$, we can rewrite the probability distribution $p(\sigma)$ as:

$$p(\sigma) = \frac{L^d}{\mathcal{Z}[h=0]} \int_q \mathrm{e}^{iqL^d\sigma + W[-iq]} \tag{A.3}$$

$$= \frac{L^d}{\mathcal{Z}[h=0]} \int_q \mathrm{e}^{L^d(iq\sigma + w[-iq])} \tag{A.4}$$

where we have furthermore defined $w[h] = W[h]/L^d$. In the thermodynamics limit, we consider $L \to \infty$, and the above integral over q can be computed by the steepest-descent method, the saddle point q_0 being given by the implicit equation:

$$\sigma = W'[-iq_0] , \tag{A.5}$$

which yields for the probability distribution:

$$p(\sigma) = \frac{1}{\mathcal{Z}[h=0]} \sqrt{\frac{L^d}{2\pi w''[-iq_0]}}\, \mathrm{e}^{L^d(iq_0\sigma + w[-iq_0])} . \tag{A.6}$$

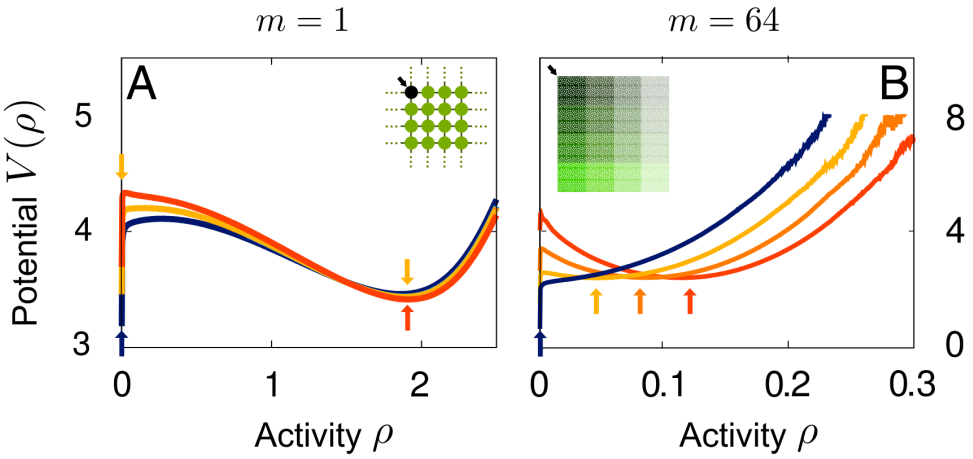

Figure A.1 – *Figure extracted from [232] of the effective potential $V(\rho)$ for the averaged activity ρ measured in cells of linear size m in a square lattice of size $N = 256\times256$. The potential V is defined for each value of m as $V = -\log p(\rho_m)$ where $p(\rho_m)$ is the steady-state probability distribution of the activity ρ averaged in boxes of linear size m, with $m = 1$* ***(left)*** *or $m = 64$* ***(right)****. Colors represent different values of a parameter of their microscopic system which is not crucial here. On the other hand, we see that as the coarse-graining scale m is increased, the shape of the effective potential V changes from its microscopic shape ($m = 1$) – which is typical of a first-order phase transition – to a shape typical of a second-order transition at larger coarse-graining scale ($m = 64$).*

Finally, we define the Gibbs free energy $\Gamma[\sigma_h]$ as the Legendre transform of $\Gamma[\sigma_h] + W[h] = h\sigma_h$ and $\sigma_h = \partial W[h]/\partial h$. The thermodynamics potential $U(\sigma_h)$ is the Gibbs free energy per unit volume and therefore yields:

$$p(\sigma) = \frac{\sqrt{L^d U''(\sigma)/2\pi}}{\mathcal{Z}[h=0]}\, \mathrm{e}^{-L^d U(\sigma)}\,. \tag{A.7}$$

This result is however no longer valid at criticality since the different thermodynamic functions W and Γ are no longer analytic.

However, in the NPRG context, the introduction of the scale k by means of the regulator renders Γ_k and U_k analytic. Since this scale k can be seen as a coarse-graining scale of the model, the potential U_k is associated to the probability distribution of a system of size k^{-1}. When $k = \Lambda$ the inverse lattice-spacing, the system is not coarse-grained and the average potential $U_{k=\Lambda}$ is the mean-field potential, while its minimum κ_Λ is the mean-field magnetization[1]. When $k \to 0$, $U_k(\psi)$ is the precursor of the thermodynamic potential $U = U_{k=0}$ and we can follow the evolution of the probability distribution along the renormalization flow.

Notice that this idea of following the evolution of the potential with the coarse-graining scale has been investigated recently via numerical simulations in [232]. In Fig. A.1, we see how the microscopic potential V is modified by the averaging over boxes of size m: Whereas the system is, at the microscopic level, described by the potential of a first-order phase transition, at the coarse-grained level one observes that it shifts to a second-order type potential.

[1] To be consistent with our notation, κ_k is the minimum of $U_k(\rho)$ and the precursor of the magnetization is therefore $\sqrt{2\kappa_k}$.

A.2 Dimensionless flow equations for the $O(2)$ model.

We give here the dimensionless flow equation for the $O(2)$ model at the LPA' and with the potential $\hat{U}(\hat{\rho})$ expanded at the third order in $\hat{\rho}$. They read:

$$\partial_s \kappa = (2-d-\eta_s)\kappa + \frac{8v_d\,(2+d-\eta_s)}{d(2+d)}\,\frac{2\kappa^2u^3+2\kappa u^2+2u+\kappa u_3}{u(2\kappa u+1)^2} \tag{A.8a}$$

$$\partial_s u = (d-4+2\eta_s)u + \frac{8v_d\,(2+d-\eta_s)}{d(2+d)}\times \frac{8\kappa^3u^6+12\kappa^2u^5+6\kappa u^4+10u^3+10\kappa u^2u_3+uu_3\left(6\kappa^2u_3-1\right)+\kappa u_3^2}{u(2\kappa u+1)^3} \tag{A.8b}$$

$$\begin{aligned}\partial_s u_3 = (2d-6+3\eta_s)u_3 - \frac{48v_d\,(2+d-\eta_s)}{d(2+d)}\,\frac{1}{(2\kappa u+1)^4}\times \\ \Big(14u^3+4\kappa^3\left(4u^6-4u^4u_3+u_3^3\right)+8\kappa^4u^5\left(u^2-u_3\right) \\ +4\kappa^2u\left(3u^4-3u^2u_3+2u_3^2\right)+\kappa\left(4u^4+8u^2u_3-5u_3^2\right)-8uu_3\Big)\end{aligned} \tag{A.8c}$$

where d is the spatial dimension, $v_d^{-1} = 2^{d+1}\pi^{d/2}\Gamma(d/2)$ is the volume factor coming from the momentum integration and we have dropped hats above the dimensionless variables to alleviate the notation.

Appendix B

Out-of-equilibrium phase transitions

B.1 Stochastic differential equations

Change of variables and Itō formula

Changes of variables in a Langevin equation are subject to rules that differ from usual calculus. Assuming we have the following stochastic Itō equation:

$$\mathrm{d}X_t = \mu_t \,\mathrm{d}t + \sigma_t \,\mathrm{d}B_t \tag{B.1}$$

with B_t a Brownian motion. Then the variable $Y_t = g(t, X_t)$ verifies the following equation:

$$\mathrm{d}Y_t = \left(\frac{\partial g}{\partial t} + \frac{\partial g}{\partial X_t}\mu_t + \frac{1}{2}\frac{\partial^2 g}{\partial X_t^2}\sigma_t^2 \right) \mathrm{d}t + \frac{\partial g}{\partial X_t}\sigma_t \,\mathrm{d}B_t \,. \tag{B.2}$$

This rule for changing variables is known as the Itō formula [184].

B.2 From the probability-generating function to the Poisson representation

In the following we will need the following formulas:

$$\partial_z^n \mathrm{e}^{y(z-1)} = y^n \mathrm{e}^{y(z-1)} \tag{B.3}$$

$$z^p \mathrm{e}^{y(z-1)} = (\partial_y + 1)^p \mathrm{e}^{y(z-1)} \tag{B.4}$$

The first formula is straightforward, while the second is simply proven by recurrence: if $p = 1$, one has the following relation:

$$(\partial_y + 1)\mathrm{e}^{y(z-1)} = \left[(z-1)+1\right] \mathrm{e}^{y(z-1)} = z\mathrm{e}^{y(z-1)} \tag{B.5}$$

then for $p > 1$:

$$(\partial_y + 1)^p \mathrm{e}^{y(z-1)} = (\partial_y + 1)^{p-1} z\mathrm{e}^{y(z-1)} = z^p \mathrm{e}^{y(z-1)} \tag{B.6}$$

which terminates the proof. Consequently, an operator $\mathcal{L}(z, \partial_z)$ acting on $\mathrm{e}^{y(z-1)}$ can be rewritten as an operator $\tilde{\mathcal{L}}(y, \partial_y)$ such that:

$$\mathcal{L}(z, \partial_z) \,\mathrm{e}^{y(z-1)} = \tilde{\mathcal{L}}(\partial_y + 1, y) \,\mathrm{e}^{y(z-1)} \tag{B.7}$$

with

$$\tilde{\mathcal{L}}(\partial_y + 1, y)\cdot = yA(\partial_y + 1)\cdot + y^2 B(\partial_y + 1)\cdot \tag{B.8}$$

B.3 Probability-generating function: the spatially-extended case

In the field-theoretic formulation, we showed in the previous section that the spatially-extended case is handled by a slight deformation of the contours in order to take care of the sub-leading term coming from diffusion. We describe here how it is treated in the probability-generating function formalism.

To take into account the spatial structure in the reaction-diffusion process, the system is now described as a d-dimensional lattice indexed by an integer i. Each site has a number $N_i(t)$ of particles at time t. A hopping reaction between nearest neighbours is introduced to account for diffusion:

$$A\emptyset \overset{D}{\leftrightarrow} \emptyset A \tag{B.9}$$

where D is the diffusion coefficient. The state of the system is now described by $P_{\{n\}}(t) \equiv \mathrm{Prob}(N_1(t) = n_1, \ldots,$ whose time-evolution is still described by the master equation with the additional diffusion term:

$$\frac{D}{h^2} \sum_{<i,j>} \left[(n_i + 1)P_{\ldots,n_i-1,n_j+1,\ldots} - n_i P_{\{n\}}\right] \tag{B.10}$$

where $< i, j >$ means that sites i and j are nearest neighbours, and h is the lattice spacing. In this context, the probability-generating function for a spatially-extended system now reads:

$$G(z_1, \ldots, z_n, t) = \left\langle z_1^{N_1(t)} \cdots z_n^{N_m(t)} \right\rangle_{\mathrm{RD}} \tag{B.11}$$

and is subject to the Fokker-Planck equation:

$$\partial_t G = \frac{D}{h^2} \sum_{<i,j>} (z_j - z_i)\partial_{z_i} G + \sum_i A(z_i)\partial_{z_i} G + \sum_i B(z_i)\partial_{z_i}^2 G \tag{B.12}$$

where the functions A and B are defined in the main text. One notices that the term coming from the diffusion defines a discrete Laplacian over $z_{\{n\}}$. After taking the continuous limit in space [$z_{\{n\}} \to z(x)$], it therefore yields the following Langevin equation for the spatialized stochastic variable $Z \equiv Z(x, t)$:

$$\partial_t Z = D\nabla^2 Z + A(Z) + \sqrt{2B(Z)}\,\zeta \tag{B.13}$$

where $\zeta \equiv \zeta(x, t)$ is a Gaussian white noise.

Appendix C

Frequencies regulator

C.1 Flow equations for the model A and the kinetic $O(N)$ model

C.1.1 Model A

One can show for the model A that the dynamical parts of the dimensionless renormalization functions read[1]:

$$\partial_s \hat{U}'|_{\text{dyn}} = -v_d \int_y y^{d/2} \frac{fg}{h^2} \tag{C.1}$$

$$\begin{aligned}\partial_s \hat{Z}|_{\text{dyn}} = 2v_d \int_y y^{d/2} \frac{g}{h^2} \Bigg[& \frac{2\hat{\rho} f^2}{h^2} \left(\frac{4}{d} \frac{y h'^2}{h} - h' - \frac{2}{d} y h'' \right) \\ & + 4\hat{\rho} \hat{Z}' \frac{f}{h} \left(1 - \frac{2}{d} \frac{y h'}{h} \right) + \frac{2\hat{\rho}}{d} (\hat{Z}')^2 \frac{y}{h} - \frac{\hat{Z}'}{2} - \hat{\rho} \hat{Z}'' \Bigg]\end{aligned} \tag{C.2}$$

$$\partial_s \hat{X}|_{\text{dyn}} = v_d \int_y y^{d/2} \frac{g}{h^2} \left(8\hat{\rho} \hat{X}' \frac{f}{h} - 3 \frac{f^2}{h^2} \hat{\rho} \hat{X} - \hat{X}' - 2\hat{\rho} \hat{X}'' \right) \tag{C.3}$$

where $\partial_t \equiv k\partial_k$, $v_d^{-1} = 2^{d+1} \pi^{d/2} \Gamma(d/2)$, $\hat{\rho} = \hat{\psi}^2/2$, $h(y, \hat{\rho}) = y(\hat{Z}(\hat{\rho}) + r(y)) + \hat{U}'(\hat{\rho}) + 2\hat{\rho}\hat{U}''(\hat{\rho})$, $f(y, \hat{\rho}) = y\hat{Z}'(\hat{\rho}) + 3\hat{U}''(\hat{\rho}) + 2\hat{\rho}\hat{U}'''(\hat{\rho})$ and $g(y) = -\eta_s r(y) - 2y r'(y)$. One notices immediately that $\hat{X}$ does not contribute to the flows of $\hat{U}'$ and $\hat{Z}$, that are the standard flows of the static Ising model. This is due to the relaxational nature of the model A.

C.1.2 Kinetic $O(N)$ model

For the kinetic $O(N)$ model, for simplicity we only consider the Local Potential Approximation prime (LPA') of the Derivative Expansion, which means we only retain U_k' as a function of ρ, and Z_k and X_k are mere numbers. While the flow of the dimensional part of the dimensionless renormalization functions is still given by Eqs. (III.50)-(III.52), the flow of the dynamical part is given this time by the following equations:

$$\partial_s \hat{U}'|_{\text{dyn}} = -v_d \int_y y^{d/2} g \left(\frac{3\hat{U}'' + 2\hat{\rho}\hat{U}^{(3)}}{h_L^2} + \frac{(N-1)\hat{U}''}{h_T^2} \right) \tag{C.4}$$

$$\partial_s \hat{Z}|_{\text{dyn}} = -8v_d \int_y y^{d/2} g \hat{\rho} \hat{U}'' \left(\frac{h_y}{h_L^2 h_T^2} + \frac{2y h_{yy}}{d h_L^2 h_T^2} - \frac{2y h_y^2}{d h_L^2 h_T^2} \left(\frac{1}{h_T} + \frac{1}{h_L} \right) \right) \Bigg|_{\hat{\rho}=\hat{\rho}_{0,k}} \tag{C.5}$$

$$\partial_s \hat{X}|_{\text{dyn}} = -4v_d \int_y y^{d/2} g \hat{\rho} \hat{U}''^2 \left(\frac{h_L^2 + 4h_L h_T + h_T^2}{h_L^2 h_T^2 (h_L + h_T)^2} \right) \Bigg|_{\hat{\rho}=\hat{\rho}_{0,k}} \tag{C.6}$$

[1] Notice that our equations differ from those of reference [91] that involve a misprint.

where $g(y) = -\eta_s r(y) - 2yr'(y)$, $h_L = y(r(y)+1) + \hat{U}' + 2\hat{\rho}\hat{U}''$, $h_T = y(r(y)+1) + \hat{U}'$, $h_y = 1 + r(y) + r'(y)$ and $h_{yy} = 2r'(y) + yr''(y)$. Notice that since we are working at the LPA', the flow equations for $\hat{Z}$ and $\hat{X}$ are evaluated at the (running) minimum of the potential $\rho_{0,k}$. Once again, $\hat{X}$ does not contribute to the flows of $\hat{U}'$ and $\hat{Z}$, that are the standard flows of the equilibrium $O(N)$ model at the LPA'.

C.2 Principle of minimal sensitivity

If we were able to solve the Wetterich equation (I.43) exactly, the precise choice of the regulator would be meaningless. Indeed, if no approximations are performed, the regulator has no physical meaning and does not influence the behaviour of the physical system when the RG scale k goes to 0, since the regulator is designed to vanish at this scale. However, the whole point of introducing a regulator is to perform controlled approximations that allows for finding approximate solutions of the Wetterich equation. These solutions, of course, depend on the approximation itself, but within a given approximation scheme (in this manuscript, usually the derivative expansion), the approximate solution also depends on the specific choice of the regulator.

For a given approximation scheme, one would therefore like to be able to choose the "best" regulator. This is a difficult task and it is often necessary to try out different types of regulators and pick out the one which provides the more satisfactory solutions.

For a given shape of regulator, for instance an exponential regulator:

$$R_k(q) = \frac{a\, q^2}{\mathrm{e}^{q^2/k^2} - 1} \tag{C.7}$$

we can add the non-physical parameter a, and ask for which value of a the solution of the Wetterich equation has the most physical meaning. An answer to this question is given by the principle of minimal sensitivity (PMS) [104], which states that if an approximant $\mathcal{A}$ depends on an unphysical parameter a, then the value of this parameter should be chosen so as to minimize the sensitivity of $\mathcal{A}$ with respect to a, that is one should choose $a = a_{\text{PMS}}$, such that:

$$\frac{\partial \mathcal{A}}{\partial a}|_{a=a_{\text{PMS}}} = 0\,. \tag{C.8}$$

The reason for this is that in the space of the unphysical parameters, the exact result is independent of these parameters, and is therefore constant. The most reliable approximate result is thus likely to lie where the dependence on the unphysical parameter is the flattest. See Stevenson's paper [104] for a more detailed discussion on this topic. See also [67, 73] for an extensive study of the PMS within the NPRG context.

C.3 Relation between R_1 and R_2

We show here that the invariance of the action under transformation (III.26) enforces constraints on R_1 and R_2. Let us define

$$\Delta\mathcal{S}_1 = \int_{\boldsymbol{x},\boldsymbol{x'}} \tilde{\phi}(x,t) R_1(x'-x, t'-t) \phi(x',t')\,, \tag{C.9}$$

$$\Delta\mathcal{S}_2 = \int_{\boldsymbol{x},\boldsymbol{x'}} \tilde{\phi}(x,t) R_2(x'-x, t'-t') \tilde{\phi}(x',t')\,, \tag{C.10}$$

in which, for notational convenience, we drop in the following the spatial dependence in the different terms. After transforming the fields by (III.26), $\Delta\mathcal{S}_i[\phi,\tilde{\phi}]$ become $\Delta\mathcal{S}_i[\phi',\tilde{\phi}'] \equiv \Delta\mathcal{S}'_i[\phi,\tilde{\phi}]$

which read:

$$\Delta\mathcal{S}'_1 = \int_{t,t'} \tilde{\phi}(t) R_1(t-t')\phi(t') - \int_{t,t'} \dot{\phi}(t) R_1(t'-t)\phi(t')\,, \tag{C.11}$$

$$\begin{aligned}\Delta\mathcal{S}'_2 = &\int_{t,t'} \tilde{\phi}(t) R_2(-t'+t)\tilde{\phi}(t') - \int_{t,t'} \tilde{\phi}(t)\left[R_2(-t'+t)\right.\\ &\left.+R_2(t'-t)\right]\dot{\phi}(t') + \int_{t,t'} \dot{\phi}(t) R_2(-t'+t)\dot{\phi}(t')\,.\end{aligned} \tag{C.12}$$

In $\Delta\mathcal{S}'_2$ we notice that the first term gives back $\Delta\mathcal{S}_2$, and the third term is symmetric in t and t' and can be rewritten as:

$$\frac{1}{2}\int_{t,t'} \dot{\phi}(t)\left(R_2(-t'+t) + R_2(t'-t)\right)\dot{\phi}(t') \tag{C.13}$$

The invariance of the action under transformation (III.26) yields the equality $\Delta\mathcal{S}'_1 + \Delta\mathcal{S}'_2 = \Delta\mathcal{S}_1 + \Delta\mathcal{S}_2$, that reads:

$$\begin{aligned}&\int_{t,t'} \tilde{\phi}(t)\left(R_1(-t'+t) + \dot{R}_2(-t'+t) - \dot{R}_2(t'-t) - R_1(t'-t)\right)\phi(t')\\ &+\int_{t,t'} \dot{\phi}(t)\left(-R_1(-t'+t) \quad + \frac{1}{2}\left(\dot{R}_2(-t'+t) - \dot{R}_2(t'-t)\right)\right)\phi(t') = 0\,.\end{aligned} \tag{C.14}$$

which should be valid for all fields ϕ and $\tilde{\phi}$. In order to deduce an identity on the integrand of (C.14), we first need to integrate it by parts and symmetrize it with respect to t and t'. This yields two equations that are in fact redundant, and hence we deduce the following sufficient condition for R_1 and R_2:

$$R_1(t) - R_1(-t) + \dot{R}_2(t) - \dot{R}_2(-t) = 0 \tag{C.15}$$

C.4 Causality and Kramers-Kronig theorem

The linear response function $\chi(t,t')$ is defined to be the variation of the mean value of the field ϕ at time t caused by the variation of the external source J coupled to ϕ at time t'. Mathematically, it reads:

$$\chi(t,t') = \frac{\langle\delta\phi(t)\rangle}{\delta J(t')}|_{J\to 0}\,. \tag{C.16}$$

Because of time translation invariance, it is a function of $t-t'$ only and we may write $\chi(t,t') = \chi(t-t')$. In the MSRDJ formalism (also called response-function formalism), the response-function reads:

$$\chi(t,t') = \left\langle \tilde{\phi}(t')\phi(t)\right\rangle\,, \tag{C.17}$$

and its Fourier transform $\chi(\omega)$ is simply given by the upper-right element of the propagator matrix G_k:

$$\chi(\omega) = \frac{1}{P(q^2,-\omega)} = \frac{1}{h(q^2,-\omega) - i\omega X_k}\,, \tag{C.18}$$

with $h(q^2,\omega) = Z_k(\rho)q^2 + R_{1,k}(q^2,\omega) + U'_k(\rho) + 2\rho U''_k(\rho)$. Causality imposes $\chi(t<0) = 0$, which means that $\chi(\omega)$ must be an analytic function of ω in the upper-part of the complex plane. In other words, the poles of $\chi(\omega)$ must have a negative imaginary part.

Let us add that the Kramers-Kronig theorem provides an alternative translation of the causality of the response function. Indeed, the fact that $\chi(t<0)=0$ yields the following equalities for the Fourier transform $\chi(\omega)$, called the Kramers-Kronig relations [7]:

$$\mathrm{Re}(\chi(\omega)) = \frac{1}{\pi}\mathcal{P}\int \mathrm{d}\omega' \, \frac{\mathrm{Im}(\chi(\omega'))}{\omega'-\omega} \tag{C.19}$$

$$\mathrm{Im}(\chi(\omega)) = -\frac{1}{\pi}\mathcal{P}\int \mathrm{d}\omega' \, \frac{\mathrm{Re}(\chi(\omega'))}{\omega'-\omega} \tag{C.20}$$

where $\mathcal{P}$ denotes the Cauchy principal value of the integral.

Appendix D

Landscape erosion

D.1 Derivation of the flow equations

In this Appendix we derive the flow of the non-linear function $A_k(\phi)$, defined in Eq. (IV.29). Having in mind this definition, we use the Wetterich equation (I.43) to deduce the following equality:

$$\partial_k \mathrm{FT}\left(\frac{\delta\Gamma_k}{\delta\tilde{\phi}(z)}\right)(\boldsymbol{p}) = -\frac{1}{2}\,\mathrm{Tr}\int_{\boldsymbol{k}_1,\boldsymbol{q}_1,\boldsymbol{q}_2} \partial_k\mathcal{R}_k(\boldsymbol{k}_1)\cdot G_k(-\boldsymbol{k}_1,-\boldsymbol{q}_1;\phi)\cdot\Gamma^{(3)}_{k,\tilde{\psi}}(\boldsymbol{q}_1,\boldsymbol{q}_2,\boldsymbol{p})\cdot G_k(-\boldsymbol{q}_2,\boldsymbol{k}_1;\phi) \tag{D.1}$$

where $\int_{\boldsymbol{q}} \equiv 1/(2\pi)^{d+1}\int_{q,\omega}\mathrm{d}^{d-1}q_\perp\,\mathrm{d}q_\parallel\,\mathrm{d}\omega$, and $\Gamma^{(3)}_{k,\tilde{\psi}} \equiv \delta\Gamma^{(2)}_k/\delta\tilde{\psi}$ reads:

$$\Gamma^{(3)}_{k,\tilde{\psi}}(\boldsymbol{q}_1,\boldsymbol{q}_2,\boldsymbol{p}) = \begin{pmatrix} p_\parallel^2\,\mathrm{TF}(A_k''(\phi))(\boldsymbol{q}_1+\boldsymbol{q}_2+\boldsymbol{p}) & 0 \\ 0 & 0 \end{pmatrix} \tag{D.2}$$

Notice that we keep the same name for a function and its Fourier transform, such that a function $f(\boldsymbol{q})$ has to be understood as the Fourier transform of $f(\boldsymbol{x})$, and we recall the convention: $f(\boldsymbol{q}) = \int_{\boldsymbol{x}} f(\boldsymbol{x})\mathrm{e}^{-i(qx-\omega t)}$.

In order to get the flow of A_k, one now has to take the derivative of the previous expression with respect to $p_\parallel^2$, and then to evaluate it at $p=0$ and uniform field ϕ. Since $\Gamma^{(3)}_k(\boldsymbol{q}_1,\boldsymbol{q}_2,\boldsymbol{p}) \propto p_\parallel^2$, the whole expression is proportional to $p_\parallel^2$ and the only non-vanishing term after the derivation and the evaluation at zero external momentum ($\boldsymbol{p}=0$) is the one obtained when deriving $\Gamma^{(3)}_k(\boldsymbol{q}_1,\boldsymbol{q}_2,\boldsymbol{p})$ with respect to $p_\parallel^2$, and evaluating every other Fourier Transform at $\boldsymbol{p}=0$. This means that one can already perform the evaluation at constant field, which simplifies drastically the computation. One therefore gets:

$$\partial_k A_k = -\frac{1}{2}\,\mathrm{Tr}\int_{\boldsymbol{q}_1}\partial_k\mathcal{R}_k(\boldsymbol{q}_1)\cdot G_k(-\boldsymbol{q}_1;\phi)\cdot\begin{pmatrix} A_k''(\phi) & 0 \\ 0 & 0\end{pmatrix}\cdot G_k(\boldsymbol{q}_1,\phi) \tag{D.3}$$

where the full propagator G_k is now evaluated at uniform field and reads:

$$G_k(\boldsymbol{q};\phi) = \begin{pmatrix} \frac{2W(\omega)}{P(q^2,\omega)P(q^2,-\omega)} & \frac{1}{P(q^2,-\omega)} \\ \frac{1}{P(q^2,\omega)} & 0\end{pmatrix} \tag{D.4}$$

with $P(q^2,\omega) = R_k(q_\parallel^2,q_\perp^2)+q_\perp^2+q_\parallel^2A_k'(\phi)+i\omega$, and $W(\omega)=1$ for an isotropic noise, and $W(\omega)=\delta(\omega)$ for a static noise. After performing the matrix product and the trace, the integration over the frequencies is straightforward and yields for the flow of A_k:

$$\partial_k A_k = -\frac{(3\kappa-2)K_d}{2}\times\int_{|q_\perp|=0}^{\infty}\int_{q_\parallel=-\infty}^{\infty}\frac{\partial_k R_k(q_\parallel^2,|q_\perp|^2)\,|q_\perp|^{d-2}A_k''(\phi)}{\left(R_k(q_\parallel^2,|q_\perp|^2)+|q_\perp|^2+q_\parallel^2A_k'(\phi)\right)^{1+\kappa}} \tag{D.5}$$

where $\kappa = 1$ for an isotropic noise, and $\kappa = 2$ for a static noise, and where $K_d = (2^{d-1}\pi^{d/2}\Gamma(d/2))^{-1} = S_{d-1}/(2\pi)^d$ with S_d the surface of the d-dimensional unit hypersphere. Notice that we have used the rotational invariance in the transverse direction to rewrite the integral over $q_\perp$ as an integral over its norm. Finally, one performs the change of variable $q_\parallel = \sqrt{y}\cos(\theta)$ and $q_\perp = \sqrt{y}\sin(\theta)$ with $y \in [0, \infty[$ and $\theta \in [0, \pi]$. If we furthermore chose the regulator R_k to be a function of $y = q_\perp^2 + q_\parallel^2$ only, we can write:

$$R_k(q_\parallel^2, |q_\perp|^2) = yk^2 r(y) \tag{D.6}$$

with $r(y)$ the usual momentum regulator, for example an exponential regulator:

$$r(y) = \frac{a}{\mathrm{e}^y - 1} \tag{D.7}$$

where a is a free parameter. Finally, using the dimensionless variables as defined in Eq. (IV.30), the particular form of regulator (D.6) and Eq. (D.5) one finally gets the dynamical part of the flow, Eq. (IV.35).

D.2 Retrieving the one-loop perturbative results

To retrieve the perturbative results from [26, 217], and from [27], we first evaluate the previous equations at the upper critical dimension d_c, which depends on the noise type: $d_c^{\text{stat}} = 4$ for a static noise, and $d_c^{\text{iso}} = 2$ for an isotropic noise. We define accordingly $\epsilon = d_c - d$.

D.2.1 Pastor-Satorras and Rothman's results

The equations derived in [26] are retrieved by performing a lowest-order expansion of the function $\hat{A}(\hat{\phi})$:

$$\hat{A}(\hat{\phi}) = \hat{\phi} + \frac{\hat{a}_3}{3!}\hat{\phi}^3 \tag{D.8}$$

where $\hat{a}_1 \equiv 1$ by definition of the anomalous dimension η_A. Then, taking derivatives of the flow equation (IV.33), and evaluating them at $\hat{\phi} = 0$, one finds:

$$\eta_A = \frac{\epsilon}{2} + \frac{3\pi K_d}{8}\hat{a}_3 \tag{D.9}$$

$$k\partial_k \hat{a}_3 = -\epsilon \hat{a}_3 + \frac{3\pi K_d}{2}\hat{a}_3^2 \tag{D.10}$$

Notice that at first order in the ϵ-expansion, the integrals of the dynamical part of the flow can be computed analytically at $d = d_c^{\text{stat}}$ or $d = d_c^{\text{iso}}$. Moreover, at the first-order in the ϵ-expansion, one notices that the flow equations do not depend on the precise shape of the regulator $r(y)$. Finally, the definition of the term in front of the cubic term in $\hat{A}$, $\hat{a}_3$, differs from that of [26] and the relation between the two is $\hat{a}_3 = 2\lambda$. Their dimensionless parameter $\bar{\lambda}$ is also proportional to ours and we have the following relation between the two: $\hat{a}_3 = 2(2\pi)^{d-1}/S_{d-1}\bar{\lambda}$ where S_d is the surface area of a d-dimensional unit sphere. Up to these notation, and up to a factor -1 which comes from the fact their equations are derived for the real-space variable l, whereas ours are derived for the momentum k, Eq. (D.10) is indeed equivalent to their Eq. (6) in [26]. We also agree with their results for the roughness (and anisotropy) exponent, and the stable fixed point of Eqs. (D.9)-(D.10) indeed yields:

$$\alpha \equiv (4\kappa - 2d - \eta_A^*)/3 = \frac{5}{12}\epsilon \tag{D.11}$$

We still emphasize that this result is not correct, even for $\epsilon \to 0$, because the expansion (D.8) discards an infinity of equally relevant coupling constants and is thus not valid.

D.2.2 Antonov and Kakin's results

Following [27], we set $\kappa = 1$ (isotropic noise), $d_c = d_c^{\text{iso}} = 2$ and we expand the function $\hat{A}(\hat{\phi})$ as:

$$\hat{A}(\hat{\phi}) = \hat{\phi} + \sum_{i=2}^{\infty} \frac{\hat{a}_i}{i!}\hat{\phi}^i \tag{D.12}$$

Notice that $\hat{A}$ is not an odd function of $\hat{\phi}$. Again, taking derivatives of the flow equation (IV.33), and evaluating them at $\hat{\phi} = 0$, we are able to retrieve the equations derived in [27], except that we do not agree on their integration over the momenta. Indeed, in [27], the integration over the momenta $\int \mathrm{d}\boldsymbol{k}$ seems to be performed as if $\boldsymbol{k}$ was isotropic, yielding a factor S_d whereas we argued it should be a factor S_{d-1}. A factor π coming from the integration over the angle θ is also missing. Up to this difference and notational discrepancies, our flow equations are in a one to one agreement with the β functions of [225] (those of the first article [27] involved a misprint in the β_2 function).

Notice also that contrary to what is stated in [27], taking $\hat{a}_i = 0$ for all $i \neq 3$ makes the RG equations of [27] boil down to those of [26, 217] (up to the factor coming from the momentum integration discussed in the previous paragraph).

D.3 An exact solution of the fixed point equation

In the special case of $\eta_A^* = 0$ (which is not interesting for the physics since it means $\zeta = 1/3 < 1$), the fixed point solution of the flow equation (IV.37) can be solved exactly. Indeed, one can show that $\hat{A}'(\hat{\phi})$ is solution of the simple differential equation:

$$4\left(2\hat{\phi}^2 + 5\right)^2 (\hat{A}')^3 - \left(9\hat{A}' + 1\right)^2 = 0 \tag{D.13}$$

which can be solved exactly in terms of an integral over an algebraic integrand. In this special case, we therefore have a proof that a well-defined function exists on the whole real axis.

Moreover, this function is in fact also solution of a *linear* ordinary differential equation of order 4, on which the study of the singularities can be performed. The main singularity lies at $\hat{\phi}^2 = -5/2$ and not on the real axis. Thus, at least in this case, the series expansion around $\hat{\phi} = 0$ of the fixed point solution coincides with the fixed point solution although it has a finite radius of convergence, $R = \sqrt{5/2}$.

Although it is difficult to extrapolate this result to the physically interesting values of η_A^*, we have nonetheless checked that our numerical integration of the fixed point equation for $\eta_A^* = 0$ matches this exact result.

Bibliography

[1] L. Onsager, "Crystal statistics. I. A two-dimensional model with an order-disorder transition," Phys. Rev. **65**, 117 (1944).

[2] E. A. Guggenheim, "The Principle of Corresponding States," J. Chem. Phys. **13**, 253 (1945).

[3] L. P. Kadanoff, "Scaling laws for Ising models near Tc," Physics **2**, 263 (1966).

[4] K. G. Wilson, "Renormalization group and critical phenomena. I. Renormalization group and the Kadanoff scaling picture," Phys. Rev. B **4**, 3174 (1971).

[5] X.-L. Qi and S.-C. Zhang, "Topological insulators and superconductors," Rev. Mod. Phys. **83**, 1057 (2011).

[6] S. Sachdev, *Quantum Phase Transitions* (Cambridge University Press, Cambridge, England, 2011).

[7] U. C. Täuber, *Critical Dynamics: A Field Theory Approach to Equilibrium and Non-Equilibrium Scaling Behavior* (Cambridge University Press, Cambridge, England, 2014).

[8] H. Hinrichsen, "Non-equilibrium critical phenomena and phase transitions into absorbing states," Adv. Phys. **49**, 815 (2000).

[9] R. F. Voss, "Fractals in nature: From characterization to simulation," in *The Science of Fractal Images* (Springer, 1988) pp. 21–70.

[10] A. Vespignani and S. Zapperi, "How self-organized criticality works: A unified mean-field picture," Phys. Rev. E **57**, 6345 (1998).

[11] D. L. Turcotte, "Self-organized criticality," Rep. Prog. Phys. **62**, 1377 (1999).

[12] A. N. Kolmogorov, "The local structure of turbulence in incompressible viscous fluid for very large Reynolds numbers," Dokl. Akad. Nauk SSSR **30**, 301 (1941).

[13] M. Kardar, G. Parisi, and Y.-C. Zhang, "Dynamic scaling of growing interfaces," Phys. Rev. Lett. **56**, 889 (1986).

[14] J. Berges, N. Tetradis, and C. Wetterich, "Non-perturbative renormalization flow in quantum field theory and statistical physics," Phys. Rep. **363**, 223 (2002).

[15] L. Canet, V. Rossetto, N. Wschebor, and G. Balarac, "Spatiotemporal velocity-velocity correlation function in fully developed turbulence," Phys. Rev. E **95**, 023107 (2017).

[16] T. Kloss, L. Canet, and N. Wschebor, "Nonperturbative renormalization group for the stationary Kardar-Parisi-Zhang equation: Scaling functions and amplitude ratios in 1+1, 2+1, and 3+1 dimensions," Phys. Rev. E **86**, 051124 (2012).

[17] J. Cardy, "Reaction-diffusion processes," Lect. Notes **100**, 26 (2006).

[18] M. F. Weber and E. Frey, "Master equations and the theory of stochastic path integrals," Rep. Prog. Phys. **80**, 046601 (2017).

[19] F. Benitez, C. Duclut, H. Chaté, B. Delamotte, I. Dornic, and M. A. Muñoz, "Langevin Equations for Reaction-Diffusion Processes," Phys. Rev. Lett. **117**, 100601 (2016).

[20] O. Deloubriere, L. Frachebourg, H. J. Hilhorst, and K. Kitahara, "Imaginary noise and parity conservation in the reaction A+A⇌ 0," Physica A **308**, 135 (2002).

[21] L. Canet, H. Chaté, and B. Delamotte, "General framework of the non-perturbative renormalization group for non-equilibrium steady states," J. Phys. A **44**, 495001 (2011).

[22] C. Duclut and B. Delamotte, "Frequency regulators for the nonperturbative renormalization group: A general study and the model A as a benchmark," Phys. Rev. E **95**, 012107 (2017).

[23] T. R. Morris and J. F. Tighe, "Convergence of derivative expansions of the renormalization group," J. High Energy Phys. **1999**, 007 (1999).

[24] I. Rodriguez-Iturbe and A. Rinaldo, *Fractal River Basins: Chance and Self-Organization* (Cambridge University Press, Cambridge, England, 2001).

[25] D. Sornette and Y.-C. Zhang, "Non-linear Langevin model of geomorphic erosion processes," Geophys. J. Int. **113**, 382 (1993).

[26] R. Pastor-Satorras and D. H. Rothman, "Stochastic equation for the erosion of inclined topography," Phys. Rev. Lett. **80**, 4349 (1998).

[27] N. V. Antonov and P. I. Kakin, "Scaling in landscape erosion: Renormalization group analysis of a model with infinitely many couplings," Theor. Math. Phys. **190**, 193 (2017).

[28] C. Duclut and B. Delamotte, "Nonuniversality in the erosion of tilted landscapes," Phys. Rev. E **96**, 012149 (2017).

[29] P. M. Chaikin and T. C. Lubensky, *Principles of Condensed Matter Physics* (Cambridge University Press, Cambridge, England, 1995).

[30] N. Goldenfeld, *Lectures on Phase Transitions and the Renormalization Group* (Perseus Books, Reading, Massachusetts, 1992).

[31] J. Zinn-Justin, *Phase Transitions and Renormalization Group* (Oxford University Press, Oxford, England, 2013).

[32] G. Jona-Lasinio, "Renormalization group and probability theory," Phys. Rep. **352**, 439 (2001).

[33] B. Delamotte, "An Introduction to the Nonperturbative Renormalization Group," Lect. Notes Phys. **852**, 49 (2012).

[34] H. Gies, "Introduction to the Functional RG and Applications to Gauge Theories," Lect. Notes Phys. **852**, 287 (2012).

[35] L. Canet, *Processus de Réaction-Diffusion : Une Approche Par Le Groupe de Renormalisation Non Perturbatif*, Ph.D. thesis, Paris 7 (2004).

[36] C. Wetterich, "Exact evolution equation for the effective potential," Phys. Lett. B **301**, 90 (1993).

[37] T. R. Morris, "The exact renormalization group and approximate solutions," Int. J. Mod. Phys. A **09**, 2411 (1994).

[38] U. Ellwanger, "Flow equations for N point functions and bound states," Z. Phys. C **62**, 503 (1994).

[39] "Supercooling Water and Black Ice," https://steemit.com/science/@timsaid/supercooling-water-and-black-ice (2016), online, accessed July 2017.

[40] "Critical Opalescence: An Optical Signature for a QCD Critical Point," https://inspirehep.net/record/838172/plots (2009), online, accessed July 2017.

[41] M. Prähofer and H. Spohn, "Universal distributions for growth processes in 1+ 1 dimensions and random matrices," Phys. Rev. Lett. **84**, 4882 (2000).

[42] P. W. Higgs, "Broken symmetries and the masses of gauge bosons," Phys. Rev. Lett. **13**, 508 (1964).

[43] F. Englert and R. Brout, "Broken symmetry and the mass of gauge vector mesons," Phys. Rev. Lett. **13**, 321 (1964).

[44] L. Landau, "On the theory of phase transitions," Zh. Eksp. Teor. Fiz. **7**, 19–32 (1937).

[45] S. Angst, S. R. Dahmen, H. Hinrichsen, A. Hucht, and M. P. Magiera, "Explosive Ising," J. Stat. Mech. **2012**, L06002 (2012).

[46] A. Coniglio and W. Klein, "Clusters and Ising critical droplets: A renormalisation group approach," J. Phys. A **13**, 2775 (1980).

[47] F. J. Wegner and A. Houghton, "Renormalization group equation for critical phenomena," Phys. Rev. A **8**, 401 (1973).

[48] J. Polchinski, "Renormalization and effective Lagrangians," Nucl. Phys. B **231**, 269 (1984).

[49] D. F. Litim, "Optimized renormalization group flows," Phys. Rev. D **64**, 105007 (2001).

[50] T. R. Morris, "Equivalence of local potential approximations," J. High Energy Phys. **2005**, 027 (2005).

[51] J.-P. Blaizot, R. Méndez-Galain, and N. Wschebor, "Nonperturbative renormalization group and momentum dependence of n-point functions. I," Phys. Rev. E **74**, 051116 (2006).

[52] J.-P. Blaizot, R. Méndez-Galain, and N. Wschebor, "A new method to solve the nonperturbative renormalization group equations," Phys. Lett. B **632**, 571 (2006).

[53] A. Chiocchetta, A. Gambassi, S. Diehl, and J. Marino, "Universal short-time dynamics: Boundary functional renormalization group for a temperature quench," Phys. Rev. B **94**, 174301 (2016).

[54] L. Canet, H. Chaté, and B. Delamotte, "Quantitative Phase Diagrams of Branching and Annihilating Random Walks," Phys. Rev. Lett. **92**, 255703 (2004).

[55] F. Benitez and N. Wschebor, "Some exact results in branching and annihilating random walks," arXiv:1207.6594 (2012).

[56] F. Rose, F. Léonard, and N. Dupuis, "Higgs amplitude mode in the vicinity of a (2+1)-dimensional quantum critical point: A nonperturbative renormalization-group approach," Phys. Rev. B **91**, 224501 (2015).

[57] F. Rose, F. Benitez, F. Léonard, and B. Delamotte, "Bound states of the $\phi 4$ model via the nonperturbative renormalization group," Phys. Rev. D **93**, 125018 (2016).

[58] S. Mathey, E. Agoritsas, T. Kloss, V. Lecomte, and L. Canet, "Kardar-Parisi-Zhang equation with short-range correlated noise: Emergent symmetries and nonuniversal observables," Phys. Rev. E **95**, 032117 (2017).

[59] W. H. Press, S. A. Teukolsky, W. T. Vetterling, and B. P. Flannery, *Numerical Recipes: The Art of Scientific Computing* (Cambridge University Press, Cambridge, England, 2007).

[60] C. Bervillier, A. Jüttner, and D. F. Litim, "High-accuracy scaling exponents in the local potential approximation," Nucl. Phys. B **783**, 213 (2007).

[61] C. Bervillier, B. Boisseau, and H. Giacomini, "Analytical approximation schemes for solving exact renormalization group equations in the local potential approximation," Nucl. Phys. B **789**, 525 (2008).

[62] C. Bervillier, B. Boisseau, and H. Giacomini, "Analytical approximation schemes for solving exact renormalization group equations. II Conformal mappings," Nucl. Phys. B **801**, 296 (2008).

[63] T. R. Morris, "On truncations of the exact renormalization group," Phys. Lett. B **334**, 355 (1994).

[64] A. Parola and L. Reatto, "Liquid state theories and critical phenomena," Adv. Phys. **44**, 211 (1995).

[65] J.-M. Caillol, "Non-perturbative renormalization group for simple fluids," Mol. Phys. **104**, 1931 (2006).

[66] F. Léonard and B. Delamotte, "Critical Exponents Can Be Different on the Two Sides of a Transition: A Generic Mechanism," Phys. Rev. Lett. **115**, 200601 (2015).

[67] L. Canet, B. Delamotte, D. Mouhanna, and J. Vidal, "Optimization of the derivative expansion in the nonperturbative renormalization group," Phys. Rev. D **67**, 065004 (2003).

[68] D. F. Litim and D. Zappalà, "Ising exponents from the functional renormalization group," Phys. Rev. D **83**, 085009 (2011).

[69] O. J. Rosten, "Fundamentals of the exact renormalization group," Phys. Rep. **511**, 177 (2012).

[70] B. Delamotte, D. Mouhanna, and M. Tissier, "Nonperturbative renormalization-group approach to frustrated magnets," Phys. Rev. B **69**, 134413 (2004).

[71] M. M. Scherer, S. Floerchinger, and H. Gies, "Functional renormalization for the Bardeen-Cooper-Schrieffer to Bose-Einstein condensation crossover," Phil. Trans. R. Soc. A **369**, 2779 (2011).

[72] G. Tarjus and M. Tissier, "Nonperturbative Functional Renormalization Group for Random-Field Models: The Way Out of Dimensional Reduction," Phys. Rev. Lett. **93**, 267008 (2004).

[73] L. Canet, B. Delamotte, D. Mouhanna, and J. Vidal, "Nonperturbative renormalization group approach to the Ising model: A derivative expansion at order $\partial 4$," Phys. Rev. B **68**, 064421 (2003).

[74] G. v. Gersdorff and C. Wetterich, "Nonperturbative renormalization flow and essential scaling for the Kosterlitz-Thouless transition," Phys. Rev. B **64**, 054513 (2001).

[75] A. A. Pogorelov and I. M. Suslov, "Estimate of the critical exponents from the field-theoretical renormalization group: Mathematical meaning of the Standard Values," JETP **106**, 1118 (2008).

[76] P. Grassberger, P. Sutter, and L. Schäfer, "Field theoretic and Monte Carlo analysis of the Domb-Joyce model," J. Phys. A **30**, 7039 (1997).

[77] M. Hasenbusch, "Finite size scaling study of lattice models in the three-dimensional Ising universality class," Phys. Rev. B **82**, 174433 (2010).

[78] M. Campostrini, M. Hasenbusch, A. Pelissetto, and E. Vicari, "Theoretical estimates of the critical exponents of the superfluid transition in He 4 by lattice methods," Phys. Rev. B **74**, 144506 (2006).

[79] M. Campostrini, M. Hasenbusch, A. Pelissetto, P. Rossi, and E. Vicari, "Critical exponents and equation of state of the three-dimensional Heisenberg universality class," Phys. Rev. B **65**, 144520 (2002).

[80] A. Pelissetto and E. Vicari, "Renormalized four-point coupling constant in the three-dimensional O(N) model with N=0," J. Phys. A **40**, F539 (2007).

[81] F. Kos, D. Poland, D. Simmons-Duffin, and A. Vichi, "Precision islands in the Ising and O(N) models," J. High Energy Phys. **2016**, 36 (2016).

[82] V. L. Berezinskii, "Destruction of long-range order in one-dimensional and two-dimensional systems having a continuous symmetry group I. classical systems," Sov. Phys. JETP **32**, 493 (1971).

[83] J. M. Kosterlitz and D. J. Thouless, "Ordering, metastability and phase transitions in two-dimensional systems," J. Phys. C **6**, 1181–1203 (1973).

[84] A. S. Krinitsyn, V. V. Prudnikov, and P. V. Prudnikov, "Calculations of the dynamical critical exponent using the asymptotic series summation method," Theor. Math. Phys. **147**, 561 (2006).

[85] N. Ito, K. Hukushima, K. Ogawa, and Y. Ozeki, "Nonequilibrium relaxation of fluctuations of physical quantities," J. Phys. Soc. Jpn. **69**, 1931 (2000).

[86] L. T. Adzhemyan, S. V. Novikov, and L. Sladkoff, "Calculation of the dynamical critical exponent in the model A of critical dynamics to order $e4$," arXiv:0808.1347 (2008).

[87] F. Jasch and H. Kleinert, "Fast-convergent resummation algorithm and critical exponents of $\phi 4$-theory in three dimensions," J. Math. Phys. **42**, 52 (2001).

[88] P. Calabrese and A. Gambassi, "Ageing properties of critical systems," J. Phys. A **38**, R133 (2005).

[89] M. Prähofer and H. Spohn, "Exact scaling functions for one-dimensional stationary KPZ growth," J. Stat. Phys. **115**, 255 (2004).

[90] K. J. Wiese, "On the perturbation expansion of the KPZ equation," J. Stat. Phys. **93**, 143 (1998).

[91] L. Canet, H. Chaté, B. Delamotte, and N. Wschebor, "Nonperturbative renormalization group for the Kardar-Parisi-Zhang equation: General framework and first applications," Phys. Rev. E **84**, 061128 (2011).

[92] L. Canet, B. Delamotte, and N. Wschebor, "Fully developed isotropic turbulence: Symmetries and exact identities," Phys. Rev. E **91**, 053004 (2015).

[93] L. Canet, B. Delamotte, and N. Wschebor, "Fully developed isotropic turbulence: Nonperturbative renormalization group formalism and fixed-point solution," Phys. Rev. E **93**, 063101 (2016).

[94] J. L. Cardy and U. C. Täuber, "Field theory of branching and annihilating random walks," J. Stat. Phys. **90**, 1 (1998).

[95] L. Canet, H. Chaté, B. Delamotte, I. Dornic, and M. A. Muñoz, "Nonperturbative Fixed Point in a Nonequilibrium Phase Transition," Phys. Rev. Lett. **95**, 100601 (2005).

[96] F. Benitez and N. Wschebor, "Branching and annihilating random walks: Exact results at low branching rate," Phys. Rev. E **87**, 052132 (2013).

[97] L. Canet and H. J. Hilhorst, "Single-Site Approximation for Reaction-Diffusion Processes," J. Stat. Phys. **125**, 517 (2006).

[98] L. Canet, "Reaction–diffusion processes and non-perturbative renormalization group," J. Phys. A **39**, 7901 (2006).

[99] K. G. Wilson and M. E. Fisher, "Critical exponents in 3.99 dimensions," Phys. Rev. Lett. **28**, 240 (1972).

[100] N. Tetradis and C. Wetterich, "Critical exponents from the effective average action," Nucl. Phys. B **422**, 541 (1994).

[101] N. Tetradis and D. F. Litim, "Analytical solutions of exact renormalization group equations," Nucl. Phys. B **464**, 492 (1996).

[102] D. F. Litim, "Convergence and stability of the renormalisation group," hep-th/0208117 (2002).

[103] D. F. Litim, "Optimisation of the exact renormalisation group," Phys. Lett. B **486**, 92–99 (2000).

[104] P. M. Stevenson, "Optimized perturbation theory," Phys. Rev. D **23**, 2916 (1981).

[105] J. M. Pawlowski, "Aspects of the functional renormalisation group," Ann. Phys. **322**, 2831 (2007).

[106] J. M. Pawlowski, M. M. Scherer, R. Schmidt, and S. J. Wetzel, "Physics and the choice of regulators in functional renormalisation group flows," arXiv:1512.03598 (2015).

[107] H. Kleinert, *Path Integrals in Quantum Mechanics, Statistics, Polymer Physics, and Financial Markets* (World Scientific, Singapore, 2009).

[108] I. Balog and B. Delamotte, "Derivative expansion at order 6," Unpublished .

[109] T. Halpin-Healy and Y.-C. Zhang, "Kinetic roughening phenomena, stochastic growth, directed polymers and all that. Aspects of multidisciplinary statistical mechanics," Phys. Rep. **254**, 215 (1995).

[110] J. Krug, "Origins of scale invariance in growth processes," Adv. Phys. **46**, 139 (1997).

[111] M. Henkel and H. Hinrichsen, "The non-equilibrium phase transition of the pair-contact process with diffusion," J. Phys. A **37**, R117 (2004).

[112] J. Ingen-Housz, "Bemerkungen über den Gebrauch des Vergrösserungsglases," Verm Schriften Phys.-Med. Inh. (1784).

[113] R. Brown, "XXVII. A brief account of microscopical observations made in the months of June, July and August 1827, on the particles contained in the pollen of plants; and on the general existence of active molecules in organic and inorganic bodies," Philosophical Magazine Series 2 **4**, 161 (1828).

[114] L. Bachelier, *Théorie de La Spéculation* (Gauthier-Villars, Paris, France, 1900).

[115] A. Einstein, "Über die von der molekularkinetischen Theorie der Wärme geforderte Bewegung von in ruhenden Flüssigkeiten suspendierten Teilchen," Ann. Phys. **322**, 549 (1905).

[116] P. Langevin, "Sur la théorie du mouvement brownien," CR Acad. Sci. Paris **146**, 530 (1908).

[117] P. Hänggi and F. Marchesoni, "Introduction: 100 years of Brownian motion," Chaos **15**, 026101 (2005).

[118] C. W. Gardiner, *Handbook of Stochastic Methods for Physics, Chemistry and the Natural Sciences* (Springer, Berlin, Germany, 1985).

[119] N. G. van Kampen, *Stochastic Processes in Physics and Chemistry* (Elsevier Science, Amsterdam, Netherlands, 1992).

[120] L. Wilhelmy, "Ueber das Gesetz, nach welchem die Einwirkung der Säuren auf den Rohrzucker stattfindet," Ann. Phys. Chem. **157**, 499 (1850).

[121] L. G. Harrison, *Kinetic Theory of Living Pattern*, Developmental and cell biology series (Cambridge University Press, Cambridge, England, 1993).

[122] A. M. Zhabotinsky, "A history of chemical oscillations and waves," Chaos **1**, 379 (1991).

[123] R. A. Fisher, "The use of multiple measurements in taxonomic problems," Annals of eugenics **7**, 179 (1936).

[124] A. N. Kolmogorov, I. Petrovsky, and N. Piskunov, "Etude de l'équation de la diffusion avec croissance de la quantité de matiere et son applicationa un probleme biologique," Moscow Univ. Math. Bull **1**, 129 (1937).

[125] G. M. Viswanathan, S. V. Buldyrev, S. Havlin, M. G. E. da Luz, E. P. Raposo, and H. E. Stanley, "Optimizing the success of random searches," Nature **401**, 911 (1999).

[126] M. C. González, C. A. Hidalgo, and A.-L. Barabási, "Understanding individual human mobility patterns," Nature **453**, 779 (2008).

[127] I. Dornic, H. Chaté, and M. A. Muñoz, "Integration of Langevin Equations with Multiplicative Noise and the Viability of Field Theories for Absorbing Phase Transitions," Phys. Rev. Lett. **94**, 100601 (2005).

[128] R. Dickman, "Numerical study of a field theory for directed percolation," Phys. Rev. E **50**, 4404 (1994).

[129] G. N. Milstein, E. Platen, and H. Schurz, "Balanced Implicit Methods for Stiff Stochastic Systems," SIAM J. Numer. Anal. **35**, 1010 (1998).

[130] H. Schurz, "Numerical regularization for SDEs: Construction of nonnegative solutions," Dynam. Syst. Appl. **5**, 323 (1996).

[131] L. Pechenik and H. Levine, "Interfacial velocity corrections due to multiplicative noise," Phys. Rev. E **59**, 3893 (1999).

[132] E. Moro and H. Schurz, "Boundary Preserving Semianalytic Numerical Algorithms for Stochastic Differential Equations," SIAM J. Sci. Comput. **29**, 1525 (2007).

[133] E. Moro, "Hybrid method for simulating front propagation in reaction-diffusion systems," Phys. Rev. E **69**, 060101 (2004).

[134] H. K. Lee, C. Kwon, and H. Park, "Equivalence of operator-splitting schemes for the integration of the Langevin equation," J. Stat. Mech. **2006**, P08021 (2006).

[135] P. C. Martin, E. D. Siggia, and H. A. Rose, "Statistical Dynamics of Classical Systems," Phys. Rev. A **8**, 423 (1973).

[136] H.-K. Janssen, "On a Lagrangean for classical field dynamics and renormalization group calculations of dynamical critical properties," Z. Phys. B **23**, 377 (1976).

[137] C. De Dominicis, "Techniques de renormalisation de la théorie des champs et dynamique des phénomènes critiques," J. Phys. Colloq. **37**, C1–247 (1976).

[138] H. Touchette, "The large deviation approach to statistical mechanics," Phys. Rep. **478**, 1 (2009).

[139] L. F. Cugliandolo and V. Lecomte, "Rules of calculus in the path integral representation of white noise Langevin equations," arXiv:1704.03501 (2017).

[140] D. Stauffer and A. Aharony, *Introduction to Percolation Theory* (Taylor & Francis, London, England, 1994).

[141] K. A. Takeuchi, M. Kuroda, H. Chaté, and M. Sano, "Directed Percolation Criticality in Turbulent Liquid Crystals," Phys. Rev. Lett. **99**, 234503 (2007).

[142] G. Lemoult, L. Shi, K. Avila, S. V. Jalikop, M. Avila, and B. Hof, "Directed percolation phase transition to sustained turbulence in Couette flow," Nat. Phys. **12**, 254 (2016).

[143] M. Henkel, E. Orlandini, and G. M. Schutz, "Equivalences between stochastic systems," J. Phys. A **28**, 6335 (1995).

[144] L. Canet, B. Delamotte, O. Deloubrière, and N. Wschebor, "Nonperturbative Renormalization-Group Study of Reaction-Diffusion Processes," Phys. Rev. Lett. **92**, 195703 (2004).

[145] J. B. Bronzan and J. W. Dash, "Higher-order ϵ terms in Reggeon field theory," Phys. Rev. D **10**, 4208 (1974).

[146] I. Jensen, "Critical behavior of the three-dimensional contact process," Phys. Rev. A **45**, R563 (1992).

[147] H.-K. Janssen, "On the nonequilibrium phase transition in reaction-diffusion systems with an absorbing stationary state," Z. Phys. B **42**, 151 (1981).

[148] P. Grassberger, "On phase transitions in Schlögl's second model," Z. Phys. B **47**, 365 (1982).

[149] J. Cardy and U. C. Täuber, "Theory of branching and annihilating random walks," Phys. Rev. Lett. **77**, 4780 (1996).

[150] F. Benitez and N. Wschebor, "Branching-rate expansion around annihilating random walks," Phys. Rev. E **86**, 010104 (2012).

[151] J. Kockelkoren and H. Chaté, "Absorbing Phase Transitions of Branching-Annihilating Random Walks," Phys. Rev. Lett. **90**, 125701 (2003).

[152] O. Al Hammal, H. Chaté, I. Dornic, and M. A. Munoz, "Langevin description of critical phenomena with two symmetric absorbing states," Phys. Rev. Lett. **94**, 230601 (2005).

[153] I. Dornic, H. Chaté, J. Chave, and H. Hinrichsen, "Critical Coarsening without Surface Tension: The Universality Class of the Voter Model," Phys. Rev. Lett. **87**, 045701 (2001).

[154] D. Gredat, H. Chaté, B. Delamotte, and I. Dornic, "Finite-scale singularity in the renormalization group flow of a reaction-diffusion system," Phys. Rev. E **89**, 010102 (2014).

[155] A. A. Ovchinnikov and Y. B. Zeldovich, "Role of density fluctuations in bimolecular reaction kinetics," Chem. Phys. **28**, 215 (1978).

[156] D. Toussaint and F. Wilczek, "Particle–antiparticle annihilation in diffusive motion," J. Chem. Phys. **78**, 2642 (1983).

[157] U. C. Täuber, M. Howard, and B. P. Vollmayr-Lee, "Applications of field-theoretic renormalization group methods to reaction–diffusion problems," J. Phys. A **38**, R79 (2005).

[158] M. Howard, "Fluctuation kinetics in a multispecies reaction-diffusion system," J. Phys. A **29**, 3437 (1996).

[159] H.-K. Janssen and U. C. Täuber, "The field theory approach to percolation processes," Ann. Phys. **315**, 147 (2005).

[160] P. Le Doussal and K. J. Wiese, "Exact Mapping of the Stochastic Field Theory for Manna Sandpiles to Interfaces in Random Media," Phys. Rev. Lett. **114**, 110601 (2015).

[161] H.-K. Janssen and O. Stenull, "Directed percolation with a conserved field and the depinning transition," Phys. Rev. E **94**, 042138 (2016).

[162] L. Anton, H. Park, and S.-C. Park, "Generating function for particle-number probability distribution in directed percolation," J. Phys. A **38**, 8187 (2005).

[163] R. Dickman and M. A. F. de Menezes, "Nonuniversality in the pair contact process with diffusion," Phys. Rev. E **66**, 045101 (2002).

[164] D. T. Gillespie, "Stochastic Simulation of Chemical Kinetics," Annu. Rev. Phys. Chem. **58**, 35 (2007).

[165] E. Moro, "Numerical schemes for continuum models of reaction-diffusion systems subject to internal noise," Phys. Rev. E **70**, 045102 (2004).

[166] R. A. Fisher, "The wave of advance of advantageous genes," Ann. Eugen. **7**, 355 (1937).

[167] D. T. Gillespie, "The chemical Langevin equation," J. Chem. Phys. **113**, 297 (2000).

[168] D. T. Gillespie, A. Hellander, and L. R. Petzold, "Perspective: Stochastic algorithms for chemical kinetics," J. Chem. Phys. **138**, 170901 (2013).

[169] M. Doi, "Second quantization representation for classical many-particle system," J. Phys. A **9**, 1465 (1976).

[170] L. Peliti, "Path integral approach to birth-death processes on a lattice," J. Phys. **46**, 1469 (1985).

[171] K. J. Wiese, "Coherent-state path integral versus coarse-grained effective stochastic equation of motion: From reaction diffusion to stochastic sandpiles," Phys. Rev. E **93**, 042117 (2016).

[172] N. G. van Kampen, "A power series expansion of the master equation," Can. J. Phys. **39**, 551 (1961).

[173] R. Grima, P. Thomas, and A. V. Straube, "How accurate are the nonlinear chemical Fokker-Planck and chemical Langevin equations?" J. Chem. Phys. **135**, 084103 (2011).

[174] D. Gredat, I. Dornic, and J. M. Luck, "On an imaginary exponential functional of Brownian motion," J. Phys. A **44**, 175003 (2011).

[175] M. Beccaria, B. Allés, and F. Farchioni, "Coherent-state path-integral simulation of many-particle systems," Phys. Rev. E **55**, 3870 (1997).

[176] C. W. Gardiner and S. Chaturvedi, "The Poisson representation. I. A new technique for chemical master equations," J. Stat. Phys. **17**, 429 (1977).

[177] S. Chaturvedi and C. W. Gardiner, "The poisson representation. II Two-time correlation functions," J. Stat. Phys. **18**, 501 (1978).

[178] V. Elgart and A. Kamenev, "Rare event statistics in reaction-diffusion systems," Phys. Rev. E **70**, 041106 (2004).

[179] P. D. Drummond, "Gauge Poisson representations for birth/death master equations," Eur. Phys. J. B **38**, 617 (2004).

[180] M. Droz and A. McKane, "Equivalence between Poisson representation and Fock space formalism for birth-death processes," J. Phys. A **27**, L467 (1994).

[181] W. Feller, *An Introduction to Probability Theory and Its Applications* (Wiley, New York, 1957).

[182] H.-K. Janssen, "Survival and percolation probabilities in the field theory of growth models," J. Phys. Condens. Matter **17**, S1973 (2005).

[183] C. R. Doering, C. Mueller, and P. Smereka, "Interacting particles, the stochastic Fisher–Kolmogorov–Petrovsky–Piscounov equation, and duality," Physica A **325**, 243 (2003).

[184] Z. Schuss, *Theory and Applications of Stochastic Processes* (Springer, Berlin, Germany, 2010).

[185] M. Ciafaloni and E. Onofri, "Path integral formulation of reggeon quantum mechanics," Nucl. Phys. B **151**, 118 (1979).

[186] L. Canet, H. Chaté, B. Delamotte, and N. Wschebor, "Nonperturbative Renormalization Group for the Kardar-Parisi-Zhang Equation," Phys. Rev. Lett. **104**, 150601 (2010).

[187] T. Kloss, L. Canet, B. Delamotte, and N. Wschebor, "Kardar-Parisi-Zhang equation with spatially correlated noise: A unified picture from nonperturbative renormalization group," Phys. Rev. E **89**, 022108 (2014).

[188] L. Canet and H. Chaté, "A non-perturbative approach to critical dynamics," J. Phys. A **40**, 1937 (2007).

[189] A. J. Bray, "Dispersion-theory approach to the correlation function for critical scattering," Phys. Rev. B **14**, 1248 (1976).

[190] R. A. Ferrell and D. J. Scalapino, "Dispersion Theory Approach for the Critical Correlation Function," Phys. Rev. Lett. **34**, 200 (1975).

[191] C. Itzykson and J.-B. Zuber, *Quantum Field Theory* (Dover Publications, Mineola, New York, 2005).

[192] F. Benitez, J.-P. Blaizot, H. Chaté, B. Delamotte, R. Méndez-Galain, and N. Wschebor, "Nonperturbative renormalization group preserving full-momentum dependence: Implementation and quantitative evaluation," Phys. Rev. E **85**, 026707 (2012).

[193] P. C. Hohenberg and B. I. Halperin, "Theory of dynamic critical phenomena," Rev. Mod. Phys. **49**, 435 (1977).

[194] A. Andreanov, G. Biroli, and A. Lefèvre, "Dynamical field theory for glass-forming liquids, self-consistent resummations and time-reversal symmetry," J. Stat. Mech. , P07008 (2006).

[195] C. Aron, G. Biroli, and L. F. Cugliandolo, "Symmetries of generating functionals of Langevin processes with colored multiplicative noise," J. Stat. Mech. **2010**, P11018 (2010).

[196] R. Guida and J. Zinn-Justin, "Critical exponents of the N-vector model," J. Phys. A **31**, 8103 (1998).

[197] V. V. Prudnikov, A. V. Ivanov, and A. A. Fedorenko, "Critical dynamics of spin systems in the four-loop approximation," JETP Lett. **66**, 835 (1997).

[198] M. P. Nightingale and H. W. J. Blöte, "Monte Carlo computation of correlation times of independent relaxation modes at criticality," Phys. Rev. B **62**, 1089 (2000).

[199] A. Pelissetto and E. Vicari, "Critical phenomena and renormalization-group theory," Phys Rep **368**, 549 (2002).

[200] P. S. Dodds and D. H. Rothman, "Scaling, Universality, and Geomorphology," Annu. Rev. Earth Planet. Sci. **28**, 571 (2000).

[201] B. Mandelbrot, "How Long Is the Coast of Britain? Statistical Self-Similarity and Fractional Dimension," Science **156**, 636 (1967).

[202] B. Mandelbrot, *The Fractal Geometry of Nature* (Freeman, San Francisco, California, 1982).

[203] J. T. Hack, *Studies of Longitudinal Stream Profiles in Virginia and Maryland*, Vol. 294 (US Government Printing Office, 1957).

[204] W. I. Newman and D. L. Turcotte, "Cascade model for fluvial geomorphology," Geophys. J. Int. **100**, 433 (1990).

[205] D. M. Mark and P. B. Aronson, "Scale-dependent fractal dimensions of topographic surfaces: An empirical investigation, with applications in geomorphology and computer mapping," Math. Geol. **16**, 671 (1984).

[206] C. G. Chase, "Fluvial landsculpting and the fractal dimension of topography," Geomorphology **5**, 39 (1992).

[207] J. Kalda, "Gradient-Limited Surfaces: Formation of Geological Landscapes," Phys. Rev. Lett. **90**, 118501 (2003).

[208] C. Paola, K. Straub, D. Mohrig, and L. Reinhardt, "The "unreasonable effectiveness" of stratigraphic and geomorphic experiments," Earth-Sci. Rev. **97**, 1 (2009).

[209] G. Caldarelli, A. Giacometti, A. Maritan, I. Rodriguez-Iturbe, and A. Rinaldo, "Randomly pinned landscape evolution," Phys. Rev. E **55**, R4865 (1997).

[210] H.-J. Kim, I.-M. Kim, and J. M. Kim, "River networks on the slope-correlated landscape," Phys. Rev. E **62**, 3121 (2000).

[211] H. Kooi and C. Beaumont, "Escarpment evolution on high-elevation rifted margins: Insights derived from a surface processes model that combines diffusion, advection, and reaction," J. Geophys. Res. Solid Earth **99**, 12191 (1994).

[212] J. D. Pelletier, "Fractal behavior in space and time in a simplified model of fluvial landform evolution," Geomorphology **91**, 291 (2007).

[213] S. Ouchi and M. Matsushita, "Measurement of self-affinity on surfaces as a trial application of fractal geometry to landform analysis," Geomorphology **5**, 115 (1992).

[214] L. E. Gilbert, "Are topographic data sets fractal?" Pure Appl. Geophys. **131**, 241 (1989).

[215] R. E. Horton, "Erosional development of streams and their drainage basins; hydrophysical approach to a quantitative morphology," Geol. Soc. Am. Bull. **56**, 275 (1945).

[216] J. D. Pelletier, "Self-organization and scaling relationships of evolving river networks," J. Geophys. Res. Solid Earth **104**, 7359 (1999).

[217] R. Pastor-Satorras and D. H. Rothman, "Scaling of a slope: The erosion of tilted landscapes," J. Stat. Phys. **93**, 477 (1998).

[218] Z. Kukal, "How are rates of geological processes measured and expressed?" Earth-Sci. Rev. **28**, 10 (1990).

[219] P. M. Kenyon and D. L. Turcotte, "Morphology of a delta prograding by bulk sediment transport," Geol. Soc. Am. Bull. **96**, 1457 (1985).

[220] S. F. Edwards and D. R. Wilkinson, "The Surface Statistics of a Granular Aggregate," Proc. R. Soc. A **381**, 17 (1982).

[221] J. J. Roering, J. W. Kirchner, and W. E. Dietrich, "Evidence for nonlinear, diffusive sediment transport on hillslopes and implications for landscape morphology," Water Resour. Res. **35**, 853 (1999).

[222] J. Kelling and G. Ódor, "Extremely large-scale simulation of a Kardar-Parisi-Zhang model using graphics cards," Phys. Rev. E **84**, 061150 (2011).

[223] T. Hwa and M. Kardar, "Dissipative transport in open systems: An investigation of self-organized criticality," Phys. Rev. Lett. **62**, 1813 (1989).

[224] T. Hwa and M. Kardar, "Avalanches, hydrodynamics, and discharge events in models of sandpiles," Phys. Rev. A **45**, 7002 (1992).

[225] N. V. Antonov and P. I. Kakin, "Scaling in erosion of landscapes: Renormalization group analysis of a model with turbulent mixing," J. Phys. A **50**, 085002 (2017).

[226] C. M. Bender and S. A. Orszag, *Advanced Mathematical Methods for Scientists and Engineers* (Mac Graw Hill, New York, 1978).

[227] A. Giacometti, A. Maritan, and J. R. Banavar, "Continuum model for river networks," Phys. Rev. Lett. **75**, 577 (1995).

[228] J. R. Banavar, F. Colaiori, A. Flammini, A. Giacometti, A. Maritan, and A. Rinaldo, "Sculpting of a fractal river basin," Phys. Rev. Lett. **78**, 4522 (1997).

[229] A. Gelimson and R. Golestanian, "Collective Dynamics of Dividing Chemotactic Cells," Phys. Rev. Lett. **114**, 028101 (2015).

[230] T. Vicsek, A. Czirók, E. Ben-Jacob, I. Cohen, and O. Shochet, "Novel type of phase transition in a system of self-driven particles," Phys. Rev. Lett. **75**, 1226 (1995).

[231] J. Toner and Y. Tu, "Long-range order in a two-dimensional dynamical XY model: How birds fly together," Phys. Rev. Lett. **75**, 4326 (1995).

[232] P. Villa Martín, J. A. Bonachela, S. A. Levin, and M. A. Muñoz, "Eluding catastrophic shifts," Proc. Natl. Acad. Sci. **112**, E1828 (2015).

Phénomènes critiques hors-équilibre: équations de Langevin exactes, érosion d'un paysage en pente.

Résumé : L'objet de cette thèse a été l'étude de phénomènes critiques hors-équilibre. Pour décrire ces systèmes, les équations de Langevin sont souvent incontournables car elles fournissent un point de départ idéal pour des simulations numériques ou des approches de théorie des champs. Dans la plupart des cas, ces équations sont obtenues de façon phénoménologique en rajoutant un terme de bruit (qui modélise les degrés de liberté microscopiques du système) à une équation déterministe. Toutefois, j'ai montré qu'il est possible, dans le cas des processus de réaction-diffusion, d'aller au delà de cette approche phénoménologique et de dériver une équation de Langevin exacte qui décrit la dynamique au niveau microscopique.

Une seconde partie de ma thèse a été consacrée à l'étude de modèles spécifiques de phénomènes critiques hors-équilibre à l'aide du groupe de renormalisation non-perturbatif (NPRG), qui est la version moderne des blocs de spins de Wilson et Kadanoff. Cet outil théorique est maintenant largement répandu dans l'étude des phénomènes critiques à l'équilibre pour lesquels il tire son succès de sa capacité à contrôler les fluctuations qui se construisent au voisinage de la transition de phase grâce à l'utilisation d'une fonction de régulation, ou régulateur. Hors équilibre, les fluctuations temporelles doivent être traitées de la même façon, et j'ai donc conçu un régulateur qui contrôle à la fois les fluctuations spatiales et temporelles.

Enfin, j'ai appliqué les techniques du NPRG à un modèle d'érosion. En effet, l'apparition générique de lois d'échelles dans les paysages naturels suggère l'existence d'un mécanisme sous-jacent qui conduit naturellement ces systèmes à leur point critique. L'équation célèbre de Kardar-Parisi-Zhang semble ainsi modéliser de façon satisfaisante l'érosion à grande échelle (> 2 km), mais ne s'accorde pas aux lois de puissance observées à plus petite échelle. Un modèle différent, qui tient compte de l'anisotropie intrinsèque de ces plus petites échelles (la pente d'une montagne), fut donc suggéré. À l'aide du formalisme du NPRG, je montre que ce modèle possède une ligne de points fixes qui correspond à un domaine continu d'exposants d'échelle, ce qui pourrait expliquer la grande variabilité observée au niveau expérimental.

Mots-clefs : Phénomènes critiques hors-équilibre, groupe de renormalisation non-perturbatif, équations de Langevin, processus de réaction-diffusion, régulateur en fréquences, érosion de paysages.

Nonequilibrium critical phenomena: exact Langevin equations, erosion of tilted landscapes.

Abstract: This manuscript is focused on the study of critical phenomena taking place out-of-equilibrium. In the description of such phenomena, Langevin equations are ubiquitous and are derived most of the time in a phenomenological way by adding a noise term to a deterministic mean-field equation. However, I show that for reaction-diffusion processes it is in fact possible to derive an exact Langevin equation from the microscopic process.

A second part of my thesis work has been devoted to the study of specific nonequilibrium critical phenomena using the nonperturbative renormalization group (NPRG), which is a modern implementation of Wilson and Kadanoff's block spin idea. This tool, well-developed and very powerful in an equilibrium context, takes care of the growing spatial fluctuations that arise near criticality through the use of a regulator function. In a nonequilibrium context, the situation is more complex and the temporal fluctuations also have to be controlled. I have therefore designed a regulator that tackles both spatial and temporal fluctuations.

Finally, I have applied the NPRG techniques to a model of landscape erosion: Indeed, the generic scaling behaviour that appear in erosional landscapes suggests the existence of an underlying mechanism naturally fine-tuned to be critical. The famous Kardar-Parisi-Zhang equation seems to give a correct model for landscape erosion at large length scale (> 2 km), but fails to predict the scaling observed at smaller scale. A different model was thus suggested which takes into account the intrinsic anisotropy at smaller length scale (the slope of the mountain). Using NPRG techniques, I show that this model possesses a line of fixed points associated with a continuous range of scaling exponents, which could explain the great variability observed in experimental data.

Keywords: Nonequilibrium critical phenomena, nonperturbative renormalization group, Langevin equations, reaction-diffusion processes, frequency regulator, landscape erosion.